Project Taking Control: Final Report

DID-10

AE3200: Design Synthesis Exercise

Team 28

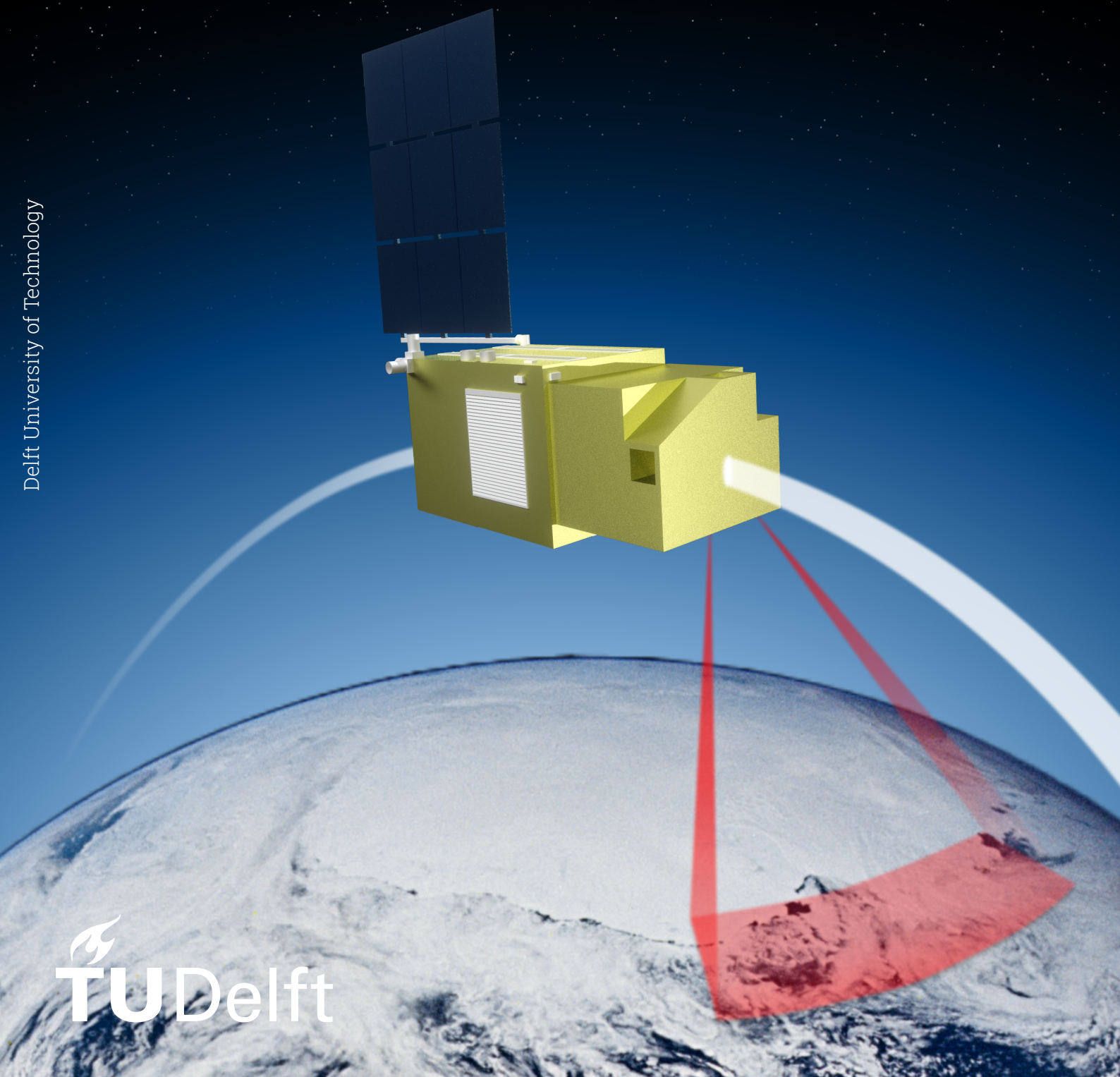

Delft University of Technology

TU Delft

(This page was left blank intentionally)

Project Taking Control: Final Report

DID-10

by

Team 28

Student Name	Student Number
Luis Ramos Archilla	5039134
Rafal Beres	5335183
Archan Chumsena	5086140
Tim Dammerman	5258634
Roland van Dijk	5208130
Bo Lee	5225604
Oskar Miller	5283507
Adriaan Ploeg	4556496
Eliot Watson	4993357
Daan van Wolffelaar	5280915

Version Control			
Version	**Date**	**Author(s)**	**Description**
0.1	08.06.2023	All	Chapter 1 for NLR
1.0	19.06.2023	All	First Draft
1.1	21.06.2023	All	Draft for Deadline
1.2	27.06.2023	All	Final Report

Tutor: M. Naeije
Coaches: H. S. Saluja, O. Stroosma
Project Duration: April, 2023 - June, 2023
Faculty: Faculty of Aerospace Engineering, Delft

Cover: Infrared Pollution Monitoring System satellite. Made by Bo Lee with 3DExperience and Figma software.
Style: TU Delft Report Style, with modifications by Daan Zwaneveld and Tim Dammerman.

TU Delft

Preface

'If you wish to be a writer, write' - Epictetus

This report represents the work of Team 28: Taking Control in the final stage of the 2023 Spring Design Synthesis Exercise (DSE) of the Faculty of Aerospace Engineering at the TU Delft; for completing the Bachelor of Science in Aerospace Engineering. The 10 team members wish to be engineers and therefore they must engineer a system (or face the wrath of Epictetus). As the final report of the degree, it is crucial to all in the group that it both represents accurately the quality of their work thus far and puts their 'best foot forward' into the future; in Delft or beyond.

The group would like to thank our tutors: Marc Naeije, Olaf Stroosma, and Harjot Sing Saluja, who have involved themselves with attention, knowledge, and enthusiasm at every step along the way. So too our client, Royal Netherlands Aerospace Centre (NLR); who welcomed us openly at their facility in Amsterdam for the review of the Midterm. The group found it to be a motivating and inspiring day, and the visit was wholly enjoyed. While the insightful discussion with all the employees we met was valued, special thanks go to Co Petersen, Nick van den Dungen, and Alexander Haagsma, who have been involved at every stage of the process and have given valuable input far beyond simply setting requirements. Finally, the team would like to extend our thanks to all of the Teaching Assistants of the DSE, particularly Crina Mihalache, who have capably assisted us at every opportunity, particularly in the earliest stages.

Team 28
Delft, June 2023

Executive Overview

'Design a space-based platform that is capable of monitoring the radiative forcing effects and dynamic evolution of exhaust trails from air-breathing vehicles in NearSpace, in 12 working days by ten students' - Project Objective Statement, Taking Control

Need, Market, and Objective

The Royal Netherlands Aerospace Centre (NLR) has requested the team Taking Control of the Technical University of Delft to design a solution to minimise the risk of collision due to the expected rapid increase of activity in the aerial regions between FL 660 to 100 km. To minimise this risk, the team has designed the NearSpace Operation Management System (NOMS) in the first half of the Design Synthesis Exercises (DSE). This system is able to surveil, communicate with, and plan the trajectories of all nominal occurring objects in the NearSpace region above Europe. However, this increase in activity in the NearSpace region also increases pollution. This pollution is expected to be more polluting than emissions on a ground level due to the limited amount of vertical air movement in these air layers. To study the effect of this pollution and the emissions of the NearSpace aerial vehicles, the Infrared Pollution Monitoring System (IPMS) is developed in the second half of the DSE.

To comply with the mission need, mission requirements are created. To observe the emissions of polluting vehicles, the system shall be able to provide data on the dispersion of H_2O, CO_2, NO_x, and CH_4 from air-breathing vehicles. Similar to the NOMS, the IPMS shall be operational in 2035 and have an operational lifetime of 30 yr. In order to ensure proper observation of NearSpace, the system shall have a downtime of at most 0.01% over its lifetime and a temporal resolution of 2 per day.

System Characteristics

With the project need and objectives, as well as the requirements in mind, the design solution of the IPMS is selected. To observe the water contrails, the observation instrument (payload) is selected first. The Infrared Atmospheric Sounding Interferometer - Next Generation (IASI-NG) is selected to perform the mission. The characteristics of this device are shown in Table 1a. Based on the lifetime of the payload, a satellite is designed to have the same lifetime of 7.5 yr.

Table 1: Payload and Astrodynamic Characteristics of the IPMS

(a) Payload Characteristics

Parameter	Value
Spectral coverage	645 cm^{-1} to 2760 cm^{-1}
Spectral resolution	0.25 cm^{-1}
Spatial resolution	24 km
Field of View	80°
Mass	360 kg
Power	500 W
Data rate	6 Mbit s^{-1}
Availability	>98%
Reliability	>84%
Lifetime	7.5 yr

(b) Orbit Characteristics

Parameter	Value
Eccentricity	0.042 09
Semi-major axis	7 258 689 m
Inclination	90°
Right ascension of the ascending node	0° - 8.57° - 17.12°
Argument of periapsis	90°
True anomaly	0°

Astrodynamics

To determine the orbit of the satellite, it is assumed that Earth-repeat orbits are the most suitable for the mission, as these cover the area of interest with relative frequency. Based on the Field of View and

spatial resolution of the payload, as well as the zone of interest of the mission, the orbit is determined. The calculations show that three different orbits are required that differ in the right ascension of the ascending node. The Keplerian elements of the orbits are presented in Table 1b. After the operational lifetime of the satellite, the satellite will perform a de-orbit manoeuvre by lowering the peri-centre altitude to zero. This manoeuvre is calculated to require a ΔV of 161.21 m s^{-1}. To maintain the selected orbit, several perturbations are taken into account to compensate for using the propulsion system of the spacecraft. The considered perturbations are third-body, non-spherical earth, atmospheric drag, and solar radiation. These calculations show that every 6.33 d a burn with a ΔV of 0.0781 m s^{-1} is required.

Electrical Power System

To provide power for the satellite, a solar array is utilised. Sparkwing solar arrays are selected to be best suitable for the spacecraft, due to the experience this company has in the field and the wide variety it provides in the possible solar arrays. The selected solar array configuration consists of three segments, each with 3 panels (0.75 m by 1.1 m). During the orbital eclipse time, energy stored in batteries provides the required electricity. The primary battery provides power to the critical subsystems, regardless of the state of the secondary battery. A pack of five modules has total capacity of 222 Wh. The secondary battery provides electricity during the eclipse time and peak power demand. The selected battery has a capacity of 2246 Wh, taking into account the required lifetime and a depth of discharge of 40%. The selected battery package is selected to be the ABSL 8s52p package. To select the required type of solar cells, a trade-off is performed. AZUR Space Quadruple Junction 4G32C is the best suitable solar cell type based on the Begin of Life maximum power, electron degradation, temperature effects and area density.

Command and Data Handling

The On-Board Computer (OBC) needs to create a data package of the acquired data and provide the State of Health (SoH) of the satellite. Since this requires relatively low computing power, one centralised OBC is used. Based on the payload data, telemetry data, and commands estimations, it is estimated that a total data rate of 6.2 Mbit s^{-1} is required. The Constellation OBC is selected as the centralised OBC, after performing a trade-off based on dry mass, average power, compatibility, storage capacity, cost, and processing capacity.

Telemetry Tracking and Control

The Telemetry and Communications (TT&C) subsystem communicates the acquired data from the payload and the system health & status. This information is communicated to a ground station through a downlink. Operational commands to the system are communicated via a ground station through an uplink. Two ground stations are selected, the SvalSat Ground Station and the Trollsat Ground Station. These were selected because of their ideal location on the north- and south-pole, respectively, which matches with a polar orbit. Because of the selected ground stations, the spacecraft will transmit in the X-band, and receive in the S-band. It is determined that the signal-to-noise ratio for the uplink has a margin of 35 dB, and for the downlink there is a margin of 9.5 dB. For the transmitter, the X-Band High Rate Mission Data Transmitter (HRT-440) by General Dynamics is selected, for its data rate capabilities, mass, and power consumption. The antenna feed was chosen to be the X Band Feed from EOSOL Group. To point the antenna, the MOOG type-3 gimbal is selected for its accurate antenna pointing, mass, and power consumption. The S-band SSTRX-3000 TM/TC Unit is used as the main component for the uplink part of the subsystem. This unit integrates Binary Phase-shift Keying modulation and is a transceiver. Using an integrated duplexer for two-way communication on one antenna is enabled. MCU-110C integrated encryption/decryption module is utilised to comply with the encryption requirements for the uplink.

Attitude Determination & Control System and Navigation

The Attitude Determination & Control System (ADCS) records the attitude of the spacecraft and ensures that disturbance torques are compensated for by changing the attitude. The disturbance torques taken into account are the gravity gradient, solar radiation pressure, magnetic field, and

aerodynamic drag. Based on the required compensation, the HR12-37.5 reaction wheels are selected. Four reaction wheels are present within the satellite, of which one is redundant. To desaturate the reaction wheels, magnetic torquers are utilised. The MTI-140-2 is selected based on its magnetic moment, length, mass, and average power consumption. Three magnetic torquers are present within the system. Star trackers are used to determine the attitude with great accuracy. Three star trackers of the type Astro APS3 are present in the system. The Inertial Measurement Unit (IMU) works together with the star tracker to determine the spacecraft's attitude. Airbus/iXBlue Astrix series is deemed most suitable for the spacecraft. Three magnetometers of type Hi-Rel FGM-A-75 are present in the system, to provide the data required for the magnetic torquers. Finally, six sun sensors of type SpaceTech CESS are present as a coarse contingency attitude determination system. To determine the three-dimensional location of the spacecraft, two Global Navigation Satellite System (GNSS) receivers of type NavRIX Integral GNSS Receiver are installed into the satellite for redundancy.

Propulsion

The propulsion subsystem is responsible for maintaining the desired orbit and for the de-orbiting manoeuvre at the End of Life (EOL) of the spacecraft. Based on the requirement that no toxic propellant can be used and the minimum thrust needed for the de-orbiting manoeuvre, the B20 thruster of DawnAerospace is selected. This thruster uses propene as fuel and di-nitrogen-oxide as an oxidiser. The oxidiser tank is pressurised using the self-pressurisation properties of N_2O. For the fuel tank, a buffer tank with nitrogen is used to pressurise it. The propellant mass is determined by making use of the Tsiolkovsky equation and the determined manoeuvres required within the mission. Both tanks are spherical and made from Ti-6Al-4V, to minimise mass. To ensure the performance of the tanks, a safety factor of 1.5 is used in the stress calculations. A series of valves, filters, and trim orifices ensure proper displacement of propellant. For the regulating valve the V1E10560-10 is used, for the fill & drain valve, the V1D10855-01 is used, both from Vacco.

Thermal

With the designed thermal system, the body of the spacecraft is able to maintain a temperature of 13.7 °C to 20.0 °C. The solar array maintains a temperature between −61.9 °C to 68.5 °C. Both of these ranges are within the operating temperature of the spacecraft's components. In order to maintain these temperatures, several techniques are applied. For the solar arrays, 3M Nextel Velvet thermal paint is utilised. To maintain the main body's temperature, a combination of insulation (Rockwell MB0135-038), radiators (Quartz mirrors), heat absorbers (Almeco Tinox), and louvres are utilised.

Structures

Spacecraft structure requirements are defined based on the identified load cases, including manufacturing & assembly, transport & handling, launch, operations, and end of life. The requirements of the payload are also taken into account, as are the specific requirements of the different subsystems. A semi-monocoque constructed of sandwich panels is selected with regard to its structural efficiency and protection against debris and micrometeorites. Material options are traded-off for their specific strength, specific modulus, specific cost, fracture toughness, and manufacturability, resulting in aluminium (7075-T6) being the best material choice. To design the sandwich panels of the system, the launch loads are considered as they are the mission's maximum. Also, the eigenfrequencies of the spacecraft are estimated to assess the risk that they resonate with the vibrations of the launch vehicle are sufficiently low. Neither loads nor oscillations were found to be limiting for the design of the structure; the resistance to debris and micrometeorites, and manufacturability were limiting. To shield internal components from radiation, a Molybdenum Oxide coating is utilised.

Concept of Operations

The mission commences with the deployment of three satellites in their polar orbits. During this initial phase, all subsystems are initiated and calibrated. Once the satellites are successfully deployed, the satellites monitor the indicated zone of interest and transmit their data twice per orbit to the designated ground stations. When self-resolution is not possible, the satellites enter safe mode, and the mission operation centre will be involved. At the end of a spacecraft's lifetime, the satellite is

de-orbited by lowering the peri-centre altitude and letting it burn up as much as possible over the South Pacific Ocean Uninhabited Area. It should be evaluated if any adjustments should be made for the next set of satellites. When the final set of satellites is de-orbited, the mission is to be evaluated. It should be researched if the data has been used as anticipated. There might have been more use cases than expected, in which case it might be beneficial to extend the mission.

Reliability, Availability, Maintainability & Safety

The lifetime of each of the respective selected components exceeds the design lifetime of the satellite. Combining all the reliabilities of the components results in satellite reliability over its lifetime of 68.3%. The availability of the system has also been determined, based on the downtime of the ground stations and the payload. This resulted in a downtime of 2.3%. Physical maintenance of a satellite is difficult since it is in orbit. However, maintaining the software of the spacecraft is considered. The On-Board Computer is designed such that it is able to receive these software updates while maintaining operation. Several safety measurements are used during the design process to ensure the safety of the spacecraft and operating with it. The hull of the spacecraft is designed to absorb the impact of micrometeorites to be compliant with current standards. Also, contingency propellant is added to the system, compensating for unexpected manoeuvres. Lastly, explosive failure of the propellant tanks is prevented by the use of venting valves throughout the propulsion subsystem.

Verification & Validation

The Verification & Validation (V&V) of the system is split into two parts, the V&V of the used models, and the V&V of the spacecraft design. The V&V of the models ensures that the software used during the design process is reliable and results in a representation of reality with the expected accuracy. The V&V of the spacecraft verifies the subsystem requirements by grouping them into functional, performance, and interface requirements. For each of the groups, a verification method is identified and a verification level. Also, it is identified in which part of the design process the specific group of requirements are to be verified.

Economics

To determine the economic feasibility of the system, an economic analysis is performed. First, the cost of the system is estimated. The costs are divided between development, production, installation, and operation. This results in a total cost of 2254 mil USD FY2023 (187.8 mil USD per satellite). Next, the market and possible clients are researched. From this an expected revenue is determined and a return on investment is calculated. It can be concluded that a minimum of fourteen sales per year are required at the market average price of approximately 6.6 million USD FY2023 in order to get a positive net present benefit during the system's lifetime.

Future Development & Recommendations

After the initial design of the system, many things are required to take place before the deployment of the system. A detailed design of the system is to be designed before 2035, in which also an extensive V&V is to take place. A more detailed production plan, including certification, is to be created. During the operation of the system, it is to be evaluated where the system can improve. The data can be used to create a model of the contrails, meaning that the later satellite constellations might not be required in the same volume as currently. Also, the end-of-life plan is to be developed in more detail. This includes a detailed plan for post-mission evaluation of the performance of the system.

During the detailed design process, there are several areas that need research for possible improvements. The orbit calculations should be reiterated, to verify that the correct orbit is chosen, or if more optimal orbits can be identified. Although multiple iterations were done to ensure the compatibility of different subsystems, further iterations are to be implemented based on the updated values of the total mass and power from the current state of the design. It is also to be investigated if the use of additional measurement systems, therefore expanding the mission, could add value to the system. Another notable recommendation for further development is for the improvement of reliability performance to reduce replacement or financial risks.

Contents

List of Symbols

α	Radiation thermal absorptivity	-
β	Angle between orbit plane and geocentric position of the sun	rad
β	Shape parameter	-
ΔL	Longitudinal shift per orbit	rad
ϵ	Thermal radiation emissivity	-
η	Efficiency	-
λ	Failure rate	yr^{-1}
λ	Magnetic latitude constant	-
μ	Gravitational parameter	$\mathrm{m}^3\,\mathrm{s}^{-2}$
ν	True anomaly	rad
Ω	Right ascension of the ascending node	rad
ω	Argument of pari-apsis	rad
ω_0	First harmonic natural frequency	Hz
Φ	Solar flux	$\mathrm{W}\,\mathrm{m}^{-2}$
ρ	Atmospheric density	$\mathrm{kg}\,\mathrm{m}^{-3}$
ρ	Density	$\mathrm{kg}\,\mathrm{m}^{-3}$
σ	Axial stress	MPa
σ_B	Stefan-Boltzmann constant	$\mathrm{W}\,\mathrm{m}^{-2}\,\mathrm{K}^4$
τ	Shear stress	MPa
θ	Nadir angle deviation	rad
φ	Sun incidence angle	rad
A	Frontal surface area	m^2
a	Acceleration	$\mathrm{m}\,\mathrm{s}^{-2}$
a	Semi-major axis	m
A_i	Availability of a component	-
A_r	Ram area	m^2
A_s	Solar flux illuminated surface area	m^2
a_x	Lateral acceleration	$\mathrm{m}\,\mathrm{s}^{-2}$
a_z	Axial acceleration	$\mathrm{m}\,\mathrm{s}^{-2}$
A_{cs}	Cross sectional area	m^2
B	Bandwidth	Hz
B	Magnetic flux density	T
C	Consequence impact	-
c	Vacuum speed of light	$\mathrm{m}\,\mathrm{s}^{-1}$
C_D	Drag coefficient	-
cm	Centre of mass	m
cp_a	Centre of aerodynamic pressure	m
cp_s	Centre of solar radiation pressure	m
D	Diameter	m
D	Residual dipole	$\mathrm{A}\,\mathrm{m}^2$
E	Solar fluence	$\mathrm{J}\,\mathrm{m}^{-2}$
E	Youngs modulus	MPa
e	Eccentricity	-
E_b	Energy per bit	J
F	Force	N
f	Frequency	s^{-1}
F_x	Lateral force	N
F_z	Axial force	N
G	Antenna gain	-
g	Gravitational acceleration	$\mathrm{m}\,\mathrm{s}^{-1}$
h	Angular momentum	$\mathrm{N}\,\mathrm{m}\,\mathrm{s}$
i	Inclination angle	rad
I_sp	Specific impulse	s
I_x	Mass moment of inertia about x-axis	$\mathrm{kg}\,\mathrm{m}^2$
I_y	Mass moment of inertia about y-axis	$\mathrm{kg}\,\mathrm{m}^2$
I_z	Mass moment of inertia about z-axis	$\mathrm{kg}\,\mathrm{m}^2$
j	Amount of orbits before ground track repeats	-
J_2	Constant of the J2 effect	-
k	Amount of days before ground track repeats	d
k	Boltzmann constant	$\mathrm{J}\,\mathrm{K}^{-1}$
k_{ax}	Axial stiffness	GPa
k_{bend}	Bending stiffness	$\mathrm{GPa}\,\mathrm{m}^4$
L	Length	m
L_d	Deviation	m
L_l	Loss	-
M	Earth magnetic field strength	$\mathrm{T}\,\mathrm{m}^3$
m	Mass	m
M_y	Moment around the y axis	$\mathrm{N}\,\mathrm{m}^2$
N	Noise per bit	J
N_{orb}	Number of orbits	-
P	Power	W
P	Probability	-
P_{in}	Incoming solar flux	$\mathrm{W}\,\mathrm{m}^{-2}$
Q	Moment of area	m^4
q	Reflectance factor	-
R	Data rate	-
R	Orbit radius	m
R	Orbit radius	m
r	Reflectivity coefficient	-
r_a	Apo-centre radius	m
R_E	Earth radius	m
r_p	Peri-centre radius	m
S	Incoming thermal irradiance	$\mathrm{W}\,\mathrm{m}^{-2}$
T	Orbital period	s
T	Temperature	-
T	Torque	$\mathrm{N}\,\mathrm{m}$
t	Lifetime	yr
t	Slew time	s
T_a	Aerodynamic drag torque	$\mathrm{N}\,\mathrm{m}$
T_D	Worst case torque	$\mathrm{N}\,\mathrm{m}$
T_g	Gravitational torque	$\mathrm{N}\,\mathrm{m}$
T_m	Magnetic field torque	$\mathrm{N}\,\mathrm{m}$
T_S	Solar radiation pressure torque	$\mathrm{N}\,\mathrm{m}$
V	Velocity	$\mathrm{m}\,\mathrm{s}^{-2}$
x	Normal distance from the yz plane	m

Abbreviations

ADCS Attitude Determination & Control System
ADS-B Automatic Dependent Surveillance–Broadcast
ADS-C Automatic Dependent Surveillance–Contract
ANSP Air Navigation Service Provider
BOL Beginning of Life
BPSK Binary Phase-shift Keying
C&DH Command & Data Handling
CAN Controller Area Network
CCSDS Consultative Committee for Space Data Systems
CESS Coarse Earth Sun Sensor
CO_2 Carbon Dioxide
COBC Constellation On Board Computer
CoG Center of Gravity
ConOps Concept of Operations
COTS Commercial Off-The-Shelf
DOD Depth of Discharge
DSE Design Synthesis Exercises
EC European Commission
ECMWF European Centre for Medium-Range Weather Forecasts
EEA European Environment Agency
EIRP Effective Isotropic Radiated Power
EM Engineering Model
EOL End of Life
EPS Electrical Power System
ESA European Space Agency
EU European Union
FABEC Functional Airspace Block
FIT Failures in Time
FM Flying Model
FoV Field of View
FSS Fine Sun Sensor
GEO Geostationary Earth Orbit
GLONASS Global'naya Navigatsionnaya Sputnikovaya Sistema
GN&C Guidance, Navigation & Control
GNSS Global Navigation Satellite System
GPS Global Positioning System
H_2O Water
HEO Highly Elliptical Orbit
HF High Frequency
IASI Infrared Atmospheric Sounding Interferometer
IASI-NG Infrared Atmospheric Sounding Interferometer - Next Generation
IMU Inertial Measurement Unit
IPMS Infrared Pollution Monitoring System
ISO International Standards Organization
ITU International Telecommunications Union
LASER Light Amplification by Stimulated Emission of Radiation
LEO Low Earth Orbit
LT Lifetime
MEO Medium Earth Orbit
MIB Minimum Impulse Bit
MIMU Miniature Inertial Measurement Unit
MLI Multi-Layered Insulation
MMOI Mass Moment of Inertia
MNS Mission Need Statement
MSI Multi-Spectral Imager
MTBF Mean Time Between Failures
MTTF Mean Time To Failure
NASA National Aeronautics and Space Administration
NLR Royal Netherlands Aerospace Centre
NO_x Nitrous Oxides
NOMS NearSpace Operation Management System
OBC On-Board Computer
OS Operating System
PCI Peripheral Component Interconnnect
POS Project Objective Statement
QM Qualification Model
RAMS Reliability, Availability, Maintainability, and Safety
S/C Spacecraft
SATCOM Satellite Communications
SBC Single-Board Computer
SF Safety Factor
SHF Super High Frequency
SHT Supersonic & Hypersonic Transport
SLOC Source Lines of Code
SoH State of Health
SRP Solar Radiation Pressure
STK Systems ToolKit
STM Structural and Thermal Model
STM Space Traffic Management
STR Spacecraft Technical Risk
SWOT Strengths, Weaknesses, Opportunities & Threats
TCS Thermal Control System
TRL Technology Readiness Level
TT&C Telemetry and Communications
TUDAT TU Delft Astrodynamics Toolbox
UHF Ultra High Frequency
UTLS Upper Troposphere, Lower Stratosphere
V&V Verification & Validation
VHF Very High Frequency
WMO World Meteorological Organisation

1 NearSpace Operation Management System

In the coming years the number of operations in NearSpace (FL 660 to 100 km altitude) is expected to increase rapidly. This creates the need for a NearSpace Operation Management System (NOMS) to manage and control these operations in a safe and efficient manner and integrate with existing Air- and Space-Traffic Management, the need for which is described further in Section 1.1. The options which were considered for this design and the selected concept are described in Section 1.2. This concept has been verified and validated with respect to the needs and expectations of the main stakeholder Royal Netherlands Aerospace Centre (NLR) but could be strengthened further with respect to some limitations, which are explored in Section 1.3.

From these limitations, it is decided that the system would benefit most from the integration of a novel observational system for greenhouse-gas emissions produced by air-breathing vehicles in NearSpace. This is chosen to enhance the sustainability of the NOMS and its emission-based fee system. The market analysis for this case determines that there is a real need for this solution, in the context of the already designed NOMS, and can be found in Section 1.4. Finally, in Section 1.5, the project development of the emission monitoring system of the NOMS is defined.

1.1. Market Analysis of NearSpace Operation Management System

With the growing number of users in NearSpace comes increased congestion and thus higher collision risk and emissions. Given the expected total value of missions in NearSpace over Europe by 2035 is >B€200 /year (and growing), a clear need, demand, and willingness to pay for a traffic management system can be seen.

Having identified this, a low-cost, highly feasible, safe, and sustainable NOMS system was detailed which met future needs by managing NearSpace traffic [1]. This introduced a fee structure as a means to pay off the initialisation and operation costs of the safety system, and by which legislators may directly enforce societal sustainability aims on the users of NearSpace. From preliminary estimates, this NOMS system would generate between M€50 and M€250 of gross profit throughout its lifetime. However, as a traffic management system in The Netherlands, it needs to have a neutral net present value[1].

The NOMS system would achieve this by charging adaptive rates between 0.15% and 4.8% of a user's mission value for use of the system. This rate would be dependent on the user's impact; the space and time which is allocated to them and their environmental footprint. It may not be preferred to reduce the fees to maintain a neutral net present value as this would reduce the effectiveness of the sustainability incentive. Instead, it may be preferred to reinvest in a system for the improvement of the NOMS, and its capabilities while retaining similar fee rates.

1.2. Summary of Trade-Off

To design the NOMS, the system was divided into six elements. Strategic Concept of Operations (ConOps), tactical ConOps, cooperative surveillance, uncooperative surveillance, communications, and system architecture [1]. After the identification of all possible design options for each element of the system, the unfeasible design options were removed. The resulting design options, considered in the trade-offs, are shown in Table 1.1.

[1]Meaning no monetary loss or profit

Table 1.1: Design Options Considered in the Trade-Offs for the NOMS

(a) Design Options for Strategic ConOps, Tactical ConOps, and Cooperative Surveillance

Option	Description
Strategic ConOps	
CONS-1	Full flight plan using 4D trajectories
CONS-2	Full flight plan using voxels
CONS-3	Partial flight plan using 4D trajectories
CONS-4	Partial flight plan using voxels
Tactical ConOps	
CONT-1	Moderated conversation-centric network where operators communicate with each other using data and voice.
CONT-2	Centralized fully-human conversation-centric communication where operators communicate with the central station using data and voice.
CONT-3	Centralized semi-automated rule-centric communication where the central station communicates with the vehicles using data only.
CONT-4	Centralized semi-automated rule-centric communication where the central station communicates with the operators using data and voice.
Cooperative Surveillance	
SURC-1	ADS-B
SURC-2	ADS-C
SURC-3	Secondary Radar

(b) Design Options for Uncooperative Surveillance, Communications, and System Architecture

Option	Description
Unooperative Surveillance	
SURU-1	Search Radar
SURU-2	Modelling
SURU-3	Assisted Tracking Radar
Communications	
COMM-1	SHF
COMM-2	UHF
COMM-3	VHF
COMM-4	HF
COMM-5	LASER
System Architecture	
PHAR-1	Renting the usage of a space-based constellation for ADS-B and communication, without the use of focused radar to assist modelling.
PHAR-2	Renting the usage of a space-based constellation for ADS-B and communication, with the creation of an array of focused radar stations to assist modelling.
PHAR-3	Building a space-based constellation for ADS-B and communication, without the use of focused radar stations to assist modelling.
PHAR-4	Building a space-based constellation for ADS-B and communication, with the creation of an array of focused radar stations to assist modelling.

With the design options shown in Table 1.1, trade-offs were performed. To ensure the validity of these decisions, a sensitivity analysis was also performed for each of the trade-offs. A summary of the results is shown in Table 1.2.

Table 1.2: Trade-Off Summary of the Elements of NOMS

(a) Trade-Off Summary of the Strategic ConOps, Tactical ConOps, and Cooperative Surveillance

Trade-Off	Concept	Weighted total
Strategic ConOps	CONS-1	286
	CONS-2	288
	CONS-3	**347**
	CONS-4	339
Tactical ConOps	CONT-1	231
	CONT-2	261
	CONT-3	329
	CONT-4	**360**
Cooperative Surveillance	**SURC-1**	**410**
	SURC-2	392
	SURC-3	367

(b) Trade-Off Summary of the Uncooperative Surveillance, Communications, and System Architecture

Trade-Off	Concept	Weighted total
Uncooperative Surveillance	SURU-1	329
	SURU-2	384
	SURU-3	**390**
Communication	COMM-1	431
	COMM-2	**448**
	COMM-3	317
	COMM-4	154
	COMM-5	314
System Architecture	**PHAR-1**	**342**
	PHAR-2	276
	PHAR-3	265
	PHAR-4	246

The best design concepts have the highest weighted total and are shown in bold. To clarify the outcomes, they are detailed fully in Table 1.3.

Table 1.3: Resulting Design Concepts from the Trade-off process of Taking Control

Function	Description
Strategic ConOps	Inform the user of the airspace availability. Users are allowed to request partial flight plans, where certain inputs (like complete trajectories or times) may be missing, or deviation is accepted. The system is then given the authority to decide this remaining direction as desired. 4D trajectories are used for this.
Tactical ConOps	Use a centralized semi-automated system with rule-centric communication to the operator. Rules are the primary means of deciding the actions that need to be conducted by users, with conversation only as a backup of edge cases. This allows for automation to operate the system while under rule-based decisions. Communication is sent to the vehicles directly, and it is the responsibility of the user to process and respond through off-vehicle forwarding, or directly. Both data and voice communication are used for communication.
Cooperative surveillance	Making use of an existing ADS-B system. Uses the principle that the vehicle broadcasts its location and velocity at a predetermined time interval.
Uncooperative surveillance	Exclusive use of modelling and flight plans to indicate the expected position of all objects. Management is conducted using exclusively these predictions, and no active means are employed. Data of STM is used to predict the trajectory of space debris.
Communi-cations	Use of SATCOM making operating on a UHF and SHF (e.g., L-Band) band for communi-cations. Optimally an already assigned band for aerospace use.

As can be seen, the resulting system comprises a connection and integration of existing systems and techniques. This gives the sum of the NOMS's parts a high TRL level, low development cost and time, and high feasibility. The lack of significant new hardware makes this system environmentally sustainable. With the components having high reliability, the downtime is expected to be low from the standpoint of the system in isolation. However, the leasing of bandwidth from service providers does present uncertainty in the corporate governance of the providers, given the long lifetime of the system. The top-level system architecture is described in Figure 1.1 for completeness.

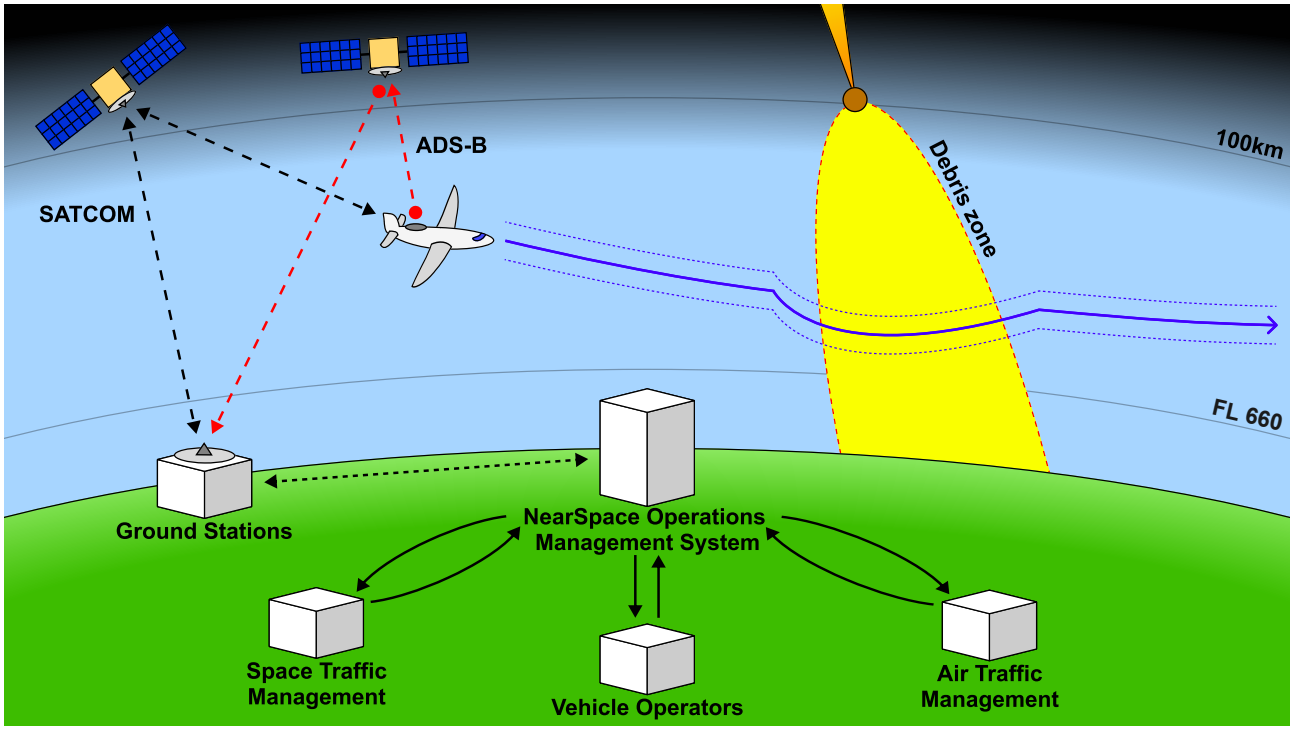

Figure 1.1: System Architecture Diagram of the Designed NearSpace Operation Management System

1.3. Analysis of Limitations

In order to identify the possible improvements to be made to the NOMS in the second full design iteration, the operational limitations faced by the system are identified, before being analysed in order to identify solutions which represent justified improvements to the NOMS.

1.3.1. Identification of Limitations

After the NOMS concept was selected, a review was undertaken with the tutors of the TU Delft and NLR. From these reviews, an analysis of the system placed in the context of current management systems and sustainability along with some of the greatest risks attributed to the system is carried out. As a result of this, some limitations or areas in which the system could be complemented are derived and described below.

- **Altitude-controlled balloons**: While 'simple' balloons have a short lifetime given their altitude increases consistently until they burst, altitude-controlled balloons can have a much longer lifetime (since they may be controlled to stay within their serviceable altitude range). As such, the area of spatial uncertainty at the time of release is much larger than the uncontrolled counterparts. Without accounting for this use-case in the ConOps, altitude-controlled balloons will cause significant issues for the strategic planning of NearSpace.
- **Small and medium space debris**: The NOMS system relies on catalogue-based models for space debris, which are derived from aperiodic observations predominantly by ground-based optical systems. This results in the catalogues not containing debris which is below a threshold dimension, while it is neither safe to assume that the small and medium debris burns up upon reentry, nor that it is too small to cause damage to a user, too little is known about this kind of debris to quantitatively assess the risk it poses.
- **Vehicles designed to reenter & disintegrate**: The NOMS ConOps's use of catalogue models for space debris means that; due to uncertainties in the exact point of atmospheric reentry, an exclusion volume of ~1000x3x80 km [2] must be projected into NearSpace for a matter of hours, in order to ensure the safety of NearSpace users. This results in a sufficiently low service reduction of ~ 0.02% based on current rates of reentry. With that said the occupation of Low Earth Orbit (LEO) and Medium Earth Orbit (MEO) regimes has increased greatly with the

introduction of mega-constellations (e.g. Starlink, OneWeb), meaning that the rate of reentering debris is equally likely to increase. This may result in an unacceptable service reduction due to debris in the current operational concept. Further to this, the catalogue is generated primarily by military-associated organisations; with the associated risk that the catalogue provider selectively omits some debris for security purposes.

- **Emissions and contrails**: The fee model for users is based on an estimation of the impact of the users on the NearSpace environment. A better understanding of the impacts of users on the environment is only possible with the development of a complementary system, which would enable dynamic re-routing and the implementation of more informed fee strategies, this is especially important considering the premature nature of many of the industries planning to expand in NearSpace. This limitation takes on further importance when it is considered that NearSpace has remained relatively untouched by human emissions, and the impact of new user groups such as super-sonic transport is unknown. The species of gasses is known but the heating impact on the environment due to these gasses (emitted for the first time at this altitude and volume) is concerning, which will require data on the amount and presence of the emissions to quantify the radiative forcing.
- **Off-Nominal use cases**: For the purposes of making the NOMS's preliminary design feasible within the limitations of time and the available engineers, only 'nominal' cases were considered. This entails the assumptions that:
  - All users operate without faults
  - All users are communicative and cooperative within the bounds of their nominal capabilities to do so
  - The environment is nominal (International Standard Atmosphere)
  - Weather and debris reentry events occur at a constant rate in line with current statistics

  Naturally, any of the above assumptions generates a list of operational cases which are excluded from consideration - e.g. stealth vehicles, vehicles with failed propulsion, debris which is not known with current statistical models, or extreme weather.
- **Service providers**: In utilising data transmission services from existing SATCOM providers, the financial and technical feasibility of the NOMS is greatly improved. With that said, it introduces a dependency of the NOMS on the service providers. Should the service provider cease to exist, change ownership, or choose to no longer provide the service; the NOMS will either cease to be able to function, or have to invest time, energy, and finances into arranging a new service level agreement with a new provider.
- **Weather**: Current weather forecasting for NearSpace is minimal and has low accuracy [3]. This results in increasing the uncertainty for high altitude balloon prediction, which makes the spatial utilisation of NearSpace less efficient with the NOMS and increased risk for users who enter the space uninformed on the intricacies of the local weather systems.

1.3.2. Description of Solutions

Following the identification of limitations of the existing solution, a table can be formulated which describes the expected actions which may be required to resolve the limitation. This action may range from a design adjustment to an entirely new 'sub-mission', or 'sub-project', and is characterised in Table 1.4.

Table 1.4: Solutions to the Limitations of the Designed NearSpace Operation Management System

Limitation	Solution	Implementable
Altitude-controlled Balloons	Further development of the NOMS ConOps to improve the efficiency of the strategic element into a dynamic process or improve the weather forecasting in NearSpace	✓As a protocol development or as a collaboration with Meteorologists

Small and medium space debris	Improvement of modelling and catalogue to reduce the volume of unknown debris, implementation of active tracking of objects entering NearSpace in the target region	✓As an international collaboration with agencies that already carry out observations and modelling, the addition of specific observation hardware for Europe
Vehicles designed to reenter & disintegrate	Improvement of modelling to reduce uncertainty induced by the moment of reentry to minimise the service reduction	✓As an international collaboration with agencies that already carry out observations and modelling
Emissions and contrails	The introduction of a space-based emissions observation system to complement the existing sample-model system	✓As a new (sub)system of the NOMS, likely space-based
Off-nominal use cases	Human-in-the-loop simulation of the designed NOMS to test edge cases and off-nominal situations, followed by a 2nd design iteration	✓As a design iteration of the NOMS, likely focussed on protocol and ConOps
Service providers	Multiple service level agreements with multiple partners, planning for inoperability of one provider as a technical risk	✓As a design consideration for the detailed design of the NOMS
Weather	Improvement of weather observation capabilities and modelling in collaboration with meteorological organisations[3]	✓As a new system, likely space-based, with collaboration

As can be seen, all of the solutions are implementable, given an unlimited number of 'engineering hours', and in some cases with additional resources. Following a preliminary analysis of the costs, challenges, benefits, and feasibility of each implementation; Taking Control identifies the emissions and contrails sensing as the solution which offers the greatest improvement to the NOMS in terms of its sustainability goals, the additional market for the product of the sensing, and the scale of the design task with relation to the number of engineering hours available to Team Taking Control.

The extensive analysis of this solution follows in Section 1.4, and describes the need for this solution not only in the context of the already designed NOMS but in the broader societal context too. Alongside this, it is identified that the radiative forcing effects which would be necessary to measure in order to assess emissions could also support meteorologists in improving NearSpace weather models, further aiding in the solution of the 'Weather' and 'Altitude-controlled Balloons' limitations.

1.4. Market Analysis of Contrail Sensing

One large environmental issue in NearSpace is the emission of water vapour (as a greenhouse gas, and as an ozone-depleting agent) into the stratosphere, alongside Nitrous Oxides (NO_x) and Carbon Dioxide (CO_2). Water vapour and ice result from the combustion of hydrogen-containing fuels in air [4]. This creates contrails which are expected to disperse slowly and remain in the lower NearSpace region (Upper Troposphere, Lower Stratosphere (UTLS)) for many years [5]. Preliminary estimates have found that 500 Boeing Type Supersonic Transport Aircraft, flying 8 hours per day for two years would triple the naturally occurring inventory of stratospheric pollutants. In order to monitor and make informed mitigation strategies on the effects of this growing market, improved data on the accumulation of greenhouse gases in the stratosphere is needed.

While the emissions of other NearSpace users are known, the air-breathing market (for both space planes and hypersonic transport aircraft) is in the least mature phase. Therefore the least is known about the effects of their use on the UTLS environment. They are also the most manoeuvrable user group and therefore present the greatest opportunity to mitigate the impact on a local and global scale. Research at an early stage may enable preventative rather than reactive sustainability actions. In line with this, the topic of UTLS emissions has garnered negative speculation from the European Environment Agency (EEA), designating the possibility that European Union (EU) investment in the

observation and management of such emissions is likely [6].

An improved observational capacity in terms of spatial and temporal resolution, targeted at the routes of airbreathing UTLS users will enable more accurate assignment of fees. Beyond this period, the system could be used as a deterrent system, where the expected emissions over a route are modelled and compared to what can be observed. This would be implemented when more is known about the most impactful flight paths, to ensure that the impact on NearSpace is minimised and those responsible are held accountable. A further design may be required to fully implement an operable strategy for policing. This can be in hybrid with ground testing and governmental agencies informed by the sampled data. It is important to note that this does not mean the system must be constantly observing the whole area of interest since intermittent observation would still prove to be a more functional deterrent than any existing solution.

1.4.1. Existing and Similar Markets

Existing solutions for the analysis of stratospheric greenhouse gases in the UTLS are carried out in a method of reanalysis. Taking sounding measurements with the use of weather balloons and small satellite trains local point data sources can be compiled to create and update large-resolution models of water vapour in this region. Improved resolution (both temporally and spatially) is required in order to achieve a more observational approach; enabling the attribution of specific peaks of vapour content to the emissions of specific user groups, routes, and missions[7]. Studies by the World Meteorological Organisation have found that the models used for the prediction of accumulation of water and pollutants in the UTLS are less accurate than previously thought. As such there would be an adjacent academic market for data generated from a higher-resolution, space-based atmospheric gas detection mission.

Existing satellite constellations such as A- and C-trains[2] provide meteorological data observations with high spatial resolution, but an insufficient temporal resolution or swath width to be effective for the purposes of assisting NOMS. Conversely, the MetOp missions[3] have a sufficient temporal resolution, though the instrument still operates on a sounding basis, leaving gaps in space between samples. In addition, neither focuses on higher than the troposphere. The purpose of the existing constellations is to support the reanalysis models of water vapour, rather than to observe directly. Improvements in either temporal resolution or ground track aspects over MetOp or the A-/C-Trains would be market-leading for meteorological applications investigating more dynamic, short-term, wider-spanning effects, representing an additional market to the NOMS application.

1.4.2. Stakeholders

Besides the stakeholders of the NOMS which have been identified [1], a number of additional stakeholders are identified. Also, a number of the existing stakeholders have redefined interest and power over the outcome of the space-based observation. As such, the stakeholders are presented here in Figure 1.2, with their area of interest and justification detailed in Table 1.5. Of note is the newfound interest of the European Environment Agency and the World Meteorological Organisation and the reduced power/interest of Air Navigation Service Providers and defence departments.

Table 1.5: Table of Stakeholder Groups for the Taking Control Space-Element and their Justifications

Stakeholder Involvement	Individual Stakeholders	Justification
Development	TU Delft and NLR	Define the mission need and requirements
Production	System Manufacturers	Define requirements related to producibility
Implementation/Launch	Launch System Provider, and EASA	Define the launch and implementation requirements, possibly including sizes and peak loads

[2]URL: svs.gsfc.nasa.gov [accessed: 02/06/2023]
[3]URL: www.esa.int/metop [accessed: 08/06/2023]

Operation	ESA, Space Agencies, ITU, and ANSPs	Define the requirements on the operation of the system
Outside Interest	National Governments, EC, EEA, WMO, FABEC, Defence Departments, and General Public	Related to the outcome/output of the system, defining expectations and wishes

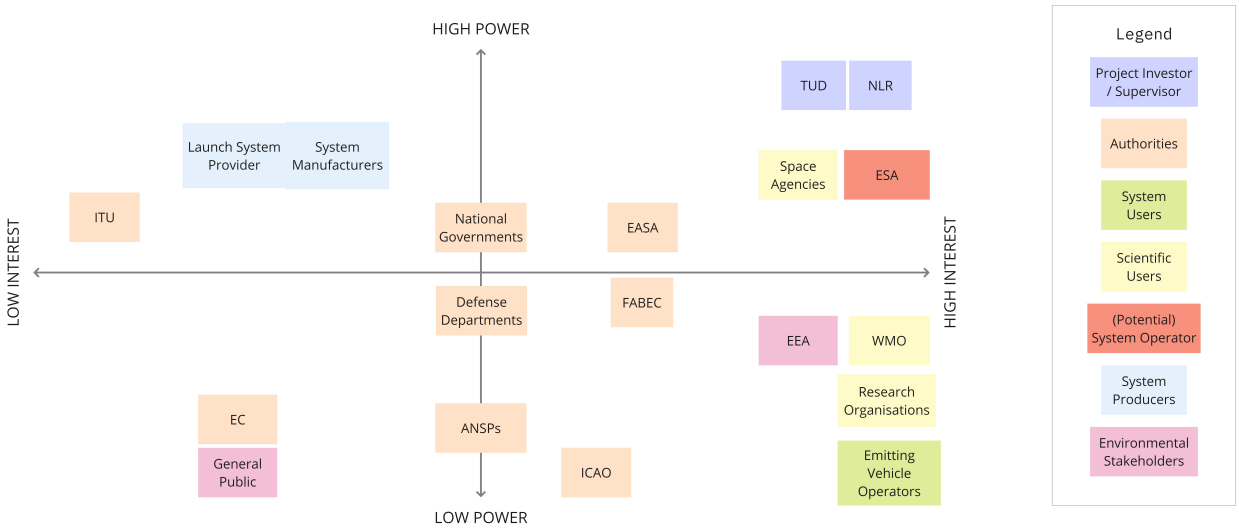

Figure 1.2: Stakeholder Map for the Space-Based Atmospheric Emissions Sensing Mission

1.4.3. Strengths, Weaknesses, Opportunities & Threats

A Strengths, Weaknesses, Opportunities & Threats analysis is performed to identify the SWOT of the system. This analysis is shown in Figure 1.3. The main strengths of the system are the high temporal and spatial resolution when compared to similar systems. As well as the benefit of added accuracy because of observation over modelling. There are two identified weaknesses of this space-based system, the difficulty with maintaining the physical parts of the system, as well as the difficulty of upgrading the system, which comes with high costs. Four opportunities have been identified for use cases of the system. There are two identified threats to the system: the possibility of collision with space debris and the change in political climate which could eliminate the support of the project.

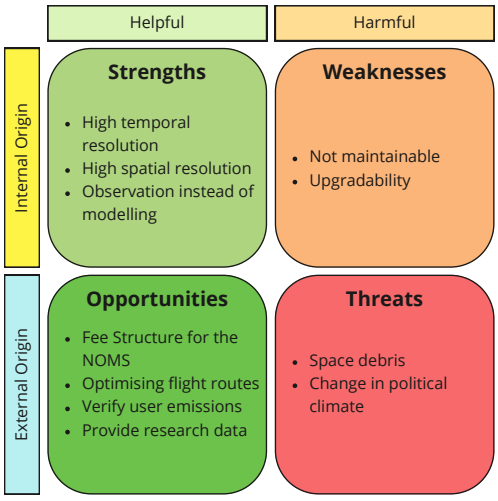

Figure 1.3: SWOT Analysis of the emissions monitoring segment of the Taking Control Project

Given that the need for the system is not purely financial, the 'return on investment' cannot be directly, completely quantified, rather a more subjective view of the system in the context of its impact on the

sustainability of society is necessary. In order to achieve the greatest social and environmental 'return on investment', the system should achieve as many of the derived opportunities as possible.

1.4.4. Target Cost for the System

The system should ideally cost less than the expected gross profits of the preliminarily designed NOMS mission, this would drive a target cost of the new observing segment to be <M€250. That said, there are opportunities to marketise the data from the emissions observing mission further, and a reasonable interest from the EEA in the field. Therefore, while <M€250 is an aim for the mission, <M€500 has been agreed as the absolute cost requirement with the key stakeholders in order to have a net present value [8]; it is assumed that public funding could be procured for the additional M€250 for the mission where required, especially when the environmental and social benefit is taken into account.

It is important to note that the success of the system (reducing the emissions of users), paradoxically, reduces the budget for the system (the fees paid by the users). This means that the tolerance of the NOMS of emissions should decrease over time, meaning that at the end of life, the same or higher fees are being applied for lower emissions. In this way, the system may remain functionally profitable for the lifetime, and achieve increasingly strong targets for sustainability in line with expected social advancements over the lifetime.

1.5. Project Definition

To start the development of the contrail sensing system, which will now be referred to as the Infrared Pollution Monitoring System (IPMS), as an element of the NOMS super-system, the aims and planning of this design process need to be defined. The aims of the IPMS and the project are given in Section 1.5.1, before the organisational approach to achieving the project aims and objectives are described in Section 1.5.2.

1.5.1. Project Aims

The Mission Need Statement (MNS) describes the purpose to be fulfilled by the end product, while the Project Objective Statement (POS) outlines the boundaries of expectations and limitations to be considered in the execution of the project. These statements for this part of the project are as follows:

Mission Need Statement:*'Monitor the radiative forcing effects and dynamic evolution of exhaust trails created by air-breathing vehicles in NearSpace supporting a more sustainable NearSpace Operation Management System.'*

Project Objective Statement:*'Design a space-based platform that is capable of monitoring the radiative forcing effects and dynamic evolution of exhaust trails from air-breathing vehicles in NearSpace, in 12 working days by ten students'*

When stating that the radiative forcing of exhaust trails should be monitored, substance concentration and heat levels are to be measured at different altitudes in NearSpace. Moreover, radiation profiles of the atmosphere should be created. This allows for better reanalysis models of water vapour and for potential weather forecasts in the stratosphere. Monitoring the dynamic evolution of exhaust trails includes the measurements of the wake effects of space planes and hypersonic transport aircraft and the wind levels. This creates the need for a sufficient temporal resolution of the exhaust trails measurements.

1.5.2. Project Planning

To achieve the POS in the project time allocated to this final part of the DSE, a comprehensive plan was created in the Midterm report [1]. Where the organisation of the team is discussed and the workflow for this phase is presented in the form of a workflow diagram, work breakdown structure and project Gantt chart. From this planning, it became evident that another simplified baseline for the new project was necessary. This is presented in Chapter 2 and 3. Afterwards, a design of the system is created in Chapter 5 to 16, which includes a detailed design of all the subsystems in Chapter 9 to 14. Then, the non-technical elements of the system are described and analysed in Chapter 17 to 23.

2 Sustainable Development Strategy

With the aims of the IPMS strongly rooted in improving the sustainability of NOMS users, it is essential that the design, development, and operation of the IPMS achieves the sustainable mission of the NOMS while also being as sustainable as possible (such that the negative impact of the IPMS is significantly less than the reduction of the negative impact of the users). This requires a sustainable development strategy which has been continuously applied throughout the Taking Control project and which places requirements and expectations on the IPMS design; described in section 2.1 and 2.2 respectively.

2.1. Sustainability Requirements

There are 2 elements to the sustainability of the NOMS. Firstly, is the need of the system to make the users of NearSpace operate more sustainably, and secondly is the need for the system itself to be sustainable. Both of these elements impose requirements on the IPMS, with the top level objective: 'the system shall make users of NearSpace operate more sustainable' being driving for the implementation of the IPMS with NOMS in the first instance.

2.1.1. The Sustainability Mission

From the top level objective on the NOMS: 'the system shall make users of NearSpace operate more sustainable', a flow down of requirements can be carried out in which 3 groups of mission requirements are derived. These are: 'the mission shall improve the environmental/economic/social sustainability of NearSpace users'; and have the requirement IDs 'SUS-ENV', 'SUS-ECO', and 'SUS-SOC' respectively. The constituent requirements are summarised in Table 2.1; rather than being requirements on the IPMS, they are used to derive the requirements on the IPMS within it's NOMS context.

Table 2.1: Sustainability Mission Requirements of the NearSpace Operation Management System Mission

ID	Requirement	Justification
SUS-ENV-01	The NOMS shall acquire data on the dispersion of CO_2, H_2O, NO_x, and CH_4 in NearSpace with a better spatial resolution than MetOp-SG	Improved Quantification the range of environmental impact of user groups
SUS-ENV-02	The NOMS shall use data to justify emissions variable fees	Incentify reduction of the environmental impact of users
SUS-ENV-03	The NOMS shall use data to route users to minimise emissions peaks	Reduce the environmental impact of operations
SUS-ENV-04	The NOMS shall provide summations of data per vehicle class, route, and time to legislators and regulators	Hold users to account for their environmental impact
SUS-ECO-01	The NOMS shall vary fees based on the economic value of the user's mission	Enable equitable use of NearSpace
SUS-ECO-02	The NOMS shall fine users for breaking emissions laws, when legal limits are in place	Ensure financial accountability of users
SUS-SOC-01	The NOMS shall make all data available to researchers	Improve knowledge about the impacts of NearSpace use
SUS-SOC-02	The NOMS shall make all data available to meteorological institutions	Improve knowledge about the weather in NearSpace

2.1.2. Sustainability of the Infrared Pollution Monitoring System

A three-pronged approach to sustainability is taken throughout the design of the NOMS and is already described in [9] and [1]. This concerns maximising sustainability of the system itself with regards to social, economic, and environmental aspects; in all stages of the lifetime of the system, inclusive of the development and End of Life (EOL). A number of system requirements for the NOMS are derived from this sustainability strategy in [1], and are used to derive sustainability requirements on the IPMS space segment ('SUS-SPA') in Table 2.2 below.

Table 2.2: Sustainability Requirements of the Infrared Pollution Monitoring System Space Segment

ID	Requirement	Source [1]
SUS-SPA-01	The space segment shall only be implemented with approval of all states whose Nearspace will be monitored	SUS-SYS-1/2
SUS-SPA-02	The space segment shall not be able to make observations at locations that are not pre-determined and communicated	SUS-SYS-2
SUS-SPA-03	The space segment shall only utilise materials or components which are supplied with an independently verified guarantee of fair working conditions	SUS-SYS-3
SUS-SPA-04	The space segment shall have an End of Life plan in which no hardware remains in LEO or GEO orbit	SUS-SYS-4
SUS-SPA-05	The space segment shall have an End of Life plan in which the expected emissions due to re-entry are < 20 t $CO_{2(eq)}$ equivalent	SUS-SYS-4
SUS-SPA-06	The space segment shall have 50 MB of data budget per year to receive software updates	SUS-SYS-8
SUS-SPA-07	The space segment shall be able to carry out up to 50 MB of software upgrades per year without causing a downtime >0.01%	SUS-SYS-8
SUS-SPA-08	The satellites of the space segment shall be replaceable	SUS-SYS-9
SUS-SPA-09	The space segment shall use only standardised connection methods	SUS-SYS-10
SUS-SPA-10	The space segment shall only source components and materials from companies who commit to having integrated or being in the process of integrating the United Nations Voluntary Sustainability Standards [1]	SUS-SYS-11
SUS-SPA-11	The space segment shall have net zero $CO_{2(eq)}$ emissions balance during operation	SUS-SYS-12
SUS-SPA-12	The space segment shall have net zero $CO_{2(eq)}$ emissions balance during manufacturing	SUS-SYS-13
SUS-SPA-13	The space segment shall not utilise toxic or potentially toxic fuels	
SUS-SPA-14	The space segment shall not utilise radioactive materials	

2.2. Sustainability Expectations

Alongside the above hard requirements, a number of expectations are also made for the final product:

- Minimise the economic risk of the space segment
- Minimise the societal negative impacts of the space segment
- Minimise the environmental negative impacts of the space segment

Notably conservationist ethics are applied here, rather than maximising the positive impacts (possibly at the cost of increased negative impacts in other areas), the 'corporate social responsibility' mandate of the European Commission (EC) expresses that this is the expected modus operandi for European organisations and projects in their decision making processes[2]. To achieve this, every decision on the space segment is weighed with its impacts (positive and negative), on social, economic, and environmental sustainability, prioritising minimal negatives.

[1]URL: www.unctad.org [accessed: 05/06/2023]
[2]URL: ec.europa.eu [accessed: 05/06/2023]

3 Requirements

To enact the subsystem of the NOMS discussed in Section 1.4, and the sustainability mission requirements set in Section 2.1, a list of mission and system requirements on the IPMS mission needs to be set up. Alongside the sustainability, there is functionality required for the space segment to function as a space segment. The mission requirements are stated in Section 3.1, followed by the system requirements in Section 3.2.

3.1. Mission Requirements

From the sustainability mission described in Section 2.1, and the need for a functional space segment, a number of mission requirements are derived. First of all, due to the NOMS having to be financially sustainable, requirements are set with respect to the business case. This includes that the system shall be able to provide data with a higher resolution than already existing meteorological instruments in order to sell it. It should also cover the up-and-coming northern transatlantic supersonic commute flight routes and be able to distribute this data[1]. Due to the system being part of the NOMS, information about trajectories and vehicles is known, and thus, measuring the scheduled flights is sufficient to monitor the emissions. Additionally, due to the almost absent vertical winds, there is not much dispersion of the emissions between 'flight levels', and thus coverage at least twice per day of the same area is sufficient to track the propagation and give semi-daily weather reports to the NOMS users [10]. Finally, as the mission is part of the NOMS operation, it should also be performed during that operational lifetime, which imposes more requirements.

Each mission, system and subsystem requirement is labelled according to the keys used in Table 3.1. Next to an identifier, the source from which each requirement is derived is reported for traceability. This can be seen for the mission requirements in Table 3.2.

Table 3.1: Groups of Categories for the Requirements.

Group	Key	Group	Key
Mission	MIS	Command & Data Handling	CDH
System	SYS	Telemetry and Communications	TTC
Subsystem	SUB	Attitude Determination & Control System	ADC
Functional	FUN	Thermal Control System	TCS
Operational	OPS	Electrical Power System	EPS
Constraints	CON	Navigation	NAV
Payload	PLD	Propulsion	PRP
Structure	STR		

Table 3.2: Mission Requirements.

ID	Requirement	Source
MIS-FUN-01	The mission shall provide data on the dispersion of emissions from air-breathing vehicles in NearSpace	SUS-ENV-01
MIS-OPS-01	The mission shall have an operational lifetime of at least 30 years	SUS-ENV-02, SUS-ENV-03
MIS-OPS-02	The mission shall have an outage time of at most 0.01% during its operational lifetime	SUS-ENV-04
MIS-CON-01	The mission shall reach initial conditions in 2035	SUS-ENV-03
MIS-CON-02	The mission shall reach final conditions in 2065	SUS-ENV-04

[1]URL: www.boomsupersonic.com [accessed: 21/06/2023]

3.2. System Requirements

From the mission requirements and the NOMS limitation, a set of requirements can be generated for a possible system which will fulfil the mission objective and requirements. This system is designed based on the requirements listed in Table 3.3. This list follows the same setup as described in Section 3.1. Moreover, when designing each of the subsystems in detail, the system requirements are developed into one level more detailed. These is presented in each of their relevant chapters.

Table 3.3: System Requirements

ID	Requirement	Source
SYS-FUN-01	The system shall be able to observe emissions over Supersonic & Hypersonic Transport (SHT) flight paths	SUS-ENV-04
SYS-FUN-02	The system shall be able to observe the change in emissions over SHT flight paths	SUS-ENV-01
SYS-FUN-03	The system shall be able to monitor within an altitude range of at least FL 660 to 100 km	SUS-ENV-04
SYS-FUN-04	The system shall be able to observe emissions in the same area at least twice per 24 hours	SUS-ENV-01, SUS-ENV-02
SYS-FUN-05	The system shall provide coverage from 40° to 60° latitude	SUS-ENV-03
SYS-FUN-06	The system shall have a minimum altitude of 100 km above the coverage area	SYS-FUN-03
SYS-FUN-07	The system shall have a maximum altitude of 800 km above the coverage area	SUS-ENV-01
SYS-OPS-01	The satellite shall have a reliability of 0.875 after its lifetime	Preliminary Weibull fit[2]
SYS-OPS-02	The system shall be able to withstand the radiation encountered during its operational lifetime	Payload[11]
SYS-OPS-03	The system shall be able to withstand the temperatures encountered during its operational lifetime	Payload[11]
SYS-OPS-04	The system shall be able to transmit the payload data to a ground station	SUS-SOC-01, SUS-SOC-02
SYS-OPS-05	The system shall be able to store payload data before transmitting it to a ground station	SUS-SOC-01, SUS-SOC-02
SYS-OPS-06	The system shall be able to transmit data to a ground station at least every orbit	SUS-SOC-02, SUS-ENV-02
SYS-OPS-07	The data transmitted to a ground station shall contain water vapour trail data from air-breathing vehicles	SUS-ECO-01
SYS-OPS-08	The data transmitted to a ground station shall contain geo-positional data	SUS-SOC-01
~~SYS-OPS-09~~	~~The system shall maintain stable pointing toward the nadir during operation~~	~~Payload[11]~~
SYS-OPS-10	The system shall meet the minimum accuracy requirements of the payload	Payload[11]
SYS-OPS-11	The system shall have attitude control in all 3 dimensions	Payload[11]
SYS-OPS-12	The system shall be able to monitor EPS functioning	MIS-OPS-02
SYS-OPS-13	The system shall be able to transmit status data to a ground station	MIS-OPS-02
SYS-OPS-14	The system shall be able to receive commands from a ground station	MIS-OPS-02
SYS-OPS-15	The system shall ensure data integrity during operation	ST-REQ-PI-8[1]
SYS-OPS-16	The system shall always receive adequate power to remain operational	MIS-OPS-02
SYS-OPS-17	The system shall maintain its orbit within 500 m	Payload[11]
SYS-OPS-18	The system shall insert into the target orbit	MIS-CON-01
SYS-OPS-19	The system shall be able to withstand all physical loads applied to it during its lifetime	MIS-OPS-02
SYS-OPS-20	The system shall correct for LEO orbit perturbations	MIS-OPS-01
SYS-CON-01	The system shall cost less than 500M€ excluding launch	Section 1.4
SYS-CON-02	The system shall be responsive to legislative demand for action from the EU	SUS-ECO-02
SYS-CON-03	The system shall adhere to the Regulations of the European Space Agency	ESA[3]
SYS-CON-04	The system shall be a project integrated by OneSky participating countries	SUS-SPA-01
SYS-CON-05	The system shall be operable within the LEO space environment	MIS-OPS-02

[2]URL ScienceDirect [accessed 13/06/2023]

SYS-CON-06	A system component shall have maximum undeployed dimensions of 4.5 x 4.5 x 10 m	Launcher
SYS-CON-07	The system components shall have a maximum launch mass of 2500 kg	Launcher
SYS-CON-08	The system components shall be compatible with current launch options	Launcher
SYS-CON-09	The system components shall have a TRL of 5	MIS-CON-01
SYS-CON-10	The system components shall have a first lateral eigenfrequency ≥10 Hz	Launcher
SYS-CON-11	The system components shall have a first longitudinal eigenfrequency ≥ 31 Hz	Launcher
SYS-CON-12	The system components shall have its center of gravity ≤ 1.9 m from the mounting point to the launcher	Launcher

In Table 3.3, some requirement sources are already based on the payload. Despite only being discussed in Chapter 5, the requirements are already presented for completeness. The same is done based on the launcher selection presented in Chapter 6.

From both the mission and the system requirements, a division can be made between key, driving and killer requirements for the design of the system and its components. This split can be seen in Table 3.4. It should be noted that the killer requirement MIS-OPS-01 is a mission requirement and can be dealt with by having multiple system components over the lifetime of the system to ensure compliance. This comes however at a cost, which might make SYS-CON-01 driving or even killer requirement.

Table 3.4: Key, Driving and Killer Requirements for the System Requirements

Key	Driving	Killer
MIS-FUN-01	SYS-FUN-04	MIS-OPS-01
SYS-FUN-01	SYS-FUN-05	
SYS-FUN-02	SYS-FUN-07	
SYS-FUN-03	SYS-OPS-09	
MIS-OPS-02	SYS-OPS-10	
SYS-OPS-01	SYS-OPS-17	
SYS-OPS-07	MIS-CON-01	
SYS-OPS-08	SYS-CON-09	
SYS-CON-01	SUS-SPA-13	

[3]URL: esamultimedia.esa.int [accessed: 13/06/2023]

4 Functional Analysis

In this chapter, the functional diagrams of the system are shown and discussed in Sections 4.1 and 4.2. Where Section 4.1 constructs the functions necessary for performing the mission in a flow, which is then expanded to breakdown form in Section 4.2.

4.1. Functional Flow Diagram

The functional flow diagram for the satellite was developed to aid with subsystem requirements discovery, as it would form the basis of the functional breakdown diagrams shown in Figure 4.1, Figure 4.4 and Figure 4.5. This in turn leads to the subsystem requirements. Arrows indicate the direction of the flow and circles containing 'OR' are junctions where the flow separates. Functions are split into a hierarchy, where lower-level functions are needed to complete a higher-level function. The total diagram is shown in Figure 4.2.

4.2. Functional Breakdown

The functional breakdown works similarly to the flow diagram, representing a hierarchy of functions necessary for the operations of the system, it is shown in Figure 4.3. However, where in the functional flow diagram dimensionality of time is mainly represented, in the breakdown the focus is made on the hierarchy. Furthermore, breakdown diagrams for the functions of the subsystems are given, these are reprinted in Figures 4.1, 4.4 and 4.5. The yellow-coloured boxes indicate that this function is connected to a function in a different subsystem.

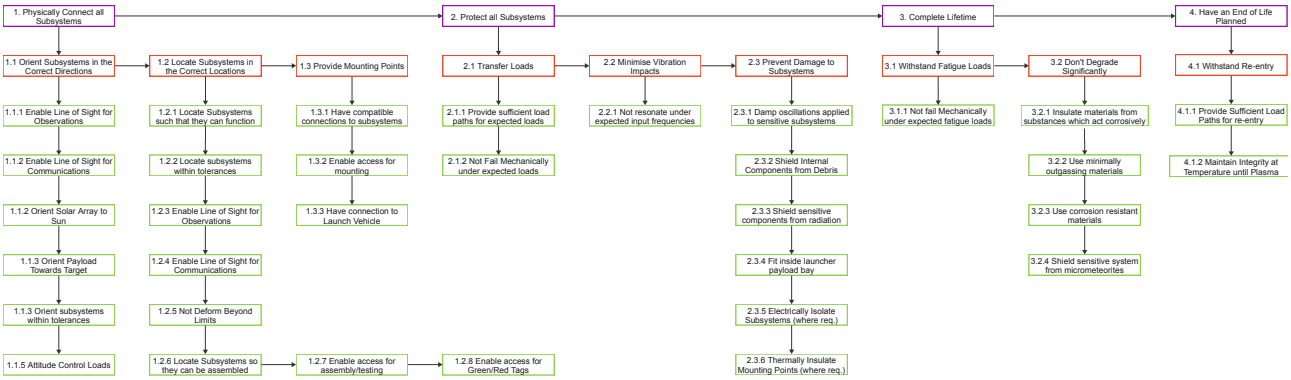

Figure 4.1: Functional Breakdown Diagram for the Structures Subsystems

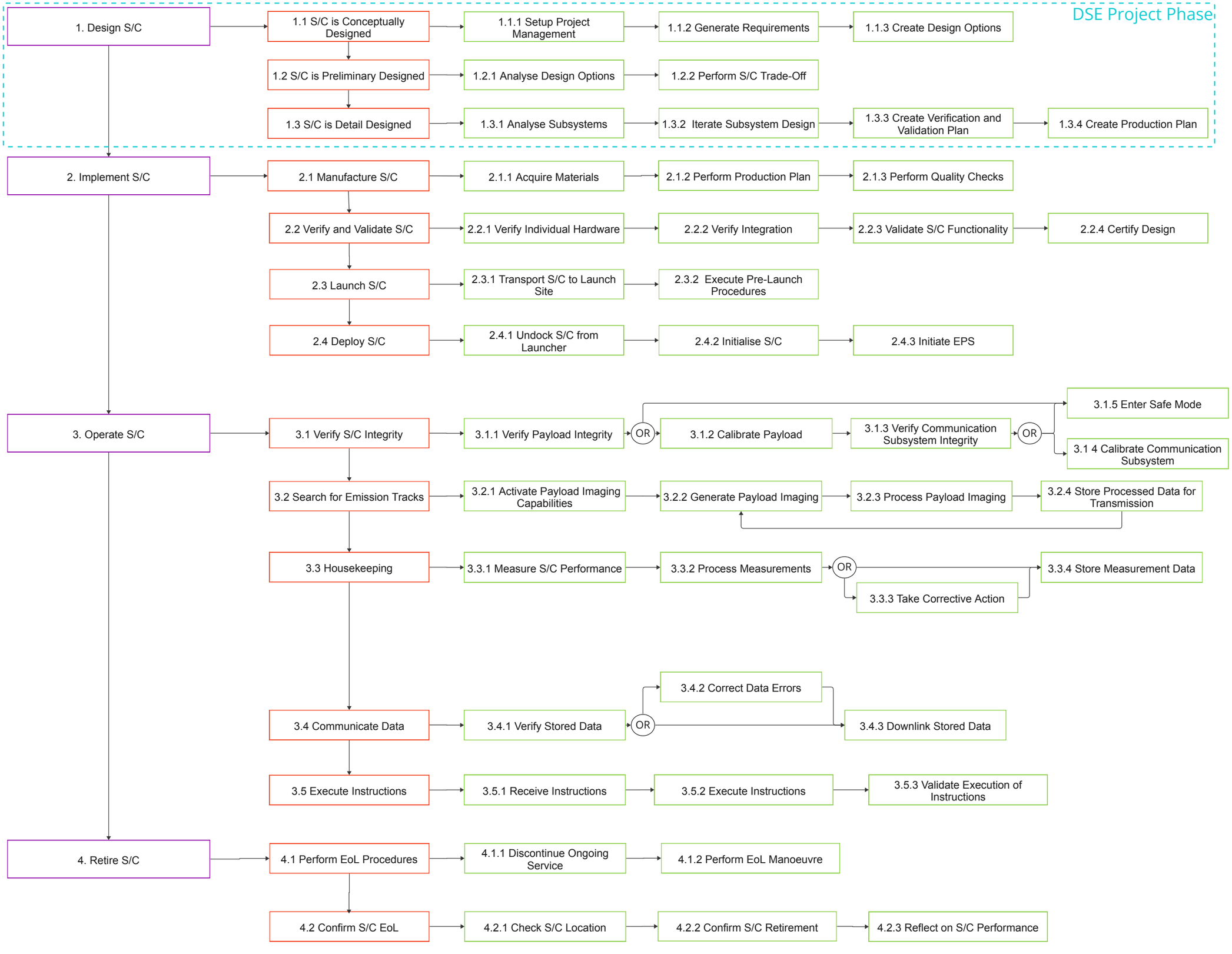

Figure 7.2: Functional flow diagram for the satellite

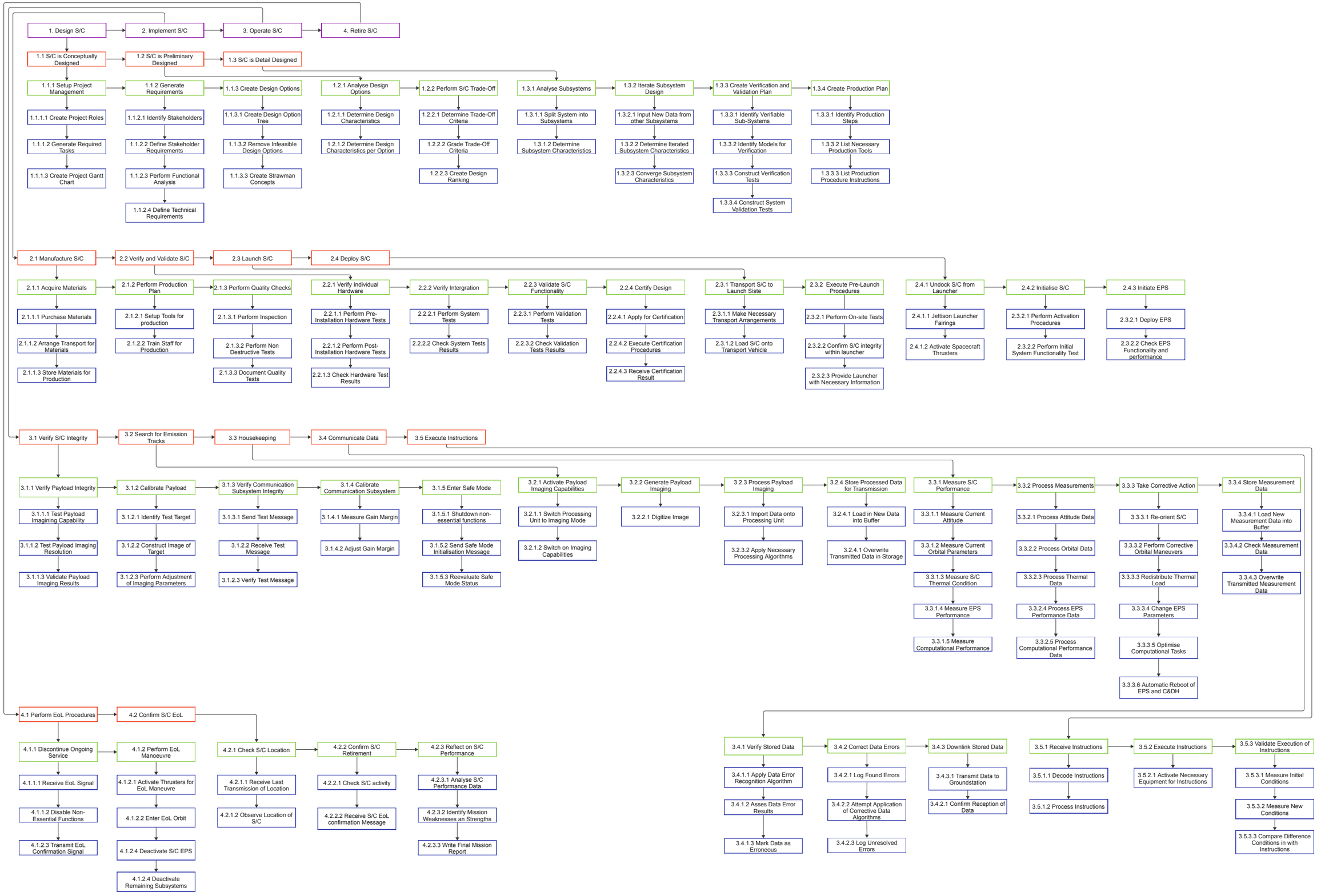

Figure 7.3: Functional breakdown diagram for the satellite

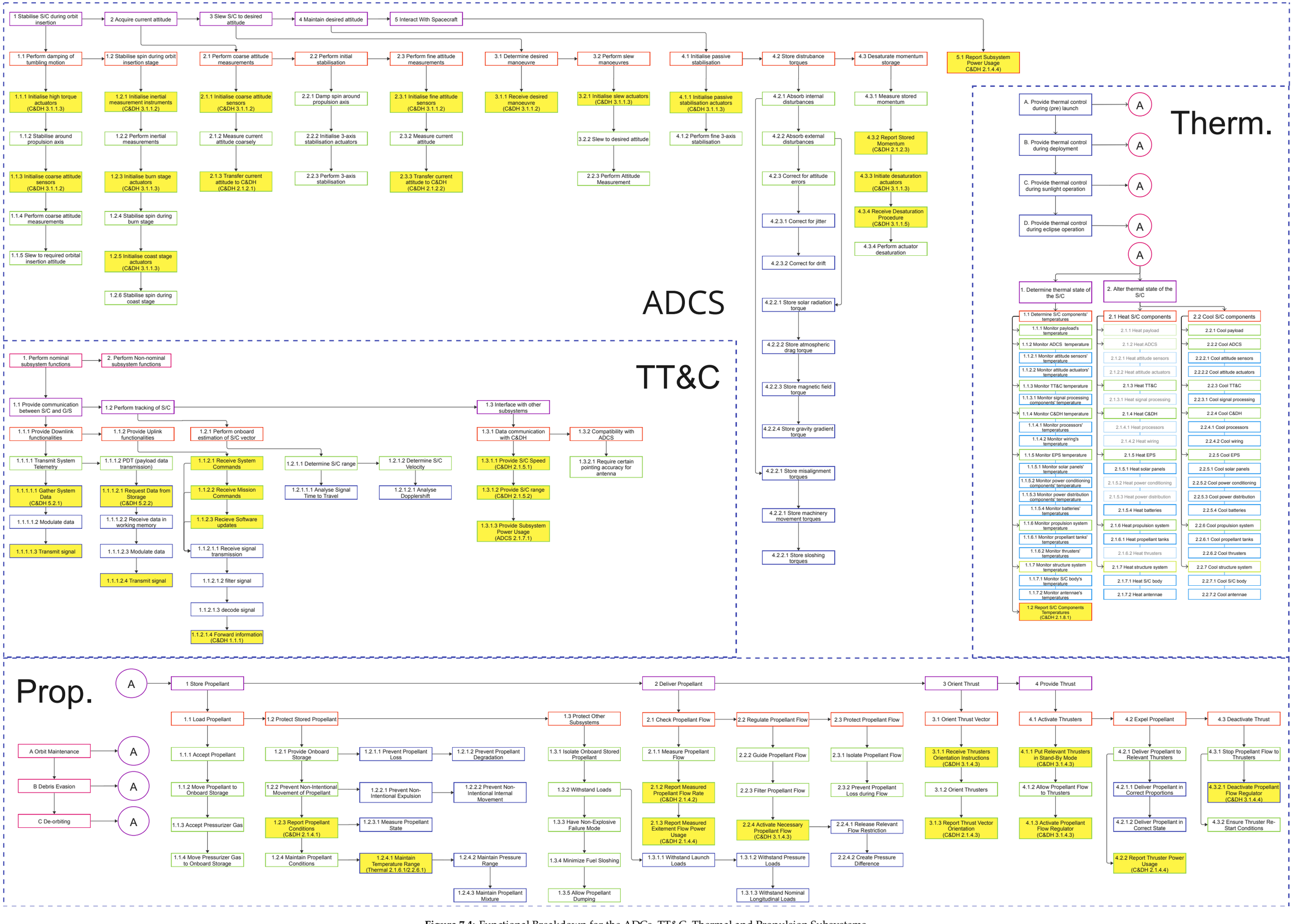

Figure 7.4: Functional Breakdown for the ADCs, TT&C, Thermal and Propulsion Subsystems

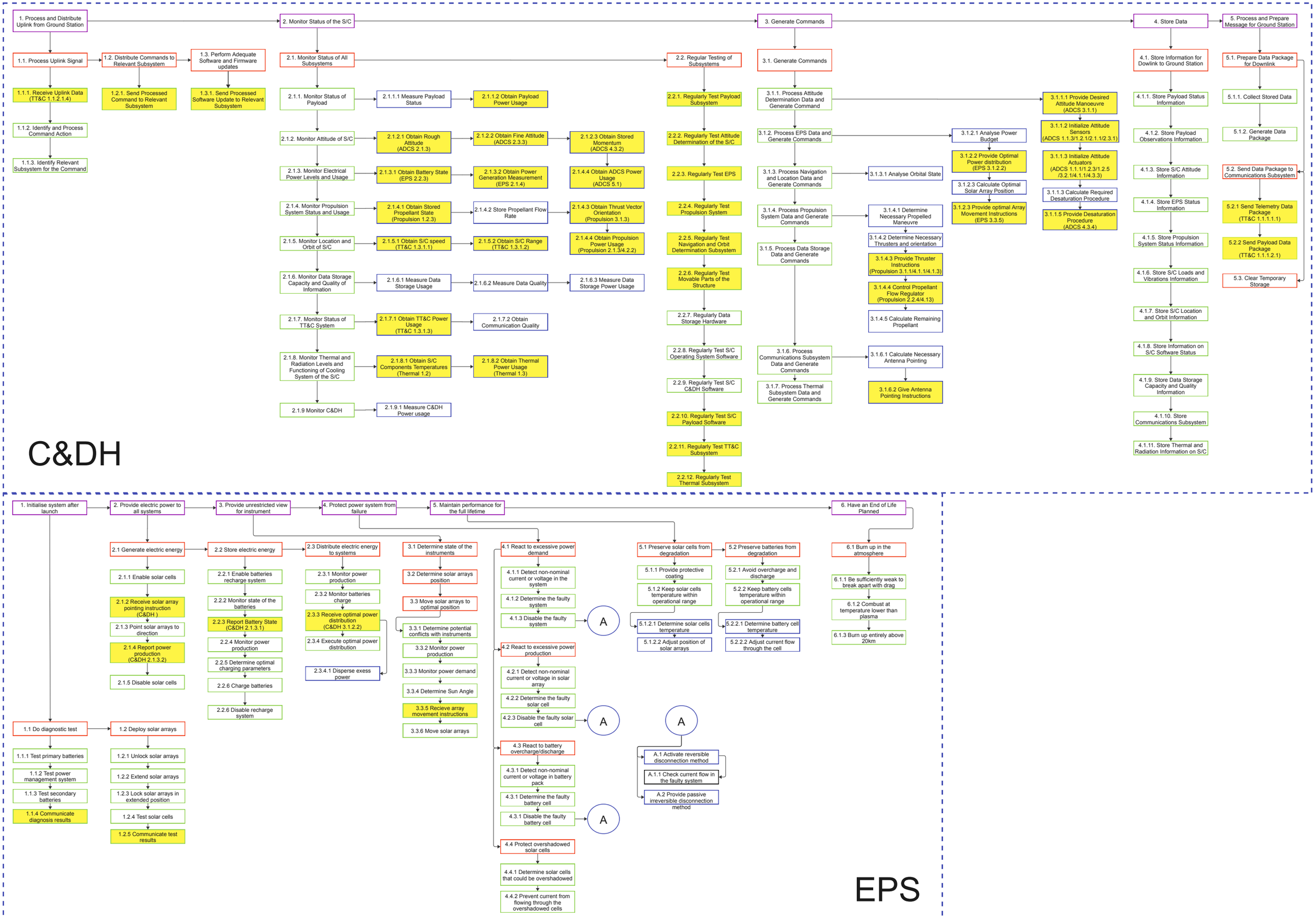

Figure 7.5: Functional Breakdown for the EPS and C&DH Susbsystems

5 Payload Design

The payload constitutes a crucial component of any space mission and often serves as the primary motivator for the operation of such ventures. Frequently, it is the payload that significantly influences the risk, cost, and size of the mission [12]. This chapter outlines the selection of the payload from defining the payload objectives in Section 5.1 to choosing the instrument in Section 5.2. The instrument characteristics will be described in Section 5.3.

5.1. Payload Objective

The primary mission objective, as defined in Section 1.5, is to "Monitor the radiative forcing and dynamic evolution of exhaust gases of air-breathing vehicles in NearSpace". Radiative forcing can be modelled when the chemical composition of the atmosphere is known [13][14][15]. This means that the payload objective could be simplified from monitoring radiative forcing to monitoring exhaust gases and their dynamic evolution. Monitoring the dynamic evolution is achieved by using a ground repeat orbit or using a constellation of satellites, measuring at different times, therefore it is not only based on the readings of one specific instrument. The future hypersonic fleets will be cruising at an altitude range of 30 km to 40 km [16], and the supersonic fleets will cruise below that altitude, hence the payload objective can be modified to monitor this specific altitude. This means that the payload instrument(s) need to be capable of detecting and quantifying the presence and concentration of exhaust gases in the FL 660 to 40km.

There are two ways of measuring these species: column measurements and profile measurements. Total column measurements represent the integrated concentration of a greenhouse gas along the entire path of light through the atmosphere, from the top of the atmosphere to the Earth's surface. It is the sum of the amount of gas in a column that extends from the Earth's surface to the top of the atmosphere. Profile measurements, on the other hand, provide detailed information about the distribution of greenhouse gases at different altitudes or layers in the atmosphere. They provide a more detailed understanding of where the gas is concentrated in the atmosphere, which is important for understanding the behaviour and impact of it on radiative forcing. It was decided that profile measurements are necessary due to the focus on NearSpace vehicles.

5.2. Payload Selection Process

With the payload objective in mind, the instrument can now be chosen. The different instrument types are identified and evaluated to choose a suitable instrument for this specific mission.

5.2.1. Potential Instrument Types

Firstly, it is needed to research different instrument types that could accomplish the mission. After thorough research, it was decided that the payload must include a spectrometer or a Fourier transform spectrometer to monitor traces of gas in the region of interest.

Spectrometers are used to analyze the properties of light and other forms of electromagnetic radiation. The primary function of a spectrometer is to split light into its component wavelengths and measure the intensity of light at each of these wavelengths. The resulting data can be used to produce a spectrogram, which can provide information about the light's source [17]. Fourier transform spectrometers, on the other hand, use a Michelson interferometer where the beam of radiation is split with one part directed to a fixed and the other to a movable mirror. After recombining the reflected beams, an interference pattern is generated which is called an interferogram [18][19][20]. In its essence, the interferogram is an inverse Fourier transform of the spectrogram. Through using broadband infrared radiation from a blackbody light source, the Fourier transform spectrometer covers the entire mid-infrared spectrum where the rotation-vibration bands of many important greenhouse gases are located[21].

5.2.2. Comparative Analyis

Spectrometric instruments are characterized by two crucial parameters: linear dispersion and spectral resolving power. Linear dispersion quantifies the physical separation between two spectral lines on the detector's image plane. It essentially represents how much the instrument can spatially separate different wavelengths at the detector. On the other hand, the spectral resolving power signifies the capacity of the instrument to differentiate between two closely spaced spectral lines at a specific wavelength, separated by a minimal difference. In essence, it tells us the smallest wavelength difference the instrument can distinguish at a given wavelength [22].

For grating spectrometers (which many space-based spectrometers are[1][2][3]), the typical values for the spectral resolving power are between 10^5 and 10^6. The Fourier transform spectrometers, on the other hand, detect all wavelengths simultaneously which allows them to provide higher signal-to-noise ratios (Fellgett's advantage [4]), leading to superior spectral resolving power [22].

This superior spectral resolving power is crucial because it allows for a different scanning method. For grating spectrometers, due to the low spectral resolving power, the only way to measure the profiles of atmospheric gases is to perform limb sounding. Limb sounding is a remote sensing technique used to probe the Earth's atmosphere by viewing the Earth's limb, or edge, rather than looking towards the nadir. The instruments measure either sunlight that has passed through the Earth's atmosphere, a method known as solar occultation, or the radiation inherently emitted by the atmosphere itself. These measurements are taken at different altitudes along the Earth's limb, enabling the vertical profiling of atmospheric constituents [23]. Although limb-sounding offers great vertical resolution (usually up to 1 km), then the horizontal resolution is significantly inferior to Fourier transform spectrometers. The average horizontal resolution of a limb-sounding grating spectrometer is around 300 km[1][2][3]. This means that the horizontal resolution of the limb sounders is too low to gather any meaningful data for the given mission and grating spectrometers had to be discarded.

This means that the only choice of instrument type is the Fourier transform spectrometers. Due to their superior spectral resolving power, the obtained transmission spectrum can be evaluated by a fitting algorithm that calculates the absorption coefficients of the individual gas components in the scan. The algorithm employs the unique absorption bands of the gases, extracted from the HITRAN database [24], to produce an initial theoretical spectrum grounded on estimated concentration values. Through an iterative process, it refines these concentration values to progressively better fit the measured spectrum. The process continues until the optimal fit is reached, which then yields the final greenhouse gas concentrations[21][25]. The only currently operational instrument that has a spectral resolution good enough to employ this method is the Infrared Atmospheric Sounding Interferometer (IASI) that is operational on the Meteorological Operational satellites from EUMETSAT[5]. The newer generation of this instrument, the Infrared Atmospheric Sounding Interferometer - Next Generation (IASI-NG)[6], is going to be operational on the second generation of Meteorological Operational satellites from EUMETSAT predicted to launch in 2025. After a performance analysis, it was found that the IASI-NG could fulfil the mission objectives and is therefore chosen due to the absence of competing instruments.

5.3. Payload Characteristics

In this section, the main characteristics of the chosen instrument are described.

5.3.1. Scanning Technique

The IASI-NG instrument has an instantaneous FoV of 5.714°. One scanning cycle consists of pointing this instantaneous FoV consecutively to 14 Earth views to cover the 40° swath. After that, the instrument

[1]URL: www.space.oscar.wmo.int/acs_limb [accessed: 14/06/2023]
[2]URL: www.space.oscar.wmo.int/gomos [accessed: 14/06/2023]
[3]URL: www.space.oscar.wmo.int/sciamachy [accessed: 14/06/2023]
[4]URL: www.olisweb.com/fellgett [accessed: 14/06/2023]
[5]URL: www.eumetsat.int/iasi [accessed: 14/06/2023]
[6]URL: www.eumetsat.int/iasing [accessed: 14/06/2023]

takes three frames, one internal black body and two deep space images, for radiometric calibration. The scanning cycle is shown in Figure 5.1.

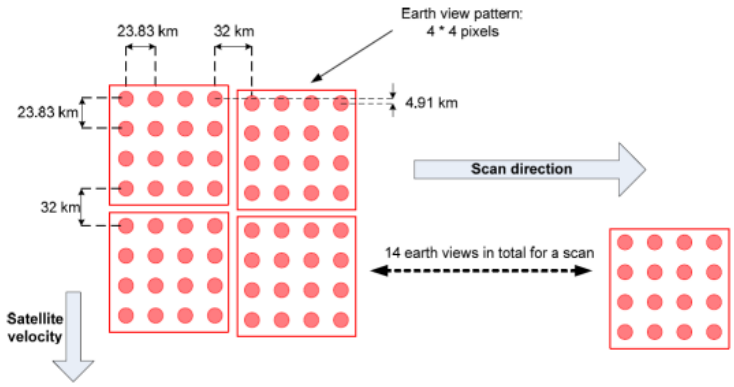

Figure 5.1: Spatial sampling of the Infrared Atmospheric Sounding Interferometer - Next Generation (IASI-NG)[7]

This cycle is repeated automatically and goes on for the entire mission. This step-and-stare technique allows for an increase in resolution on demand. If the user wants an increased resolution over an area of interest, the instrument may be commanded to take consecutive images so that the frames partially overlap. This would mean that the gaps between the pixels (red dots in Figure 5.1) would be filled by pixels from the following images[7].

5.3.2. Data Processing

As a Fourier-transform spectrometer, the raw data coming from the IASI-NG instrument needs a lot of processing to be made into useful data. The majority of the processing of spectra will be performed on the ground. The raw data rate from the sensors of the instrument is 200 Mbit s^{-1} which is roughly divided into 175 Mbit s^{-1} from raw interferograms and 25 Mbit s^{-1} for other data (mainly metrology and images. After the processing in the instrument, the data is compressed to 6 Mbit s^{-1}[7].

Firstly, non-linearity correction is applied and after that spike detection is performed. When a spike is found, the frame is labelled as contaminated. Following that, the interferogram is centred and the Inverse Fourier Transform is computed. After that, the data is in useful form so the wavenumber range of interest is extracted and the data is quantized and encoded. This marks the end of data processing on-board and further processing is done outside of the instrument [7].

5.3.3. Summary

The IASI-NG characteristics are given in Table 5.1.

Table 5.1: Payload Characteristics[7]

Parameter	Value
Spectral coverage	645 cm^{-1} to 2760 cm^{-1}
Spectral resolution	0.25 cm^{-1}
Spatial resolution	24 km
Field of View	80°
Mass	360 kg
Power	500 W
Data rate	6 Mbit s^{-1}
Availability	>98%
Reliability	>84%
Lifetime	7.5 yr

[7]URL: www.eumetsat.int/iasingfactsheet [accessed: 14/06/2023]

It can be seen that the spectral coverage is between 645 cm^{-1} to 2760 cm^{-1} with a spectral resolution of 0.25 cm^{-1}. The unit cm^{-1} indicates the wavenumber and is commonly used in spectrometry to measure spectral resolution. These are both greatly improved from the original IASI instrument and allow for better retrieval algorithms leading to better spatial resolution in the final measurements. This instrument choice also has multiple implications for the design of the satellite. Firstly, it must be noted that the instrument has relatively high mass and power consumption which must be taken into account when designing the structures and the EPS. Secondly, this instrument is going to already operate on the second generation of Meteorological Operational satellites from 2025 which means that to provide meaningful and useful data, the satellite has to have a lower altitude than the existing missions that use that instrument to have a superior resolution. While lower altitudes lead to better resolution, it must be kept in mind that the atmospheric composition changes when going lower and this might lead to differences in the calibration algorithms. The instrument also has a high data rate due to its extensive sensing method. This has to be taken into account when designing the C&DH subsystem.

6 Launch Vehicle Selection

The choice of the launch vehicle, while not a subsystem of the spacecraft, is equally driven by and a driver of the system and subsystem requirements. Therefore a selection must be made from launch vehicles which feasibly launch the required payload to the right orbit (presented in section 6.1). The vehicle must be selected; in section 6.2, before finally the selected launch vehicle can be described in detail, especially regarding the launch characteristics; driving requirements for the system which are presented in section 6.3.

6.1. Launch Vehicle Options

Given the mission's Euro-centric focus and interests; it is preferred that the launch will be undertaken either by ESA as a partner of the mission, or by a commercial space launch system provider, and not by any extra-European national space agency. This gives the options for launch vehicles which are technically capable of lifting sufficient mass into an Earth Orbit which is described in Table 6.1.

Table 6.1: Launch Vehicle Options for the Taking Control Mission

ESA	Notes	SpaceX	Notes
Ariane 5	Not accepting new orders	Falcon 9	
Ariane 6	First commercial launch Q4 2023	Falcon Heavy	
Vega C		Starship	Unknown first commercial launch date
Soyuz 2			

6.2. Launch Vehicle Selection

To first reduce the number of considered options, those which are not certified or in use for commercial launches are removed: *Starship* introduces too great of an operational uncertainty, while *Ariane 5* is expected to be retired by the launch date in 2035, so is also eliminated. *Ariane 6* is to be considered, given it is near-certain to be commercially operating by the same time.

Secondly, the launches of *Soyuz 2* are currently on hold from ESA due to the ongoing military actions of the Russian State and their implications on supply and social acceptability of such use [1]. While this may be resolved before the required launch date, the Soyuz is also disregarded as an option to launch the Taking Control mission.

As a third elimination; *Vega C*, while technically capable of the launch of sufficient weight to a polar orbit is barely capable of carrying out such a launch for the expected weight of 1 satellite. In order to launch a constellation, a launch would be required for each satellite, which is viewed to be less sustainable than a launch vehicle which enables the piggybacking of multiple satellites.

Finally, while *Falcon Heavy* can sufficiently launch the weight of the 3 Taking Control spacecraft, it cannot do so into a polar orbit as required for the mission, therefore the final selection is the choice between Ariane 6 and Falcon 9, for which the key differentiating data is described in Table 6.2.

Table 6.2: Key Characteristics of Falcon 9 and Ariane 6

Variable [units]	Falcon 9	Ariane 6
Number of Flights per Vehicle	>10	1

[1] URL: www.spacenews.com [accessed: 09/06/2023]

Cost per kg to Polar Orbit [USD FY 2023]	2,720 [2]	4,033 (based on Ariane 5 known cost, scaled to Ariane 6) [3]
Fuel Type	Liquid Kerosene [4]	Liquid Hydrogen, Ammonium Perchlorate, Hydroxyl-terminated polybutadiene (HTPB) [5]
Mass to Polar Orbit of 600km radius and 90 °inclination (kg)	7783	3500

From the table, it can be seen that the cost for *Ariane 6* per kg is significantly higher than that of the *Falcon 9*. Besides this, the Falcon 9's reusability means that the associated emissions per flight of the launch hardware are lower. Accurate numbers on the associated equivalent CO_2 emissions per flight are difficult to come by, as little research has been carried out. With that said, while the emissions from Falcon 9's liquid kerosene are CO_2, H_2O, and NO_x, the emissions from Ariane 6 also include toxic chlorine-based byproducts of the Ammonium Perchlorate/HTPB combustion [26].

Based on this, the economic feasibility, environmental sustainability, and social sustainability of the Falcon 9 are superior to the Ariane 6, and therefore the *Falcon 9* is selected as the launch vehicle.

6.3. Launch Vehicle Description

The launch vehicle selected is the Falcon 9, with an extended fairing (shown in Figure 6.1. With the extended fairing, it is deemed possible to launch the 3 IPMS satellites to the required Polar Orbit in a single launch. This significantly reduces the required costs for launches for the mission.

In order to be compatible with the launch vehicle, the total geometry of all satellites must be contained within the fairing, but it (and its subsystems) must also withstand the static loads described in Figure 6.2. There are 4 limiting load cases (lateral acceleration in g, axial acceleration in g): (2, 8.5), (3, 4), (3, -1.5), and (2, -4). Alongside this, it must not oscillate with a natural frequency matching the oscillations of Falcon 9. This means that the 1st harmonic frequency of the IPMS must be >10 Hz laterally, and >31 Hz in the launch direction.

Finally, these loads must be imparted on the spacecraft through an interface with the launch vehicle. While SpaceX will allow customers to design and manufacture a proprietary interface, the use of SpaceX's 1575 mm launch vehicle interface enables the reduction of associated launch costs, emissions, and workload, with increased reliability. Therefore wherever possible, the IPMS shall interface to this standard, as shown in Figure 6.3

[2]URL: ntrs.nasa.gov [accessed: 09/06/2023]
[3]URL: www.yumpu.com [accessed: 09/06/2023]
[4]URL: www.spacex.com [accessed: 09/06/2023]
[5]URL: www.esa.int [accessed: 20/06/2023]
[6]URL: SpaceX [accessed: 21/06/2023]
[7]URL: SpaceX [accessed: 21/06/2023]
[8]URL: SpaceX [accessed: 21/06/2023]

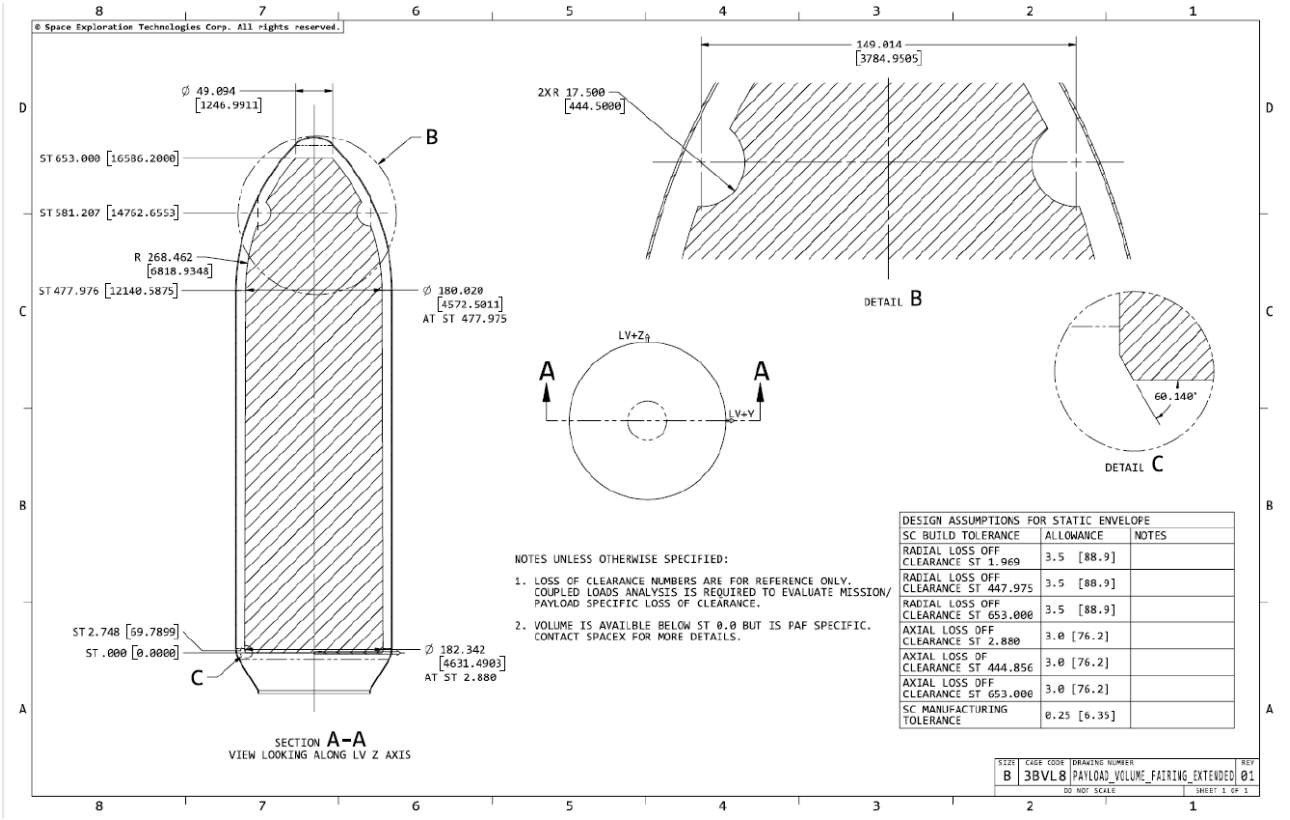

Figure 6.1: Volume of the Extended Payload Fairing of the Falcon 9[6]

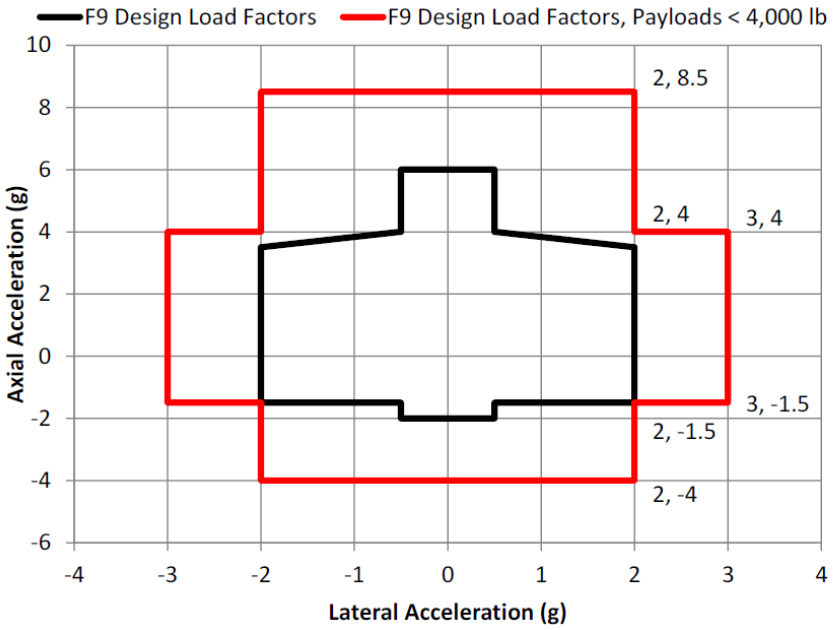

Figure 6.2: Loading Diagram for Payloads of the Falcon 9[7]

Figure 6.3: SpaceX Falcon 1575 Interface Unit[8]

7 Astrodynamic Characteristics

In this chapter, the orbit of the mission and the number of satellites needed are determined based on the mission requirements defined in Chapter 3. In Section 7.1, the orbit is determined and it is verified that this orbit meets the mission requirements. In Section 7.2, the perturbations are identified and quantified. The ΔV-budget required to maintain the orbit over the mission lifetime is also determined.

7.1. Orbits and Trajectories

For the determination of the orbit of the satellites, Keplerian orbits are applied. The Keplerian elements need to be identified to describe the orbit completely. The Keplerian elements are the semi-major axis a, eccentricity e, inclination i, argument of periapsis ω, right ascension of the ascending node Ω, and the true anomaly ν[1]. The other orbital parameters can be determined from these, or vice versa.

7.1.1. Earth Repeat Orbits

With the main focus of the system being in the range of 40° to 60° latitude, it needs to be ensured that that band is observed repeatedly. To ensure this, Earth-repeat orbits have been selected. These types of orbits repeat its ground track every certain amount of orbits in a certain number of days. The equation of Earth repeating orbits is shown in Equation (7.1)[2].

$$j\,|\Delta L| = k2\pi \qquad\qquad \Delta L = -2\pi\frac{2\pi\sqrt{\frac{a^3}{\mu_E}}}{T_E} - \frac{3\pi J_2 R_e^2 \cos i}{a^2\left(1-e^2\right)^2} \tag{7.1, 7.2}$$

In this equation, besides the Keplerian elements mentioned before, μ_E is the gravitational parameter of the Earth, T_E is the rotation time of the Earth, and J_2 is the orbital perturbation constant due to the oblateness of the Earth. This equation can be rewritten to find the cosine of the inclination angle, and substituting Equation (7.4)[2] results in Equation (7.3). It should be noted that only the negative version is considered, since the positive version results in inclinations of more than 180°.

$$\cos i = \pm 2\pi\frac{k}{j} - \frac{4\pi^2\sqrt{\frac{a^3}{\mu_E}}}{T_E}\cdot\frac{a^2\left(1-\left(1-\frac{r_p}{a}\right)^2\right)^2}{3\pi J_2 R_E^2} \qquad\qquad e = 1 - \frac{r_p}{a} \tag{7.3, 7.4}$$

To ensure the required spatial resolution, the peri-centre needs to be in this region. The peri-centre radius is determined using Equation (7.5). Where N_{orb} is the number of types of orbits, where the orbits differ in right ascension of the ascending node, and the true anomaly, and FoV is the selected Field of View of the payload.

$$r_p = R_E + \frac{111139\cdot\Delta L}{2\cdot N_{orb}}\cdot\frac{1}{\tan\frac{FoV}{2}} \qquad\qquad r_a = a\cdot(1+e) \tag{7.5, 7.6}$$

It was decided to minimise the number of orbits/days before the orbits repeat, j and k respectively, since this would minimise the number of satellites required and hence the cost. Concurrently using Equation (7.3) and Equation (7.5) showed that it is required to have at least three orbit types while ensuring the spatial resolution. The resulting k and j are one and fourteen, respectively. ΔL follows directly from this, Equation (7.1). The peri-centre altitude is now determined, using Equation (7.5). To ensure the coverage of the zone of interest, the ascending nodes are equally spread over ΔL. It

[1] URL: www.grc.nasa.gov [accsessed: 07/06/2023]
[2] URL: ocw.tudelft.nl [accessed: 09/06/2023]

is also decided that the three satellites are to fly parallel, meaning the true anomalies are the same. Knowing that the orbits repeat after one day in fourteen orbits, it is calculated that the orbital period should be 6155 s. From this, the semi-major axis is determined using Equation (7.7)[2]. Equation (7.3) is used to determine the required inclination for this orbit. e can be calculated from the r_p and a, using Equation (7.4). The apo-centre radius is calculated using Equation (7.6)[2]. The peri-apsis, given that it is a polar orbit, is equal to the latitude at which it needs to be. This is set to be in the middle of the latitude range of interest of 50°. An overview of the determined and calculated orbital parameters is shown in Table 7.1.

$$a = \sqrt[3]{\mu_e \left(\frac{T}{2\pi}\right)^2} \tag{7.7}$$

Table 7.1: Overview of the Determined and Calculated Orbital Parameters

(a) Determined Parameters Using Equation (7.3) and Equation (7.5)

Parameter	Value	Unit
N_{orb}	3	[-]
k	1	[day]
j	14	[-]
ΔL	25.71	[°]
FoV	80	[°]
$r_{p_{alt}}$	575	[km]
Ω	0 - 8.57 - 17.12	[°]
ν	0 - 0 - 0	[°]

(b) Calculated Parameters from the Determined Parameters

Parameter	Value	Unit
T	6154.6	[s]
a	7 258 689	[m]
e	0.042 09	[-]
r_p	6 953 137	[m]
r_a	7 564 241	[m]
i	90	[°]
ω	90	[°]

7.1.2. Coverage & Visibility

The coverage over the globe is simulated using STK, a systems toolkit from Ansys [3]. This simulation shows the coverage of the northern hemisphere from 13° latitude and up in just over twelve hours. Although a good visualisation is not present, it has been observed from the simulations of STK that covering the region of interest twice per day is guaranteed due to Earth repeat orbit of one day.

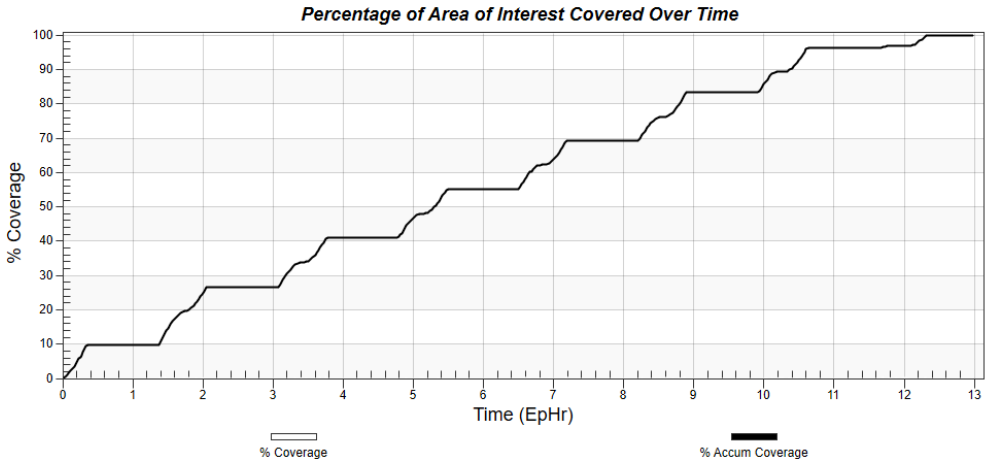

Figure 7.1: Coverage over time of simulation using STK from 13° Latitude and Above

To verify that the spatial resolution is sufficient in the zone of interest, it was calculated that the maximum latitude where the spatial resolution is still sufficient is 13°, using Equation (7.8)[2], so the

[3]URL: www.ansys.com [accessed: 26/06/2023]

requirement is met. Where r is the radius of the orbit, set to be at 800 km altitude, and ν is the true anomaly. Which, in the case of a polar orbit, is related to the latitude by Equation (7.9).

$$\nu = \arccos \frac{\frac{a\left(1-e^2\right)}{r}-1}{e} \qquad lat = \frac{\pi}{2} - \nu \tag{7.8, 7.9}$$

It must be noted that, as addressed in Section 5.3, the calibration algorithms may need to be changed due to a different altitude.

7.1.3. Orbit Insertion

Orbit insertion is not part of the ΔV budget, because of the large amount of propellant required for changing the orbital plane. It was therefore taken into consideration when choosing the launcher in Chapter 6, that it would be capable of inserting the spacecraft in an orbit with the correct inclination and the correct right ascension of the ascending node.

7.1.4. De-Orbit

To de-orbit within the 25 yr required, the orbit's peri-centre is to be lowered to an altitude of 220 km[27]. It can not be ensured that the satellites will burn during re-entry. In general, satellites burn up until a mass of around 1000 kg[28]. Since this spacecraft's mass is above this, a controlled re-entry is required. To ensure this, the peri-centre radius of the orbit is to be lowered to the radius of the Earth. To change the peri-centre to this altitude, a Hohmann transfer orbit is used. The ΔV required for this transfer is determined by Equation (7.10)[12].

$$\Delta V = V_1 - V_2 = \sqrt{\mu_E \left(\frac{2\left(1 + e_1 \cos \nu_1\right)}{a_1\left(1 - e_1^2\right)} - \frac{1}{a_1} \right)} - \sqrt{\mu_E \left(\frac{2\left(1 + e_2 \cos \nu_2\right)}{a_2\left(1 - e_2^2\right)} - \frac{1}{a_2} \right)} \tag{7.10}$$

In this equation, V_1 is the velocity at the apo-centre of the original orbit, and V_2 is the velocity of the apo-centre of the EOL orbit. μ_E is Earth's gravitational parameter, e is the orbit's eccentricity, nu is the true anomaly, 180° at the apo-centre, and a is the semi-major axis. Subscripts 1 and 2 indicate the original mission orbit and EOL orbit, respectively. From this calculation, it is determined that a ΔV of 161.21 m s^{-1} is required for the de-orbiting procedure. This is in line with the expected ΔV required from literature [28].

7.2. Perturbations

With an orbit determined and adequate coverage ensured, the different orbit perturbations affecting the spacecraft during its operational lifetime can be described and quantified. First, the influence of other celestial bodies is discussed in Section 7.2.1, after which the effect of a nonspherical central body is discussed in Section 7.2.2. Moreover, nongravitational forces were also considered. As the spacecraft is in LEO, atmospherical drag will need to be accounted for, which is discussed in Section 7.2.3. Additionally, the effect of solar radiation will be explored in Section 7.2.4, before the total required ΔV over the lifetime is determined in Section 7.2.5.

7.2.1. Third-Body Perturbations

Due to the gravitational forces of the other bodies in the solar system, there are variations in the right ascension of ascending node and the argument of pericenter. These effects are more present in higher orbits, however, should also be accounted for in LEO orbits. Due to that low orbit, only the influence of the moon and sun are considered. Especially the change in Ω over time will be of influence, as it changes the ground tracks of the Earth repeating orbit. As the orbit has little eccentricity, it is possible to approximate this effect for a circular orbit with an error in the order of e^2, which is 0.18%. The used formulas from the *Space Mission Engineering: The New SMAD* are Equation (7.13) and Equation (7.14).

$$\dot{\Omega}_{moon} = -0.00338 \cdot \frac{\cos i}{j} \qquad \dot{\Omega}_{sun} = -0.00154 \cdot \frac{\cos i}{j} \tag{7.11, 7.12}$$

However, due to having a polar orbit with an inclination of 90 °, both effects on the right ascension of ascending note from the moon and sun are zero over time. A similar calculation was done for the change in the argument of perigee ($\dot{\omega}$) using Equation (7.13) and Equation (7.14) from *Space Mission Engineering: The New SMAD*. From these, the moon and sun effect on the argument of perigee is 1.061×10^{-4} °/d and 4.8327×10^{-5} °/d, respectively.

$$\dot{\omega}_{moon} = -0.00169 \cdot \frac{4-5 \cdot \sin i^2}{j} \qquad \dot{\omega}_{sun} = -0.00077 \cdot \frac{4-5 \cdot \sin i^2}{j} \tag{7.13, 7.14}$$

7.2.2. Nonspherical Earth

As the Earth is not spherical, the orbit calculations performed before can be made a bit more accurate. The spacecraft will experience a drift due to the oblateness of the Earth, which is the J_2 effect being used to create an Earth repeat orbit in Section 7.1.1. Therefore, there should be no significant additional perturbation present due to this zonal coefficient. This was verified using Equation (7.15) and Equation (7.16), from which deviations of zero and -1.0055×10^{-10} °/d were calculated for $\dot{\Omega}$ and $\dot{\omega}$, respectively [12].

$$\dot{\Omega}_{J_2} = \frac{-2.06474 \cdot 10^{14} \cdot a^{-\frac{7}{2}} \cdot \cos i}{\left(1-e^2\right)^2} \qquad \dot{\omega}_{J_2} = \frac{1.03237 \cdot 10^{14} \cdot a^{-\frac{7}{2}} \cdot (4-5 \cdot \sin^2 i)}{\left(1-e^2\right)^2} \tag{7.15, 7.16}$$

The effect of other zonal coefficients was also explored, however, due to their effect being three orders of magnitude smaller than the J_2 effect, they were deemed insignificant[4]. These terms could be added for a higher degree of accuracy if that is required for the payload or functioning of another subsystem.

7.2.3. Atmospheric Drag

With an orbit in LEO, the presence of an atmosphere causes a reduction of energy and thus velocity and altitude of the spacecraft. Using Equation (7.17), the acceleration due to drag can be determined, where ρ is the density in $\mathrm{kg\,m^{-3}}$, C_D the drag coefficient and A the frontal surface area in $\mathrm{m^2}$[12].

$$a_D = -\frac{1}{2} \cdot \frac{\rho C_D A V^2}{m} \tag{7.17}$$

For this, the average circular velocity was taken and the mean atmospheric density of $1.5645 \times 10^{-13}\,\mathrm{kg\,m^{-3}}$ at pericenter height [12]. Additionally, from the sizing of the spacecraft described in Chapter 16, a wet mass of 1437.8 kg and a frontal surface area of $2.79\,\mathrm{m^2}$ with the added solar array frontal area of 3.5 m by 0.0155 m were used. For the corresponding drag coefficient, a value of 2 was used as input to this equation, which was derived from a MetOp satellite simulation [29]. This led to an initial estimate of $-1.700 \times 10^{-8}\,\mathrm{m\,s^{-2}}$. However, it should be noted that high variations in density are present in this altitude range due to variable solar activity. This can make the density differ by an order of magnitude. Therefore, using the maximum density of $1.188 \times 10^{-12}\,\mathrm{kg\,m^{-3}}$ at the pericentre altitude results in an increase of 660% of the deceleration. This results in an acceleration of $-1.291 \times 10^{-7}\,\mathrm{m\,s^{-2}}$. Using the acceleration and mass to obtain the force and assuming that all the drag force is converted into heat, the power generated by the drag is calculated to be 1.200 W, an insignificant amount compared to the heat flows considered in Section 14.1.1.

Moreover, due to its low eccentricity and thus near-circular orbit, a simplified set of equations could already be used for the change in the semi-major axis and velocity per day with again an inaccuracy of e^2. These can be seen in Equation (7.18) and Equation (7.19)[12].

$$\Delta a_{day} = -2\pi \cdot \frac{C_D A \rho a^2 j}{m} \qquad \Delta V_{day} = \pi \cdot \frac{C_D A \rho a V j}{m} \tag{7.18, 7.19}$$

[4]URL: ocw.tudelft.nl [accessed: 09/06/2023]

With the same initial inputs and a mean density, a semi-major axis reduction of $2.87\,\mathrm{m\,d^{-1}}$ and velocity reduction of $0.001\,46\,\mathrm{m\,s^{-1}\,d^{-1}}$ was calculated. However, for the worst case density, a semi-major axis reduction of $21.8\,\mathrm{m\,d^{-1}}$ and a velocity reduction of $0.0111\,\mathrm{m\,s^{-1}\,d^{-1}}$ was calculated. Additionally, aerodynamic lift is also a cause of perturbations for the spacecraft, however, these have a bigger effect during launch and reentry and not during its operational lifetime[12].

7.2.4. Solar Radiation

Another non-gravitational force which could perturb the spacecraft is the acceleration due to solar radiation pressure. Dependent on the mass-to-surface area ratio, or the inverse ballistic coefficient, of the spacecraft this could result in a significant acceleration over time. To determine the magnitude of this acceleration, Equation (7.20) was used using the bottom side surface area of the satellite and arrays and the mass calculated in Chapter 16 [12]. From this, a value of $-1.406 \times 10^{-8}\,\mathrm{m\,s^{-2}}$ was determined when using a reflectivity of 0.58 from Chapter 14.

$$a_R \approx -4.5 \cdot 10^{-6} \cdot (1 + r) \cdot \frac{A}{m} \tag{7.20}$$

7.2.5. Orbit Lifetime & Maintenance

With all the different gravitational and non-gravitational forces resulting in perturbations to the spacecraft's trajectory, an initial estimate of the required orbit maintenance in ΔV during a year and its lifetime can be made. The expected lifetime is mostly dependent on the solar cycle and the ultraviolet radiation in altitudes between 120 km to 600 km. The unpredictable solar activity influences the density, which can change over two orders of magnitude between solar maximum and minimum, which results in different decay rates[12]. As a result, starting an orbit during a solar maximum will drastically decrease the orbiting lifetime. According to Figure 7.2 by Larson and Wertz, starting a mission around 600 km altitude results in a preliminary estimate of the lifetime between 1 to 40 years, depending on the starting solar activity.

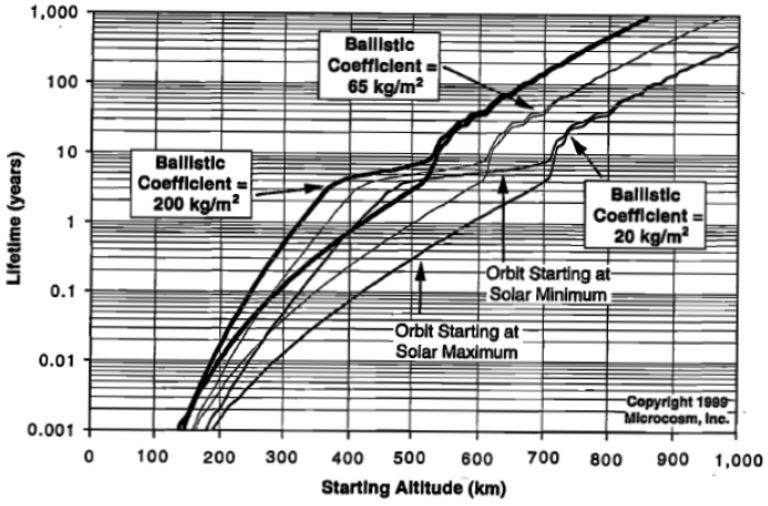

Figure 7.2: Satellite Lifetime as Function of Altitude, Relationship to the Solar Cycle and Representative Ballistic Coefficients[12]

From the 43rd COSPAR Scientific Assembly, it was estimated that Solar Cycle 26 will start in 2031 with its maxima in 2036 and ending in 2041[5]. Similarly, it was estimated by A. K. Singh and A. Bhargawa that Solar Cycle 26 will appear between February 2031 and February 2043, with a maximum in June 2036 [30]. This estimation over time can be seen in Figure 7.3, where the amount of sunspots is an indicator of solar activity. Therefore, a higher density should be taken into consideration when operating in the years around 2036. When starting operations in 2035, the worst case should definitely

[5]URL: ui.adsabs.harvard.edu [accessed: 08/06/2023]

be taken into account. With the typical lifetime of a LEO satellite being between 7 to 10 years [31], an estimate can be made on the worst case ΔV. Taking the lifetime of the payload into account and being aware of the solar cycle, a realistic orbital lifetime of 7.5 years should be designed for per satellite.

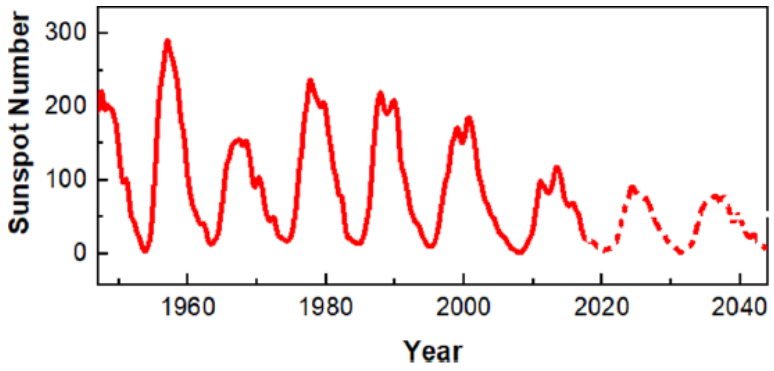

Figure 7.3: Monthly variations of the observed and predicted (dotted) values of the sunspot numbers [30]

During that lifetime, the orbit should perform manoeuvres to stay in a ground repeat orbit and not shift due to any disturbances. The gravitational perturbations can be neglected compared to the non-gravitational ones, due to their lower influence. Bearing in mind that the J_2 effect is not neglected, as it is already accounted for in the determined orbit. The combined changes in Ω are approaching zero and can thus be neglected, while the combined perturbations in ω are 0.4226 ° over the whole lifetime. Corresponding to this is a ΔV of 0.0200 m s^{-1}, which was calculated using Equation (7.21), which was derived from a dog-leg manoeuver[6].

$$\Delta V_\omega = 2 \cdot \sqrt{\frac{\mu}{a \cdot (1 - e^2)}} \cdot \sin \frac{\Delta\omega}{2} \tag{7.21}$$

When it comes to the non-gravitational forces, acceleration on the vehicle due to the solar radiation is 10.90% of the atmospheric drag acceleration. For a worst-case simplification, the mass stays constant and the radiation will act in the same direction as the drag, and can thus be added to the required ΔV. When converting the calculated velocity reduction due to drag to the whole lifetime, a ΔV of 30.44 m s^{-1} is lost. Adding the 10.89% to this, a total ΔV of 33.76 m s^{-1} is required for orbital maintenance during operation to ensure an Earth repeat orbit. This is in line with the range of speed reduction per year of 1.94 m s^{-1} to 13.9 m s^{-1} defined for orbits around 500 km altitude by *Space Mission Engineering: The New SMAD*. However, not just Singh and Bhargawa conclude that the solar maximum of Cycles 25 and 26 will be less severe, Abdusamatov also supports this claim [32]. This might result in a longer lifetime per satellite due to the lower actual density.

Moreover, as the semi-major axis can be reduced by 21.78 m per day due to drag, a total reduction of 24.16 m must be accounted for when taking into account the solar radiation. This maximum reduction becomes problematic when there is no overlap between the coverage areas of the three satellites anymore, which will happen first either at the pericenter or at the lowest latitude with the biggest separation. Due to having a polar orbit, there will be full overlap when approaching the pericenter, thus this is not the limiting case. Therefore, at 800 km altitude at 13° latitude, the satellite must stay above 554.0 km. As there is a spacing of 8.57 ° in Ω, the minimum width to both sides of the ground view is 4.286 °, which is equal to 464.9 km when converting to meters at 13 ° latitude. Using half of the FoV, an altitude of 554.0 km is the lowest height possible for complete ground coverage. This is 246 km below the pericenter altitude, which means that every 27.89 years orbit maintenance would be required. This would indicate that no maintenance is required for overlap, due to the lower lifetime of the satellite.

[6]URL ocw.tudelft.nl [accessed 09/06/2023]

A limit is also set by the ADCS. Due to having a limit on the amount of momentum that can be stored every two days, there is an upper boundary for the density due to the corresponding aerodynamic torque. The lowest altitude at which this is possible is at 540 km. This is 35 km below the pericenter and thus limiting. With losing 24.16 m of the semi-major axis every day, orbit maintenance is required at least every 3.96 years with corresponding burns of 17.86 m s^{-1}.

Another more limiting factor is the payload requirement SYS-OPS-17, which states that the system shall maintain its orbit within 500 m (L_d). Using Equation (7.22), where $\dot{a}$ is the change in a over time, Ω_e the Earth rotation rate and Ω the drift rate, a corresponding reduction of the semi-major axis can be calculated for the maximum deviation[33].

$$\Delta a = \sqrt{\frac{-4a\dot{a}L_d}{3\cdot(\Omega_e-\dot{\Omega})R_e}} \qquad t = \frac{-2\Delta a}{\dot{a}} \tag{7.22, 7.23}$$

From Equation (7.22) a reduction of 76.48 m in the semi-major axis is found critical, which implies that every 6.33 days orbital maintenance is required when increasing a by $2\Delta a$ each burn, according to Equation (7.23). Moreover, at each burn a ΔV of 0.0781 m s^{-1} is required to maintain the lifetime during the solar maximum. This is by far the limiting case for orbital maintenance. Finally, it should be noted that unexpected changes in a might occur, due to for example manoeuvring around space junk when there is a chance of collision.

8 Resource Allocation

As the design process of a spacecraft is an iterative process, an initial estimate should be given for different available resources. This enables each subsystem to design for certain constraints and allows for uncertainties when contingencies are used and start the snowball effect. The initial total estimations are given in Section 8.1, Section 8.2 and Section 8.3 for mass, power and cost, respectively. Finally, in Section 8.4 an overview is given of all the different budgets and allocations per subsystem.

8.1. Mass Estimation

One of the most important parameters of the spacecraft is its mass. The higher the mass, the more ΔV is required for launching and thus the higher the costs. Therefore, getting a somewhat accurate initial estimation of the total dry and wet mass of the satellite is of crucial importance for a successful iterative design. To do so, empirical relations or regression models between the payload mass and the dry or wet mass can be used. To reduce the amount of uncertainty, multiple methods can be used and compared. With a payload mass of 360 kg a dry mass of 1254 kg is estimated based on payload mass being approximately 28.7% of the dry mass [12]. Zandbergen estimates a dry mass of 1083.68 kg, based on Equation (8.1), which is an empirical relatioship based on nineteen data points of Earth-orbiting spacecraft for a payload range between 50 kg to 950 kg[1].

$$m_{dry} = 2.058 \cdot m_{pl} + 342.8 \qquad m_{wet} = 3.78 \cdot m_{pl} \tag{8.1, 8.2}$$

In a similar approach, the wet mass of the satellite was determined. This time B. Zandbergen provided Equation (8.2), which was based on 16 Earth observation spacecraft. This resulted in a wet mass of 1360.8 kg. When using the approach taken in *Space Mission Engineering: The New SMAD* and collecting information on eleven similar Earth-observing spacecraft, a wet mass of 1691 kg was estimated. Taking the higher estimate, which includes some contingency, gives some room for inaccuracies. Moreover with a dry mass of 1254 kg and a wet mass of 1691 kg the propellant mass is determined to be 436 kg. The budget breakdown per subsystem can be seen in Section 8.4.

8.2. Power Estimation

Another important parameter of the spacecraft is its power usage. Higher power requirements, often lead to greater solar arrays and batteries, which both again increase costs and mass. Therefore, getting an initial estimation of the power used by the satellite is required. Similarly to the mass estimation, empirical relations between the payload and the satellite power usage can be used. For this, *Space Mission Engineering: The New SMAD* provided Equation (8.3) for large satellites' power usage, from which a total value of 687 W was calculated from the payload power of 500 W. Similarly, Brown used eight meteorology satellites to get to Equation (8.4) [34], from which P_{sat} was 980 W.

$$P_{sat} = 1.13 \cdot P_{pl} + 122 \qquad P_{sat} = 1.96 \cdot P_{pl} \tag{8.3, 8.4}$$

Again, the higher estimation was taken as a benchmark for the power budget. This again allows for some safety margin by overestimating the amount of power required. The actual allocation of power per subsystem can be seen in Section 8.4.

8.3. Cost Estimation

The third parameter of importance to the spacecraft is the cost. Higher costs are of course not desired, thus making sure that each subsystem stays within its allocated budget is of crucial importance to

[1]URL: Zandbergen reader [accessed: 15/06/2023]

not break through the budget requirements. Again, two different estimation methods were used. Zandbergen provides a cost estimation based on Earth Observation satellites' dry mass, together with converting it to million USD FY2023, Equation (8.5) was used[2]. Similarly, the SVLCM from NASA was used and converted to million USD FY2023 in Equation (8.6)[3].

$$C_{sat} = (0.0264 \cdot m_{dry} + 192.95) \cdot 1.76 \qquad C_{sat} = 0.3531 \cdot (m_{dry})^{0.839} \cdot 1.76 \tag{8.5, 8.6}$$

From Equation (8.5) and Equation (8.6), 390 and 294 million USD FY2023 were estimated, respectively. Again the higher estimate was taken as a basis for the budgeting of the subsystems. However, as the payload is already known, an estimation of that can be made already and subtracted from the total. According to its mass of 360 kg, it can be estimated that the production cost is 96 million USD FY2023, which was determined by scaling the value according to the price per unit mass of a NASA model-based cost engineering space missions estimation[4].

8.4. System Budgets Overview

With the estimations for mass, power and costs defined, one can now deduce how much of that total is allocated to each subsystem. These budget allocations serve as subsystem expectations in Chapter 9 to Chapter 15 and can get budgeted in more detail per subsystem. The relative budget allocation for the mass has been retrieved from the *Spacecraft Design and Sizing* reader by Zandbergen[2], which was a combination of *Space Mission Engineering: The New SMAD* and the TU Delft Space Systems Engineering propulsion webpages[5]. The relative division for power was taken for average power distribution at EOL for several large geostationary telecom satellites[2]. Finally, the relative cost budget was estimated by Zandbergen from four data points and it is thus not that accurate due to the limited dataset. It should be noted that no cost has been assigned to the propulsion subsystem due to the lack of data on it as well. These subsystem proportions can be applied to the total mass, power, and cost estimates made above to derive the absolute allocations, as can be seen in Table 8.1. Moreover, the payload has an increased allocation in power than the nominal 500 W due to the budgeting method. These values also have contingency due to the higher total estimations of the mass, power and costs.

Table 8.1: System Budget for Mass, Power and Cost

Subsystem	Mass [kg]	Power [W]	Cost [million USD FY2023]
Payload	360	753.52	96.10
Structures	262	45.08	41.19
TCS	54	61.74	5.88
EPS	366	14.70	88.27
TT&C	55	15.68	35.31
ADCS	77	33.32	38.25
Propulsion	61	1.96	-
C&DH	19	49.00	82.83
Total	1254	980	386
Bus	894	221	291

[2]URL: Zanbergen reader [accessed 15/06/2023]
[3]URL www.globalsecurity.org [accessed 15/06/2023]
[4]URL www.nasa.gov [accessed: 20/06/2023]
[5]URL research.tudelft.nl [accessed: 15/06/2023]

9 Electrical

The Electrical Power System (EPS) provides electric power to all spacecraft subsystems from the pre-launch phase to the EOL. The design of EPS is shaped mostly by power budget, orbit and reliability requirements. The structure of this chapter is as follows. First, functional analysis (Section 9.1) and the environment (Section 9.2) are presented, followed by system requirements (Section 9.2.3). Then, system configuration and components selection are given. It is finished with a sensitivity analysis (Section 9.5) and a summary.

9.1. Functional Analysis

From the initial sizing (Section 8.2), the EPS should provide an average of around 222 W of power for the bus subsystems and 500 W for the payload. Based on that budget and mission profile, and following the design guidelines from *Space Mission Engineering: The New SMAD*, it is assumed that the EPS uses solar arrays to produce energy and batteries to store it. This section focuses on phenomena that affect energy production by the solar arrays, storage by the battery and distribution by the management system. Sizing is only addressed in later sections, once the configuration is selected.

9.1.1. Energy Production

Solar cells produce electric energy while illuminated thanks to the photovoltaic effect [1]. According to *Space Mission Engineering: The New SMAD*, solar cells convert the input solar flux P_{in} to electric power with a type-specific energy conversion coefficient, which varies from 18% for silicon cells to more than 30% for multi-junction cells [2]. This is the ideal efficiency. The real efficiency of the solar system is lower due to assembly losses[3] often in the range 0.77 - 0.90. Temperature loss, when the temperature of the solar cell is higher than the reference temperature [4], in the range 0.8-0.98. For simplicity, it is assumed performance decreases linearly with an increase in temperature. Energy transfer efficiency accounts for conversion losses between solar cell circuits and spacecraft bus. It depends on the conversion method. Peak-power transfer that requires a voltage converter has an efficiency of 0.60 according to [12]. However, commercially available power control units often have higher efficiency of around 90% [5], that value will be used for sizing. The direct transfer has an efficiency of 0.65. All given quantities are derived from *Space Mission Engineering: The New SMAD* unless otherwise stated.

Solar flux depends on the intensity of the solar irradiance and the angle of incidence (or Sun incidence angle). Misalignment (non-zero angle of incidence) introduce the Kelly Cosine loss[6], which for simplicity will be approximated by trigonometric cosine loss.

The power performance of solar cells degrades over time due to the space environment, hence it strongly depends on the mission orbit. The degradation rate is a relative decrease in power per year of the mission, often between 2% and 4% [12].

Aside from efficiencies, the voltage-current relation is too an influence on power generation. Every solar cell type has a peak power point - a voltage-current combination for which the highest power is produced. It varies with cell temperature and degradation

[1] URL: https://www.energy.gov [accessed: 20/06/2023]
[2] URL: www.azurspace.com [accessed: 20/06/2023]
[3] It is not possible to cover the entire solar array with solar cells, hence the loss.
[4] Reference temperature depends on certification standard, often T = 25 ° °C
[5] URL: https://www.airbus.com/ [accessed: 21/06/2023]
[6] URL: https://digitalcommons.usu.edu [accessed: 20/06/2023]

9.1.2. Energy Storage

Rechargeable batteries (or secondary batteries) store electric energy as electrochemical energy. They must store energy for the eclipse phase and peak power moments. The capacity of a battery depends on its type, size and state of health. Capacity decreases with the number of charge-discharge cycles. The battery health can be maintained for longer by utilising a low Depth of Discharge (DOD), keeping the cells balanced (at an optimal potential) and within the operational temperature [35]. A battery has maximum charge and discharge rates that depend on battery type and configuration. It limits the maximum power that can be delivered. The transition of energy between batteries and loads comes with energy loss quantified by transmission efficiency that depends on battery type and electrical connections.

9.1.3. Energy Distribution

Distribution system transfers and converts electric energy from the solar arrays to the batteries and spacecraft bus and payload. It provides appropriate voltage and current draw for each electric bus and provides a connection between the power source and the user.

9.1.4. Subsystem Relations

The EPS performance is related to other subsystems and design decisions. Orbit selection determines the Sun incidence angle and solar array temperature. The thermal system affects the performance and health of both solar arrays and batteries. The structures can potentially limit solar array configuration and cause shadowing.

9.2. Environment Analysis

Analysis of the environment focuses on two aspects: effects on energy production and impact on systems performance degradation. The former concerns solar irradiance, solar panel incidence angle, eclipse times and working temperature. The latter concerns the degradation of solar cells due to radiation and oxidation.

9.2.1. Energy Production

The amount of energy collected by the solar panels directly depends on three geometric quantities: distance to the Sun, panel incidence angle and shadowing. These quantities change in short-time scale due to the orbital motion of the spacecraft and in the long term due to the Earth's revolution. Solar irradiance changes depending on the season. To make the design conservative, the smallest value of $1360.3\,\mathrm{W\,m^{-2}}$ is used [36]. The incidence angle also depends on the season. For the given polar orbit with the longitude of the ascending node of 0°, the incidence angle to the spacecraft zenith direction varies in every orbit. At the equinox, it spans from 0° at the equator to 90° at the poles. At the solstice, it spans from 66.56° [7] at the poles to 90° at the equator. At any other time, the incidence angle is a transition between these two extrema. Finally, the shadowing depends on spacecraft configuration and eclipse region. In general, for low earth polar orbits, the eclipse time varies from around 35 minutes at the equinox to 0 minutes at the solstice [37]. The working temperature of a solar array depends on the received solar flux and its thermodynamic properties. It is assumed that the thermal design of the spacecraft keeps the solar array within the temperature range from 23.15 °C to 80 °C during operation.

9.2.2. Degrading Effects

Spacecraft in orbit are exposed to a space environment that can affect their performance. As of EPS, solar arrays and (to a lesser extent) the batteries can be damaged by energetic particles suspended in space, mostly protons and electrons. Further, solar arrays are eroded by atomic oxygen in a process called oxidation.

According to NASA's report on solar array design [38], protons are less harmful than electrons since shielding against the former can be applied easily. Hence, the driving factor of solar array performance degradation is electron fluence. Often, the fluence of 1 MeV electrons is considered

[7] 90° minus the Earth's tilt.

as an estimator of degradation [38]. According to Samwel et al. [39], the AE-8 model[8] of trapped electrons indicates 10^{11} cm^{-2} MeV^{-1} collected in a polar orbit during one-year long mission. However, to accommodate for electrons with other energies, an equivalent fluence should be used. According to *Space Mission Engineering: The New SMAD*, it is 10^{11} cm^{-2} MeV^{-1} for a five-year mission in LEO. Oxidation particularly affects polymers since a collision with atomic oxygen releases the energy of roughly 5 eV, which is enough to break bounds in polymers [40]. The protective coating should be used to protect organic materials on solar arrays.

9.2.3. Requirements

Power demand and working environment, system configuration together with mission profile lead to the following subsystem requirements shown in Table 9.1.

Table 9.1: Electric Power System Requirements

ID	Requirement	Derived From
SUB-EPS-01	The EPS system shall have a maximum mass of 366 kg (see Section 8.1).	SYS-OPS-07
SUB-EPS-02	The EPS shall cost less than 109 M€ (see Section 8.3).	SYS-CON-01
SUB-EPS-03	The EPS shall constantly provide 1020 W of power at the EOL, with an eclipse time of 35 minutes (see Section 8.2, Section 9.2).	SYS-OPS-16
SUB-EPS-04	The EPS shall provide 1100 W of peak power for 10 minutes every orbit at the EOL.	SYS-OPS-16
SUB-EPS-05	The EPS shall provide voltage on the main power bus with an average of 28 V.[9]	SYS-OPS-16
SUB-EPS-06	The harness of EPS shall not exceed 15% of the total EPS mass *Space Mission Engineering: The New SMAD*.	SYS-CON-07
SUB-EPS-07	The EPS shall have direct energy transfer efficiency of >0.65 (see Section 9.1).	SYS-OPS-16
SUB-EPS-08	The EPS shall have peak-power tracking efficiency of >0.6 (see Section 9.1).	SYS-OPS-16
SUB-EPS-09	The EPS shall not degrade more than 5% in performance throughout the lifetime.	SYS-OPS-16
SUB-EPS-10	The EPS shall have power interface compatible with all other subsystems.	SUS-SPA-09
SUB-EPS-11	The EPS shall distribute power between subsystems according to their demand.	SYS-OPS-16
SUB-EPS-12	The EPS shall provide primary power source for critical systems.	SYS-OPS-16
SUB-EPS-13	The EPS shall have safety procedures for excess power demand.	SYS-OPS-16
SUB-EPS-14	The EPS shall have no heat signature within the field of view of the scientific instrument.	SYS-OPS-10
SUB-EPS-15	The EPS shall not obstruct the field of view of any of the subsystems.	SYS-OPS-10
SUB-EPS-16	The EPS shall be able to generate power on 3-axis stabilised spacecraft pointed to nadir.	SYS-OPS-09
SUB-EPS-17	The EPS shall withstand 5 eV collisions with atomic oxygen without excess degradation (see Section 9.2).	SYS-OPS-02
SUB-EPS-18	The EPS shall withstand 10^5 electrons per cm^2 of equivalent 1 MeV electron fluence without excess degradation (see Section 9.2).	SYS-OPS-02
SUB-EPS-19	The EPS shall be equipped with measures against electrostatic charging.	SYS-OPS-02
SUB-EPS-20	The EPS shall provide diagnostic information.	SYS-OPS-12
SUB-EPS-21	The EPS shall not utilise more than 0 g of radioactive materials	SYS-OPS-14

9.3. Configuration

This section presents a configuration of the solar array, the batteries and the power management system. Next, preliminary sizing is presented, followed by components selection.

9.3.1. Solar array

The solar array must be configured such that it can collect enough solar flux each time of the year. This primarily concerns the segmentation and rotation of the solar array. To meet the SUB-EPS-14, the solar

[8]URL: https://ntrs.nasa.gov [accessed: 20/06/2023]

[9]Standard voltage for US instruments, also compatible with European instruments [12]

array should be extended away from the spacecraft in a configuration similar to the one of MetOp satellite [10]. It is decided that the solar array should consist of one block since it reduces the number of drive mechanisms (one per block) and boom deployment systems. The block can consist of multiple segments, but they must have a common mounting point. Furthermore, while deployed, the solar array should be in the aft part of the spacecraft, so as not to interfere with the instrument.

Array rotation

Considering the change of Sun angle throughout the year as described in Section 9.2, 3 potential configurations of the rotation system are analysed. One axis rotation around the direction of motion. One axis rotation around the limb direction (perpendicular to the nadir and to the direction of motion). Combination of the two options: biaxial rotation. The options are graded based on the sun incidence angle φ throughout the year, which directly translates to the total solar radiation the array could collect.

The first option provides a constant φ of 0° during the solstice. During equinox, φ varies from 0° to 90° (in magnitude) during every orbit. Compared to constant 0° φ, over half orbit, it leads to the reduction of solar fluence (E) of:

$$E_{reduced} = 2\int_0^{\frac{1}{2}T} E_0 cos(\frac{\pi}{2}\frac{t}{T})dt = \frac{2}{\pi}E_0 \approx 0.63E_0, \tag{9.1}$$

which is equivalent to an average incidence angle of approximately 50°.

The second option provides a constant φ of 0° during the equinox. However, during the solstice, the smallest value of φ is approximately 67° (consult Section 9.2, incidence angle).

Both options result in the solar array working at a suboptimal incidence angle at some point in the year. Considering the EPS must be sized to function at the worst scenario, using either of these configurations would lead to an oversized solar array. Therefore, the third configuration (biaxial rotation) is selected as the most suitable one. Such configuration has been used in other LEO missions, for instance on the Hubble Space Telescope [11].' With that configuration, φ can be set to 0° at all times.

Array Power Sizing

Analysis of power consumption of other subsystems leads to an estimated average power of 667.3 W (bus + payload). With a safety factor of 50% that leads to 1001 W of power. The critical scenario for array power sizing is the longest eclipse which lasts for 35 minutes Section 9.2, at the EOL. The corresponding daytime is 68 minutes Section 7.1. The solar array must produce enough energy to charge the batteries for the eclipse time, hence the power should be as listed in Equation (9.2)(adopted from *Space Mission Engineering: The New SMAD*[12]):

$$P_{array} = \frac{P_{demand}(T_{eclipse} + T_{day})}{X_e T_{day}}, \tag{9.2}$$

where X_e is the converter efficiency, here assumed to be 0.9 both in daylight and eclipse Section 9.1. This leads to total power of 1707 W

9.3.2. Batteries and power management system

Batteries store energy for eclipse time and provide redundant power for critical subsystems. The power management system converts power from the solar arrays and distributes it to other subsystems. The driving requirement for this design is redundancy - the management system should have at least one redundant connection to each of the subsystems. Batteries should be connected to the system through multiple links.

[10]URL: https://www.eumetsat.int/metop [accessed: 20/06/2023]
[11]URL: https://asd.gsfc.nasa.gov/archive/

Management system configuration

The power system consists of three regulated power buses, with a voltage of 28 V. Power is delivered to those buses through four independently connected DC-DC regulators (DC1, DC2, DC3, DC4). One has high power capacity (BUS 1) and is used to power the payload, propulsion and TCS. The other two (BUS 2 and BUS 3) have lower power capacity and are used to power the remaining systems and provide a redundant power source for the payload. The regulators are directly connected to the solar array, they act like peak power trackers. Two charge/discharge battery modules are independently connected to the battery and the main power bus and to all DC-DC converters. The primary battery is directly connected through a separate bus (Primary) to the critical systems, that is the C&DH and TT&C. Subsystems are segregated into power groups according to their profile, voltage sensitivity and power demand. A summary is given in Table 9.2.

Power group	Bus	Power source	Max. power [W]	Max. current [12] [A]
Payload, Propulsion, TCS	BUS 1 / BUS 2&3	DC1 / DC2&3	578	21
ADCS, Propulsion, TCS	BUS 2 / BUS 3	DC2 / DC3	242	9
C&DH, TT&C, EPS, Navigation	BUS 2 / BUS 3 / Primary	DC3 / DC4 / Primary	106	4

Table 9.2: Configuration of the power management system.

9.4. Components Selection

The EPS configuration with subsystem requirements forms a basis for the selection of EPS components. The commercial offer of EPS components optimised for small satellite LEO missions is wide and exhaustive. Therefore, most of the components are selected from off-the-shelf products. That is the case for solar panels with a deployment system and drive mechanisms, solar cells, primary and secondary batteries and power management systems.

9.4.1. Solar array

Sparkwing was selected as the solar array manufacturer. Sparkwing is experienced with delivering solar arrays for small and medium satellites and other space missions e.g. Rosetta and ExoMars[13]. The company provides a short manufacturing time of 6 to 9 months and allows for the usage of customer-specific solar cells.

Sparkwing provides customisable panel assemblies, however, only some parameters can be modified. The number of panels per segment can be 1, 2 or 3. Panels of different sizes can be selected. Each panel size has a corresponding number of solar cells, which translates to the total power produced by that panel. Sparkwing specifies power per panel based on the default solar cells[14]. This power approximation is used to select the correct panel size. The cells can be grouped into strings of 19 or 26 cells. The former results in lower system voltage (around 36 V) than the latter (50 V).

The selected solar array configuration consists of 3 segments, each with 3 panels (0.75 m by 1.1 m), with 19 cells per string configuration. The total number of cells is 1881. Thanks to the short hinge-side edge (0.75 m), the folded panel fits on the side of the spacecraft.

9.4.2. Battery

First, the primary battery is sized and selected. The identified critical subsystems are the C&DH and TT&C. To size the primary battery, it is assumed that it must be able to power the computer for one orbit and handle two communication cycles. Such a sequence is assumed to happen twice during

[13]URL: https://sparkwing.space/ [accessed: 15/06/2023]
[14]AZUR 3G30A

one spacecraft mission. The primary battery should be at least 173 W h, or 6.2 A h[15] (assuming 28 V). Five battery packs of 44.4 W h each will be used. EXA BA0x High Energy Density Battery Array[16] was selected. Multiple similar models are available, due to high similarity, this model is given as an example and could be changed in the future.

The secondary battery should store energy for the duration of the longest eclipse, that is for 2144 s. The spacecraft is assumed to demand the average power, that is 1001 W. Assuming the battery transmission efficiency of 0.9 [12], it leads to the required battery capacity of 662 W h. However, the battery cannot be discharged completely as this affects its health, reducing its lifetime number of cycles [35]. To provide a sufficient number of battery cycles, the Depth of Discharge (DOD) was set to 40%, leading to the required capacity of 1655.77 W h. There are many commercially available batteries that have been certified for usage in space. A battery that is close to the required capacity is the ABSL 8s52p package [17]. It has a capacity of 2246 W h, included cell balance and operates on a nominal voltage of 28 V, making it a suitable choice for the EPS.

9.4.3. Solar cell

The selection of solar cells is done through a trade-off between four commercially available cells, selected from the types most commonly used in the space industry. These are OCE Triple Junction GaAs[18], Spectrolab Ultra Triple Junction[19], AZUR Space Quadruple Junction 4G32C[20], AZUR Space Triple Junction 3G30C[21]. From the following options, the most suitable component was selected by means of trade-off against the following criteria: BOL peak power, performance degradation due to electrons fluence, the voltage drop due to the temperature gradient and area weight.

BOL peak power, expressed in W, is the power produced by one uncovered 30.15 cm^2 solar cell at 28 °C, exposed to zero-atmospheres (AM0) spectrum sunshine with intensity of 1367 $W\,m^{-2}$. Multi-junction GaAs solar cells often reach from 1 W to 1.5 W. The peak power depends on their photo-electrical efficiency and the absorbed spectrum. This criterion received a high 60 % weight in the trade-off, as more powerful solar cells result in a smaller total array area, which is strongly constrained by spacecraft dimensions and structural limitations.

Performance degradation due to electrons fluence, expressed in %, is a relative decrease in peak power after a fluence of 5×10^{14} 1 MeV electrons per cm^2. Performance degradation of multi-junction GaAs cells is often within 4% to 15% [41]. Effects of performance degradation cannot be easily mitigated since once the mission has been launched, the potential increase in energy generation would require orbit modification. Therefore, this criterion received a weight of 20 %.

Voltage drop due to temperature gradient, expressed in $mV\,°C^{-1}$, describes a decrease in the potential of a solar cell with growing temperature. In general, this change is moderate, from $-5\,mV\,°C^{-1}$ to $-10\,mV\,°C^{-1}$ per cell, but when the entire assembly is affected, then the resulting voltage drop reduces the power. Note should be made that the potential drop occurs alongside an increase in current intensity, however, it is too small to compensate for the potential drop. Potential negative consequences to the power budget can be mitigated by appropriate power margins and thermal control. Therefore, this criterion received a weight of 10 %. Trade-off criteria, weights and corresponding values are presented in Table 9.3

[15] Two times 35 W for one orbit + 14 W for 94% of orbit + 40.45 W for 6% of orbit
[16] URL: https://www.cubesatshop.com/product/ [accessed: 21/06/2023]
[17] URL: www.enersys.com [accessed: 15/06/2023]
[18] URL: https://satsearch.co [accessed: 15/06/2023]
[19] URL: www.spectrolab.com [accessed: 15/06/2023]
[20] URL: www.azurspace.com [accessed: 15/06/2023]
[21] URL: www.azurspace.com [accessed: 15/06/2023]

Table 9.3: Trade-Off Criteria of the Solar Cell Type

Criterion	Weight %	1	2	3	4	5
BOL max. power [W]	60	< 1.15	1.15-1.20	1.20-1.25	1.25-1.30	> 1.30
Electron degradation [%]	20	> 10	8 - 10	6 - 8	5 - 6	< 5
Temperature effects [$mV\,°C^{-1}$] (negative)	10	> 8.0	8.0 - 7.5	7.5 - 7.0	7.0 - 6.5	< 6.5
Area density [$mg\,cm^{-2}$]	10	> 100	100 - 95	95 - 90	90 - 85	< 85

Components were graded based on their performance for each of the criteria. The values were derived from manufacturers' data sheets[18] [19] [20] [21]. Table 9.4 shows the grading, the winning option is AZUR Space Quadruple Junction 4G32C, which was selected as a solar cell for the EPS.

Table 9.4: Analysis of the Solar Cell Type Trade-Off Criteria

Criterion	Weight [%]	OCE Tech	AZUR 3G30C	Spectrolab UTJ	**AZUR 4G32C**
BOL max. power	60	3	3	2	5
Electron degradation	20	1	4	2	4
Temperature effects	10	5	3	4	1
Area density	10	1	4	5	4
Weighted total		260	330	250	**430**

The selected solar cell, AZUR Space Quadruple Junction 4G32C, placed on the Sparkwing panels constitute the solar array. 1881 4G32C cells produce 2467 W at BOL and 2307 W at EOL operating at 25 °C. At 60 °C it produces 2222 W and 2066 W, respectively. At 80 °C (highest allowable operating temperature) it produces 2081 W and 1926 W. The lowest produced power is higher than the required power of the solar array.

9.5. Sensitivity Analysis

Sensitivity analysis of the EPS investigates how a change of mission parameter affects the performance of the EPS. Six influential parameters have been determined: change of orbital inclination, inaccurate power budget, high battery degradation rate, high solar panels degradation rate, and increased lifetime. Potential mitigation strategies are analysed for each case.

A lower orbital inclination would result in more days with a high eclipse time orbit fraction. The maximal eclipse time will not change, remaining at around 35% of the period, hence required capacity is not affected. More frequent, long eclipses will result in higher battery fatigue. The battery is designed to handle polar orbit eclipses with a depth of discharge of 40%. To keep the battery's health at acceptable levels, the depth of discharge should be reduced accordingly if long eclipses appear frequently. A decrease of the depth of discharge to 30% will result in a growth of required battery capacity: from 1655.77 W h to 2207.7 W h, which is smaller than the selected battery capacity.

Increased battery degradation rate might be caused by a faulty temperature control system or poorly tuned battery management system. Suboptimal charge/discharge battery temperature will lead affect battery health. A potential mitigation is to design the thermal system to keep the batteries' temperature in the middle of their operational range so that the potential deviations might not lead to suboptimal working conditions. Unbalanced cells will age at different rates, leading to an excess loss of capacity. A lower depth of discharge is a potential mitigation that will lower the degradation of the imbalanced cells. Alternatively, a 50% safety margin on battery capacity can be applied. However, if cell imbalance is caused by a poor charging/discharging system, added battery capacity would not solve the problem, because redundant cells would also get damaged. Hence, it is better to lower DOD and thoroughly validate the battery management system.

Extended lifetime will pose a challenge to solar cells and secondary batteries, as they both degrade with

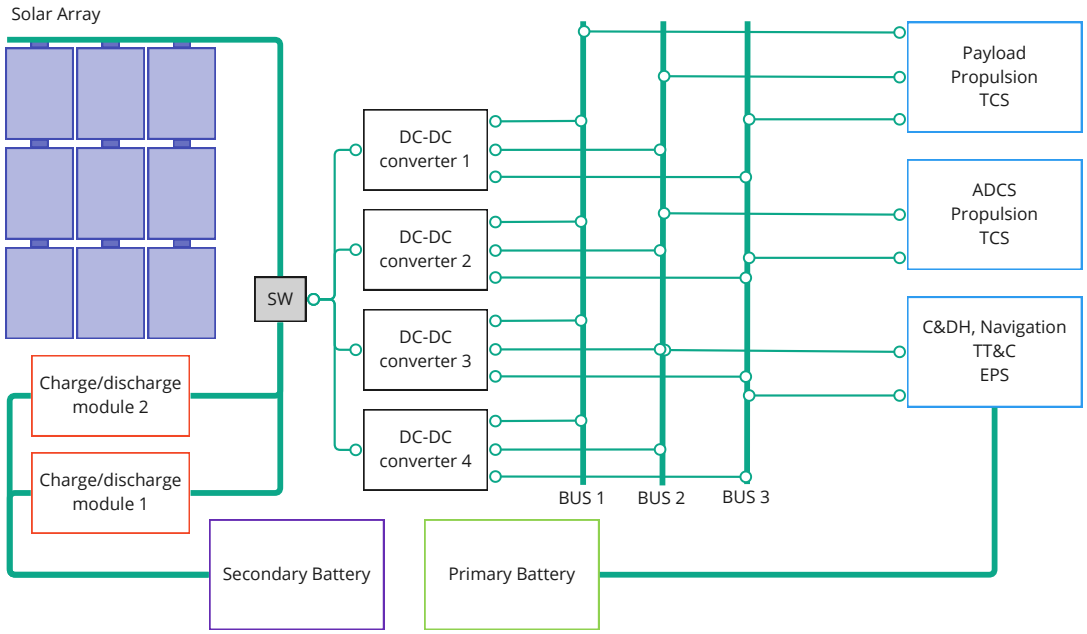

Figure 9.1: Block Diagram of the EPS.

time. Solar cell degradation grows in time due to radiation flux or molecular oxygen concentration. These effects can be mitigated by using solar cells with a protective coating and high radiation hardness, and by using a safety factor on the ageing rate. The battery capacity was sized with an assumed depth of discharge of 40%, leading to an expected lifetime of 70000 cycles (with acceptable capacity at the EOL). 70000 cycles correspond to 13.7 years of operation. That is with an assumption that each orbit has a 35% eclipse time, whereas for the selected polar orbit it happens only during the equinox (Section 9.2), making the capacity estimation even more conservative. The energy storage system is prepared to operate for 15 years.

9.6. Summary

The EPS system with Sparkwing solar array with AZURSpace 4G32C produce from 1926 W (EOL) to 2467 W (BOL). Energy for the eclipse phase is stored in ABSL cell-balanced Lithium Ion battery pack with a capacity of 2246 W h. The power distribution and management system is based on four DC-DC converters and two battery chargers that are assembled into an Airbus EVO power control unit. Table 9.5 gives a summary of the EPS components. Figure 9.1 is a block diagram of the EPS that shows connections between the main components and gives an overview of the system.

Table 9.5: Summary of the components used in EPS

Component	Name	Total Mass [kg]	Power [W]	Quantity
Solar array	Sparkwing panel	32	-	9
Solar cell	AZURSpace 4G32C	-[22]	-	1881[23]
Primary Battery	EXA BA0x	1.05	-	5
Secondary Battery	ABSL 8s52p	23	-	1
Drive Mechanism	Moog Type2 SADA	7	5	2
Power Management	Airbus EVO PCDU	4[24]	-	1

[22]Included in the Solar Array mass
[23](99 strings of 19 cells)
[24]Exact mass not specified for that model. The mass is of a unit with similar power capacity DHV PCDU

10 Command and Data Handling

The Command & Data Handling (C&DH) subsystem is a crucial part of the spacecraft design. It is responsible for connecting and controlling the different components of the spacecraft, acting as its "brain", encompassing all of the data and command processing tasks, carrying commands, preparing data for downlink, monitoring the State of Health (SoH) or performing regular testing on the on-board equipment[1]. This chapter includes the functional analysis of the C&DH subsystem in Section 10.1, a requirement identification in Section 10.2, the architecture and the configuration in Section 10.3 and Section 10.4, respectively. Finally a sensitivity analysis is presented in Section 10.5 and a summary in Section 10.6.

10.1. Functional Analysis

For the C&DH subsystem, five main functions were identified in the functional breakdown structure. These are the processing and distribution of the uplink signal from ground station, the monitoring of the spacecraft, the generation of commands, data storage and processing and message packaging for downlink to ground station. From these functions, two parameters were identified to have the greatest impact on the design of the subsystem; data rate and data storage. These are estimated in Section 10.1.1 and Section 10.1.2.

10.1.1. Data Rate Estimation

In regards to the payload, two sources of data rate must be considered; the payload data, which is known to be 6 Mbit s^{-1} already compressed on the payload itself, as explained in Section 5.3.2, and the telemetry data, for which no information is provided, and therefore a statistical approach has been used to estimate it [11].

Telemetry points comprise both sensors of the subsystems, and transducers distributed all over the S/C. They provide information about attitude, temperature, S/C location and orbit, the status of valves, forces, vibrations and radiation amongst many others [42][43]. To estimate the number of telemetry points each satellite will use, a linear regression was performed using the information on the number of telemetry points, their mass and the data rate of eight different spacecraft. Whilst the R-value of this regression can be visually determined to be rather low, it is used for a very preliminary estimation and is hence deemed sufficiently accurate. This table can be found on Table 10.1. A 1 Hz sample rate and 16 bit per sample are deemed sufficient [42]. Using an estimated weight for the spacecraft of 1450 kg, it is found that around 1650 telemetry points are needed, which translates to a data rate of 18 640 bit s^{-1}.

Table 10.1: Number of Telemetry Points per Spacecraft (Sampling Frequency: 1 Hz; 16 bits per sample)[42]

Spacecraft	Telemetry Points	Mass of S/C [kg]	Data Rate [bit s^{-1}]
Delfi C3	114	3	1824
Delfi n3Xt	135	3	2160
IntelSat 5	520	2519	8320
Eutelsat II	840	1878	13 440
SPOT	500	1907	8000
MSX	400	2700	6400
ERS	6600	2384	105 600
Envisat	13 700	8211	2 192 000

In relation to ground commands, which are explained in Section 10.2, an estimation is used based on the Sentinel-2 mission, in which 64 kbit s^{-1} are required[2]. A factor of 1.5[3] was applied in order to stay

[1] URL: www.mars.nasa.gov [accessed: 12/06/2023]

[2] URL: www.esa.int [accessed: 13/06/2023]

[3] URL: `https://ntrs.nasa.gov/api/citations/20140011147/downloads/20140011147.pdf` [accessed: 23/06/23]

within safe margins. For the internally produced commands, used to adjust the subsystems as required to maintain the desired performance, the same data rate as the uplink commands was assumed. This is considered a conservative approach as the internal commands tend to be less required. All of these estimations are summarised in Table 10.2.

Table 10.2: Estimation on Required Data Rate

Source	Required Data Rate [bit s^{-1}]
Payload	6×10^6
Telemetry	18 640
Commands	192 000
Total	6.21×10^6

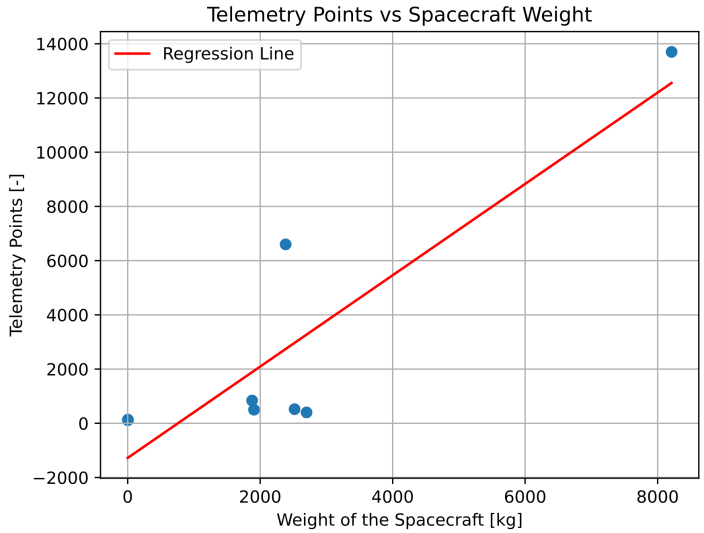

Figure 10.1: Telemetry Points vs Spacecraft with Regression Line

10.1.2. Base Data Storage Estimation

The two main sources of base data storage are the operating system and software data storage. The operating system used was selected to be VxWorks by WindRiver[4]. This is the case due to its high reliability, robustness and usage throughout the industry. It may not be the most user-friendly operating system, however, it is well documented and supported and via review of design it can be assumed that it should perform all the functions identified for it. From the developer of this operating system, the most conservative storage recommendatation was taken, that of 2 MB[5].

In regards to the software data storage, from an extensive literature research it was concluded that there is no standard, or agreement on the estimation of software size. Literature is available on the estimation of Source Lines of Code. This is a convenient parameter for the cost estimation of the software, however, it is not an accurate way of estimating the storage size of it. Therefore an analogical approach is taken. The OBC selected is currently being used in satellites with more complex architectures and similar weights. It was therefore deemed that if these satellites use the Constellation OBC to store this data, our spacecraft will be able to do it too. In later stages of the design, as components are designed or obtained, and the software can be written for them, more accurate measures can be obtained, and, if necessary, changes to the design can be made.

[4]URL: www.windriver.com [accessed: 21/06/2023]
[5]URL: www.uio.no [accessed: 20/06/23]

10.2. Requirements

The subsystem is divided into three main components: *Hardware*, *Software* and *Documentation*. The hardware comprises the physical segments of the subsystem. The software drives the hardware and determines how it will behave. Finally, all of these parameters have to be documented for manufacturers, users, clients or operators to understand the functioning of the system and interact with it, as well as test and understand its capabilities and limitations [12].

As with all the subsystems, the design process of this component has been driven by the functions it should perform. These are identified as five: process and distribute the uplink signal, monitor SoH, generate commands, store data, and process and prepare packages for downlink. This leads to the derivation of requirements, which are used to shape the final design of the subsystem. These are presented in Table 10.3.

Table 10.3: Command & Data Handling Subsystem Requirements.

ID	Requirement	Derived From
SUB-CDH-01	The C&DH subsystem shall be able to gather payload data	SYS-OPS-05
SUB-CDH-02	The C&DH subsystem shall manage the functioning of all subsystems and payload on-board	SYS-OPS-04, 08
SUB-CDH-03	The C&DH subsystem shall be able to store payload data up to a maximum of 5 Gb until it is transferred	SYS-OPS-05
SUB-CDH-04	The C&DH subsystem shall be able to transfer all produced data during two time dump fractions in one transmission window to the TT&C subsystem.	SYS-OPS-04
SUB-CDH-05	The C&DH subsystem shall be able to correct errors in the payload data	SYS-OPS-04
SUB-CDH-06	The C&DH subsystem shall be able to verify payload data	SYS-OPS-04
SUB-CDH-07	The C&DH subsystem shall be able to provide data link connections for interfacing with all subsystems and payload on board	SYS-OPS-04
SUB-CDH-08	The C&DH subsystem shall be able to gather S/C status data	SYS-OPS-08
SUB-CDH-09	The C&DH subsystem shall be able to store S/C status data up to a minimum of 132 Mb until it is transferred	SYS-OPS-08
SUB-CDH-10	The C&DH subsystem shall be able to process ground control commands	SYS-OPS-14
SUB-CDH-11	The C&DH subsystem shall be able to decode, authenticate, validate, process and distribute ground commands to all subsystems and payload	SYS-OPS-14
SUB-CDH-12	The C&DH subsystem shall receive data from the TT&C at a minimum data rate of 96 Kbps	SYS-OPS-14, SYS-OPS-14
SUB-CDH-13	The C&DH subsystem shall be able to transfer ground control commands to subsystems at a data rate of 96 Kbps	SYS-OPS-14
SUB-CDH-14	The C&DH subsystem shall transfer all stored data packages for downlink to TT&C	SYS-OPS-06, SYS-OPS-13
SUB-CDH-15	The C&DH subsystem shall have a maximum mass of 19 kg	Section 8.4
SUB-CDH-16	The C&DH subsystem shall operate at a peak power no higher than 49 W	Section 8.4
SUB-CDH-17	The C&DH subsystem shall have a outage time below 0.01%	MIS-OPS-02
SUB-CDH-18	The C&DH subsystem shall be able to receive upgrades 2 times per year without increasing mission downtime over 0.01%	MIS-OPS-02, hyperref[req:SUS-SPA-06]SUS-SPA-06, SUS-SPA-07
SUB-CDH-19	The C&DH subsystem shall verify all subsystems are meeting their functional and performance requirements every scanning cycle	SYS-OPS-13
SUB-CDH-20	The C&DH subsystem shall report functional and performance errors of any subsystem and payload to the ground station with a maximum delay of 24 hours	SYS-OPS-13
SUB-CDH-21	The C&DH subsystem shall comply with the CCSDS and ISO standards	SUS-SPA-09
SUB-CDH-22	The C&DH subsystem shall provide at least one level of redundancy	SYS-OPS-01
SUB-CDH-23	The C&DH shall provide SpaceWire connection to the payload unit	Payload Specifications [44]

As can be seen, each of the subsystem requirements has one or various associated system requirements. SUB-CDH-03 and SUB-CDH-09 is derived from the time dump fraction. As per the need of storing the data produced by both the payload and SoH acquisition. SUB-CDH-04 is driven by the transmission time and needs to downlink the stored data on a limited time interval. The obtention of the specific values can be found in Section 10.3.1.

Both SUB-CDH-12 and SUB-CDH-13 relate to the uplink. These were derived from the Sentinel-2 mission, which required 64 kbit s^{-1} [6]. A similar or even lower command uplink is expected as, although the missions have high similarity, the Sentinel-2 MSI instrument has higher complexity compared to IASI-NG [7]. Nonetheless, due to the scale and cost of the mission, a factor of 1.5[8] has been applied to this parameter.

The remaining requirements relate the functions to be performed (SUB-CDH-01, -02, -05, -06, -07, -08, -14, -19, -20), processing of signals (SUB-CDH-10, -11), weight of the hardware (SUB-CDH-15), power consumption (SUB-CDH-16), availability (SUB-CDH-17), upgradability (SUB-CDH-18), standardisation (SUB-CDH-21), and redundancy (SUB-CDH-22).

10.3. Command and Data Handling Architecture

As mentioned in Section 10.2, the C&DH subsystem is divided into three main components: *Hardware*, *Software* and *Documentation*. The design process and final options for each category are presented in this section. However, several defining decisions have to be taken first with respect to the architecture and functioning of this component. Primarily, either having space- or ground-based data processing, performing processing on either hardware or software and selecting between either a centralized or decentralized processing system [12].

Regarding whether the data processing is made on space or ground and the (de)centralization of the system; this can greatly influence the processing power and energy required. The solutions are straightforward. As explained in Section 5.3, the data processing from IASI-NG is performed on the processing unit of the instrument; which provides a 6 Mbit s^{-1} encoded signal, compliant with CCSDS 121 [11]. This means that no data processing from the instrument is necessary. The OBC only needs to create a data package of the IASI-NG and telemetry data for downlink. Because the SoH and command processing requirements are relatively low, a centralized OBC system is used. One exception is made for the EPS which will use its own control unit; the OBC will only transmit uplink commands and monitor the system.

In regards to performing the processing on either hardware- or software-based platforms; due to the technological capabilities, flexibility, reduced cost, upgradability and simplicity of software-based processing, this option is used [12][45]. In short, the C&DH subsystem will be a centralized, software-based processing arrangement without additional measured data processing than packing it with the downlink telemetry for the TT&C subsystem.

10.3.1. Hardware

On-Board Computer

The hardware of the C&DH subsystem is usually comprised of an On-Board Computer (OBC), a data storage unit, and the bus connectors. Once the general overview of the C&DH subsystem has been decided, and an estimation of the data rates is performed, the OBC and data storage device selection follow.

Respecting the OBC, a COTS solution is used due to available design time, reliability and legacy. A list of commercially available computers which met the requirements was made and a trade-off between them was performed. The criteria and analysis can be seen in Table 10.4 and Table 10.5 respectively.

[6] URL: www.esa.int [accessed: 13/06/23]
[7] URL: www.space.oscar.wmo.int [accessed: 13/06/23]
[8] URL: `https://ntrs.nasa.gov/api/citations/20140011147/downloads/20140011147.pdf` [accessed: 23/06/23]

Table 10.4: Trade-Off Criteria of the OBC

Criterion	Weight %	1	2	3	4	5
Dry Mass [kg]	20	> 12.9	≤ 9.9	≤ 6.8	≤ 3.4	≤ 3.4
Average Power [W]	20	> 47.5	≤ 47.5	≤ 36.6	≤ 25	≤ 12.5
Compatibility [-]	20	Very Low	Low	Medium	High	Very High
Storage Capacity [GByte]	15	<1.3	≥ 1.3	≥ 2.5	≥ 3.7	≥ 4.8
Cost [-]	15	Very High	High	Medium	Low	Very Low
Processing Capacity [DMIPS]	10	< 900	≥ 900	≥ 1800	≥ 2600	≥ 3420

Table 10.5: Analysis of the On-Board Computer Trade-Off Criteria

Criterion	Weight [%]	ICDE-NG[9]	Athena 3 SBC[10]	NextGen-eration OBC[11]	**Constella-tion OBC[11]**	OSCAR [12]	AMETHYST [13]
Dry Mass	20	1	5	3	3	4	4
Average Power	20	3	5	2	3	4	1
Compatibility	20	4	3	4	5	4	4
Storage Capacity	15	5	1	5	4	2	4
Cost	15	1	2	5	4	3	3
Processing Capacity	10	1	4	1	5	1	1
Weighted score		260	345	340	**390**	325	295

From the trade analysis in Table 10.5 it can be seen that the clear winner is the Constellation OBC from Beyond Gravity. The main processing characteristics can be found in list below:

- 2 x e500Core 800 MHz
- 3600 DMIPS
- 1600 MFLOPS
- 32 KB L1 instruction cache with parity
- 32 KB L1 data cache with parity
- 512 KB L2 cache with ECC
- 1 GiB DDR3 processing memory with ECC
- 4 GB non-volatile storage with ECC

This option outperformed its counterparts in both compatibility and processing capacity. It contains a total of 57 core interfaces for the most widely used connection standards in the industry: SpaceWire, CAN buses, Ethernet, RS422/RS485 UART, GPIO and M1553 BC. Despite having all these options, once the final connectors are chosen, in a later stage of the design, non-used interfaces are to be removed as they would only add weight without added value or redundancy. It also has the most powerful processing capabilities of all. Being higher by a factor of 10 or more for all other options but Athena 3 SBC, for which it is still 70% higher. Processing capacity and speed were especially important

[9]URL: www.airbus.com [accesed: 16/06/23]
[10]URL: www.seakr.com [accesed: 16/06/23]
[11]URL: www.beyondgravity.com [accesed: 16/06/23]
[12]URL: www.airbus.com [accesed: 16/06/23]
[13]URL: www.airbus.com [accesed: 16/06/23]

parameters as there is only limited sensor data processing, but mostly command and housekeeping processing which should be hard-real time, where processing time is critical.

The only inconveniences of this option are the relatively high mass and power consumption. Nonetheless, because it outperforms the other options in the rest of the parameters, as well as ensuring such a high degree of redundancy and reliability [14], and having a wide usage in the industry, it was decided to tolerate this.

For both storage capacity and cost it is still one of the best options. Providing 4 GByte non-volatile storage; enough to store the 49.4 49.4 Mbit required for the software and operating system. It is not capable however of holding the produced data from IASI-NG during a full orbit (only NextGeneration OBC would), which is 4.6 GB. For this reason, an additional data storage component is also used; namely GEN3 Flash Memory Card from SEAKR Engineering LLC., with a capacity of 192 GByte. Allowing the storage of data for both the instrument and telemetry for 41 full orbits. It also contains two memory mezzanine cards, allowing for redundancy.

Furthermore, the internal architecture of the computer is fully duplicated, creating full redundancy. If the main core fails, the redundancy takes on and allows for software updates without service disruption. Also enabling hot sparing, allowing for periodical function, reducing the possibility of a second failure [46]. The selected OBC's flight heritage includes: Göktürk-1, ExoMars Trace Gas Orbiter or Sentinel 2A and 2B further bolsters confidence in it.

In regards to cost, this option scored the second highest grade as the system cost is below 200k€. Furthermore, it was deemed more convenient, in this aspect, to make use of a OBC rather than a SBC, due to the simplicity of implementation and reduced costs in further compatibility and structural aspects.

Interfaces

The interfaces are also an important component to make a decision on. It is mainly driven from the OBC, for which compatibility was an important criterion. Two main types of connection have been identified for the spacecraft: payload and subsystems.

The payload connection is restricted to the use of SpaceWire, as this is the only interface available for IASI-NG [44]. It allows for speeds of between 2 Mbit s^{-1} and 100 Mbit s^{-1}. This is well within the need of 6 Mbit s^{-1} [47], and it is fully compatible with the OBC selected. Spacewire offers a latency of only 10 µs.

In regard to telemetry and command transmissions, the RS485 protocol was selected. Although being a relatively old protocol it is widely used in the industry, has low latency (1.1 ms), allows for a data rate of up to 10 Mbit s^{-1} and low noise due to its working principle, and is highly reliable. Moreover, the OBC has 18 ports for RS485, allowing for more connections with reduced extra components [15]. All data connections, both inside and outside the OBC, as seen in Figure 10.2, are doubled for redundancy.

10.3.2. Software

As mentioned previously, all the processing on-board is to be made software-based. In this sense, several dedicated software components are to be used for each subsystem. In this sense, at least 7 components are required: *executive*, *communications*, *attitude and orbit sensor processing*, *attitude determination and control*, *actuators processing*, *fault detection*, *SoH sensors processing* and *utilities* [12]. The development of this software has been left open for future actions in the design and production of the satellite. Furthermore a testing software is also included in order to regularly test the components of the spacecraft (at least once per scanning cycle).

In order to assess the quality of the software developed, as it will be made in house, a requirement is set to comply with CCSDS standards. In regards to software, the most important CCSDS document to

[14] URL: www.escies.org [accessed: 16/06/23]
[15] URL: www.analog.com/RS485quickguide [accessed: 21/06/23]

comply with is the Spacecraft On-Board Interface Services Green Book. Therefore the ISO 49.140 set of standards on space systems and operations - standards regarding software and interfaces - will be used for the development of the on-board software.

10.3.3. Documentation

Documentation is also an important aspect of the C&DH subsystem design. Namely all the components, from the OBC and software to interface/bus should be documented in detail for different types of audiences and therefore different levels of detail. Five main categories of documents can be identified for different purposes and phases of the design, namely: requirements, program management, design, implementation, testing and deployment. Around 27 documents are to be made to get an idea of how the C&DH subsystem will look and behave (both hardware- and software-wise), to the full functioning of it.

10.4. Data Handling Configuration

After the preliminary design and selection of the components and links for the C&DH subsystem previously explained, an overview can be obtained on how the subsystem will look. The block diagram can be seen in Figure 10.2.

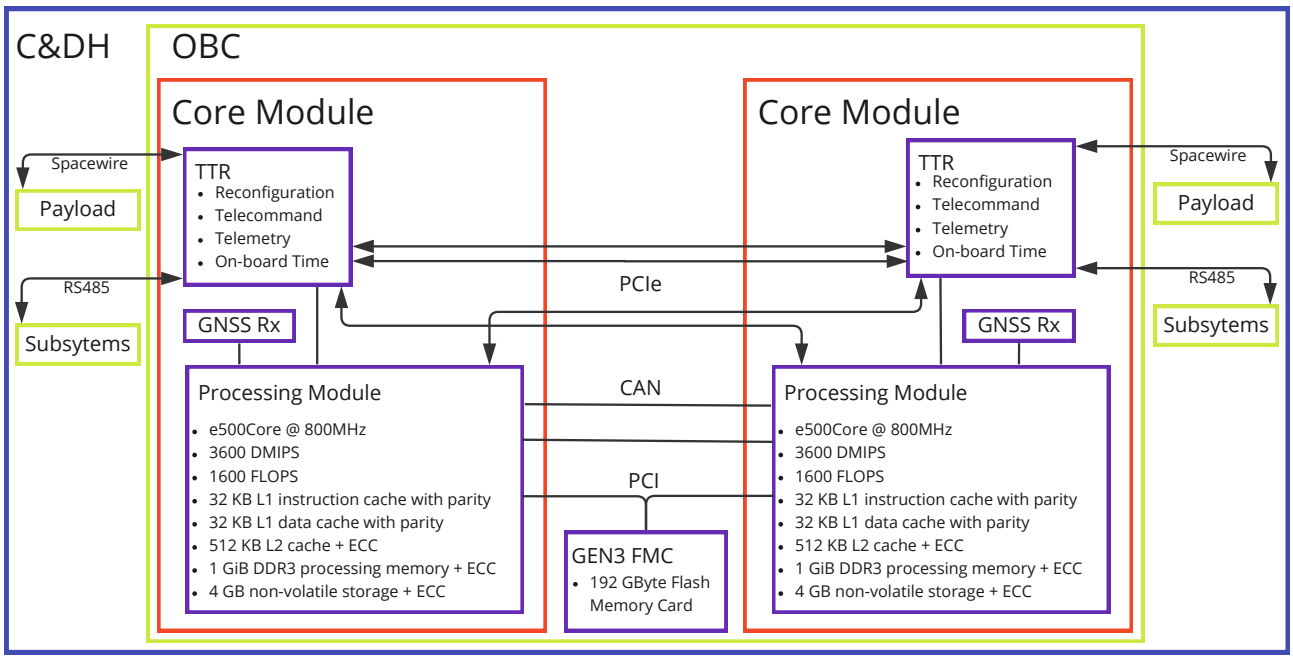

Figure 10.2: Command and Data Handling Block Diagram.

As can be seen in the block diagram, the C&DH subsystem will be composed of a fully redundant OBC, an extra data storage device (located inside the computer) and Spacewire/RS485 external connections, as well as Peripheral Component Interconnnect (PCI) express, PCI and Controller Area Network (CAN) internal conectors.

In regards to the OBC, as it can be seen in Figure 10.2, it is formed by three main components: telemetry and telecommand module, GNSS receiver, and processing module. The telemetry module is the one connecting to the payload and subsystems for data acquisition. The processing capabilities of the processing module can be seen in Figure 10.2. The GNSS recevier for navigation is implemented into the computer itself. The extra storage device has also been placed inside the OBC adding 192 GBytes to the current 4GBytes it provides standalone.

In regards to interfaces and conectors, SpaceWire will be used to connect to the payload as this is the only interface the latter provides. For receiving telemetry information and sending commands to the subsystems, RS485 Bus will be used. Inside the computer, PCIe connections are used between

the telemetry modules. PCI connectors are also used between the processing modules and the extra storage device, and CAN connectors between the two processing modules. Finally, software is also a core segment of the C&DH subsystem. Which will be stored in the OBC integrated memory and processed by the processing module.

10.5. Sensitivity Analysis

A sensitivity analysis is performed on the C&DH subsystem in order to assess the limitations and strong points of the design, as well as its susceptibility to strong changes due to a change in the requirements. The most critical mission parameters that could affect the subsystem design are the instrument, the lifetime of the spacecraft, the mass and power budget, and the zone of interest.

The biggest effect would come from the instrument. If it is changed, a different data storage capacity and bus/interface could be required. If the new requirements lower the volume of data, the spacecraft design would not be affected. The C&DH could be optimized by using less performing equipment, and if the total volume decreases below 3.75 GB, the external storage unit would not be necessary, with OBC sufficing. This would result in a cost reduction. On the other hand, if the new instrument requires a rise of 435% in data storage, an extra storage device would be needed. Data storage devices, with their small dimensions, would primarily affect power consumption and cost.

In regard to the bus/interface, the new instrument may, or may not be compatible with Spacewire. Nonetheless, the OBC was chosen such that it could offer the highest compatibility, therefore it would be expected that due to standardisation, the new instrument would be compatible with some of the current OBC bus/interface connectors, directly or through a converter.

Another major sensible parameter on the C&DH design is the lifetime of the spacecraft. The current lifetime of the COBC is at least 10 years in LEO. Current LEO missions only last between 7 to 10 years [31], and most of the components of these satellites are designed for such a period. Nonetheless, as it has already been proven before with Landsat 5, satellites with a 3-year lifetime design can last up to 30 years[16]. Hispasat 36W-1, which currently uses the same OBC has a lifetime of 15 years, meaning the critical part of the C&DH subsystem can withstand a lifetime rise up to 15 years. For longer lifetimes, necessary tests and further investigation should be done for the need of plausible but unlikely design changes.

The mass and power budgets are highly influencing factors in the design of the subsystem. If the weight and power requirement were to decrease by 65% and 17%, a new OBC or bus/interface would be required to meet the requirements. Lastly, a change in the zone of interest of the mission would result in no effects on the C&DH design, as it is already designed to cover - store and manage data - for the whole of the Earth.

10.6. Summary

The C&DH is made up of the following components. An OBC with a fully redundant architecture, 32-bit e500 processor, 10 GB processing memory and 4 GB non-volatile memory. In addition to this, inside the OBC hardware a 192 GB Flash Memory Card is also installed. The total mass of this is of 6.7 kg with power consumption of 35 W, and an estimated cost of around 100 k€.

The subsystem takes care of the SoH, uplink and downlink command processings and payload data storage until downlink, requiring a total storage of 4,6 GBytes for a full orbit, and around 2,3 GBytes between transmissions. For this, two connection protocols will be used: SpaceWire for payload connection, allowing speeds of up to 100 $\mathrm{Mbit\,s^{-1}}$ and latency of 10 µs; and RS485 for telemetry and command data, allowing speeds of up to 10 $\mathrm{Mbit\,s^{-1}}$ and latency of 1.1 ms.

The VxWorks operating system from WindRiver will be used together with around 7 software to perform all the functional processing tasks of the spacecraft and its subsystems as well as regular testing throughout the mission.

[16]URL: www.landsat.gsfc.nasa.gov [accessed: 16/06/23]

11 Telemetry, Tracking & Communication

This chapter will focus on the design of the Telemetry and Communications (TT&C) system. Firstly, the functions and requirements of the TT&C will be discussed in Section 11.1 and Section 11.2, respectively. After that the components of the TT&C will be chosen and the functioning of the TT&C will be established in Section 11.3. Finally, the robustness of the TT&C configuration will be discussed in Section 11.4 and the subsystem will be summarized in Section 11.5.

11.1. Functional Analysis

The primary function of the TT&C subsystem is to facilitate communication with the satellite. It serves as an interface between the C&DH system and the ultimate data recipient. This process involves two distinct parts: downlink and uplink. Downlinking refers to the transmission of data to the ground, whereas uplinking involves receiving data from the ground.

The process of downlinking information includes two key components. The first component pertains to the spacecraft's principal function—the transmission of acquired mission data. This payload data is received by the ground segment and subsequently relayed to the operational command. Additionally, system health and status information gathered by the C&DH are transmitted to the ground station, ensuring that the operational command remains informed about the spacecraft's current state.

When the operational command needs to send instructions to the spacecraft, an uplink is established, and commands are transmitted. This process allows for the control of both the spacecraft and the scientific mission. The uplink also provides the possibility of upgrading system software components [48]. However, this uplink could expose the system to potential malicious attacks. Malicious attempts to input commands could jeopardize or harm the mission [49]. Therefore, ensuring the secure transfer of information is a key principle of the uplink process [50]. It was deemed that, as opposed to uplink, downlink would not expose the system to attacks because there is no way to directly impact the functioning of the satellite through intercepting downlink.

11.1.1. Concept of Data Dissemination

The scientific payload generates mission-specific data. This data, along with geolocation information, is processed through the C&DH. The C&DH compiles this data with all other system information. The resulting data packages then pass through the TT&C and are received at the ground station. Subsequently, this information is transmitted to the operational command, which uses it for its specific purposes.

The mission serves a dual purpose. It aids in monitoring radiative forcing of exhaust trails to expand scientific knowledge. Concurrently, it contributes to improving the economic position and pricing strategy of the NOMS. Therefore, the data acquired by the satellite is sensitive and requires protection. A point-to-point data dissemination architecture is selected for its secure and robust communication link. Although this increases pointing complexity and requires higher precision antennas, it results in a higher signal-to-noise ratio at equivalent output powers [12].

11.2. Requirements

The functions of the TT&C, system configuration, and the mission profile lead to the following subsystem requirements shown in Table 11.1.

Table 11.1: Sub-system Requirements for the TT&C Subsystem

ID	Requirement	Source [1]

SUB-TTC-01	The TT&C subsystem shall always be able to establish a link to ground stations during nominal operations	SYS-OPS-04, SYS-OPS-06
SUB-TTC-02	The TT&C subsystem shall adhere to compatibility standards set by authoritative institutions	SYS-OPS-04, SYS-OPS-06
SUB-TTC-03	The TT&C subsystem shall be able to receive data from ground stations at a data rate of 96 kbps	SYS-OPS-13
SUB-TTC-04	The TT&C subsystem shall be able to transmit all produced data by the C&DH subsystem during two time dump fractions in one transmission window. MIS-FUN-01, SYS-OPS-04, SYS-OPS-06	
SUB-TTC-05	The TT&C subsystem shall be able to transfer data to the C&DH subsystem at a data rate of 96 kbps	SYS-OPS-13
SUB-TTC-06	The TT&C subsystem shall be able to receive all produced data by the C&DH subsystem during two time dump fractions in one transmission window.	
SUB-TTC-07	The TT&C subsystem shall have a maximum mass of 55 kg	SYS-CON-08
SUB-TTC-08	The TT&C subsystem shall provide redundancy during non-nominal operation	MIS-OPS-02, SYS-OPS-01
SUB-TTC-09	The TT&C subsystem shall make use of standardised sub-system interfaces	SUS-SPA-09
SUB-TTC-10	The TT&C subsystem data throughput shall have a bit error rate not exceeding 10^{-4}.	*Space Mission Engineering: The New SMAD*
SUB-TTC-11	The TT&C subsystem shall provide uplink encryption in accordance with FCC standards	47 CFR Part 97[1]

It can be seen that requirements SUB-TTC-03 until SUB-TTC-06 define the volume of data handling needed during transmission windows. The data rate needed for uplinks and sending data to the TT&C system is defined as 96 kbit s^{-1} (64 kbit s^{-1} with a 1.5 margin) derived in Section 10.1.1. The required data volume for downlink is defined using the data production rates derived in Section 10.1.1, and the time dump fraction determined later in this chapter. Requirement SUB-TTC-11 defines the maximum allowed bit error rate which was derived from [12].

11.3. Configuration

For the configuration of the TT&C, a ground station needs to be selected first, which is done in Section 11.3.1. Afterwards, a link budget is designed in Section 11.3.2 before the downlink and uplink components are selected in Section 11.3.3 and Section 11.3.4, respectively.

11.3.1. Ground Station Selection

In order to guarantee robust and efficient communication with the three polar-orbiting satellites, the strategic selection of ground stations and communication frequency bands is crucial.

Given that the satellites are in polar orbits, they pass over the Earth's poles more frequently than any other location. This situation points towards the need for locations near the poles, providing enhanced visibility and communication opportunities. Locations near the equator would offer fewer communication opportunities due to the high inclination of the satellites' orbits. Another essential aspect is the minimization of potential radio frequency interference, which calls for a preference towards sparsely populated areas or regions with strict controls over local radio frequency emissions.

Taking these considerations into account, it was decided to use two ground stations: one near the north pole and one near the south pole. Both of the ground stations will be part of the Kongsberg Satellite Services[51]. The ground station near the north pole will be the SvalSat Ground Station on Svalbard. The SvalSat site is located on the Platåfjellet plateau at 78°14'N and 15°24'E at 450 m above sea level. The ground station near the south pole will be the Trollsat Ground Station in Antarctica. The Trollsat site is located 72°S and 2°E at 1365 m above sea level. Both ground stations have a similar 7.3 m antenna for transmitting in X-band and receiving in S-band [52] [53].

11.3.2. Link Budget

The link budget is an important tool in the TT&C subsystem design. It allows for a trade-off between antenna size, input power and data rate. The link budget equation is given in Equation (11.1).

$$\frac{E_b}{N_0} = \frac{PL_l G_t L_s L_a G_r}{kT_s R} \tag{11.1}$$

In Equation (11.1), $\frac{E_b}{N_0}$ is the ratio of received energy per bit to noise density, P is the transmitter power, L_l is the transmitter-to-antenna loss, G_t is the transmitting antenna gain, L_s is the space loss, L_a is transmission path loss, G_r is the receiving antenna gain, k is the Boltzmann's constant, T_s is the system noise temperature, and R is the data rate. For this case, STK was used to change the free variables and find the optimal configuration and this configuration was validated by hand. After modifying the free variables in STK, the optimal values were found and are given in Table 11.2.

Table 11.2: Optimal Free Variables for Uplink and Downlink

	S/C Antenna Size [m]	S/C Antenna Power [dB W]	Link Frequency [GHz]	Transmitting Data Rate [Mbit s^{-1}]
Downlink	0.5	-10	8.03	100
Uplink	0.05	0	2.2	0.192

The uplink and downlink link budgets were calculated with the Svalbard ground station over 24 h and 15 transmission windows. The lowest energy per bit to noise density ratio of every transmission window was inspected to be similar. One transmission of both uplink and downlink is given in Figure 11.1.

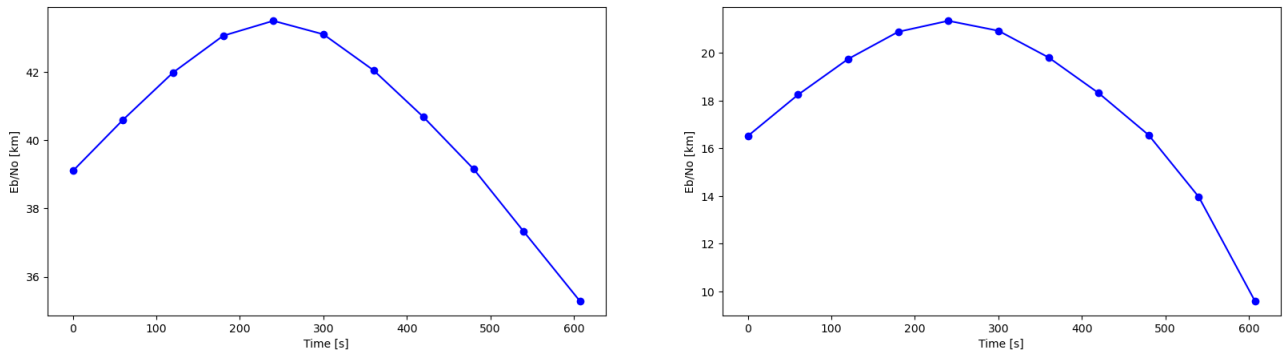

(a) Uplink Margin

(b) Downlink Margin

Figure 11.1: $\frac{E_b}{N_0}$ of One Transmission Window over the Svalbard Ground Station Simulated using STK

It can be seen that the uplink has a significant margin at around 35 dB. It was decided that going lower than 0.05 m for the S/C antenna size is not sensible and therefore the link budget for uplink could not be further optimized. The lowest link margin for the downlink will be around 9.5 dB. The full link budget tables are given in Table 11.3.

Table 11.3: Link Budgets for Uplink and Downlink

	Downlink	Uplink
Transmitter Power (P) [dB W]	-10.00	16.99
Transmitter Gain (G_t) [dB]	29.88	41.93
Effective Isotropic Radiated Power (EIRP) [dB W]	19.88	58.92

[1]URL: www.law.cornell.edu [accessed: 21/06/2023]

Free Space Loss (L_s) [dB]	179.6	168.4
Atmospheric Loss (L_a) [dB]	2.04	1.74
Rain Loss (L_r) [dB]	2.41	0.04
Propagation Loss (L_p) [dB]	184.1	170.2
Received Power [dB W]	-164.2	-111.3
Flux Density [dB W m^{-2}]	-124.7	-82.96
Receiver Gain (G_r) [dB]	53.17	-1.36
Atmospheric Noise Temperature (T_{atmos}) [K]	77.72	68.52
Rain Noise Temperature (T_{rain}) [K]	111.7	5.06
Antenna Noise Temperature ($T_{antenna}$) [K]	189.5	172.6
Earth Noise Temperature (T_{earth}) [K]	0	98.98
System Noise Temperature (T_s) [K]	627.9	611.0
Gain-to-Noise-Temperature ($\frac{G}{T}$) [dB K^{-1}]	25.19	-29.22
Bandwidth (B) [kHz]	2.00×10^5	384.0
E_b/N_0 [dB]	9.58	35.28
Bit Error Rate	1.01×10^{-5}	1.00×10^{-30}

In Table 11.3, the transmitter power and transmitter gain were free variables for downlink and specifications of the ground stations for uplink. EIRP was a function of the transmitter power and gain. The free space loss was calculated using the Friis transmission formula[54]. The atmospheric loss was calculated using the ITU-R P676 model[2] and the rain and propagation loss were calculated using the ITU-R P618 model[3]. The received power and flux density are functions of the previous parameters and were calculated by STK. Receiver gain was given by the ground stations for the downlink and was a free variable (dependent on antenna size) for the uplink. The atmospheric, rain, earth, and thus also the system noise temperatures were also calculated by STK using ITU-R models[2][3]. The antenna noise temperature was calculated by STK dynamically using the angles between the transmitter and receiver. After that, the Gain-to-Noise-Temperature, E_b/N_0, and Bit Error Rate are functions of previous variables.

It must be noted that the link budget given in Table 11.3 is calculated for the end of the transmission period, which is the most limiting due to high noise temperature figures. It was determined that the system noise temperature during the end of transmission is a factor of 1.4 larger than the system noise temperature in the middle of the transmission. This is due to increased atmospheric and rain noise temperatures when the signal has to go through more matter. This numerical link budget calculation was verified with Equation (11.1) and similar values were achieved. The values obtained from this calculation were used to choose the components making up the TT&C subsystem.

11.3.3. Downlink Component Selection

The primary function of the TT&C subsystem is to act as an interface between the spacecraft and entities on the ground or in space. For data transmission, the TT&C needs to convert data from the C&DH subsystem into a format suitable for antenna transmission. For data reception, the TT&C must convert the signal from the antenna into a format readable by the C&DH. This is typically accomplished using a transmitter and a receiver, or a combination of the two, a transponder. In this case, due to different downlink and uplink frequencies, the transmitter and receiver must be separate.

The downlink system generally consists of a modulator, amplifier, low-pass filter, antenna feed, and reflector. The chosen instrument is the X-Band High Rate Mission Data Transmitter (HRT-440) by General Dynamics, which integrates an SQPSK modulator, forward error correction coding, and a solid-state power amplifier[4]. This instrument was selected due to its compatibility with other subsystems and adherence to the requirements. It supports up to a 440 Mbit s^{-1} uncoded data rate and 384 Mbit s^{-1} with encoding. Additionally, it weighs 2.3 kg and operates at 30 W. To ensure compatibility with the C&DH subsystem for data transmission, the onboard computer was verified

[2]URL: www.itu.int/P676 [accessed: 13/06/2023]
[3]URL: www.itu.int/P618 [accessed: 13/06/2023]
[4]URL: www.gdmissionsystems.com [accessed: 15/06/2023]

to allow an 8-bit parallel connection. The transmitter power was compared to the −10 dB W power calculated in Section 11.3.2 to confirm the link budget closure. With the solid-state power amplifier, the transmitter can provide −8.24 dB W, enough to close the link budget. The transmitter does not have built-in redundancy and therefore two identical instruments are added to the system. The next part of the downlink sequence, the low-pass filter, will be implemented manually rather than purchased commercially. The antenna feed selected is the X Band Feed from EOSOL Group[5]. Due to the small size requirement for the reflector and the need for control over the link budget, it was decided to manufacture the reflector manually. Both downlink and uplink antennas are mounted on a 4.4 kg Type 33 Biaxial Gimbal produced by Moog, which allows for 0.02° accurate antenna pointing and consumes 10 W during operation[6].

11.3.4. Uplink Component Selection

To provide a reliable uplink and ensure a seamless interface between the spacecraft and ground control, the TT&C subsystem consists of a distinct set of components. In addition to a reflector and antenna feed for capturing radio wave transmissions, the system requires components to amplify, demodulate, decode, and decrypt the transmission before forwarding the information to the C&DH. After careful consideration and referencing the requirements discussed in Section 11.2, the core of the uplink functionality is performed by the 7.5 kg S-band SSTRX-3000 TM/TC Unit[7]. This unit integrates Binary Phase-shift Keying (BPSK) modulation, adhering to the modulation standards set by the ground stations. It is a transceiver, thus combining a transmitter module with a receiver module. The integrated diplexer enables two-way communication on a single antenna. Section 11.4 elaborates on the considerations of redundancy, enabled by using this component. The unit supports data reception rates ranging from 2 kbit s^{-1} to 256 kbit s^{-1}, and filtering is performed using a low-pass filter. Under nominal operating conditions during uplink, the transceiver consumes 4 W. To meet the encryption requirements for uplink, the receiving module is connected to the 0.75 kg MCU-110C integrated encryption/decryption module[8]. Operating at 8.45 W, it enables uplink data decryption at a rate of 5 Mbit s^{-1}. Similar to the downlink reflector, the uplink S-band reflector will be developed in-house.

11.4. Sensitivity Analysis

To check the robustness of the configuration, its redundancy is analysed for non-nominal operations in Section 11.4.1. Moreover, the chosen TT&C configuration is also analysed for its performance for changing mission parameters. This is done in Section 11.4.2.

11.4.1. Design for Redundancy and Non-nominal Operation

One of the most critical and high-impact risks is the loss of link with the ground station. This situation could be triggered by a variety of causes, including atmospheric anomalies, volcanic eruptions, or radar site outages.

Incorporating gimballed antennas into the design permits operational flexibility. In the event of detected anomalies in communication links, these antennas, capable of precise yet flexible pointing, enable the utilisation of backup data relay via space-based satellite communication networks [55], such as SpaceLink[9] or the Kepler Network[10].

For the downlink components, there are two X-band transmitters to guarantee operation during the nominal lifetime. Similarly, the S-band transceiver is fully redundant, incorporating two S-band transmitters and two S-band receivers. This redundancy provides fail-safe two-way communication over the S-band using a space-relay satellite. While the system still relies on a single gimbal which

[5]URL: www.satsearch.co/XBandFeed [accessed: 15/06/2023]
[6]URL: www.moog.com/type33 [accessed: 15/06/2023]
[7]URL: www.satcatalog.com/SSTRX-3000 [accessed: 15/06/2023]
[8]URL: www.l3harris.com/MCU-110C
[9]URL: www.eosspacelink.com [accessed: 16/06/2023]
[10]URL: www.kepler.space [accessed: 16/06/2023]

mounts the antennas, the actuator of the gimbal integrates redundant three-phase motors[11] and is electrically and mechanically isolated from the TT&C subsystem.

11.4.2. Sensitivity to Mission Parameters

The current design of the TT&C subsystem incorporates performance margins, as discussed in section 11.3.2. Nevertheless, altering mission parameters can still influence the design of the TT&C. The most sensitive parameters include cost budget, power budget, and zone of interest.

If the cost budget is reduced or funds allocated to the TT&C are shifted to a different subsystem, the performance of the TT&C will degrade. The selection of less expensive components will negatively affect factors such as pointing accuracy, bit-error rate, and EOL performance.

Changes in the power budget will also necessitate component changes. Components with lower power consumption will be needed, which will degrade the system's performance. A significant reduction in input power will eliminate the link margin redundancy, prompting a comprehensive redesign of the reflector and other components. While the development and manufacturing of the reflectors are controlled in-house, they are subject to geometrical constraints and budget restrictions. The X-band is more sensitive to changes in the power budget as the link margin is smaller, compared to the S-band link, which has a larger margin.

A direct consequence of changing the zone of interest is a change in orbit, which influences the selection of the concept of data dissemination. These changes can be mitigated by extending the transmission window from the currently lax window of just over a minute or selecting different locations for ground stations. If no ground station is available, both X-band and S-band communication links can utilize a space-based relay system to maintain communication. Changes in orbits could lead to a redesign of the reflectors to alter the required beamwidth, which in turn impacts the link design. These impacts are minimal on the subsystem design itself, but significant upon on the concept of data dissemination.

11.5. Summary

In summary, the TT&C enables two-way communication between the ground and the spacecraft. It utilizes high data rate X-band protocols for payload data downlink and less weather-affected S-band protocols for command uplink. The spacecraft is linked to the ground stations twice per orbit since the stations are situated at polar locations. Both the Antarctic Trollsat and Svalbard SvalSat sites are equipped with a 7.3 m antenna dish. The spacecraft is equipped with a 0.5 m downlink antenna and a 0.05 m uplink antenna. With a transmission data rate of 100 Mbit s^{-1}, this setup allows for a 9.58 dB downlink margin and, at 0.192 Mbit s^{-1}, a 35.28 dB uplink margin. To ensure operation even in non-nominal conditions, the critical components are redundantly integrated. Furthermore, a reliably designed redundant gimbal enables the relay of information using different ground stations or space-based relay networks. The components integrated into the TT&C subsystem are summarized in table 11.4.

Table 11.4: Summary of the Chosen TT&C Components

Type	Component	Instrument	Quantity	Average power [W]	Peak power [W]	Mass [kg]
Downlink	Transmitter	GD HRT-440	2	0	15	2.3
	Reflector	in-house	1	0	0	2
	Feed	EOSOL X-band	1	0	0	1.25
	Gimbal	MOOG type-3	1	10	10	4.4
Uplink	Transceiver	SSTRX-3000 TM/TC	1	4	16	7.5
	Reflector	in-house	1	0	0	0.02
	Decryptor	L3Harris MCU-110C	1	0	9.45	0.75
Total				14	50.45	20.52

[11] URL: www.moog.com/type3actuator [accessed: 16/06/2023]

12 Control Systems

This chapter discusses the design of the control systems of the spacecraft, this includes the design of the Attitude Determination & Control System (ADCS) and the design of the navigation system. Section 12.1 breaks down the control modes and their resulting requirements for the ADCS. The disturbance torques resulting from the orbit are then discussed in Section 12.2 with the required components to control the spacecraft against these torques chosen in Section 12.3. Section 12.4 defines the requirements for the navigation system and Section 12.5 then discusses the components needed to meet the positioning requirements of the satellites. The sensitivity of the control system to mission changes is analysed in Section 12.6 and the chosen components for the system are summarised in Section 12.7.

12.1. Attitude Determination and Control System Requirements

The Attitude Determination & Control System (ADCS) is a vital subsystem that ensures the spacecraft's and to that extent, the payload's, pointing is controlled and accurate. There are a number of ADCS methods which vary between spacecraft and the first step in designing the ADCS is to determine the desired control method. Based on the mission design and payload requirements a *zero-momentum 3-axis stabilised* control method needs to be used in order to provide stable pointing towards the nadir during operation. This decision constrains the design in a number of ways, primarily, it indicates that the spacecraft will require a high level of control on a day-to-day basis to accurately point to locations of interest and to maintain stable pointing against disturbance torques.

12.1.1. Control Modes

For sub-system requirements to be set the control modes of the ADCS are determined. These control modes flow down from the mission and subsystem design completed thus far. These modes define the operation of the ADCS in every situation the spacecraft may encounter. This ranges from the initial launcher ejection to End of Life (EOL) procedures. These modes are defined in Table 12.1.

Table 12.1: The Control Modes of the Attitude Determination & Control System (ADCS) Subsystem

Control Mode	Description
Acquisition	Tumble stabilisation with coarse attitude measurements. This mode is entered when the spacecraft separates from the launcher in order to damp out disturbances. It is entered in recovery situations if the spacecraft is disturbed from the nominal control mode.
Nominal	3-axis stabilisation towards the nadir and strict attitude maintenance with fine attitude measurements for nominal operations. This mode is entered into from the acquisition mode to provide stable and robust pointing for the payload system.
Slew	Stabilisation and fine attitude control while providing a change in attitude about one axis. This mode is entered into from the nominal mode and provides accurate pointing and stabilisation while performing a slew. This mode can also be entered at EOL to turn the spacecraft in the nadir direction so that a de-orbit burn may be performed.
Contingency	Tumble stabilisation and coarse pointing with minimum thermal output and power consumption. This mode is entered in emergency situations and utilises redundant systems to provide independency from the nominal control mode.

12.1.2. Requirements

The control modes in combination with the pointing required by the payload and overall mission design dictate the sub-system requirement development. These sub-system requirements are shown in Table 12.2.

Table 12.2: Subsystem Requirements for the Attitude Determination & Control System (ADCS)

ID	Requirement	Derived From
SUB-ADC-01	The ADCS subsystem shall have a fine measurement attitude knowledge accuracy of 0.01°	SYS-OPS-10
SUB-ADC-02	The ADCS subsystem shall have a pointing stability of at least 0.1° over 60 s in its nominal control mode	SYS-OPS-10
SUB-ADC-03	The ADCS subsystem shall have a maximum absolute pointing accuracy of 0.1°	SYS-OPS-10
SUB-ADC-04	The ADCS subsystem shall be 3-axis stabilized in its nominal control mode	SYS-OPS-09
SUB-ADC-05	The ADCS subsystem shall limit the bias error of fine sensors to a maximum of 15″ in its nominal control mode	SYS-OPS-10
SUB-ADC-06	The ADCS subsystem shall have a minimum slew rate of $0.05\,^{\circ}\,s^{-1}$ about all axes	SYS-OPS-11
SUB-ADC-07	The ADCS subsystem shall correct for torques arising from solar radiation	SYS-OPS-20
SUB-ADC-08	The ADCS subsystem shall correct for torques arising from gravity gradients	SYS-OPS-20
SUB-ADC-09	The ADCS subsystem shall correct for torques arising from Earth's magnetic field	SYS-OPS-20
SUB-ADC-10	The ADCS subsystem shall be able to receive pointing commands from the C&DH subsystem	Functionality
SUB-ADC-11	The ADCS subsystem shall be able to transfer current pointing to the C&DH subsystem	Functionality
SUB-ADC-12	The ADCS subsystem shall have a maximum mass of 90 kg	SYS-CON-07
SUB-ADC-13	The ADCS subsystem shall have a average power usage of 150 W	SYS-OPS-16
SUB-ADC-14	The ADCS subsystem shall have a average power usage of 100 W in its contingency mode	SYS-OPS-16
SUB-ADC-15	The ADCS subsystem shall be able to stabilise along all axes from tumbling within one orbit	SYS-OPS-09

The requirements from SUB-ADC-01 to SUB-ADC-06 comprise of the pointing requirements of the ADCS. These are generated from the pointing requirements of the IASI-NG payload [11]. The remaining requirements stem from the need to maintain stable pointing during disturbances and basic subsystem functionality requirements. By analysing these requirements, key and driving requirements are found to be the following:

- **Key**: SUB-ADC-07, SUB-ADC-08, SUB-ADC-09
- **Driving**: SUB-ADC-01, hrefreq:SUB-ADC-03SUB-ADC-03, SUB-ADC-04, SUB-ADC-05

12.2. Attitude Determination and Control System Disturbance Environment

The environment of LEO presents a greater number of challenges for satellites than that of MEO or GEO due to the close proximity to Earth. This results in greater disturbances from gravity gradient effects, magnetic field influence and aerodynamic drag resulting in a greater overall torque felt by the spacecraft [56]. The ADCS will need to manage and counteract these torques in order to meet the stability and pointing requirements of the mission and the magnitude of these torques allows the components of the ADCS to be selected

12.2.1. Gravity Gradient

Gravity gradient torques are induced by a misalignment between spacecraft axes and the nadir direction. Due to gravity following the inverse square law, when a spacecraft's mass is not evenly distributed around its horizontal axis, masses at lower altitudes will experience a greater downward gravitational force than those at higher altitudes. This gives rise to a rotational torque about the axis normal to the nadir. The maximum gravity gradient torque experienced by the spacecraft can be

calculated with Equation (12.1) [12].

$$T_g = \frac{3\mu}{2R^3}|I_z - I_x| \sin(2\theta) \tag{12.1}$$

Where T_g indicates the gravity gradient torque in N m, μ is the gravitational parameter of the Earth in $m^3\,s^{-2}$ and R is the orbit radius of the satellite in m. I_z and I_x are the Mass Moment of Inertia (MMOI) of the spacecraft about the z and x axes and thus they are spacecraft dependent. Finally, θ is the maximum angle between the z-axis and the nadir direction of the spacecraft in rad.

12.2.2. Solar Radiation Pressure

Solar Radiation Pressure (SRP) torques arise from the spacecraft's relatively close orbit to the sun. Subsequently, this torque remains constant throughout the majority of the spacecraft's lifetime. However, as the spacecraft's body is generally uniform it will not be subject to a notable SRP torque and thus neglected. Instead, the largest torque will be produced by the gimbaled solar array unit due to its large surface area and moment arm, as is described in Section 9.3.1. As the solar array is constantly sun-pointed the incidence angle remains near zero resulting in a constant maximum solar radiation pressure outside of eclipse regions. The torque that this creates can be calculated with Equation (12.2) [12].

$$T_s = \frac{\Phi}{c} A_s (1 + q)(cp_s - cm) cos(\varphi) \tag{12.2}$$

The torque is defined by T_s in N m with the solar pressure determined by the solar flux, Φ, in $W\,m^{-2}$ and the speed of light, c, in $m\,s^{-1}$. The spacecraft-dependent variables are the illuminated surface area, A_s, in m^2, the reflectance factor, q, and the SRP moment arm determined by the difference between the centre of solar pressure, cp_s, and the centre of mass, cm, in m. Finally, the angle of incidence of the sun on the solar array is given by φ in rad.

12.2.3. Magnetic Field

Due to the polar LEO regime of the spacecraft, magnetic field disturbance torques will have a significant effect on pointing stability. As the spacecraft components are primarily metallic it holds a residual magnetic moment which results in an interaction between the Earth's magnetic field and the spacecraft causing a magnetic torque if the poles are misaligned. Since the residual moment will likely not be aligned with Earth's magnetic field there is a constant magnetic field torque experienced by the spacecraft. The maximal strength of this can be calculated using Equation (12.3) and Equation (12.4) [12].

$$T_m = DB \qquad\qquad B = \frac{M}{R^3}\lambda \tag{12.3, 12.4}$$

Torque is indicated by T_m in N m and the satellite dependent residual dipole is defined by D in $A\,m^2$. The orbit-dependent magnetic field strength, B, in T is calculated with the Earth's magnetic field strength, M, in $T\,m^3$, orbit radius, R, in m and the magnetic latitude constant, λ, which ranges from 1 to 2 depending on the orbit inclination.

12.2.4. Aerodynamic Drag

Finally, due to the LEO regime, a thin layer of the atmosphere is still present at the spacecraft's orbit altitude. Air particles in the region will induce drag on the spacecraft and a misalignment between the point at which the drag force acts and the centre of mass results in the creation of a torque. Similarly, this misalignment will primarily be an effect of the gimbaled solar array due to its large area and moment arm. An expression for the maximum aerodynamic torque experienced by the spacecraft is given in Equation (12.5) [12].

$$T_a = \frac{1}{2}\rho C_d A_r V^2 (cp_a - cm) \tag{12.5}$$

T_a notates this maximal torque in N m. This is the output of the atmospheric density, ρ, in kg m^{-3}, the coefficient of drag of the spacecraft, C_d, and the ram area, A_r, in m^2. The total magnitude is then found by multiplying with the moment arm of the centre of aerodynamic pressure, given by the difference between cp_a and cm in m. As the solar panel will create the largest aerodynamic torque, the ram area is assumed to be the area of the solar panel, and the moment arm is assumed to be the distance to the centre of the solar panel. The torque caused by the main body of the satellite will be neglected due to assumed symmetry.

12.2.5. Disturbance Torques

The values used to calculate the disturbance torques were determined from subsystems with complete designs where possible and first-order estimates otherwise. While not fully accurate these values will provide a baseline to initiate the sizing of the ADCS. Table 12.3 displays these key system-dependent variables.

Table 12.3: Key Values for the Calculation of Disturbance Torques

Variable	Value	Unit	Source
I_x	1610	kg m^2	Chapter 15
I_y	639	kg m^2	Chapter 15
I_z	470	kg m^2	Chapter 15
R	6 953 137	m	Chapter 7
θ	5.24×10^{-3}	rad	SUB-ADC-03
A_s	7.43	m^2	Chapter 9
$cp_s - cm$	3.00	m	Chapter 15
φ	0.00	rad	Chapter 9
D	3.00	A m^2	First-order estimate
λ	2.00	-	Polar orbit effect
ρ	1.39×10^{-14}	kg m^3	Atmospheric density at 580 km[1]
C_d	2.00	-	First-order estimate
A_r	7.43	m^2	Chapter 9
V	7100	m s^{-1}	Chapter 7
$cp_a - cm$	3.00	m	Chapter 15

Inputting these values into the disturbance torque calculations provided torquers shown in Table 12.4. These will be used going forward to calculate the sizing of ADCS actuators and other required pointing components.

Table 12.4: The Maximum Disturbance Torques Caused by the Environment on the Spacecraft

Disturbance	Torque N m
Gravity gradient	2.12×10^{-5}
SRP	1.63×10^{-4}
Aerodynamic drag	1.68×10^{-5}
Magnetic field	1.42×10^{-4}

12.3. Attitude Determination and Control System Configuration

Stemming from the disturbance environment and control method the base components of the ADCS were selected. The components are as follows:

- **Actuators**: Magnetic torquer, reaction wheel, thrusters

[1]URL: www.braeunig.us [accessed: 13/06/2023]

- **Sensors**: Magnetometer, sun sensor, Inertial Measurement Unit (IMU), star tracker

The selection of these components was motivated individually based on the subsystem requirements of the ADCS. The sun sensors provide coarse, low-power attitude measurements for acquisition and contingency modes, and the IMU measures rotation rates and orientation for nominal, contingency and acquisition modes. The star sensors provide fine attitude measurements and the reaction wheels provide 3-axis stabilisation for the nominal mode. For slewing and reaction wheel desaturation magnetic torquers are used with magnetometers to provide the required magnetic field data. Thrusters can also be used for slewing and desaturation maneuvres but with added propellant weight, therefore, their use is tentative.

Sizing mainly needs to be performed for the actuators as counteraction torque and momentum storage highly depend on the design of the spacecraft. The sizing of the sensors will differ and be based primarily on the requirements of the payload as these components depend less overall on the size of the spacecraft. Additionally, the Sentinel-2 ADCS system [57] serves as a case study to assist in the development of the ADCS. This is due to its similar mission profile and accessible design information.

12.3.1. Reaction Wheel Selection

Reaction wheels can provide torque for slewing and stabilisation, however, in this spacecraft, they are primarily used for stabilisation. Therefore the most critical sizing consideration is the momentum storage of the reaction wheels. Assuming the worst-case torque acts over an entire orbit then the root mean square average of this provides the minimum required momentum storage, this is given in Equation (12.6) [12].

$$h = (0.707 \cdot T_D)\, T \tag{12.6}$$

Where h is the angular momentum to be stored in N m s, T_D is the worst-case torque due to SRP of 1.63×10^{-4} N m and T is the period of one orbit give to be 6154 s. This gives a total of 1.06 N m s to be stored per orbit. Assuming desaturation of the reaction wheels occurs every 1 to 2 days (every 14 to 28 orbits) the maximum momentum to be stored is calculated to be 27.7 N m s with a Safety Factor (SF) of 1.4 [58].

Now that the required size is known, market options were analysed for off-the-shelf reaction wheel options that met the required momentum storage. Due to the limited number of large satellites the majority of off-the-shelf options were designed to CubeSat specification, however, three viable and realistic options were found. The Honeywell HR12-37.5[2] used on the Sentinel 2 [57], the Bradford W45[3] and the Rockwell Collins RSI 30-280/30[4]. These three options were chosen as they met the required momentum storage size while being low in mass and power usage compared to other reaction wheels. These were analysed on the basis of the criteria shown in Table 12.5.

[2]URL: Honeywell HR12-37.5 Data Sheet [accessed: 13/06/2023]
[3]URL: Bradford W45 Data Sheet [accessed: 13/06/2023]
[4]URL: Rockwell Collins RSI 30-280/30 Data Sheet [accessed: 13/06/2023]

Table 12.5: Trade-Off Criteria of the Reaction Wheels

Criterion	Weight [%]	1	2	3	4	5
Momentum storage [N m s]	20	< 32	≥ 32	≥ 34	≥ 36	≥ 38
Volume [kg m^{-3}]	10	> 0.015	≤ 0.015	≤ 0.014	≤ 0.013	≤ 0.012
Mass [kg]	30	> 8.5	≤ 8.5	≤ 8.0	≤ 7.5	≤ 7.0
Average power [W]	30	> 28	≤ 28	≤ 26	≤ 24	≤ 22
Maximum power [W]	10	> 160	≤ 160	≤ 140	≤ 120	≤ 100

From these criteria, the reaction wheels were traded-off to find the best option. Mass and average power were determined to be the most important criteria as these are the parameters that typically constrain reaction wheel selection when it comes to budgeting. The trade-off analysis can be seen in Table 12.6.

Table 12.6: Analysis of the Reaction Wheel Trade-Off Criteria

Criterion	Weight [%]	**HR12-37.5**	W45	RSI 30-280/30
Momentum storage	20	4	5	1
Volume	10	4	3	5
Mass	30	2	5	1
Average power	30	4	1	5
Maximum power	10	4	1	3
Weighted score		**340**	320	280

From the trade-off, it can be seen that the Honeywell HR12-37.5 wins the trade-off by a score of 20 points above the next option. While it underperforms in mass its overall high score in all other areas deems it an appropriate choice for the mission. If mass constraints become more strict then it may be possible to use the Bradford W45 as an alternative while trading off power usage.

12.3.2. Magnetic Torquer Selection

Due to the polar orbit of the spacecraft magnetic torquers provide an appealing option for slewing and desaturation manoeuvres. The one drawback of magnetic torquers is the relatively low slew rate, however, since the mission does not require any rapid manoeuvres to be performed they still provide a viable approach to attitude control. Equation (12.7) [12] can be used to calculate the required dipole moment.

$$D = \frac{T_D}{B} \tag{12.7}$$

In this equation, D indicates the magnetic dipole moment in A m^2, T_D represents the most disturbing torque in N m and B is the Earth's magnetic field strength in T calculated with Equation (12.4). If a desaturation manoeuvre is assumed to take 1 orbit then the required torque to desaturate can be determined to be 4.5×10^{-3} N m and this gives a total required dipole moment of 133 A m^2 with a SF of 1.4 [58]. Additionally, to check that the minimum slew requirement can be met by this the required torque can be calculated using Equation (12.8) [59].

$$T = 2\frac{\theta I}{t^2} \tag{12.8}$$

Where T is the required torque in N m, I is the greatest axial inertia in kg m^2, θ is the slew angle in rad, and t is the time of slew in s. Using this formula a minimum required torque of 3.90×10^{-4} N m for a slew rate of 5×10^{-2} ° s^{-1} (SUB-ADC-06) can be calculated. This is less than the torque required for desaturation, therefore, magnetic torquers that meet the required dipole moment of 133 A m^2 will also meet the slew requirement.

A trade-off is performed similarly to the last for three differing off-the-shelf magnetic torquers. Similar to reaction wheels a lack of large satellite options limited the available offerings, however, 3 possible options were still determined. The Sentinel 2's [57] ZARM Technik MTI-140-2[5], the IAI P/N 1286-0009[6] and the O.C.E. Technology MQ200[7]. These were analysed on the criteria shown in Table 12.7.

Table 12.7: Trade-Off Criteria of the Magnetic Torquers

Criterion	Weight [%]	1	2	3	4	5
Magnetic moment [A m^2]	30	< 120	≥ 120	≥ 130	≥ 140	≥ 150
Length [m]	30	> 0.80	≤ 0.0.75	≤ 0.70	≤ 0.65	≤ 0.60
Mass [kg]	20	> 5.5	≤ 5.5	≤ 5.0	≤ 4.5	≤ 4.0
Average power [W]	20	> 6	≤ 6	≤ 5	≤ 4	≤ 3

The most important criteria here regarded magnetic moment and length. As the magnetic torquers should ideally be placed on the edges of the structure a length that is too large may cause an increase in structure size. The magnetic moment is also an important criterion as the greater it is, the more rapidly manoeuvres can be performed. The analysis of the trade-off is shown in Table 12.8.

Table 12.8: Analysis of the Magnetic Torquer Trade-Off Criteria

Criterion	Weight [%]	**MTI-140-2**	P/N 1286-0009	MQ200
Magnetic moment	30	4	4	5
Length	30	4	4	1
Mass	20	3	4	5
Average power	20	5	2	4
Weighted score		**400**	360	360

ZARM Technik's MTI-140-2 provides the best possible option for the magnetic torquer as it wins the trade-off with a score of 40 points above the next option. This torquer provides high values for the most important criterion, magnetic moment and length, while also providing efficient power usage. While the other two torquers provide relatively high values for most criteria each suffers very negatively on either length or average power.

12.3.3. Thruster Selection

Finally, the thrusters must be sized, however, since the use of thrusters is tentative their use in the ADCS will be determined by their sizing. Thrusters are useful but not necessary for the ADCS, they allow for more flexibility when it comes to manoeuvres but the drawback is added propellant weight and complexity from the need for 6 degrees of freedom movement. Once again, assuming that desaturation manoeuvres will be the most constraining, the total required force and propellant mass for these manoeuvres can be calculated using Equation (12.9) and Equation (12.10) [12].

[5]URL: ZARM Technik MTI-140-2 Data Sheet [accessed: 13/06/2023]
[6]URL: IAI P/N 1286-0009 Data Sheet [accessed: 13/06/2023]
[7]URL: O.C.E. Technology MQ200 [accessed: 13/06/2023]

$$F = \frac{h}{Lt} \qquad M_p = \frac{Ft}{I_{sp}g} \tag{12.9, 12.10}$$

Where F is the thruster force in N, t is the burn time in s, L is the moment arm in m, I_{sp} is the specific impulse in s, M_p is the propellant mass in kg and g is gravitational acceleration in m s^{-2}. The minimum required force can be calculated to be 37.5 N assuming a minimum momentum arm of 1 m and burn time of 1 s. Then assuming a desaturation of the reaction wheels is performed maximally every 2 days for the spacecraft lifetime of 7.5 years the pulse life can be calculated to be 4110. The required propellant mass can then be calculated using an assumed specific impulse of 250 s and a total impulse of 154 000 N s calculated from the pulse life and burn parameters. Consequently this results in a required propellant mass of 87.9 kg with a SF of 1.4.

If the total propellant mass required for the ADCS is compared to the maximum mass specified by the subsystem requirements of 90 kg (SUB-ADC-12) then it can be seen that the use of thrusters is not feasible. A total of 2.1 kg will be left available for the other ADCS components which is unrealistic. It is therefore decided that the ADCS will not use thrusters as a system component and rely solely on magnetic torquers for actuation.

12.3.4. Star Tracker Selection

Following on from the actuators the sensors need to be selected in order to meet the pointing requirements of the mission. The most mission-critical sensor will be the star trackers as they provide the required fine attitude measurements. Due to the large range of different star trackers for all sizes of satellites, a trade-off will be performed for the star trackers while the other sensors will be selected through logical reasoning and research.

Three similar star trackers are chosen which can provide the required pointing accuracy (SUB-ADC-03) and pointing knowledge accuracy (SUB-ADC-01) and which had spacecraft heritage on other Earth observation missions. The chosen sensors are the Jena-Optronik Astro APS3[8], the Leonardo SPACESTAR[9] and the Space Micro μSTAR Tracker[10]. These star trackers are all traded-off on the criteria shown in Table 12.9.

Table 12.9: Trade-Off Criteria of the Star Trackers

Criterion	Weight [%]	1	2	3	4	5
Maximum bias error [″]	30	> 11	≤ 11	≤ 9	≤ 7	≤ 5
Sampling rate [Hz]	30	< 9	≥ 9	≥ 10	≥ 11	≥ 12
Mass [kg]	20	> 2.1	≤ 2.1	≤ 1.9	≤ 1.7	≤ 1.5
Average power [W]	20	> 10	≤ 10	≤ 8	≤ 6	≤ 4

Here the two most important criteria were determined to be the maximum bias error and the sampling rate. While there is a requirement on maximum bias error the lower it is the better as this will remove erroneous data from the ADCS. The sampling rate was chosen as the second most important criterion as this defines how often the attitude can be measured and is vital when strict pointing must be constantly kept. The analysis of the star trackers with respect to each criterion can be found in Table 12.10.

The Astro APS3 comes out as the top star tracker for this mission with a score of 60 points greater than the next option. This star tracker has an overall high performance, especially in regard to sampling rate and average power. The Space Micro μSTAR Tracker provides a suitable secondary option if a lower error rate is required by the system with a loss of mass and average power.

[8]URL: Jena-Optronik Astro APS3 Data Sheet [accessed: 13/06/2023]
[9]URL: Leonardo SPACESTAR Data Sheet [accessed: 13/06/2023]
[10]URL: Space Micro μSTAR Tracker Data Sheet [accessed: 13/06/2023]

Table 12.10: Analysis of the Star Tracker Trade-Off Criteria

Criterion	Weight [%]	**Astro APS3**	μSTAR Tracker	SPACESTAR
Maximum bias error	30	3	5	2
Sampling rate	30	5	3	3
Mass	20	3	2	4
Average power	20	4	2	3
Weighted score		**380**	320	290

12.3.5. Inertial Measurement Unit Selection

IMU components are critical for an ADCS as they work in parallel with star trackers and other reference locating sensors to provide complete and accurate attitude measurements. IMUs usually contain at least 3 gyroscopes and an accelerometer to provide accurate rotational rate and orientation. IMUs have a large range of options as they are one of the most vital components of the ADCS. IMUs also provide image localization which is key for IASI-NG payload as it is Earth observing.

For the selection of the IMU instead of a trade-off a research-based approach was taken due to the limited number of fibre-optic IMUs available for large satellites. The research was performed on the flight heritage of a number of IMUs in order to find the option with the highest performance that would perform sufficiently for the IASI-NG. It was found that the most common IMUs for high-performance European Earth observation satellites was the Airbus/iXBlue Astrix series [60]. These are also on the Sentinel 2 [57] and used on recently launched similarly sized satellites with weather observing missions[11].

From the Airbus/iXBlue Astrix series the Astrix 200 was chosen due to its balance between mass and power requirements. It is also the Astrix unit with the most heritage on Earth-observing satellites out of all the Astrix units[12].

12.3.6. Coarse Sensor Selection

The final sensors to be selected are the coarse sensor units, these are the magnetometer and the sun sensors. The magnetometer is an instrument that is primarily required for the operation of the magnetic torquers, it also provides coarse attitude sensing for the spacecraft's heading direction. This is done through the measurement of Earth's magnetic field in and around the satellite in orbit. Sun sensors, unlike the magnetometer, are used primarily for coarse attitude measurements and are primarily used in contingency and acquisition modes due to their low power usage. The selection of these was done on logical reasoning and research on similar missions.

To provide compatibility with the magnetic torquers magnetometers manufactured by ZARM Technik were researched. ZARM Technik provides one flagship magnetometer for large satellite missions which has a high heritage[13] and is lightweight and power efficient. This unit, the ZARM Technik Hi-Rel FGM-A-75 [14], will be therefore be used as the magnetometer for the mission.

For sun sensor selection reliability is the highest priority due to the use of the sensors in contingency mode. For many large Earth-observing spacecraft in LEO, including Sentinel 2 [57], a common sensor known as the SpaceTech (originally Astrium) CESS is used [15]. [61] [62]. This sensor picks up infrared flux and solar flux from both the Earth and Sun to provide coarse attitude measurements, it is also a passive sensor so it requires no power[16]. Therefore the SpaceTech CESS will be used due to its low

[11]URL: French Gyroscopes Picked for U.S. Weather Satellite [accessed: 13/06/2023]
[12]URL: Airbus/iXBlue Astrix 200 Data Sheet [accessed: 13/06/2023]
[13]URL: ZARM Technik Products [accessed: 13/06/2023]
[14]URL: ZARM Technik Hi-Rel Magnetometer FGM-A-75 Data Sheet [accessed: 13/06/2023]
[15]URL: SpaceTech CESS Sensors [accessed: 13/06/2023]
[16]URL: SpaceTech CESS Data Sheet [accessed: 13/06/2023]

weight, reliability and zero power usage.

12.4. Navigation System Requirements

The navigation subsystem works in turn with the ADCS to provide accurate location determination and tracking of the spacecraft in its orbit. Navigation systems communicate with external sources in order to provide geopositioning and time synchronisation. This usually requires the use of multiple external transmitters, a receiver configured to receive these signals and a processing unit to extract useable data out of the signals. As the payload is Earth-observing and needs to correlate its information with a position on the Earth, accurate location mapping is essential. Therefore a majority of the subsystem requirements for the navigation system arise from the base requirements of the payload. These subsystem requirements can be seen in Table 12.11.

Table 12.11: Subsystem Requirements for the Navigation Subsystem

ID	Requirement	Derived From
SUB-NAV-01	The navigation system shall determine the radial position on orbit with an accuracy of at least 5 m	SYS-OPS-10
SUB-NAV-02	The navigation system shall determine the cross-track position on orbit with an accuracy of at least 10 m	SYS-OPS-10
SUB-NAV-03	The navigation system shall determine the along-track position on orbit with an accuracy of at least 10 m	SYS-OPS-10
SUB-NAV-04	The navigation system shall determine the velocity on orbit with an accuracy of at least 1 m s^{-1}	Functionality
SUB-NAV-05	The navigation system shall have a time accuracy of at least 1 ms	Functionality
SUB-NAV-06	The navigation system shall use GNSS as its primary source of location data	Functionality

From these requirements, it can be seen that the spacecraft will require a high-performance GNSS system in order to reach the positional accuracies defined by the payload. Analysing these requirements provides key and driving requirements which will determine the selection of the navigation system components. These requirements are given as follows:

- **Key**: SUB-NAV-02, SUB-NAV-03, SUB-NAV-04
- **Driving**: SUB-NAV-01, SUB-NAV-05

12.5. Navigation System Configuration

The navigation system is one which is heavily integrated with both the ADCS and C&DH therefore component selection should take both of these into account. As it is required that the system use GNSS the specific GNSS system to be used needs to be determined. The primary systems that offer GNSS are currently; Galileo, Global Positioning System (GPS), BeiDou and Global'naya Navigatsionnaya Sputnikovaya Sistema (GLONASS) where Galileo and GPS are the most common. As this system is a European-based constellation Galileo will be selected as the main GNSS provider with GPS as an auxiliary provider in case Galileo is not functioning as intended.

Analysing off-the-shelf navigation receivers that can interface with Galileo and GPS is done on the basis of ensuring compatibility with the OBC, Beyond Gravity's Constellation On Board Computer (COBC) (Section 10.3.1). The COBC provides the option for an integrated GNSS unit known as NavRIX Integral[17], this unit is able to provide suitable 3D root mean squared accuracies for position, timing and velocity of <1 m, <25 mm s^{-1} and <100 ns respectively. Additionally, since this is integrable with the OBC no external computing unit is required for the receivers compared to other Beyond Gravity receivers[18]. Therefore the Beyond Gravity NavRIX unit will be used as the primary GNSS receiver.

[17]URL: Constellation On Board Computer Data Sheet [accessed on 13/06/2023]
[18]URL: Podrix GNSS Data Sheet [accessed on 13/06/2023]

12.6. Sensitivity Analysis

A sensitivity analysis is performed for the entire control system, both the ADCS and navigation system, as both subsystems are sensitive to the same changes in mission changes. The mission parameters that both systems are most sensitive to are a change in orbit regime/altitude, a change in mass budget and a change in the power budget. This is due to the design of the system being focused on LEO and high accuracy pointing.

First analysing the ADCS, the effect of a change in orbit altitude/regime is analysed. The most sensitive components in regard to this are the sun sensors and magnetic torquers. The chosen sun sensors, the SpaceTech CESS, have a maximum altitude of 1500 km [61] as they are not sensitive to pick up the required electromagnetic radiation at higher altitudes. Therefore a change from LEO to a higher orbit will result in a lack of coarse attitude measurement and therefore all the control modes will not be useable and the requirements will not be met. A remedy for this problem would be to swap to fine sun sensors such as the Bradford FSS[19] which has functionality up to HEO. However, this comes with an increase in cost and power usage and a decrease in reliability.

Regarding the magnetic torquers, an increase in orbit to above LEO (2000 km) would lead to the current 140 A m^2 torquers becoming insufficient for desaturation due to weakening of Earth's magnetic field. If a higher orbit is required it is possible to increase the strength of the magnetic torquers. This would lead to a maximum orbit in MEO at an altitude of 10 000 km) as there would be a required magnetic moment of over 400 A m^2, calculated from Equation (12.3) and Equation (12.4). 400 A m^2 cannot be exceeded as this is the upper limit of magnetic torquers currently available off the shelf. This also assumes that magnetic torquers will still function as expected above LEO. Magnetometers, however, will function up to 10 000 km as shown by M-SAT [63] but this requires a much more sensitive magnetometer set-up than currently selected. It should be noted that there would be a decrease in disturbance torques above LEO which would lead to a decrease in the size of the ADCS. However, at greater altitudes, the use of purely magnetic torquers for slewing and desaturation becomes risky due to the deterioration of Earth's magnetic field, therefore, a thruster based ADCS would need to be considered above LEO.

Compared to the ADCS the navigation system as a whole is much less sensitive to large altitude changes. The navigation system primarily uses GNSS therefore it is limited by the pointing and orbit of the GPS and Galileo satellites. Both GNSS constellations orbit within MEO at altitudes of roughly 20 000 km and point directly to Earth. Therefore at altitudes above 3000 km GNSS spacecraft are no longer in the direct signal of the GNSS constellations [64]. While this does lead to a decrease in accuracy it has been shown that GNSS navigation systems can be used above 76 000 km, however, positional accuracy degrades to approximately 50 m [64]. The navigation subsystem would therefore be most sensitive to an increase of orbit altitude to above 3000 km and at this height an alternative positional system should be used if the positional error becomes unacceptable.

Ultimately, for the control system, it is most sensitive to a change in orbit altitude above 2000 km to above LEO. At this altitude, the current actuators will be insufficient and the positional accuracy of the navigation system will decay. If the orbit parameters are altered to change the altitude to greater than 3000 km then it is recommended to create a new control system (both navigation and ADCS) altogether.

12.7. Summary

To summarise the final selection of the components used in the control system a table is shown in Table 12.12. This includes every component used and its quantity including redundant components. The redundant design of each component was based on the ADCS design of a similarly sized Earth-observing satellite Sentinel-2 [57] as it uses related components and has comparable pointing requirements. Additionally, all chosen components have significant mission heritage and at least a TRL of 9.

[19] URL: Bradford Fine Sun Sensor Data Sheet [accessed on 13/06/2023]

Table 12.12: Summary of the Chosen Control System Components

Type	Component	Instrument	Quantity	Average power [W]	Mass [kg]
Sensor	Magnetometer	ZARM Technik FGM-A-75	3	1	0.3
	Sun sensor	SpaceTech CESS	6	0	0.8
	IMU	Airbus/iXBlue Astrix 200	1	5.5	4.7
	MIMU	Honeywell MIMU	1	25	12
	Star tracker	Jena-Optronik Astro APS3	3	6	1.8
Actuator	Magnetic torquer	ZARM Technik MTI 140-2	3	1.9	5.3
	Reaction wheel	Honeywell HR12-37.5	4	22	8.25
Navigation	GNSS receiver	NavRIX Integral GNSS Receiver	2	1	0.216

The full control system has been designed with the redundancy of each component in mind and each system has at least one redundant component, redundancy levels have also been set such that critical systems always have hot redundancy[20]. The magnetometers operate with triple hot redundancy as multiple measurement units are required to operate at once. This is so that the measurements of the units may be verified with each other. The sun sensors are triple redundant with hot redundancy in order to coarse sensing at all times. The IMU has double cold redundancy with the addition of the MIMU. The star trackers are two out of three redundancy with the inclusion of a third tracker. ZARM Technik magnetic torquers come with in-built double cold redundancy thus only 3 are required. Reaction wheels have three out of four hot redundancy in order to maintain 3-axis stability with the failure of one reaction wheel. Finally, the GNSS receiver has double cold redundancy, however, they may also operate in hot redundancy using alternate GNSS constellations if there is a risk of GNSS outage.

The total power and mass usage of each control system component is given in Table 12.13 in order to provide budgets for the EPS.

Table 12.13: Mass and Power Budgets of the Chosen Control System Components

Type	Component	Total average power [W]	Total peak power [W]	Total mass [kg]
Sensor	Magnetometer	3	3	0.9
	Sun sensor	0	0	4.8
	IMU	5.5	7.5	12
	MIMU	25	32	4.7
	Star tracker	18	24	5.4
Actuator	Magnetic torquer	5.7	5.7	15.9
	Reaction wheel	88	420	33
Navigation	GNSS receiver	2	2	0.432
	Total	147	494	77

These total budgets meet the requirements for average power and total mass with a safety margin as the total average power is calculated with all components in operation. The total contingency mode total average power with the usage of only 1 magnetometer, the sun sensors, the MIMU, the magnetic torquers, 3 reaction wheels and 1 GNSS receiver totals to 98.7 W which also meets requirements. It should be noted that the total peak power is highly inflated due to the total peak power of the reaction wheels including torquing power. As the reaction wheels are not used for torque in this mission their total peak power will be closer to the total average power of 88 W resulting in a total peak power of 162 W.

[20]URL: European Cooperation for Space Standardization Redundancy [accessed on 13/06/2023]

13 Propulsion System

The propulsion subsystem of this satellite is only responsible for orbit maintenance and the EOL de-orbit manoeuvre. The ADCS does not impose any requirements for propulsion to conduct desaturation and pointing manoeuvres. The orbit maintenance is to compensate for ΔV losses due to perturbations. The perturbations considered are third-body, non-spherical Earth, atmospheric drag, and solar radiation. These perturbations are described in Section 7.2. The EOL procedure ensures that the spacecraft de-orbits within 25 years after EOL. To achieve this, the propulsion system will lower the peri-centre radius of the orbit to an altitude of 220 km, as described in Section 7.1.4. To ensure the system is capable of performing these functions, the subsystem requirements are set up in Section 13.1. With the requirements identified, the subsystem is divided into several parts that are designed in sequence, as elaborated in Section 13.2. In Section 13.3, a sensitivity analysis is performed to ensure the proper operation of the subsystem in non-nominal conditions. Finally, a summary of the subsystem is provided in Section 13.4.

13.1. Requirements

The ΔV requirement imposed by orbit maintenance follows from the calculations performed in Section 7.2. From these calculations, the maximum allowable Minimum Impulse Bit (MIB) of the thruster can be determined. To determine this, the satellite mass is multiplied by the ΔV of the manoeuvre of the orbit maintenance. The ΔV EOL requirement follows from the calculations performed in Section 7.1.4. In addition to this requirement, the minimum thrust required by the propulsion system based on the maximum required burn time and ΔV is determined. The other requirements follow directly from the mission and system requirements described in Chapter 3. An overview of the subsystem requirements is provided in Table 13.1

Table 13.1: Propulsion Subsystem Requirements.

ID	Requirement	Derived from
SUB-PRP-01	The propulsion system shall provide 0.078 055 m s^{-1} station keeping ΔV every 6.33 d	Section 7.2.5
SUB-PRP-02	The propulsion system shall provide 161.21 m s^{-1} ΔV for the de-orbit burn	Section 7.1.4
SUB-PRP-03	The propulsion system shall have a maximum dry mass of 61 kg	Section 8.1
SUB-PRP-04	The space segment shall not utilise toxic or potentially toxic propellant	SUS-SPA-13
SUB-PRP-05	The propulsion system shall have a maximum MIB of 97.88 N s	Section 13.1
SUB-PRP-06	The de-orbit burn shall be performed within less than 24 h	SUS-SPA-04

13.2. Configuration

The thrusters are considered the most critical part of this subsystem; therefore the thrusters are selected before any other part is designed. Once the thrusters are selected and their associated propellant is determined, the propulsion concept is decided upon. This flows into the design of the propellant tanks and the valves used within the propulsion subsystem.

13.2.1. Thruster Selection

To start the thruster selection process, the different types of thrusters are identified. Mono-propellant, bi-propellant and cold gas thrusters are considered. Electric propulsion systems are disregarded due to the low thrust they are able to provide. The possible thrusters are selected from SatCatalog [1]. Based on SUB-PRP-04, only two thrusters are feasible for the satellite. The B1 thruster [2] and the B20 thruster [3],

[1] URL: www.satcatalog.com/PropulsionSubsystem [accessed: 09/06/2023]
[2] URL: satcatalog.s3.amazonaws.com/B1 [accessed: 09/06/2023]
[3] URL: satcatalog.s3.amazonaws.com/B20 [accessed: 09/06/2023]

which both use N_2O as its oxidiser and C_3H_6 as the fuel. Due to the low thrust of the B1, the B20 thruster is selected for the propulsion subsystem. An overview of the properties of the B20 thruster is shown in Table 13.4a.

13.2.2. Propulsion Concept

One thruster is needed for the performance of the required manoeuvres. However, because of redundancy and the alignment of the thrust vector with the centre of gravity, four thrusters are placed on the wake side of the satellite. From the thruster selection, the propellant is known and the rest of the propulsion system can be designed. Three configurations of the propellant tanks are considered [65]. The first concept is to make use of the self-pressurisation of both N_2O and C_3H_6. However, this option is disregarded due to the low self-pressurisation pressure of C_3H_6. The second concept uses for both the oxidiser and fuel tank a buffer tank with nitrogen gas to pressurise the propellant. The third concept makes use of the self-pressurisation of the oxidiser and uses a buffer tank with nitrogen to pressurise the fuel tank. It was opted to use the third option, because of the additional mass and complexity that comes with the extra nitrogen tank in the second option.

The configuration of the propulsion subsystem is then set up, shown in the self-made diagram in Figure 13.1, based on the propulsion diagram in *Space Mission Engineering: The New SMAD*. It shows the three main tanks in the system, as well as valves and other components. The fill & drain valves are used to fill and drain the propellant and nitrogen, but also to check for any leaks in the system. The explosive valves fully restrict any flow until operation. This prevents any leakage or flow of propellant before the satellite is in operation. The relief valve releases the pressure of the system when needed by expelling the propellant. The check valve ensures a one-way flow in the system. The burst valve is similar to the explosive valve but is triggered by an overload of pressure. The trim orifice ensures that the propellant flow is less turbulent. The regulator valve regulates the amount of propellant that flows through the system. And the bi-propellant valve combines the oxidiser and fuel just before entering the combustion chamber. Besides these components, there are also multiple filters present in the system. These filters ensure the purity of the species throughout the flow of the system.

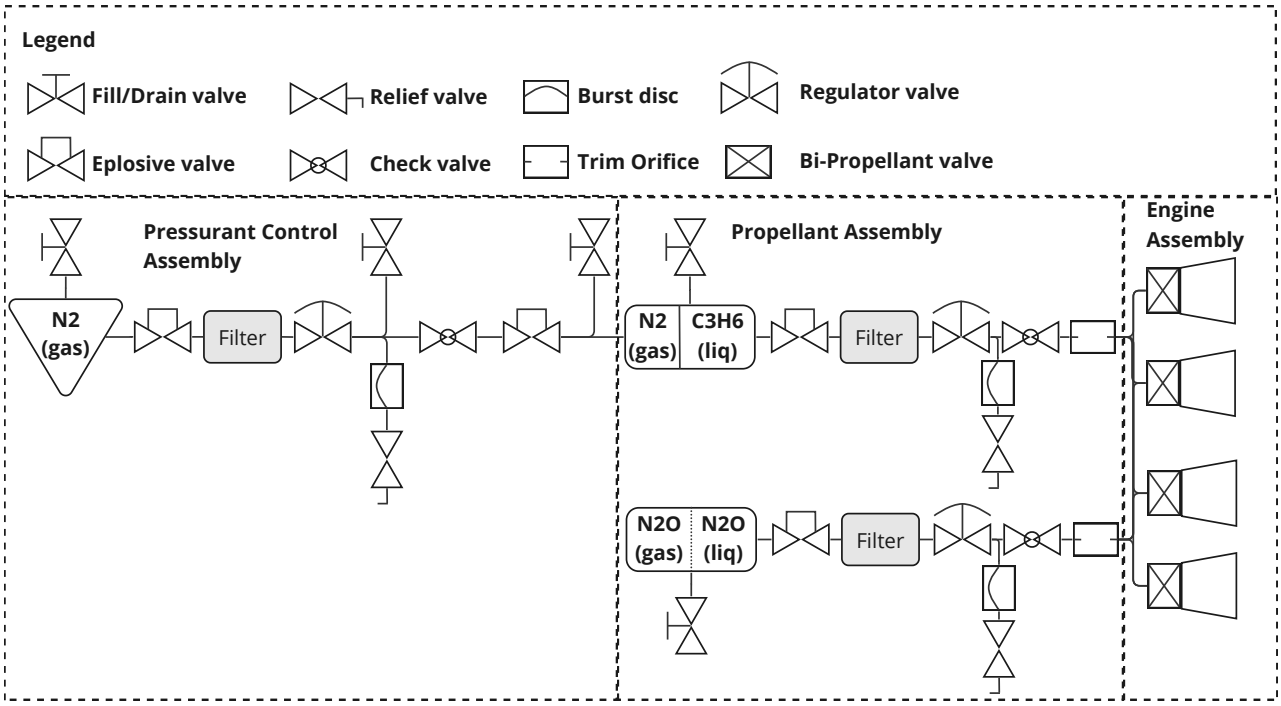

Figure 13.1: Diagram of the Propulsion System

13.2.3. Propellant Tanks Design

Before the propellant tanks can be designed, the amount of propellant needs to be determined. Based on this propellant mass, the three tanks are designed individually in series. It was chosen to use

Ti-6Al-4V as the material of the propellant tanks, common for space-craft propellant tanks, for their high yield stress, relatively low density, and resistance to corrosion.

Propellant mass

To determine the propellant mass needed throughout the mission, the manoeuvres performed by the subsystem are simulated over the spacecraft's lifetime. Based on the frequency of the orbit maintenance, it is identified on which days of the mission a manoeuvre is performed and with what ΔV. At the end of the mission, the de-orbit manoeuvre is performed. The model loops from the end of the spacecraft's lifetime, where it is assumed the mass of the spacecraft is equal to the spacecraft's dry mass plus the propellant for unexpected manoeuvres. To calculate the propellant mass needed for a manoeuvre, Tsiolkovsky's equation is adapted and applied in the form of Equation (13.1).

$$M_p = M_1 \cdot \left(e^{\frac{\Delta V}{g_0 I_{sp}}} - 1 \right) \tag{13.1}$$

In this equation, M_1 is the mass of the spacecraft at the end of the manoeuvre, ΔV is the change in velocity required for the manoeuvre, g_0 is the gravitational acceleration of Earth at sea level, and I_{sp} is the specific impulse of the thruster. Summing all the propellant masses of the manoeuvres results in the required propellant mass of the mission.

To determine the fuel and oxidiser reaction ratio, the chemical reaction is established, Equation (13.2). That shows that the molar ratio is 1:9. This is used to find the mass ratio of the propellant by dividing the molar mass of C_3H6 by the molar mass of $9N_2O$.

$$9N_2O + C_3H_6 \Rightarrow 3H_2O + 3CO_2 + 9N_2 \tag{13.2}$$

To find the masses of the oxidiser and fuel (M_{OX} and M_F respectively), Equation (13.3) and Equation (13.4) are utilised. Where RAT_{mass} is the mass ratio of fuel over oxidiser, as determined above.

$$M_{OX} = \frac{M_p}{1+RAT_{mass}} \qquad M_F = \frac{M_p}{\frac{1}{RAT_{mass}}+1} \tag{13.3, 13.4}$$

Propellant Tanks

Based on the masses of the oxidiser and fuel, their volumes can be determined by dividing the masses by their respective densities. The propellant will be stored on board the spacecraft in its liquid form, and their densities are therefore assumed to be constant with pressure. The tanks are of spherical form to minimise the mass, thus the radii of the tanks needed can be determined from the volume. The required thickness of the tanks is determined using Equation (13.5) [12]. Where P is the pressure in the tank, σ_y is the yield strength of the material, and FoS is the factor of safety of 1.5. The pressure of the fuel tank is set to be 14.7×10^5 Pa, based on the maximum inlet pressure of the thruster. The pressure of the oxidiser tank is 6 MPa, based on the saturation pressure of N_2O at the maximum temperature of the spacecraft of 20 °C [66].

It was found that the chosen alloy can be manufactured with a minimum thickness of 0.2 mm and with an accuracy of 0.1 mm [4]. Therefore, the thickness is taken to be the minimum value, even if less thickness is needed structurally, and the calculated thickness is rounded up to the next tenth of a mm. The mass of the tank is then determined using Equation (13.6). Where $\rho_{Ti-6Al-4V}$ is the density of the titanium alloy.

$$t = \frac{1}{2}\frac{PR}{\sigma_y FoS} \qquad m = \frac{4}{3}\left((R+t)^3 - R^3 \right) \rho_{Ti-6Al-4V} \tag{13.5, 13.6}$$

[4] URL: www.spacematdb.com [accessed: 12/06/2023]

13.2.4. Nitrogen tank

To design the nitrogen tank, two assumptions are made. Firstly, the pressure of the nitrogen tank is equal to the pressure of the fuel tank when all fuel is consumed. And secondly, the pressure of the nitrogen tank is limited by the operating pressure of the selected valves. These assumptions stand if the fuel tank is filled up with fuel and all the nitrogen is in the nitrogen tank. Following the ideal gas law, these two assumptions result in Equation (13.7) and Equation (13.8).

$$n_{N_2} = \frac{P_{C_3H_6} V_{N_2}}{RT} + \frac{P_{C_3H_6} V_{C_3H_6}}{RT} \qquad n_{N_2} = \frac{P_{N_2} V_{N_2}}{RT} \tag{13.7, 13.8}$$

Where n_{N_2} is the number of moles of nitrogen in the tank, $P_{C_3H_6}$ is the pressure in the fuel tank, P_{N_2} is the maximum pressure in the nitrogen tank, $V_{C_3H_6}$ is the volume of the fuel tank, V_{N_2} is the volume of the nitrogen tank, R is the gas constant, and T is the lower temperature of the spacecraft. P_{N_2} and V_{N_2} are unknown. Rewriting these equations results in Equation (13.9) and Equation (13.10).

$$V_{N_2} = \frac{P_{C_3H_6} V_{C_3H_6}}{P_{N_2} - P_{C_3H_6}} \qquad n_{N_2} = \frac{P_{N_2} V_{N_2}}{RT} \tag{13.9, 13.10}$$

The mass of nitrogen can be determined by multiplying the number of moles of nitrogen with its molar mass. The dimensions of the nitrogen tank can then be determined from the volume and the assumption of a spherical tank, using Equation (13.5) & Equation (13.6).

13.2.5. Valve Selection

In this stage of the design, two main valves are selected. The fill & drain valve and regulating valves. Fill & drain valves are utilised before the operation to fill the propellant tanks. The regulating valves regulate the flow of propellant to the thrusters during the operating phase of the satellite. In total, eleven valves from several suppliers are identified as possible design solutions. To determine the optimal valve, a trade-off is performed. Three criteria were found to be relevant for this trade-off, shown in Table 13.2. The scale of these criteria is based on the range of performance of the considered valves. Due to the significant difference in mass between the regulator and fill & drain valves, two scales are set up. For the weighing of the criteria, the operating pressure was deemed most important, since this drives the design of the nitrogen propellant tank as described in Section 13.2.4. Leakage is also deemed important since this could cause catastrophic and system functionality inhibiting problems when in operation. Mass is relatively less significant, due to the small mass with respect to the total dry mass of the satellite.

Table 13.2: Trade-Off Criteria of the Valve Trade-Off

Criterion	Weight [%]	1	2	3	4	5
Operation pressure [Pa]	50	$< 6 \times 10^6$	$< 15 \times 10^6$	$< 30 \times 10^6$	$< 40 \times 10^6$	$> 40 \times 10^6$
Leakage [Scc/s]	40	$> 10^{-3}$	$> 10^{-4}$	$> 10^{-5}$	$> 10^{-6}$	$< 10^{-6}$
Mass (fill/drain) [g]	10	> 1000	> 750	> 500	> 250	< 250
Mass (regulating) [g]		> 200	> 125	> 75	> 20	< 20

Using the data provided by the manufacturers of the valves, the trade-off is performed using the before mentioned criteria. The grading of the criteria of each of the valves is shown in Table 13.3. In this table, the regulator valves are traded off on the left-hand side and the fill & drain valves are on the right-hand side. This shows that for the regulator valves the V1R10560-06 is optimal, and for the fill&drain valves the V1D10855-01 is optimal.

Table 13.3: Analysis of the Valve Trade-Off Criteria

		Regulating valve					Fill & Drain valve					
Criterion	*Weight [%]*	*Latch valve*[5]	*V1E10535-01*[6]	*V1E10763-01*[6]	***V1E10560-01***[6]	*V8E10580-01*[6]	*FDV*[7]	*FVV/FDV*[8]	*V1E10430-01*[9]	*V1E10811-01*[9]	*V1E10845-01*[9]	***V1D10855-01***[9]
Operation pressure	50	1	3	4	4	3	1	4	3	4	5	5
Leakage	40	3	2	1	2	2	5	3	5	5	3	5
Mass	10	4	4	4	2	5	4	4	3	3	4	5
Weighted total		210	270	280	**300**	280	290	360	380	430	410	**500**

13.3. Sensitivity Analysis

Four factors of the mission design are identified to be relevant for the sensitivity analysis of the propulsion subsystem. The four mission properties are the spacecraft lifetime, the dry mass, the semi-major axis of the orbit, and the addition of a (partial) orbit insertion to the desired ascending node. For each of these aspects, it should be investigated how much the parameter can be altered while the propulsion system is still able to perform its intended functions. For all of the parameter changes, the contingency propellant is used to compensate for the change in propulsion needs. The calculation procedure to determine the required propellant mass as described in Section 13.2.3 is applied again to calculate the required propellant mass for the changed situation. The parameter is slowly increased until the propellant required exceeds the propellant on board the spacecraft.

The design lifetime of the mission is 7.5 yr, for which the propulsion system is also accordingly designed. It is determined how long the spacecraft can maintain the orbit using the available propellant in case the design lifetime is extended. The calculations conclude that there is enough propellant on board to perform for 28.5 yr. In case the dry mass increases with respect to the currently estimated dry mass during the following phases of the design process, the propulsion system should still be able to perform the mission. It was determined that the dry mass could increase to 2240 kg, an increase of almost 80% from the original weight estimate used during sizing. This is an even greater 2.9 times that of the latest dry weight estimate.

In case it is decided that the orbit needs to be altered, the propulsion system should still be able to maintain the orbit during the mission. For the calculations, it is assumed that the peri-centre is reduced (and the semi-major axis) while keeping the eccentricity constant. The density estimations of SMAD are interpolated to define the density at the new peri-centre [12]. Based on this the new orbit maintenance strategy is determined similarly to the method described in Section 7.2.5. From this, it was determined that the current propulsion system is capable of maintaining an orbit with a peri-centre altitude of 375 km, which is 200 km below the currently selected peri-centre altitude.

If the right ascension of the ascending node deviates from the expected orbit after orbit insertion by the launcher, the propulsion system is to correct for this. For polar orbits, changing the right ascension of the ascending node is similar to changing the inclination of an orbit, but then performing the manoeuvre at one of the poles[10]. Therefore, Equation (13.11) can be used to determine the required ΔV of the manoeuvre.

[5]URL: satcatalog.com/Latch_Valve [accessed: 12/06/2023]
[6]URL: www.vacco.com/latch [accessed: 12/06/2023]
[7]URL: satcatalog.com/FDV [accessed: 12/06/2023]
[8]URL: `https://www.nammo.com/product/fdv-fvv/` [accessed: 12/06/2023]
[9]URL: www.vacco.com/filldrain [accessed: 12/06/2023]
[10]URL: www.faa.gov [accessed: 09/06/2023]

$$\Delta V = 2V \sin \frac{\Delta\Omega}{2} \qquad V = \sqrt{\mu_E \frac{2(1+e\cos\nu)}{a\left(1-e^2\right)} - \frac{1}{a}} \qquad (13.11, 13.12)$$

Where $\Delta\Omega$ is the change in ascending node required. V is the velocity of the satellite when the manoeuvre is performed. This should be as low as possible, hence the manoeuvre is performed above the south pole, with a true anomaly of 180°. This velocity can be determined with Equation (13.12)[12]. From this, it was determined that the maximum change in the right ascension of the ascending node that the propulsion system can provide is 0.75°.

The previous calculations show that the propulsion system would not be able to perform the full orbit insertion. Therefore, if the selected launcher were to change, it is crucial that the newly selected launcher is able to insert the satellites into the required inclination and the correct right ascension of the ascending node.

As a further consideration, it is also possible that space debris is detected to be in a collision path with one of the satellites. In this situation, the satellite needs to perform evasive manoeuvres. This would cost propellant and ΔV, which will lower the budget available for any of the other unexpected events. A further full analysis could be performed to quantify the exact impacts of the various possible and plausible evasive maneuvers.

13.4. Summary

Four thrusters are placed on the back side of the satellite, of which two are redundant. The selected thruster is the B20 thruster of DawnAerospace[11]. An overview of the properties of this thruster is shown in Table 13.4a. Based on the selected thruster, the configuration of the propulsion system has been decided.

Spherical tanks are used, made of Ti-6Al-4V to minimise the mass of the propulsion subsystem. The self-pressurisation properties of the oxidiser, N_2O, are utilised for the pressurisation of the oxidiser. The fuel, C_3H_6, is stored in a diaphragm tank and is pressurised using a buffer tank with nitrogen gas. The sizing of the tanks is based on the propellant mass calculations, of which the results are shown in Table 13.4b. Using this information, the tanks are designed, of which the results are shown in Table 13.4d.

Lastly, two trade-offs are performed to select both the regulating valves and fill&drain valves. The properties of these valves are presented in Table 13.4c. Mass estimation of the subsystem has been set up and is presented in Table 13.4e. The *other* category assumes that all elements present in the flow chart have an average mass of 400 g. Power consumption is also shown in Table 13.4f. Here, a division is made between the nominal power, when the system is idle, and peak power, when the system is starting a manoeuvre. The peak power will occur for 50 ms.

[11]URL: satcatalog.com/B20 [accessed: 09/06/2023]

Table 13.4: Summary of Propulsion Subsystem Properties

(a) Summary of the B20 Thruster Properties

Property	Value
Propellants	N_2O and C_3H_6
Dry mass	610 g
Operational temperature	−5 °C to 35 °C
Inlet pressure oxidiser	27.5×10^5 Pa to 72.0×10^5 Pa
Inlet pressure fuel	5.0×10^5 Pa to 14.7×10^5 Pa
Specific impulse	285 s
Maximum thrust	19.3 N
MIB	1 N s

(b) Summary of the Propellant Mass Division

Property	Value
ΔV contingency	100 m s^{-1}
ΔV de-orbit manoeuvre	161.21 m s^{-1}
Total propellant mass	140.50 kg
Propellant mass contingency	45.68 kg
Propellant mass orbit maintenance	17.65 kg
Propellant mass de-orbit manoeuvre	77.17 kg

(c) Summary of the Selected Valves' Properties

Property	Value
Regulator Valve	
Name	V1D10855-01
Operating pressure	31.0 MPa
Mass	800 g
Leakage	1×10^{-3}
Temperature range	−25 °C to 45 °C
Fill&Drain Valve	
Name	V1E10560-01
Operating pressure	46.2 MPa
Mass	10 g
Leakage	1×10^{-6}
Temperature range	10 °C to 30 °C

(d) Summary of Tank Properties

Property	Value
Material	
Material Properties (For All)	Ti-6Al-4V
σ_y	880 MPa
Density	4430 kg m^{-3}
Fuel tank (N_2O)	
Mass N_2O	127.042 kg
Pressure	7.5 MPa
Density N_2O	1.22×10^3 kg m^{-3}
Volume	104.13 L
Radius	0.292 m
Thickness	0.9 mm
Mass tank	1.362 kg
Fuel tank (C_3H_6)	
Mass C_3H_6	13.459 kg
Pressure	1.47 MPa
Density C_3H_6	613.9 kg m^{-3}
Volume	21.92 L
Radius	0.174 m
Thickness	0.2 mm
Mass tank	0.107 kg
Fuel tank (N_2)	
Mass N_2	0.403 kg
Pressure	31 MPa
Density N_2	-
Volume	1.022 L
Radius	0.062 m
Thickness	0.8 mm
Mass tank	0.056 kg

(e) Summary of the Mass Distribution

Component	Mass [kg]
Fill&Drain valves	0.05
Regulator valves	2.4
Tanks	1.525
Thrusters	2.44
Other	7.2
Total	13.615

(f) Summary of the Power Consumption

Property	Nominal Power [W]	Peak Power [W]
Thrusters	3.2	42
Valves	2.4	36
Total	5.6	78

14 Thermal

The primary functions of the Thermal Control System (TCS) are to monitor and provide the spacecraft with a thermal environment within the range acceptable to its respective components. It is therefore essential for the successful operation of the spacecraft, but not for satisfying the mission objectives directly. This nature lends towards its primary goals being entirely mission independent and determined by the specifications of the other systems. A standard 10 °C margin is placed upon the limiting values to decrease the probability of failure [12].

The ranges as dictated by the other subsystems are summarized in Table 14.1. Note that the ranges are already inclusive of the 10 °C margin. Component groups with multiple items are specified for the most strenuous range. It can be derived that among the body-mounted components, the batteries are the most limiting. The propellant management system is also unique in that the fill and drain's allowable range is small such that the 10 °C margin does not make sense, it will be considered as a special case. Thermally sensitive subcomponents of the payload are managed by their own internal thermal control systems, and only power needs to be provided. Other components, primarily electronic, are not explicitly specified for their allowable range [11]. It will be assumed to utilize the same allowable range as the other space-compatible electronics being used.

Table 14.1: Allowable Temperature Ranges of Taking Control Spacecraft Components

Components	Operability Temperature Range [°C]	Survivability Temperature Range [°C]
Solar Array Assembly		
Solar arrays	23.15 to 80	−190 to 120
Solar array actuators	−30 to 50	−50 to 50
Body Mounted Components		
Electronics (GNSS receiver limited)	0 to 35	−10 to 45
Batteries	10 to 20	10 to 30
Antennae (Transmitter limited)	−20 to 60	−40 to 85
ADCS actuators (Magnetorquer limited)	0 to 35	−10 to 45
ADCS sensors (IMU limited)	0 to 40	−10 to 50
Propellant management	10 to 20	10 to 20

14.1. Operational Environment

The operation of the thermal system considers the "thermal environment" that the spacecraft and its components are subjected to. This includes the temperature of each item in that environment and the heat flows between them. This can be considered from the macroscopic scale of the spacecraft as a whole and its interactions with external radiations, dictating the thermal equilibrium temperature. Alternatively, the internal heat flows between individual heat-generating and dissipating elements can be considered for their temperature gradient implications.

14.1.1. Temperature Equilibrium

The thermal equilibrium of the spacecraft is characterized by the heat flows between it and the environment. These flows can be simplified to solar radiation absorption, Earth infrared diffusion absorption, reflected Albedo absorption, the spacecraft's own thermal radiation, and internally generated heat from electronic equipment. Radiation's positive relationship with temperature leads towards a stable heat balance that will stabilize around a particular temperature. The various scenarios during the lifetime of the spacecraft will hence subject it to a multitude of different temperatures that

must be regulated to allow for component operability and survivability.

Firstly, the spacecraft will be subjected to a controlled external temperature of (21 ± 3) °C during pre-launch procedures. The spacecraft must then endure the radiation heat transfer from the launch vehicle fairing and free molecule aero-thermal heating during the launch phase [67]. During operation, the polar orbit will continually process through the entirety of the orbital plane-to-sun location angle (β) range, including full solar exposure and eclipse and solar array-blocking portions of orbit. These scenarios must be managed so that the spacecraft temperature remains within the component-specific allowable ranges.

14.1.2. Temperature Gradient

The stage of part and configuration design particularly with respect to the individual connectors is not fully established; nor the sufficient available resources to conduct a full temperature gradient analysis. However, considerations and recommendations can be made for the implementation of equipment to conduct thermal control in this regime.

14.2. Requirements

From system requirements on the thermal equilibrium and thermal gradient control, high-level subsystem requirements can be created. These can then be detailed for the subsystem components which have an operational thermal range. Moreover, additional requirements were generated based on the initial budget breakdown. The TCS requirements are listed in Table 14.2.

Table 14.2: Thermal Control System Requirements

ID	Requirement	Derived From
SUB-TCS-01	The TCS shall be able to determine its component temperatures with an accuracy of 10 °C	SYS-OPS-05
SUB-TCS-02	The TCS shall be able to provide a thermal environment for each component within a 10 °C margin of their operational temperature limit	SYS-OPS-05
SUB-TCS-02.1	The TCS shall maintain the electronic components' temperature within 0 °C to 35 °C during operation	SYS-TCS-02
SUB-TCS-02.2	The TCS shall maintain the batteries' temperature within 10 °C to 20 °C during operation	SYS-TCS-02
SUB-TCS-02.3	The TCS shall maintain the solar arrays' temperature within −23.15 °C to 80 °C during operation	SYS-TCS-02
SUB-TCS-02.4	The TCS shall maintain the antennae's temperature within −20 °C to 60 °C during operation	SYS-TCS-02
SUB-TCS-02.5	The TCS shall maintain the ADCS actuators' temperature within 0 °C to 35 °C during operation	SYS-TCS-02
SUB-TCS-02.6	The TCS shall maintain the ADCS sensors' temperature within 0 °C to 40 °C during operation	SYS-TCS-02
SUB-TCS-02.7	The TCS shall maintain the propellant management system's temperature within 10 °C to 20 °C during operation	SYS-TCS-02
SUB-TCS-03	The TCS shall be able to provide a thermal environment for each component within a 10 °C margin of their survivability temperature limit	SYS-OPS-05
SUB-TCS-03.1	The TCS shall maintain the electronic components' temperature within −10 °C to 45 °C during survivability state	SUB-TCS-03
SUB-TCS-03.2	The TCS shall maintain the batteries' temperature within 10 °C to 30 °C during survivability state	SUB-TCS-03
SUB-TCS-03.3	The TCS shall maintain the solar arrays' temperature within −190 °C to 120 °C during survivability state	SUB-TCS-03
SUB-TCS-03.4	The TCS shall maintain the antennae's temperature within −40 °C to 85 °C during survivability state	SUB-TCS-03
SUB-TCS-03.5	The TCS shall maintain the ADCS actuators' temperature within −10 °C to 45 °C during survivability state	SUB-TCS-03
SUB-TCS-03.6	The TCS shall maintain the ADCS sensors' temperature within −10 °C to 50 °C during survivability state	SUB-TCS-03

SUB-TCS-03.7	The TCS shall maintain the propellant management system's temperature within 10 °C to 20 °C during survivability state	SUB-TCS-03
SUB-TCS-04	The TCS shall provide thermal management for the spacecraft during all mission phases	SYS-OPS-05
SUB-TCS-04.1	The TCS shall provide thermal management while receiving 350 K, 0.9 emissivity radiation from the fairing	SYS-CON-11
SUB-TCS-04.2	The TCS shall provide thermal management under 1135 W m^{-2} free molecular aero-thermal heating post-fairing release launch phase	SYS-CON-11
SUB-TCS-05	The TCS shall have a maximum mass of 54 kg	SYS-CON-10

14.3. Configuration

The thermal control system consists of passive and active external components to influence the heat flows and heat generation to various parts of the spacecraft; while internal heat flow devices control the temperature gradient within the spacecraft.

14.3.1. Material selection

The primary method, by intention, is to implement passive components to regulate the temperature. Specific materials are selected for their specific thermal absorptivity and emissivity. The various external faces of the spacecraft are subjected to distinct thermal loads and will hence hold varying desirable thermal influences. A multitude of materials will need to be selected to satisfy all the external environments faced.

Materials - Cost and availability are key drivers towards the preferability of a smaller range of materials to be used. A single material has been selected for each role to be performed by the external coatings, and area balance is used for finer temperature control.

For insulation, vaporized deposited gold upon a Kapton polyimide tape was selected due to its exceptionally low emissivity and sufficiently low absorptivity. The most common and prolific product of Rockwell MB0135-038 can be acquired from providers of the like of Sheldahl [68]. [1]. This material features exceptionally low emissivity.

Radiators are satisfied by 8 mil Quartz mirrors, providing among the highest emission-to-absorption ratios among available options. They are readily available due to their use as mirrors for optics. [2] Radiation absorption is performed by Tinox surfaces with their complementarily exceptional absorption-to-emission ratio. With an absorptivity of 0.95 and emissivity of 0.04, it is sufficiently performant, whilst also being more readily available than alternatives such as MAXORB. [3]

3M Nextel Velvet paint in black provides a particular combination of characteristics to maintain the isolated solar array within its required temperature range. With limited possibilities to implement measures beyond just the coating material, this particular combination of characteristics must be used. It is readily available for purchase. [4]

Passive louvres are also applied to control and limit the effect of highly emissive or absorbent surfaces when heat balances shift. The particular sizes of the regions to be louvred lead towards the high likelihood of having to design a completely new and proprietary louvre. Design concepts and performance metrics within the realm of 0.7 changes to the emissivity or absorptivity of the underlying coating closer towards the performance of bare aluminium as with currently available hardware can be expected [12].

Material Thermal Performance - The radiation absorptivity (α) and thermal emissivity (ϵ) of the materials are known and can be applied to determine the heat flows for each surface. Manufacturer specifications can be taken for the start-of-life performance as well as incorporating similar materials

[1] URL: www.sheldahl.com [accessed: 14/06/2023]
[2] URL: www.ecoptik.net [accessed: 12/06/2023]
[3] URL: www.almecogroup.com [accessed: 13/06/2023]
[4] URL: www.nextel-coating.com [accessed: 13/06/2023]

and predictive models to estimate the performance degradation at the end of the 7.5-year spacecraft lifetime [12][68]. A summary of the thermal properties of the products selected is summarized in Table 14.3.

Table 14.3: Thermal Properties of Coatings Used

Material	α_{start}	α_{end}	ϵ_{start}	ϵ_{end}
Quartz Mirrors	0.05	0.05	0.08	0.08
Rockwell MB0135-038	0.19	0.20	0.03	0.03
Almeco Tinox	0.95	0.95	0.04	0.04
3M Nextel Velvet	0.97	0.87	0.84	0.74

Equation (14.1) and Equation (14.2) can be used to predict the area normalized thermal absorption and emission for a surface exposed to a radiation flux (S), with an absorptivity of α, an emissivity of ϵ, and temperature of T. The Stefan-Boltzmann constant (σ_B) is also used.

$$Q_{in} = S\alpha \qquad Q_{out} = \epsilon\sigma_b T^4 \qquad (14.1, 14.2)$$

Integration of all panel areas for the total heat flow, as well as the known incoming solar, Earth infrared, and albedo radiations, leaves the only unknown as the temperature. The equilibrium temperature of the thermal body is the only unknown. The internal temperature gradients will not be fully modelled but will be considered in Section 14.3.5.

14.3.2. Material Allocation

Firstly, the significant thermal loading as well as more relaxed temperature range requirements of the solar array assembly compared to the rest of the spacecraft, as well as its already significant physical separation allows for an insulative material to be used to isolate the parts as their own thermal bodies.

As described in Section 9.3.1, the solar array is angled to minimize incidence angle when feasible, often able to achieve 0°. The front side of the panel is an attribute of the cell technology used and cannot be covered up. The backside, however, allows for the selection of a medium absorbtivity and high emissivity to radiate away absorbed heat whilst also providing additional Earth infrared heating during eclipses; Nextel black velvet adequately manages the temperature range

The top and sides of the spacecraft are the faces additionally subjected to significant direct sun facing, depending on the ascending node of the current orbit state. β of 0 and 90 correlating to the top and side being exposed respectively. They must hence serve the dual roles of reflecting away solar radiation when sun-facing, but also providing insulation when the spacecraft would otherwise be losing heat. This is achieved through a mixture of both goldized Kapton MLI and louvred radiative quartz mirrors with the balance between their coverages selected to provide temperatures within the component-dictated allowable range.

The front and rear of the spacecraft also receive sunlight when the sun's position is coplanar with the orbit. But the smaller areas of these and reduced exposure time compared to the top face allows for them to only be covered in MLI and still satisfy the temperature requirements. No mirrors or louvres are implemented onto this face.

The bottom face of the spacecraft is of particular interest as it is always held in the nadir direction. It is the spacecraft's only source of receiving Earth radiation, being the sole source of heat during eclipses. It is otherwise covered in mirrors and passive louvres are implemented to reduce the heat intake from this side when solar radiation becomes the alternative source of heat for the spacecraft. The extensive louvre coverage allows for greater authority in influencing the heat should a thermal balance not be naturally met with the material sections implemented.

14.3.3. Design Concept

The full freedom of material selection, section sizing, and louvre design allows for a large set of viable design solutions. A set of combinations were determined along particular approach ideologies to identify the merits of each. The criteria that will be used to compare these concepts are temperature control, sensitivity to ageing, and louvre area.

The first two concepts emphasize the use of louvres with option one utilizing both radiators and absorbers whilst option two is entirely radiator based. They differ simply by the areas of the various radiator and absorber areas. The third option, on the other hand, is constructed to help identify the merits and limitations of minimizing the use of louvres. It instead utilizes vapour-deposited aluminized Kapton as a less efficient insulator to allow for smaller radiators.

The areas of the radiators and absorbers were not specified beyond increments of $0.1\,m^2$; the configurations were adapted for the best temperature range about the desired central value of 15 °C. These temperature ranges are compared to determine the relative insensitivity of the concepts to indicate the error margins available in achieving the desired temperature. This is a highly valued criterion as it is the primary objective of the TCS, hence with a weight of 45%.

The average increase in temperature of each scenario at the start and end of life can be compared whilst also including potential louvre effects that would offset the increase. This compares the type of material used, which is similar for all the options, but also the range of influence available to the louvres as deviations from the starting equilibrium point. Performance in this aspect significantly helps in offsetting the difficulty of accurately predicting material degradation behaviour, giving it a weight of 35%.

Lastly, the louvre areas can be directly compared. The additional cost, complexity, volume, and weight of these louvres are preferably avoided. With the likely use of proprietary louvres of adaptable sizes, the areas are the most straightforward metric for comparison. The flight heritage of louvres means that this should not be a significant concern [12]. It is therefore allocated a weight of only 20%.

Table 14.4: Trade-Off Criteria of the Thermal Control Configuration

Criterion	Weight [%]	1	2	3	4	5
Thermal half-range [°C]	45	<0 to >30	0 to 30	5 to 25	10 to 20	12.5 to 17.5
Aging deviation [°C]	35	> 4	≤ 4	≤ 3	≤ 2	≤ 1
Louvre area [m^2]	20	> 10	≤ 10	≤ 7.5	≤ 5	≤ 2.5

Table 14.5: Analysis of the Thermal Control Configuration Trade-Off Criteria

Criterion	Weight [%]	Minimal Louvres	Only Radiators	**Radiators and Absorbers**
Thermal half-range	45	3	4	4
Ageing deviation	35	4	3	5
Louvre area	20	4	2	3
Weighted total	100	355	325	**415**

The numerical values are only representative of an example of each design approach, but provide some insight into the general trends present. The thermal range is generally easier to control when more louvres are implemented. Additional radiators allow for reducing the temperature of a scenario that is too hot and can be louvred for all the other scenarios. Vice versa applies to the implementation of absorbers. The high heat in-flow of absorbers allows them to more easily heat the coldest situations than rebalancing the general materials and other section areas.

Ageing is in actuality more determined by the construction and exact properties of the product used;

but also in part affected by the system's ability to adapt its heat flows. This is evidently an advantage for the louvred systems. An additional benefit that should be considered is the passive aspect of the louvres allowing them to be adaptable to unexpected rates of coating degradation. The difference between the louvre setups can primarily be attributed to the non-extensive optimization of the louvre areas and openings conducted.

The louvre area is again not of significant importance considering the current constraints and direction of the spacecraft design. The efficacy of absorbers is again seen with their relatively small area increase to increase heat intake being disproportionately smaller than the radiator increase necessary to add heat through additional insulation. The first option had the objective of minimizing the louvre area to identify the magnitude of deficiency and perhaps any benefits. If the drawbacks of louvres were to become suddenly problematic for whatever reason, it can be more highly weighted for future iterations.

14.3.4. Thermal Section Dimensions

A mixed radiator and absorber panels upon an insulated base with louvre implementation appears to be the preferable design approach. Particular attention can then be given towards optimizing the exact numeric values of this design beyond the preliminary ones derived during the trade-off. The final values are summarized in Table 14.6. Radiators are rounded where possible to increments of $0.2\,m^2$ to ease the potential implementation of standardised louvres of that size.

The material selection elaborated in Section 14.3.1 is maintained with the insulator being goldized kapton, radiators with quartz mirrors, and absorbers with Tinox coating. All radiator and absorption panels are to be louvred where possible, taking into account obstruction by exterior mounted components.

Table 14.6: Thermal Coatings of Exterior Surfaces

Section	Material	Area [m^2]
Front-facing surfaces of structural panels' insulation	Golidzed Kapton	0.47
Front-facing surfaces of payload optics module insulation	Golidzed Kapton	1.80
Rear structural panel insulation	Golidzed Kapton	2.33
Right structural panel insulation	Golidzed Kapton	2.28
Right structural panel radiator	Radiator	0.80
Right-facing surfaces of optics module insulation	Golidzed Kapton	1.24
Left-facing surfaces of payload electronics module insulation	Golidzed Kapton	0.50
Left-facing payload electronics module radiator	Radiator	1.00
Left structural panel insulation	Goldized Kapton	1.59
Nadir structural panel absorber	Tinox	0.40
Nadir structural panel radiator	8 Mil quartz mirrors	2.20
Nadir-facing surfaces of structural panels radiator	8 Mil quartz mirrors	0.55
Nadir-facing surface of optics module	8 Mil quartz mirrors	1.78
Top structural panel insulation	Goldized Kapton	1.80
Top structural panel radiator	8 Mil quartz mirrors	0.80
Top-facing surfaces of optics module insulation	Goldized Kapton	2.68

The louvres are to be calibrated to a temperature of 15 °C causing the mirrors to shutter close during eclipses, and the absorber closed during sun-facing portions of orbit. It should be noted that when $\beta = 90°$ the absorber does not need to be louvred, the passive system will adapt accordingly for other β angles.

The equilibrium temperature can be calculated for the extreme loading cases. The implementation of louvres means that other scenarios between those points will fall within the range that can be accommodated by the TCS. Louvre closure amount is intentionally set to maintain the desired temperatures and is to be used as the basis for calibrating their behaviour.

These extreme scenarios include in-sun with maximum solar and Earth radiation and a β angle of 0,

likewise with a β angle of 90, and lastly an equilibrium during eclipse with minimum Earth radiation. The launch scenario with fairing heating to all external surfaces in a stowed undeployed configuration (solar array at a third of the area, top of the body covered by array, front and back attached to adapters. Electrical power is assumed to be converted entirely into heat and introduced into the system. The degradation values are based on NASA's general guidelines on spacecraft coating characteristics and have high uncertainty [68]. The final values for each scenario are summarized in Table 14.7.

14.3.5. Heat Transfer Components

Internal components can be implemented to control the temperature gradient between components. They can regulate the temporal flow rate of heat between components. This is relevant for both temporary heat sources, as well as flow-limited temperatures. These components, perhaps most importantly, can allow for the reduction or compensation for deficiencies in the use of louvres as the design progresses and further details become established.

Firstly, a sufficiently insulating connection can be implemented to delay the heat transfer for a non-permanent heat source or sink. This will be implemented to thermally isolate the solar array assembly from the rest of the spacecraft body. Whilst some heat transfer is expected, it will be analyzed along with the final design of the boom arm to determine if it is excessively detrimental to the predicted equilibrium state. It can also delay excessive heating or cooling of the most sensitive components, helping them remain safe during thermal extremes.

Thermal transfer acceleration can also be done with components such as heat pipes, straps, or any other thermally conductive part to connect components [12]. Particularly useful for electronics that are both heat-generating and desire to operate at lower temperatures; allowing them to more directly transfer heat to the radiators. The final operating procedures and protocols would be necessary to conduct a full thermal analysis of the time-related power use of each component. Only this basic concept is established currently. No components were identified as preferring to be particularly hot. Because of this, most of these connections are expected to be between internal heat-generating components to more quickly transfer to the spacecraft body if not to the radiators themselves. The presence of radiators on the top, bottom, and both sides of the structural panels should allow for feasible connection lengths.

Lastly, flow-limited connections can be established around heat-generating sections that are intentionally kept hot. Within the cold periods of orbit, the heat loss can be limited such that the component never falls to the equilibrium temperature of the rest of the thermal body. Such an implementation can allow for a local temperature range higher than its surrounding. This will be applied as an absorber on the solar array boom actuation motor with insulation to adjacent components. This allows it to remain above the rest of the array's minimum temperature and within its own minimum operability temperature of $-50\,^{\circ}\text{C}$. Likewise will be done with the isolation of the coupled nadir absorber and propellant management system to maintain its desired temperature range of $10\,^{\circ}\text{C}$ to $20\,^{\circ}\text{C}$ that is within, but of a significantly smaller range than the rest of the spacecraft components.

14.4. Sensitivity Analysis

The thermal control system must also be analysed with consideration to how it is able to perform its required tasks under different design constraints. This will be considered from the aspect of mission parameter variation, additional design constraints, and changes to the thermal environment. These aspects are more concisely categorized into increased coating degradation, changed allowable temperature range, louvre restrictions, and significant radiation environment changes.

Mission duration is particularly interesting due to the limited predictability of the exact combination of materials, orbit, and space environment. The implementation of additional louvred mirrors remains a possibility for mitigation. If the predicted degradation of materials is expected; in an extreme case completely quartz mirrored body would allow for an end-of-life body temperature between $-98.3\,^{\circ}\text{C}$ to $-76.8\,^{\circ}\text{C}$ (no louvres) with current duration and degradation predictions. While such a configuration may not be convenient, it indicates a significant margin for degradation predictions or the mission

duration to increase before a complete change in design approach will be necessary.

Another consideration is if the components will then require a tighter temperature range. The utilization of louvres means that the temperature for each scenario can be very finely set through a very particular louvre setting. For example, increasing the nadir absorber to $0.63\,m^2$ results in a start-of-life temperature range of 22.3 °C to 23 °C; hence a range magnitude of only 0.7 °C. This temperature is no longer within the spacecraft's preferred temperature range but is an example that such optimizations are possible with sufficient fine-tuning of the radiator and absorber areas and louvring. However, such accurate manipulation may not be feasible with passive means. A detailed analysis should be conducted on the accuracy of passive louvres if the intended control range is to be reduced. For example, Sierra Space's passive louvre is variable but cannot be assured for exactness within a 6 °C range.

Central temperature shifts, on the other hand, can be more easily shifted with the ratios of radiator-to-absorber patches. On the low end is the full mirror configuration mentioned with a central temperature of −87.6 °C. A fully insulated body on the other hand is already able to achieve temperature ranges upwards of 370 °C. Absorbers can increase this even further, but such ranges are extremely unlikely with any current equipment. Louvring can be applied around these new central equilibrium temperatures to manage the range due to the various thermal scenarios of the orbit.

The application of mechanical louvres introduces additional reliability risks. A potential theoretical constraint against the use of louvres can be considered. Removing any louvre effects from the previously derived minimal-louvre approach results in a temperature range of −24.2 °C to 16.5 °C. The fluctuation of approximately 40 °C is evidently outside of the acceptable range. This approach used vapour-deposited aluminized Teflon insulation and as much radiator space as necessary. A more optimized design may be possible, but sensitivity results from altering values do not indicate significant performance gains. Such a change would hence invalidate the current design approach, and require more additional active means for component heating, louvre-less adaptable coatings, or a full analysis of internal heat flows with consideration for temporal flow rates throughout the orbits.

The radiation environment experienced by the spacecraft is also a very significant determinant of the design concept chosen. Solar radiation is relatively consistent everywhere within the Earth's sphere of influence [12]. Temporal variation however commonly exists within the order of $100\,W\,m^{-2}$ [12]. Such variations would cause only 1.54 °C to 1.82 °C differences to in-sun temperatures, such values are considered acceptable with respect to the 10 °C margin already implemented. Exceptional solar events would need to occur for this effect to be non-marginal. Equilibrium temperatures are also considered, negating eclipse and solar exposure time variations.

The last analysis conducted is the complete thermal coupling of the solar array and spacecraft body. Such a reconfiguration, without a panel size change or louvring, would result in a temperature range of −53.6 °C to 105.0 °C. Full louvring of the radiators, for example, would only increase the minimum temperature to −43.8 °C, still far from the desired range. It will be exceptionally difficult to still make this design approach work. To remain feasible, there would be a need to implement active means to maintain an acceptable temperature range.

14.5. Summary

The body of the spacecraft is thermally segregated from the solar array assembly. This isolation is accommodated by the spatial separation of the parts and thermally insulating material used in the boom arm. The array is controlled within the more variant range of approximately −70 °C to 70 °C. Whilst the more sensitive body components are contained within 10 °C to 20 °C. Individual components with special requirements are locally controlled within their desired bounds, this includes the solar array drive motor, and the fill/drain valve.

Solar array thermal control is conducted using 3M Nextel Velvet black paint on the back and side surfaces of the array. The drive motor will be additionally insulated to allow for a hotter temperature during eclipses. No other means are necessary to maintain the array assembly components within

their desired operational and survivability ranges.

The body is primarily insulated with Rockwell MB0135-038 goldized Kapton single-layered insulation. All non-operational outer surfaces are to be covered in insulation unless otherwise stated. Quartz mirrors are used as radiators and Almeco Tinox coating as absorbers on key surfaces exposed to significant radiative heating. Louvres are implemented upon the radiator and absorber surfaces to limit their absorptivity, centralizing as much as possible around 15 °C.

The spacecraft's equilibrium temperature is calculated for the identified critical scenarios during its life cycle. These values are summarized in Table 14.7 below. The spacecraft body will experience a temperature fluctuation between 13.7 °C to 18.8 °C at the start of life and increasing to 14.6 °C to 20 °C at the end-of-life. The array will experience a temperature range from −59.6 °C to 63 °C widening to −61.9 °C to 68.5 °C for the start and end of life respectively.

Table 14.7: Temperature Ranges Experienced by the Spacecraft

Phase of Life	In Sun	β	Array Temperature °C	Body Temperature °C
Launch	Fairing heating		-36.9	11.0
	Aero Heating		-12.5	29.2
Start	Sun	90	63	13.7
	Sun	0	63	18.8
	Eclipse	0	-59.6	18.4
End	Sun	90	68.5	14.6
	Sun	0	68.5	20.0
	Eclipse	0	-61.9	18.4

The masses of each coating are known and provided by the respective manufacturers. An average louvre mass-per-area is used from existing flight-proven examples. The summation of all surfaces provides the total mass of the Thermal Control System. The entirely passive nature of the thermal control components leads to no power usage. Thermal sensors use a marginal amount of power when measurements are taken, and are the only electrical power-consuming component of the TCS itself. These values are summarized in Table 14.8.

Table 14.8: Mass and Power Characteristics of Thermal Control System

(a) Mass Characteristics of the Thermal Control System

Component	Mass [kg]
Insulation	2.05
Radiators	1.45
Absorbers	0.12
Louvres	42.68
Total	46.30

(b) Power Characteristics of the Thermal Control System

Component	Power [W]
Pulse power	4.7
Average power	2.0

15 Structures

The structural subsystem of the spacecraft comprises all physical interfaces between subsystems and to the launch vehicle. The requirements that are placed on the structures in order to fulfil this function are described in Section 15.1. The structural concept is highly interdependent on the layout and packaging of the spacecraft, so a first idea of important considerations for the configuration are discussed in Section 15.2. In Section 15.3, the concept options are detailed and one is selected; it is to be designed hand in hand with the materials selected in Section 15.3.1. Finally Section 15.3.2 provides the results of the detailing and analysis of the structural subsystem, before Section 15.4 analyses the sensitivity of the Structural Subsystem to changes in design parameters. The structural subsystem is summarised in Section 15.5.

15.1. Spacecraft Structural Requirements

The structural requirements of the spacecraft are essential for the design of the structural subsystem. Primarily, they are derived from the loading under launch and operation, and the environments under which the spacecraft operates.

15.1.1. Spacecraft Loading and Environments

The spacecraft (and structure) experiences many loads and environments, all of which must be accounted for. These are described in Table 15.1. The EOL requires that the spacecraft returns to Earth's atmosphere, so should be considered in order to ensure compatibility, but does not constitute a load case which must be withstood.

Table 15.1: Load Cases and Environments experienced by the Structure of the Infrared Pollution Monitoring System spacecraft [12]

Phase	Types of Loads	Environments
Manufacture & Assembly	Welding/Joining/Machining stresses, Handling	Workshops/Cleanrooms
Transport & Handling	Crane/Dolly loads	Land, Sea, Air Transport
Testing	Vibrations/Acoustics	Workshops/Cleanrooms
Launch	Steady-state accelerations, Vibro-acoustic noise, Transient events and Pyrotechnic shock	Payload bay, under fairing, exposed to change in air pressure
Operations	Steady-state accelerations, transient loads in pointing manoeuvres, thermal stresses from solar heating	Vacuum, changing solar loading, space-dust, radiation
End of Life	Aerodynamic heating and drag	Exposed to air at high velocity

15.1.2. Structures Requirements

The requirements on the structural subsystem and their derivations from system requirements are described in Table 15.2.

Table 15.2: Requirements on the Structural Subsystem of the Taking Control Spacecraft

ID	Requirement	Derived From
SUB-STR-01	The structure shall be able to withstand + 8.5 g / - 4 g longitudinal acceleration in launch configuration[1]	SYS-CON-12
SUB-STR-02	The structure shall be able to withstand ± 3 g lateral acceleration in launch configuration[1]	SYS-CON-12

[1]URL: www.spacex.com [accessed: 06/06/2023]

SUB-STR-03	The structure shall interface with the SpaceX 1575mm interface according to it's datasheet[1]	SYS-CON-08
SUB-STR-04	The structure shall be able to withstand 100 station-keeping burns at 0.004 g	SYS-OPS-20
SUB-STR-05	The structure shall have a maximal outer dimension defined by a cylinder of diameter 4 m and length 4.4 m	SYS-CON-08
SUB-STR-06	The structure shall have a maximum mass of 262 kg	Section 8.1
SUB-STR-07	The structure shall isolate the mission instruments and payload from vibratory disturbances as specified in their datasheets	SYS-OPS-19
SUB-STR-08	The structure shall provide standardised mounting points to all spacecraft subsystems	SYS-OPS-19
SUB-STR-09	The structure shall have a first harmonic eigenfrequency (perpendicular to launch direction) > 10 Hz[1]	SYS-CON-10
SUB-STR-10	The structure shall have a first harmonic eigenfrequency (in the launch direction) > 31 Hz[1]	SYS-CON-11
SUB-STR-11	The structure shall shield all internal components from micrometeorites and cosmic dust below 1 cm at 8 km s^{-1}	SYS-OPS-19
SUB-STR-12	The structure shall not plastically deform during the expected lifetime of the spacecraft	SYS-OPS-19
SUB-STR-13	The structure shall protect corrosion-sensitive components to the standard NASA STD 6012A	SYS-OPS-19
SUB-STR-14	The structure shall utilise outgassing materials with Total Mass Loss <1%	SYS-OPS-19
SUB-STR-15	The structure shall utilise corrosion-resistant materials to the standard NASA STD 6012A	SYS-OPS-19
SUB-STR-16	The structure shall be sufficiently weak to break into multiple pieces during reentry	SUS-SPA-04
SUB-STR-17	The structure shall melt at a temperature below 4500 °C	SUS-SPA-04
SUB-STR-18	The structure shall not melt at a temperature below 500 °C	SYS-OPS-19
SUB-STR-19	The structure shall enable access to subsystems for testing	Functionality
SUB-STR-20	The structure shall enable access to subsystems for assembly	Functionality
SUB-STR-21	The structure shall comprise only elements with TRL>5	SYS-CON-09
SUB-STR-22	The structure shall not comprise of toxic materials	SUS-SPA-13
SUB-STR-23	The structure shall not comprise of radioactive materials	SUS-SPA-14
SUB-STR-24	The structure shall reduce the dose of cosmic radiation which reaches the internal components to below 500 Sv over the lifetime	SYS-OPS-02

15.2. Spacecraft Configuration

When considering the physical configuration of the system; a key driver of the structure, a few key considerations are made. Firstly, there are requirements imposed by the payload; it must be unobstructed during observation, thermally, electromagnetically, and mechanically insulated from the rest of the system, and it must point nominally to the Nadir. This means that the solar array, which must be free to rotate on two axes, must be placed at the opposite end of the spacecraft to the payload. Primarily so as not to obstruct the sensor, but equally to avoid reflecting heat towards the sensitive infrared sensing equipment.

To minimise the mass and power required for ADCS, as much of the mass of the spacecraft as possible should be located on or near the central axes of the spacecraft, while the actuators (magnetic torquers and reaction wheels) are to be placed at the extremities of the Spacecraft, while the thrusters for propulsion must be placed with their line of action passing through the centre of gravity of the spacecraft. There are various requirements on the location of the sensors, some require specific pointing directions, while others require to be free from sources of noise such as electromagnetic interference. Most must be placed on the outside of the spacecraft.

By comparing the electrical and data block diagrams of the system, locations can be found for the relevant subsystems which minimises the complexity and size of the wiring harness, reducing additional weight. Equally, by isolating the propulsion subsystem from the rest of the spacecraft, it is possible to reduce the mass of tubing required for the propulsion system, finally resulting in the

preliminary layout described in Figure 15.1.

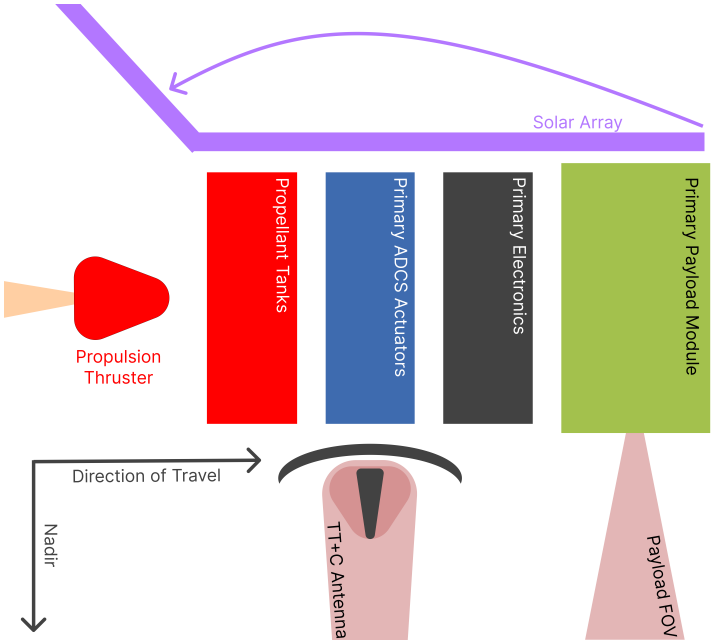

Figure 15.1: Layout of Subsystems and Structure

15.3. Structural Concept and Configuration

From the requirements, 4 concepts were determined: a full monocoque, partial monocoque, spaceframe, and a backbone structure. Each of these concepts is utilised in existing spacecraft and therefore they are all proven to have a sufficient TRL for use in the Taking Control Spacecraft. Diagrams of each option are provided in Figure 15.2, and a concept is selected in Section 15.3.2.

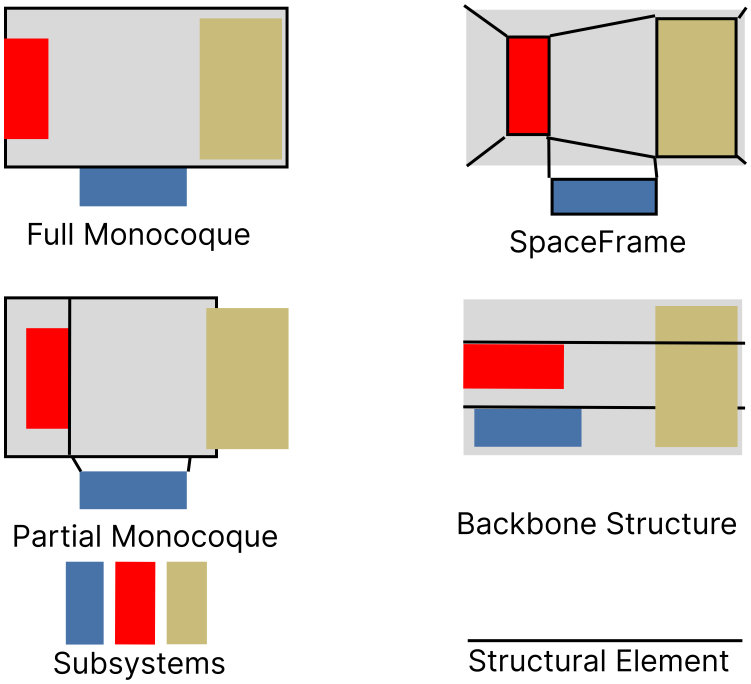

Figure 15.2: Concepts for the structural subsystem of the IPMS

15.3.1. Structural Materials

From *Space Mission Engineering: The New SMAD*, a number of material options can be derived for the Taking Control Spacecraft, each with its own strengths and weaknesses. These are:

- **Aluminium** High strength/weight, ductile, easy to machine, but with low hardness and high thermal expansion
- **Steel** High strength, but difficult to machine, ferromagnetic, and high density
- **Magnesium** Low density, but susceptible to corrosion and low strength/volume
- **Titanium** High strength/weight and low thermal expansion but expensive, difficult to machine, and low toughness
- **Composites** Can be tailored to achieve ideal characteristics, high strength/weight, but costly and the quality is dependent on workmanship and difficult to inspect

There are also commercially available solutions for sandwich panels formed of any of the above materials but also formed of combinations of the above materials. For metals, it is also possible to use alloys of any of the above materials to achieve varying material characteristics.

Sandwich panels, particularly with an aluminium honeycomb core are known to be great protectors of internal components against micrometeorites and small-medium debris, without losing significant structural integrity [69]. Equally, these panels provide improved bending and shear strength/weight performance over the same material in a normal configuration, given that the moment of inertia around the central plane is increased without a large increase in the weight of the material. Aluminium (and its alloys) is also the most likely material to wholly burn-up, up due to its significantly lower melting temperature than pure steel and titanium.

15.3.2. Structures Selection and Sizing

Given that the structure must protect the internal components from debris, it is decided that in any case, the outer shell of the structure will be made from honeycomb sandwich panels. Since these panels are also strong, stiff, and lightweight structural elements, while there is a need to mount components to the perimeter of the spacecraft; it is logical and therefore decided to use either a partial monocoque for the spacecraft structure; with the sandwich panels as the main structural elements. From this, it is possible to carry out a trade-off for the binding/skin material of the sandwich structure, with an aluminium honeycomb as the core. Magnesium is not offered as an option given it fails the requirement for corrosion resistance.

The criteria utilised are specific-strength, -modulus, -cost, fracture toughness, and manufacturability. Specific strength is expected to be limiting for the mass of the system, which should be minimised to minimise launch emissions and maximise the possibility of loading the spacecraft. Cost is of secondary importance, given the need for a financially feasible structure. Finally, specific modulus assists in the minimisation of vibrations and displacement, toughness aids in the protection against debris and micrometeorites, while manufacturability is an important consideration for the ability of the spacecraft to be produced.

Table 15.3: Trade-Off Criteria of the Structures Material

Criterion	Weight [%]	1	2	3	4	5
Specific Strength [$kN\,m\,kg^{-1}$]	40	≤100	≤125	≤150	≤175	≥175
Specific Modulus [$Mm^2\,s^{-2}$]	10	≤ 10	≤ 20	≤ 50	≤ 100	≥ 100
Specific Cost [$\$kg^{-1}$]	25	≥ 100	≥ 50	≥ 25	≥ 5	≤ 5
Fracture Toughness [$MN/m^{3/2}$]	15	≤ 5	≤ 10	≤ 30	≤ 60	≥ 60
Manufacturability	10	Only at Specialist Plant	Only with Specialist Equipment	Specialist Tool	Specialist Training	No Specialism

Table 15.4: Trade-off analysis of the Structures Material Options, with Data from [70]

Criterion	Weight [%]	**Aluminium (7075-T6)**	Steel (4340)	Titanium (6Al4V)	CFRP	GFRP
Specific Strength	40	5	4	5	3	1
Specific Modulus	10	3	3	3	1	2
Specific Cost	25	5	5	4	1	5
Fracture Toughness	15	3	5	5	4	4
Manufacturability	10	5	4	3	1	2
Weighted total		**450**	430	435	225	265
Rank		1	3	2	5	4

From the trade-off, it is clear that any of the proposed metals would be a good option, though aluminium comes out as the winner. Being significantly cheaper than titanium and an already established industry standard material, aluminium will be used for the skin of the sandwich panels.

15.3.3. Sandwich Panel Sizing

In order to preliminarily size the sandwich panels, the spacecraft is simply modelled for the highest load case: launch, for which the loads are defined in Figure 6.2, and the critical cases are detailed in Table 15.5. For the purposes of the analysis, the structure is modelled as a mass-spring model, described in the free body diagram of Figure 15.3a, and made with a number of assumptions:

- The cross-section described in Figure 15.3b is the only load-bearing element of the structure
- There is no in-plane stiffness in the honeycomb - it acts similarly to an infinitely thin flange of an I-beam
- Angular deflections are small
- The cross-section of the structure remains constant
- The mass of the spacecraft is concentrated at the Center of Gravity
- The interface with the launch vehicle acts as a support fixed in all degrees of freedom
- The skin panels are continuous (there are no local concentrations due to joining)

The effect of these assumptions cannot be accurately quantified at this stage, in the following development of the structure, it would be advisable to use a finite element model of the structure to validate the preliminary calculations made here. For the preliminary purpose of global sizing to understand the order of magnitude of stresses, this model is sufficient, but will not describe the

accurate, local, stress concentrations.

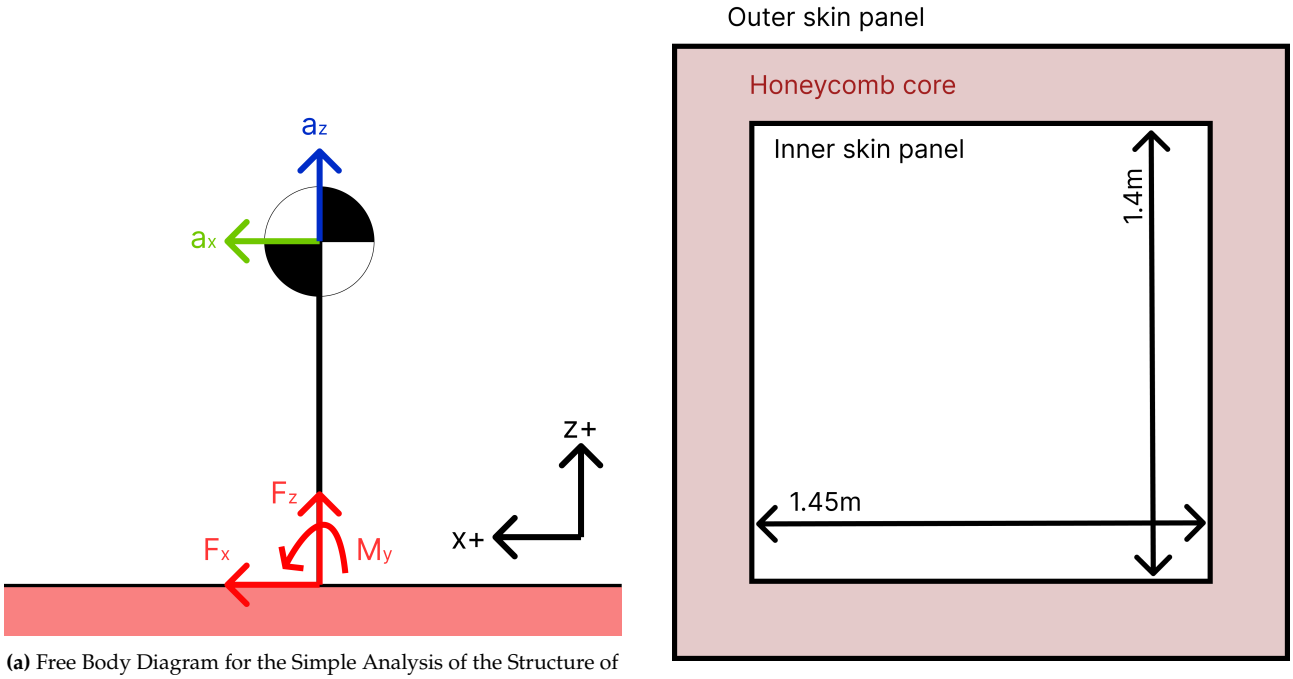

(a) Free Body Diagram for the Simple Analysis of the Structure of the IMPS

(b) Cross Section of the Structure of the IPMS

Figure 15.3: Diagrams describing the analytical setup of the Structures Analysis

To calculate the stresses in the root of the structure, it is first required to transform the accelerations applied to the spacecraft into forces and torque about the root, as described in Table 15.5. These loads assume a Spacecraft Mass of 1691 kg (Section 8.1), in the launch configuration, with Center of Gravity in the longitudinal axis of the launch vehicle, at 1.5 m from the connection interface.

Table 15.5: Load Cases for the Structural Subsystem of the IPMS

Loads	A	B	C	D
a_x [g]	2	3	3	2
a_z [g]	8.5	4	-1.5	-4
Reaction Loads at Root				
F_x [N]	-3382	-5073	-5073	-3382
F_z [N]	14373.5	6764	-2536.5	-6764
M_y [Nm]	-5073	-7609.5	-7609.5	-5073

Firstly, the normal (σ) and shear (τ) stresses are calculated with Equations (15.1) and (15.2) respectively; from the Axial Load (F_z), Lateral Load (F_x), Torque (M_y), Cross-Sectional Area (A), the furthest distance from the yz plane (x), Moment of Inertia (I_{xx}), and Moment of Area (Q).

$$\sigma = \frac{F_z}{A_{cs}} + \frac{M_y x}{I_y} \qquad \tau = \frac{F_x Q}{I_y b} \tag{15.1, 15.2}$$

Secondly, the stiffnesses (k) in the axial and lateral directions are calculated with Equations (15.3) and (15.4). Here L is the distance from the root to the Center of Gravity, while E is the E- (Young's-) Modulus of the skin material.

$$k_{ax} = \frac{EA}{L} \qquad k_{bend} = \frac{EI_y}{L^3} \tag{15.3, 15.4}$$

This enables the calculation of the first harmonic resonant frequency (ω_0) in both axial and lateral modes with Equation (15.5), where m is the lumped mass of the spacecraft.

$$\omega_0 = \sqrt{\frac{k}{m}} \tag{15.5}$$

Research shows that 2.5 cm thick honeycomb, with a density of 740 kg m^{-3} is considered in the industry to be sufficient to shield against reasonably likely micrometeorites and debris[2]. To ensure this safety, a factor of safety of 2 is applied, giving a minimum core thickness of 5 cm.

Taking this minimum core thickness, and a limit load of 95 MPa (the fatigue strength of Aluminum 7076-T6), the required skin thickness is 0.0055 mm (still giving eigenfrequencies that fulfil SUB-STR-09/10), hence the structure is possibly limited by manufacturability and by shielding against β and γ radiation, rather than by strength or eigenfrequency requirements. Typical γ radiation exposure for a spacecraft in LEO with high inclination (over the poles) is 10 Sv yr^{-1} to 100 Sv yr^{-1}[3], the maximum lifetime dose of the electronics is 500 Sv. Therefore some radiation shielding for γ photons is required in order to achieve the required lifetime of the system.

Advanced heavy metal oxide (such as Molybedinum Oxide) coatings have been developed, which can be applied to the internal skin of the structure; this has been proven to result in a factor 300 reduction in γ radiation and a factor 2 reduction in β and neutron radiation without adding significant mass to the subsystem [71]. The use of these coatings will, with a low mass increase, shield the internal components sufficiently from all forms of radiation such that radiation is not limiting for the lifetime of the spacecraft. In having been demonstrated, this technology has a TRL 5 to 7.

Finally, this means that the skin thickness is not limited by structural integrity, eigenfrequency, or radiation absorption. The limiting factor is manufacturability. Hence a skin thickness of 2 mm is selected, to combine with the core thickness of 50 mm.

15.4. Sensitivity Analysis

There are a number of mission variables which are deemed to have either a direct or indirect effect on the structures. Some would result in conceptual changes to the structures, while others would result in the need to resize the structure. These are the duration of the mission, the target cost of the mission, the selected instrument, and the total wet/dry masses of the spacecraft (alongside the location of the Center of Gravity (CoG)). For each, the possible changes to the structures are investigated in this section.

Were the duration of the mission to be extended, more propellant and therefore larger tanks are be required. This would likely result in cylindrical rather than spherical tanks, which would be better suited to being the central structural element of the spacecraft, meaning that a backbone concept could become leading for the structures, so as to save the total mass of the spacecraft.

If the mission could be achieved at a greater cost per satellite, then the use of more advanced materials could be preferable, such as composite panels, titanium, or 3D-printed metals. This could result in a much more structurally optimal subsystem, resulting in a greater mass budget for other subsystems - enabling the extension of the lifetime or the increasing of the payload mass.

Should the instrument have a different FoV or thermal requirements (being unable to manage its own temperature, for example) then a different layout may be preferable to either minimise the obstruction to the instrument or the additional cooling required. If this mandates a different shape to the simple 'box' currently used, then a semi-monocoque could become much less preferable to implement due to the complex forms of the spacecraft. Equally, if the instrument was significantly smaller or less structurally rigid, a full monocoque would be preferred over a partial monocoque, in order to retain structural rigidity.

Currently, the limiting factor in the sizing of the skin panels in the existing concept is driven by

[2]URL: encyclopedia.pub [accessed: 16/06/2023]
[3]URL: llis.nasa.gov [accessed: 16/06/2023]

resistance to debris, manufacturability, resistance to radiation, strength, and stiffness; in that order. Assuming that debris, manufacturability and radiation set minimum limits which do not change significantly with the parameters of the spacecraft, then one can investigate the point at which the peak stress and the eigenfrequencies would become dominant factors (thus increasing the requirement on the thickness of skin or stiffness/strength of the skin material.

Using the same calculations as those which are described in Section 15.3.2, one can find that the mass of the spacecraft must increase by a factor of 35x in order for the peak stress (in shear) to exceed the fatigue strength of Aluminium, while a 417x increase is required for the eigenfrequency to be limiting (in the launch direction), clearly, the sizing is unlikely to be affected by such an increase in mass, as it would take the spacecraft mass well beyond the capabilities of any existing launcher.

Equally, the distance of the CoG from the base can be examined; a 12x increase in distance from the base is required in order to reduce the bending eigenfrequency below the requirement, while a 53x increase is required for the peak stress (in the normal direction) to be limiting. Clearly, the structure sizing is not sensitive to either the location of the CoG or the mass; in its current configuration.

15.5. Summary

Resulting from the analysis carried out in this chapter is the structural subsystem in a preliminary state. In further design, radiation shielding, reinforcement, and assembly must be considered in more detail. It is estimated that radiation shielding will add $1\,\mathrm{kg\,m^{-2}}$ over the $16.4\,\mathrm{m^2}$ surface area of the structures, while additional reinforcement (nuts, bolts, reinforcement plates, and the launch vehicle adapter) for localised load transfer are preliminarily estimated to be 20% of the initial structural mass. The calculated maximum stress includes a 1.5x safety factor in order to ensure that the spacecraft is safe from unexpected peak loads. The structure subsystem characteristics are summarised in Table 15.6, with a render of the subsystem's preliminary design shown in Figure 15.4, where all other subsystems are made seethrough.

Table 15.6: Summary of Key Characteristics of the Structural Subsystem

Variable	Units	Value
Structures Height	mm	2100
Structures Width	mm	1554
Structures Length	mm	1504
Wall Thickness	mm	54
Skin Thickness	mm	2
Core Thickness	mm	50
Structural Mass	kg	135.4
Radiation Shielding Mass	kg	16.64
Reinforcement Mass Estimate	kg	27.08
Total Subsystem Mass	kg	179.12
Structures Peak Power Usage	W	0
1st Eigenfrequency in Launch Direction	Hz	566.2
1st Eigenfrequency Orthogonal to Launch	Hz	382.7
Peak Axial Stress During Launch	MPa	3.25
Peak Shear Stress During Launch	MPa	3.1

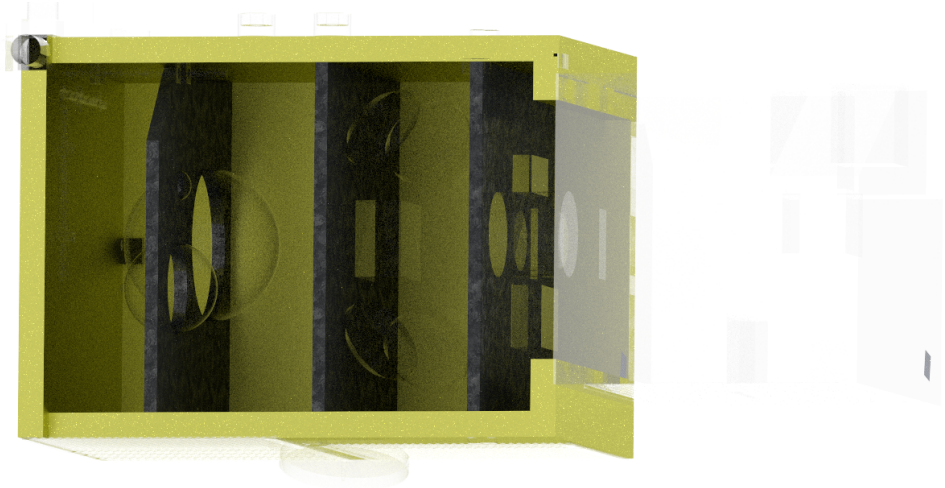

Figure 15.4: Render of the Structural Subsystem, With All Other Subsystems Seethough

16 Configuration & Layout

With the IPMS spacecraft design complete, it is possible to summarise both the hardware and software aspects of the solution by first describing the physical configuration and layout in section 16.1 and Section 16.2, with block diagrams further describing the interrelation between subsystems in section 16.3. Finally section 16.4 details the use of resources by the subsystems and system as a whole.

16.1. Configuration/Layout

There are 2 key configurations of the spacecraft: the deployed (operational) state, and the undeployed (launch, transfer, insertion) configuration. Besides these, the internal configuration of the IPMS does not change dependent on the state. Both states are described, alongside the internal layout, in the following subsections.

16.1.1. Deployed Configuration

The deployed configuration (annotated with the orbital direction and the observation direction - earth facing) is shown in Figure 16.1, while a sketch of the profiles of the spacecraft is shown in Figure 16.2

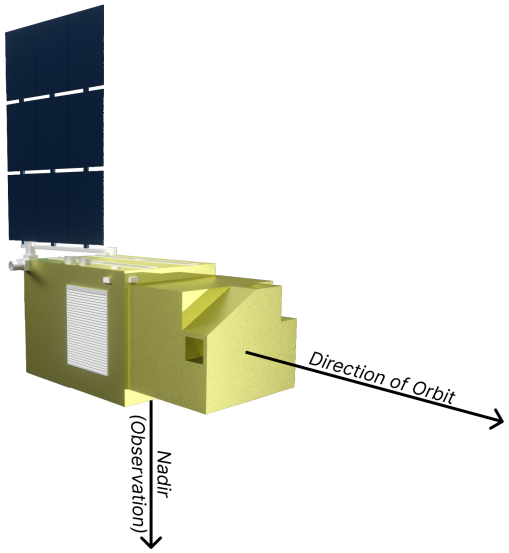

Figure 16.1: Render of the full Infrared Pollution Monitoring System Satellite in the deployed configuration

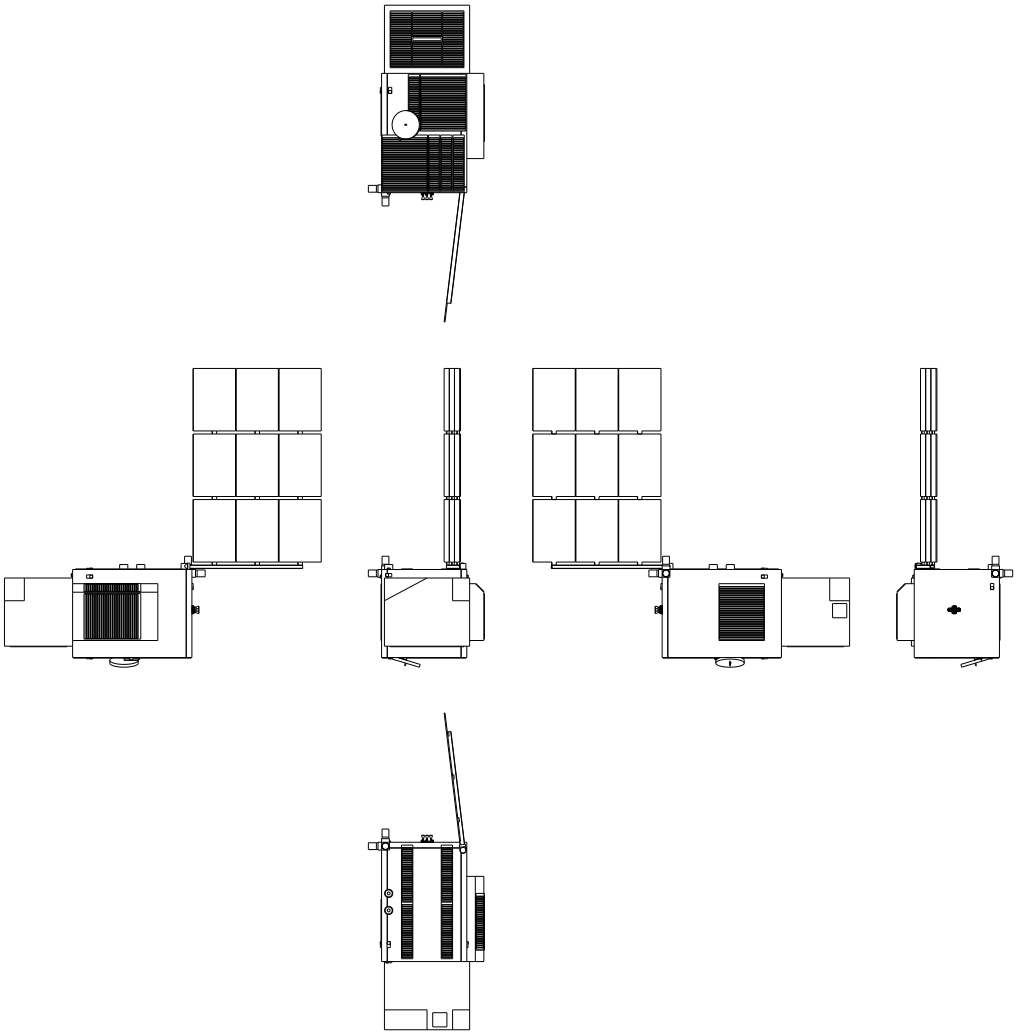

Figure 16.2: Sketch of the full Infrared Pollution Monitoring System Satellite in the Deployed Configuration

16.1.2. Undeployed Configuration

In the undeployed configuration, the volume and moments of inertia of the satellite are minimised for the purposes of launch and insertion. Firstly, a sketch of the profiles of the satellite in this configuration is shown in Figure 16.3, while the launch configuration (in which 3 IPMS Satellites are launched simultaneously), is shown in Figure 16.4, as proof of compliance with the geometric requirements of the selected Falcon 9 Launch Vehicle.

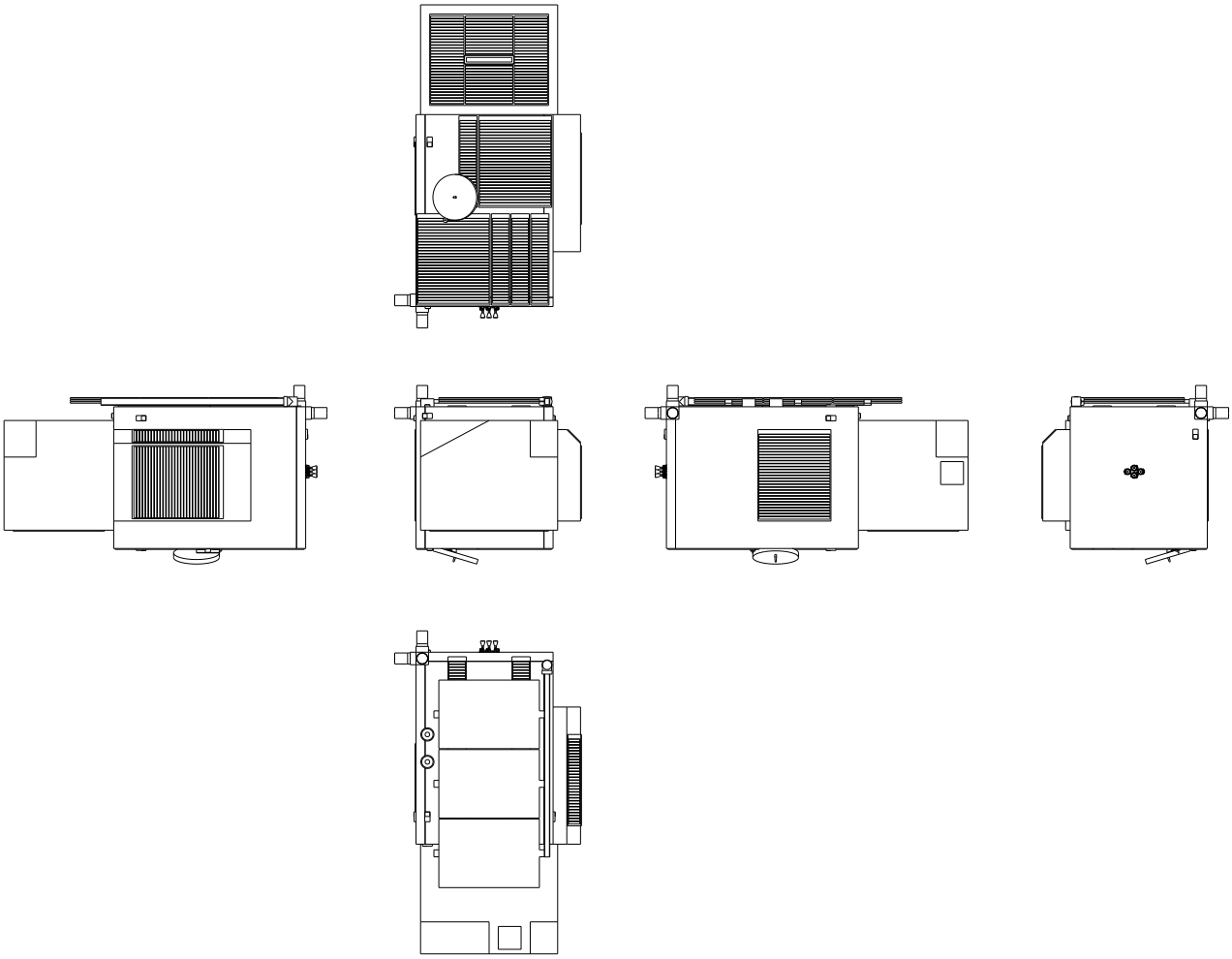

Figure 16.3: Sketch of the full Infrared Pollution Monitoring System Satellite in the Undeployed Configuration

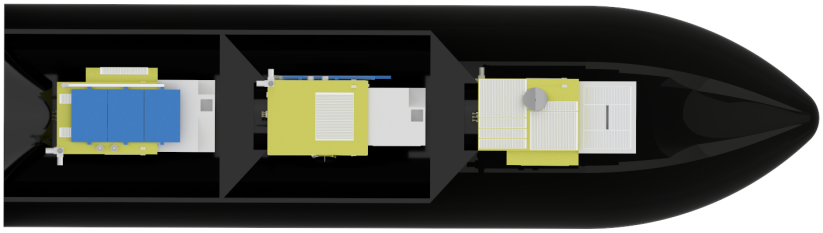

Figure 16.4: Falcon 9 Extended Fairing with 3 Infrared Pollution Monitoring System satellites in the Launch Configuration[1]

16.2. Internal Layout

Internally to the spacecraft, the subsystems are laid out in such a manner to reduce the unaccounted mass of wiring harness, tubing, and structural reinforcement, as such the subsystems are laid out over 3 'shelves', or otherwise attached to the outer skin of the spacecraft. This is in line with Section 15.2. It can be seen that from 'front-to-back' in the orbital direction, there is: payload, primary electronics, primary ADCS actuators and battery, and propulsion, while power generation arrays, sensors, thermal devices, some additional actuators, and antennae are mounted externally on the required surfaces.

[1]The figure illustrates the three satellites in three configurations to show compliance to geometry. In actual launch configuration the satellites will be in the same configuration

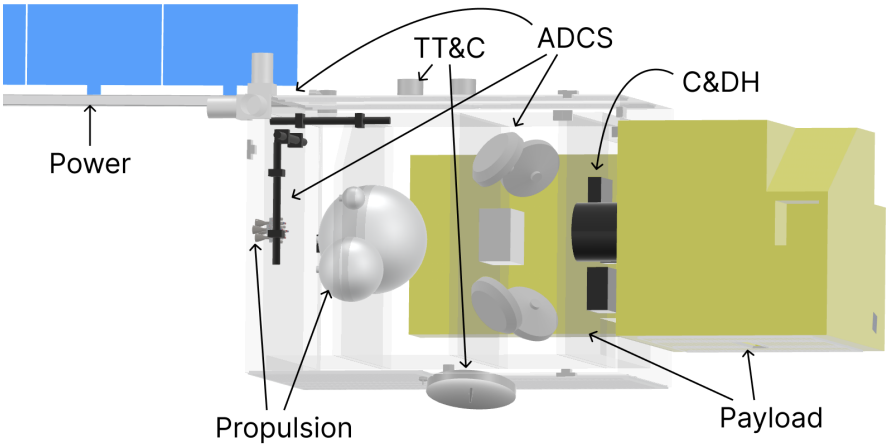

Figure 16.5: Internal View of the Infrared Pollution Monitoring System Satellite with the key components of each subsystem annotated

16.3. Block Diagrams

To facilitate the study and testing of the system in a more abstract manner, multiple diagrams are used to represent the spacecraft and demonstrate its functions. The Hardware and Electrical Block Diagram illustrates the physical interfaces. The Software Block Diagram outlines the operations pertaining to the data generated from the payload. Lastly, the Communication Block Diagram depicts the content and flow of information between subsystems.

16.3.1. Hardware and Electrical Block Diagram

Figure 16.6 presents the hardware of one satellite, along with the electrical flow for each system. It thus illustrates the hardware, electrical connections, data connections (both digital and analogue), and propellant connections. The arrows indicate data flow directions, and the subsystem boxes represent subsystem responsibility, not the physical layout. Please note that for simplicity and readability of the figure, the bus structure proposed in Table 9.2 is thought of. With all necessary bus and primary bus connections made.

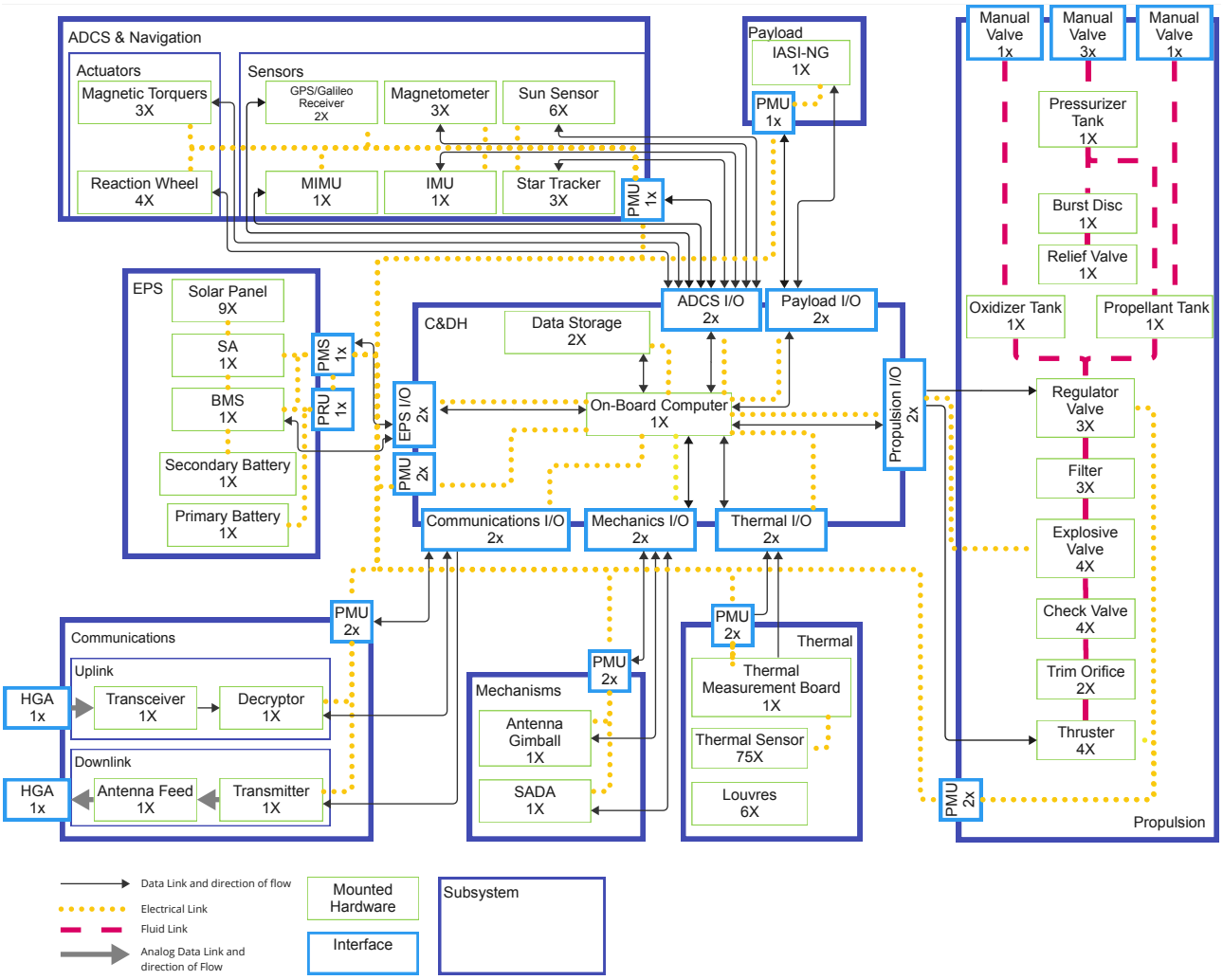

Figure 16.6: Hardware, Data handling and Electrical Block Diagram for one satelite

16.3.2. Software Block Diagram

Within Figure 16.7, the software diagram, only the data handling when generated by the payload is shown, as this is a specific method for the satellite. All other subsystems could be controlled with software that has been developed before.[72] Where the propulsion and ADCS subsystems would require direct control software and both the EPS and TT&C subsystems through the control of an actuator and power regulation. Within the diagram, the circular blocks show the start and stop moments, managed by the satellite OS. Square blocks show functions to be executed by the CPU, and diamond blocks show software comparative conditions.

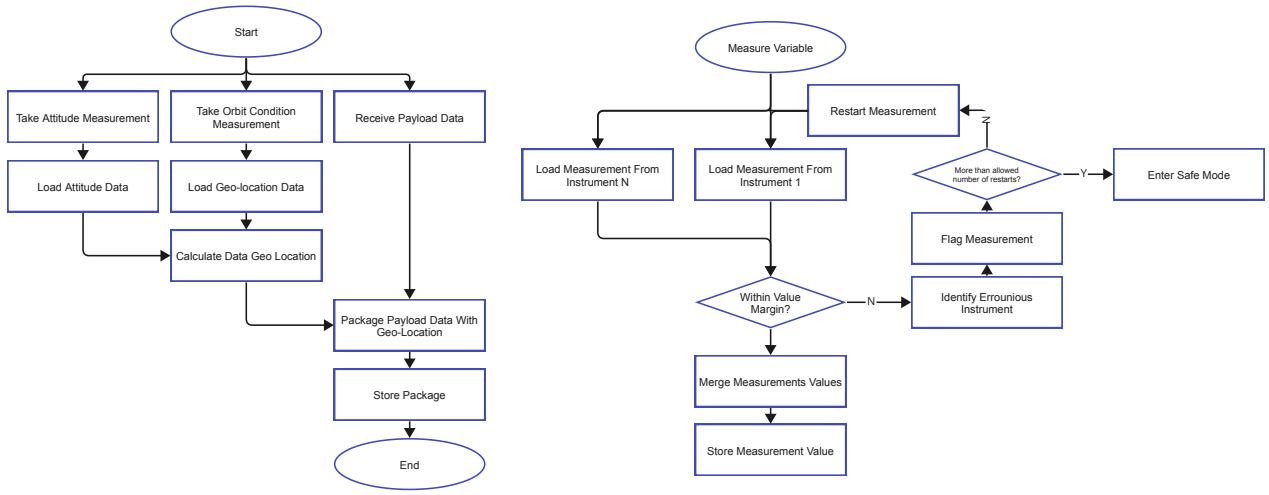

Figure 16.7: Software Block Diagram for the data handling

16.3.3. Communication Block Diagram

The communication block diagram in Figure 16.8 shows the data contents as well as the direction of informational flow. This diagram should be used in conjunction with the hardware diagram in Figure 16.6, as this shows the sources and end-point of all internal data. Note that the navigation subsystem does not communicate the power usage to the C&DH, as the responsibility of that is distributed to ADCS, as shown in Figure 16.6.

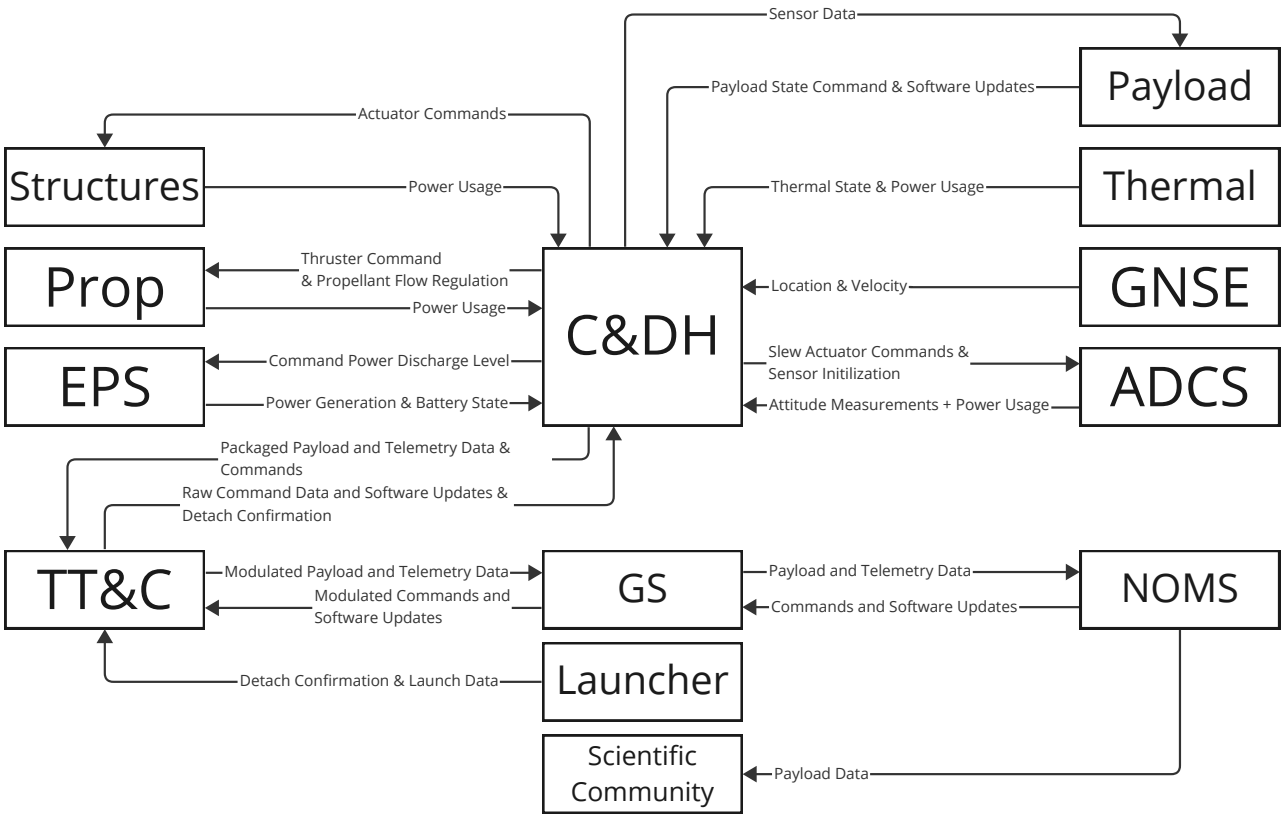

Figure 16.8: Communicational Block Diagram for the mission

16.4. Technical Resource Breakdowns

With the satellite's layout set and all subsystems designed, a breakdown of all system resources (mass, power, link, propellant, and cost) can be made. This process enables us to verify whether the complete

system adheres to the requirements and budgets allocated in Chapter 3 and Chapter 8. The link budget, already determined and reported in Chapter 11, encompasses both command and telemetry. As the TT&C link budget matches the system one, it is not included here. Additionally, the cost breakdown is presented in Chapter 22. The breakdowns for mass and power are provided in Section 16.4.1, while the propellant breakdown is given in Section 16.4.2.

16.4.1. Mass & Power Breakdown

By combining the different components of each subsystem, the total mass and power per subsystem can be determined. These values have been inserted in Table 16.1. From this, it can be seen that the total mass is 911.24 kg wet and 770.74 kg dry while having a peak power usage of 839.75 W and average usage of 667.3 W. Compared to the initial values of 1254 kg and 980 W for dry mass and power, it can be noted that the parameters have reduced in value. This allows for another iteration to be performed where these values are taken as the inputs to further iterations until they converge to an insignificant difference. The peak power usage time was calculated for subsystems where it was applicable based on the mean activation time per orbit.

Table 16.1: Mass and Power Breakdown for the System

Subsystem	Mass [kg]	Average Power[W]	Peak Power [W]	Peak Power Usage Time [%]
Payload	360	500	500	-
Structures	179.12	0	0	-
TCS	46.30	2	4.7	-
EPS	67.05	10	10	-
TT&C	20.52	14	50.45	5.91
ADCS	77	98.7	162	3.45
Propulsion	13.62	5.6	78	9.1×10^{-8}
Navigation	0.43	2	2	-
C&DH	6.7	35	35	-
Dry Mass Total	770.74	667.3	842.15	-
Propellant	140.5	-	-	-
Total	911.24	667.3	842.15	-

16.4.2. Propellant Breakdown

The propellant in the spacecraft is used on several occasions. When adding all these separate amounts, one gets to a total propellant mass of 140.5 kg. The actual breakdown can be seen in Table 16.2. Moreover, this value is 25% of the initially allocated 436 kg in Chapter 8 and thus fulfils the budget.

Table 16.2: Propellant Breakdown

Propellant Usage	Mass [kg]
Orbit Insertion	0
Orbit Maintenance	17.26
Maneauvres	0
Contingency	45.68
De-orbiting	77.17
Total	140.5

17 Concept of Operations and Logistics

17.1. Launch and Early Orbit Phase

The mission commences with the deployment of three satellites into their designated polar orbits. Following deployment, an early orbit phase takes place during which each satellite's subsystems are progressively activated and evaluated. This initial period, estimated to last approximately a week, focuses on calibrating the instruments, validating the subsystems and interfaces, and ensuring their optimal functioning. Special attention is paid to the Infrared Atmospheric Sounding Interferometer - Next Generation (IASI-NG) instrument's scanning mechanism, which remains locked during launch and must be unlocked prior to operational commencement. This early phase serves to identify any potential anomalies before transitioning into full-scale operations.

17.2. Operations

After the successful conclusion of the early orbit phase, operational proceedings begin. The full functional breakdown diagram is given in Section 4.1. Throughout the mission, the satellites monitor the specified zone of interest and transmit data twice per orbit to the preselected ground stations. The received data is processed further by the NearSpace Operation Management System (NOMS) operators.

The safe mode is included in the functional flow diagram in Figure 7.2. It allows the system to react quickly when failures occur in orbit, thereby increasing the reliability of the system. A safe mode means that non-essential subsystems are disabled, meaning that the payload would be disabled. Safe mode is lifted when a command from the ground station is received when proper diagnostics have been performed and a solution, to the problem, has been uplinked to the satellite.

In situations where self-resolution is not feasible, the satellite enters safe mode, triggering the mission operation centre's involvement. Depending on the anomaly's severity, the satellite might be decommissioned (as per Section 17.4.1) or continue operations with partial capabilities. The operational mode selection procedures are summarized in Figure 17.1.

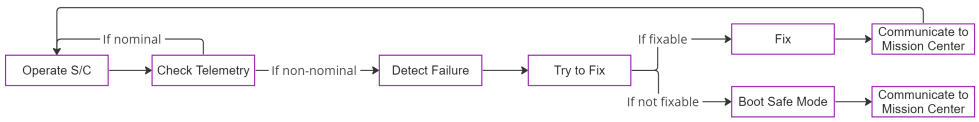

Figure 17.1: Concept of Operations of the Satellite

17.3. Replacement of satellites

As each satellite reaches the end of its operational life, a prearranged decommissioning plan, as described in Section 17.4.1, is implemented. It is crucial to request a flight plan from the NOMS before de-orbiting as each satellite's pericenter is brought down to an altitude of 0 km so that they can enter the atmosphere to burn up and crash. Given the mission's 30-year duration, continuity measures are necessary once the initial fleet of satellites is retired. Three options present themselves:

- The deployment of a new fleet of satellites to ensure continuous and consistent data collection over the entire mission duration
- Usage of the data from the first fleet to develop models simulating exhaust gases, eliminating the need for a full-fledged replacement fleet, with a single new satellite for model validation,

resulting in a considerable reduction in mission costs
- Usage of the data from the first fleet to develop models simulating exhaust gases with validation performed by existing satellites equipped with the same instrument, presenting the most cost-effective, though less precise, solution due to the different resolution of the data

The option to be chosen is primarily dependent on the quality of the data obtained by the first constellation of satellites. Higher-quality data will enable superior model accuracy, thus reducing the need for validation. Following the first half-year of operation, the collected data will be analysed and a replacement option will be decided. This allows for sufficient time in the case that a new fleet needs to be developed.

17.4. End of Life Plan

End of Life (EOL) plans are constructed for both the initial satellite fleet which has a lifetime of 7.5 yr and the mission as a whole with a lifetime of 30 yr. These EOL plans concern both physical and technical procedures that need to be performed. Physical procedures concern the de-orbiting and retirement of equipment and technical procedures concern performance evaluation processes.

17.4.1. Satellite End of Life

As described in Section 7.1.4, each of the satellites within the system will perform a de-orbit manoeuvre. This manoeuvre ensures that the satellite de-orbits in a relatively short amount of time. This scheduled de-orbit allows for reliability as the new satellite can enter a phase-shifted orbit and therefore provide redundancy. It needs to de-orbit in a relatively short amount of time because if all satellites stay in orbit, the space environment of Earth would get cluttered. Due to the mass of the satellite, it can not be guaranteed at this stage of the design, that the satellite would burn up during re-entry. Hence, it was chosen to perform a controlled re-entry by lowering the peri-centre radius to an altitude of 0 km. This controlled re-entry ensures a low chance of casualties and environmental impact. To ensure this, the satellites must be planned to impact the Earth in an uninhabited area with low environmental importance.

The selected area is the South Pacific Ocean Uninhabited Area[1] the most human-isolated area on Earth which is often utilised for the de-orbiting of larger satellites. Due to the Earth-repeating orbit, it is actually possible to re-enter at this location. The timing of the burn to ensure re-entry at this location are to be performed at a later stage of the design since they require a more detailed aerodynamic description of the satellite than is available in this instance. However, due to its isolation, any form of recovery effort would cause more damage than it would help sustainability.

During the operation of the first set of three satellites and especially when approaching EOL, the functioning of the individual satellites will be evaluated. This is done to enhance future designs as in case the satellite overperforms, mass can be saved, reducing costs. Conversely, if there are unexpected limitations in the system, upgrades can be made for the next generation of satellites. It might also be the case that there is a need for unexpected additional data. In this case, the addition of more measurement devices should be considered.

17.4.2. Mission End of Life

After the expected 30 yr lifetime of the mission, several things should happen to evaluate the performance of the system. An analysis is to be performed of how the data has been used and how this compares to the expected usage of the data. In case the data is not used in the expected manner, it should be evaluated why this is the case. In case there is still a relatively high demand for the data and/or more use cases have been identified by the market than initially identified, it should be evaluated if a possible continuation of the mission is economically profitable. Since the technology is likely to be developed at the EOL, it should also be evaluated if possible upgrades to the satellites and/or orbital parameters are possible.

[1] URL: blogs.esa.int [accessed: 16/06/2023]

18 RAMS Analysis

The Reliability, Availability, Maintainability, and Safety (RAMS) aims to ensure the operation of the system over the desired period of time and to enable the fulfilment of requirement MIS-OPS-01. These tools are not exact and should only serve to provide insight into the working of the system and point to possible points of failure. This is done by analysing the maintenance in Section 18.1, as this helps define the reliability analysis. With the reliability in Section 18.2, and the maintenance schedule, the availability in Section 18.3 can be calculated. Lastly, safety is briefly discussed in Section 18.4, as it flows from the other three sections.

18.1. Maintenance

Satellite maintenance is a difficult topic, as with the discontinuation of the space shuttle, satellites are hardly accessible for manual maintenance. Therefore no physical maintenance schedule is made and maintenance is now considered to be the ability to maintain the system, for this purpose the system is able to receive software updates and maintain its own safety, which will be discussed later. Receiving software updates is facilitated by the TT&C and C&DH, as discussed in Section 11.1 and Section 10.3.2 respectively. This functionality increases availability, by allowing the correction of software bugs discovered during operations.

18.2. Reliability

To start with the reliability analysis first the reliability diagram is constructed, shown in Figure 18.1, this helps to visualise the reliability risks posed to the system. This allows for the straightforward incorporation of redundancy measures into the final calculation. Secondly, the method of calculating reliability is defined. This is done in Equations (18.1) and (18.2) [73]. Equation (18.2) is used since no maintenance can be performed.

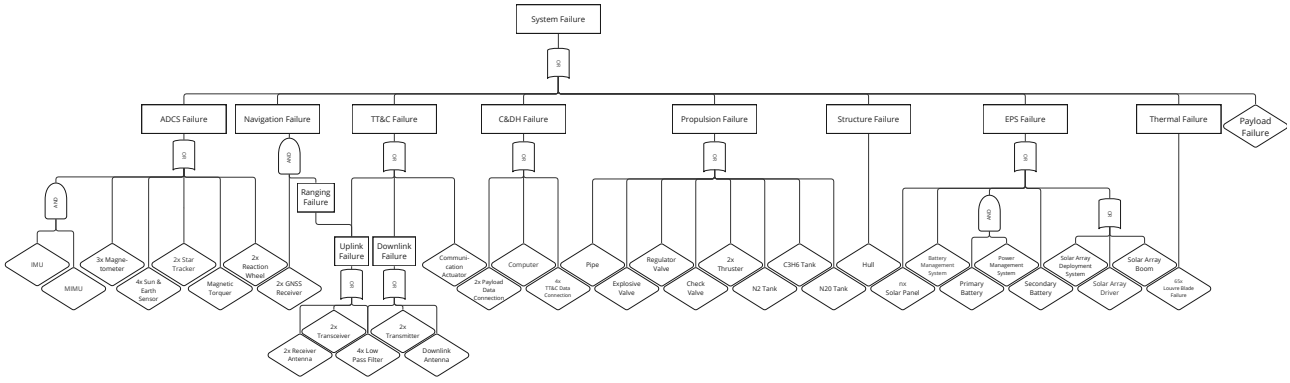

Figure 18.1: Failure Events of Each Subsystem and their Connection to Overall Reliabillity

$$R = \exp^{-(\lambda t)^{\beta}} \qquad \lambda = \frac{1}{MTTF} = \frac{10^9}{8766FIT} \approx \frac{-LT}{\ln 0{,}95} \tag{18.1, 18.2}$$

Where R is the reliability, λ is the failure rate per year, t is the satellite's lifetime in years and β is the shape parameter. Mean Time To Failure and Lifetime are parameters to be obtained and both are expressed in years, while Failures in Time is given per 10×10^9 s and must therefore be converted using the second version of Equation (18.2) and can only be used when the FIT is given. If only a component lifetime is available Equation (18.1) is to be used with the third version of Equation (18.2). For some exposed components failure rate is determined by the object impact chance, and for those systems (specifically the solar array, solar array boom, and hull) this probability determines the reliability. If

none of these are given Table 2 from Castet and Saleh [73] is used as a reference for the values. The results of these calculations with the structure of Figure 18.1 is given in Table 18.1.

Table 18.1: The Reliability Values of All Subsystems

Subsystem	Reliability
ADCS	0.9856
Navigation	≈1
TT&C	0.9680
C&DH	0.9995
Propulsion	0.9303
Structure	0.9648
EPS	0.9492
Thermal	≈1
Payload	0.84
Bus Reliability [1]	0.8125
Satellite Reliability	0.6825

As can be seen in Table 18.1, the reliability of the ADCS, navigation, C&DH and Thermal subsystem are sufficiently high. While the reliability of both the propulsion and EPS are calculated to be lower, however as these calculations are overestimations of the reliability of a non-refined design, these values are acceptable, as the lifetime guarantee of all components is still above the lifetime of a single satellite.

The reliability of the payload however is suboptimal as it significantly decreases the satellite reliability. Though this is a risk that must be accepted at this stage as no realistic alternative was found, during the research presented in Section 5.2. It could also be that the definition of the reliability given for the IASI-NG within the scienceplan[11] is different from the one used here, with the mean time between failures used, where these failures would be resolved through software updates.

The launch success rate is excluded from the table, as it is a one-time probability that does not degrade with mission duration. It must however still be mentioned, as it is a source of mission failures. The Falcon 9 series has 3 (partial) failures over all executed launches, this gives it a launch success rate of 98.88%[2]

18.3. Availability

Availibillity is normally calculated using Equation (18.3) [74], with MTBF and $\bar{M}ct$ the mean corrective maintenance time, however as is discussed during Section 18.1, no physical maintenance is expected to be performed during the lifetime of the satellite. Therefore this value is discarded and only the downtime of the ground stations and instrument are considered, these are 0.003%[3][4] and 2% respectively, leading to a cumulative availability of 97.7% and therefore a downtime of 2.3%.

$$A_i = \frac{MTBF}{MTBF + \bar{M}ct} \tag{18.3}$$

18.4. Safety

Considerations for safety include the launch, operations and EOL. With risks for humans being most prominent during launch and EOL, environmental pollution is a risk during all stages of operations. To ensure safety during launch, standard launch procedures will be adhered to, these procedures ensure that launcher failures will not cause damage on the ground[5]. Furthermore, safety during EOL

[1] Reliabillity of all subsystems, without the Payload
[2] URL: spacexstats.xyz [accessed: 20/06/2023]
[3] URL: www.icao.int [accessed: 20/03/2023]
[4] The source starts counting at #6 with 2 failures considered
[5] URL: www.airbus.com [accessed: 20/06/2023]

has already been discussed in Section 17.4.1 and necessary considerations have been made.

To guarantee safety in the space environment a few design choices have been made. Firstly, the hull of the satellite has been designed to absorb the impact of satellites and been designed to be worthy of current standards as discussed in section 15.3.2. Another safety measure is the addition of extra propellant mass for contingency as listed in Section 16.4.2, this ensures that maneuvres can be executed when a collision warning is received. Lastly, an explosive failure is prevented by the inclusion of venting valves which relieve pressure in the event that some part of the propulsion system fails and is discussed in Section 13.2.2.

19 Technical Risk Assessment

Risks need to be identified for the satellite and then mitigated to ensure the design is viable. This process is shown in this chapter. Identification is done in Section 19.1, while mitigation is done in Section 19.2, lastly these risk are mapped in Section 19.3.

19.1. Risk Identification

Risks are identified before and during design, these are listed in Table 19.1. With a short description of the risk event, cause and consequence. These are then scored on probability and consequence impact, as defined in Table 19.1. These serve to complete the risk mitigation plan[9] and adhere to the method defined there. Where a risk would constantly be monitored and mitigation by the responsible person.

As was stated before, risks were identified prior to starting the design. As well as when design options were reduced and components were selected, as these came with their own risk. Each risk carries its own unique ID. To clarify that these risks differ from risks previously identified, these risks are given the new identifier Spacecraft Technical Risk (STR).

Table 19.1: Definition for the Probability and Consequence Impact Indices used for the Mapping of Organisational Risks

(a) Definition for the Probability Indices

Index	Probability
1	Negligible
2	Highly unlikely
3	Plausible
4	Probable
5	Very likely
6	Definite

(b) Definition for the Consequence Impact Indices

Index	Consequence Impact
1	Negligible
2	Marginal performance deficit
3	Significant performance deficit
4	Customer expectations not met
5	Mission critical deficit
6	Catastrophic failure

Table 19.2: Identified risk of the Taking Control Satelite

ID	Description	Cause	Consequence	P	C
STR-1	Materials very scarcely available	Materials shortage	Project delay and cost increase	2	3
STR-2	Materials do not arrive	Interrupted transportation	Project delay and cost increase	1	3
STR-3	Material loss	Insufficient material storage	Project delay and cost increase	2	3
STR-4	Component not produced as required	Production plan unclear	Project delay and cost increase	4	3
STR-5	Component not produced as required	Inaccurate tooling	Project delay and cost increase	2	3
STR-6	Not enough available staff for training	Manpower Shortage	Project delay and cost increase	3	2
STR-7	Production flaw goes unobserved	Inspection not up to standard	Lifetime of product is reduced	4	5
STR-8	Production flaw goes untreated	Incomplete Documentation	Lifetime of product is reduced	2	5
STR-9	Hardware failure	Unnoticed hardware flaw	Lifetime of product is reduced	3	5
STR-10	Subsystems fail to interoperate	Incompatible subsystem interfaces	Lifetime of product is reduced	4	5

STR-11	Structural damage during launch	Launcher Vibrations / Loads	Lifetime of product is reduced	2	5
STR-12	Mission certification denied	S/C does not meet certification requirements	Project delay and cost increase	3	2
STR-13	S/C gets damaged during transport	Inadequate transportation	Project delay	1	5
STR-14	Lost satellite	Launcher Failure	Mission failure	2	6
STR-15	S/C cannot undock	Launcher fairings do not jettison	Mission failure	2	6
STR-16	S/C cannot reach parking orbit	Thruster failure	Mission failure	2	6
STR-17	S/C fails to initialise	C&DH Hardware failure	Mission failure	3	6
STR-18	S/C fails to initialise	C&DH Software failure	Mission failure	3	6
STR-19	S/C EPS deployment failure	EPS hardware failure	Mission failure	3	6
STR-20	Image has inadequate quality	Uncalibrated Imaging tool	Devaluation of mission	4	2
STR-21	Image displays incorrect data	Imaging tool not functioning as intended	Devaluation of mission	2	4
STR-22	Unresponsive S/C	Incorrect data protocol usage	Loss of data	2	4
STR-23	Unresponsive S/C	Insufficient link budget	Delay in mission and cost increase	3	4
STR-24	Loss of control	Non essential Subsystem malfunction	Mission failure	4	6
STR-25	Payload lifetime is shorter than expected	Payload is active while not used	Lifetime of product is reduced	4	3
STR-26	Digital storage fills up	Imaging data has a too high file size	Loss of scientific data	4	4
STR-27	Overwritten data	Insufficient buffer storage	Loss of data	4	4
STR-28	Data not written to storage	Buffer failure	Loss of data	4	4
STR-29	Misaligned S/C	Incorrect attitude reading	Loss of scientific data	2	3
STR-30	Spacecraft misses observational target	Misaligned orbit	Loss of scientific data	2	3
STR-31	Hardware failure	Over- or under-heating	Lifetime of product is reduced	4	5
STR-32	Battery does not store sufficient energy	Insufficient power budget	Devaluation of mission	1	6
STR-33	Insufficient available power	Unexpected EPS degradation	Devaluation of mission	2	5
STR-34	Overloaded processing unit	Insufficient processing capacity	Loss of data	2	4
STR-35	EPS overloads	Under-utilization of EPS	Loss of a satellite	1	6
STR-36	Subsystem receives insufficient power	EPS hardware failure	Lifetime of product is reduced	2	4
STR-37	Electronic malfunction	Geomagnetic Storm	Loss of operateabillity	4	5
STR-38	Electronic malfunction	Space Dusts	Loss of operateabillity	3	5
STR-39	Unncessary instructions are performed	Unclear chain of command	Temporary loss of operateabillity	2	2
STR-40	Faulty Status Measurement	Sensor Malfunction	Temporary loss of operateabillity	4	3
STR-41	Unreadable data	Corruption of data	Loss of data	5	3
STR-42	Data is not received by GS and overwritten	Inoperable GS	Loss of data	3	3
STR-43	In orbit collision	Orbit intersects with space debris or other S/C	Loss of a (or part of a) satelite	3	5
STR-44	Instruction is misexecuted	Hardware failure	Loss of scientiffic data	2	3
STR-45	S/C Collides with object after operations	Insufficient Planning	Environmental Pollution	3	3

STR-46	S/C Collides with object after operations	EoL plan not executed properly	Envioremental Pollution	3	3
STR-47	Hostile Interference	Hostile Interference	Loss of a satelite	1	6
STR-48	Thermal coating gets damaged	Micro miteorite or debris impact	Thermal range becomes wider	2	1
STR-49	Thermal overheating	Louvres don't function as intented	Lifetime of product is reduced	3	2
STR-50	Misalligned Spacecraft	Incorrect intertial measurment	Loss of scientiffic data	2	3
STR-51	System information is not received	Data Connection Faillure	Lifetime of product is reduced	3	4
STR-52	System becomes unresponsive	OS system failure	Loss of data	2	4
STR-53	Battery does not store sufficient energy	Fast battery degredation	Devaluation of mission	5	5
STR-54	Damage to solar array	Collision with an micro meteorite or debris	Devaluation of mission	2	4
STR-55	Insufficient available power	Solar array rotation failure	Devaluation of mission	1	4
STR-56	Debris re-enters the atmosphere	Structure does not burn up	Envioremental Pollution	4	5
STR-57	Electric Arching	Too close electric components	Mission failure	3	5
STR-58	Hardware components unaivalable	Producer cannot deliver product	Project delay and cost increase	2	3
STR-59	Payload unavailable	Producer cannot deliver product	Mission failure	1	6
STR-60	Co-channeling	Frequency conjestion	Loss of data	5	4
STR-61	System does not meet requirements	Verifcation and validation failure	Devaluation of mission	2	5

19.2. Risk Mitigation

Some risks within Table 19.2 cause an unacceptable danger to the system, they must therefore be mitigated. The mitigation strategy for each risk is shown in each table as well as the old and new probability and consequence impact score, listed as P, C and P* and C* respectively. Two risks, STR-6 and STR-47 are accepted as they fall outside the control of the mission, without excessive and unnecessary intervention. All other risks are mitigated.

Table 19.3: Risk probability and consequence for technical risks after mitigation

ID	P	C	Mitigation	P*	C*
STR-1	2	3	Design with material choice in mind	2	2
STR-2	1	3	Locally source and thoroughly arrange transport	1	1
STR-3	2	3	Have a logistics plan for manufacturing	1	3
STR-4	4	3	Verify production plan	2	2
STR-5	2	3	Inspect and test tools	1	2
STR-6	3	2	Train staff to cover for colleagues	2	1
STR-7	4	5	Implement structured inspection training and methods	1	5
STR-8	2	5	Implement structured documentation training	1	5
STR-9	3	5	Perform hardware and system tests	1	5
STR-10	4	5	Perform system tests	1	5
STR-11	2	5	Perform system validation tests	1	5
STR-12	3	2	Verify and validate during design	2	2
STR-13	1	5	Locally source and thouroughly arrange transport	1	2
STR-14	2	6	Partly accept and perform pre-flight checks on the S/C	1	6
STR-15	2	6	Partly accept and perform pre-flight checks on the S/C	1	6
STR-16	2	6	Thruster redundancy	1	6

STR-17	3	6	Perform hardware and system tests	1	6
STR-18	3	6	Perform software verification	1	6
STR-19	3	6	Perform hardware and system tests	1	6
STR-20	4	2	Perform payload verification and calibration	1	1
STR-21	2	4	Perform payload verification and calibration	1	3
STR-22	2	4	Perform communication verification and calibration	1	2
STR-23	3	4	Perform communication verification and calibration	1	2
STR-24	4	6	Implement safe operations mode	1	2
STR-25	4	3	Disable payload when not in use	2	3
STR-26	4	4	Perform processing on images	2	2
STR-27	4	4	Buffer redundancy	1	3
STR-28	4	4	Buffer redundancy	1	2
STR-29	2	3	ADCS sensor redundancy	1	3
STR-30	2	3	Implement navigation and propulsion system	1	2
STR-31	4	5	Implement thermal control subsystem	1	3
STR-32	1	6	Redundancy and system tests	1	5
STR-33	2	5	Plan and check EPS performance	2	3
STR-34	2	4	Implement safety margins on data handling	1	4
STR-35	1	6	Include power discharge capabilities	1	1
STR-36	2	4	EPS hardware redundancy	1	4
STR-37	4	5	Shield Electronics and allow for system reboots	3	2
STR-38	3	5	Shield Electronics and allow for system reboots	1	2
STR-39	2	2	Log corrective actions taken	1	2
STR-40	4	3	Sensor redundancy and comparison	2	2
STR-41	5	3	Error checking data	3	2
STR-42	3	3	Data storage safety margin	3	2
STR-43	3	5	Shield vulnerable areas of satelite; Allow evasive manoeuvres	2	3
STR-44	2	3	Validate execution of instruction	2	2
STR-45	3	3	Make extensive EOL plan	1	1
STR-46	3	3	Validate completion of EOL plan	1	1
STR-47	2	6	Do not publish sensitive information	1	5
STR-48	2	1	Use safety factors in Thermal Design	1	1
STR-49	3	2	Calibrate Louvres	1	2
STR-50	2	3	ADCS sensor redundancy	1	3
STR-51	3	4	Connection redundancy	3	4
STR-52	2	4	Allow reboots and software updates	1	4
STR-53	5	5	Use a battery management system	2	5
STR-54	2	4	Shield sollary array	2	2
STR-55	1	4	Perform hardware and system tests	1	4
STR-56	4	5	Design for EoL	1	2
STR-57	3	5	Design for arching	1	5
STR-58	2	3	Design with product availabillity in mind	2	2
STR-59	1	6	Use similar instrument with design changes	1	3
STR-60	5	4	Obtain communication frequency certificate	1	4
STR-61	2	5	Implement structured documentation training	1	5

19.3. Risk Map

The risk map helps visualise the process described in the previous two sections. Therefore the risks before mitigation and after mitigation are shown in Figures 19.1a and 19.1b respectively.

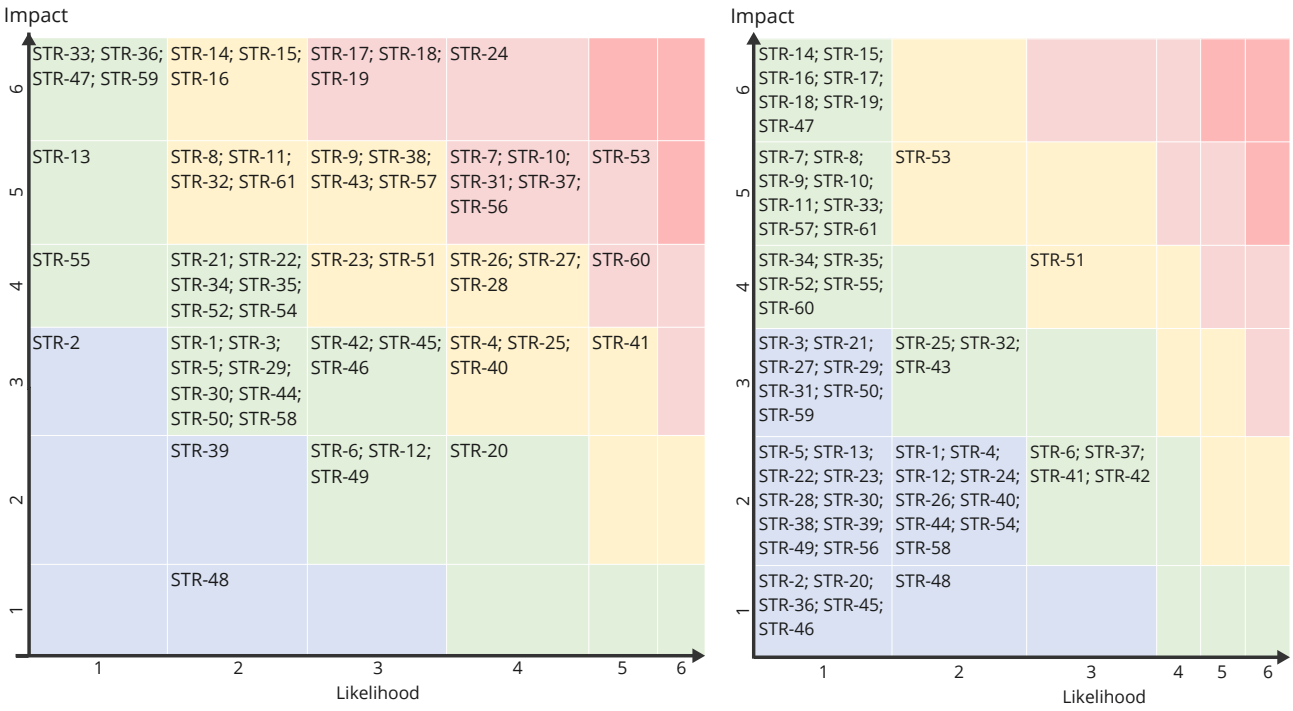

(a) Technical Risks Before Mitigation

(b) Technical Risks After Mitigation

Figure 19.1: Risk Maps for the Infrared Pollution Monitoring System (IPMS)

20 Verification & Validation Procedures

In order to ensure that the spacecraft fulfils its mission requirements and that these requirements fulfil the mission need, it is essential that it is verified and validated at every stage of the design process. Similarly, for each model that is used, the correct functioning must be verified in order to be sure that decisions made based upon these models are fully founded. As such, a brief description of the successfully completed verification measures for all of the models utilised in the design of the IPMS is given in section 20.1, before discussing the further V&V activities from the completion of this project to the acceptance of the spacecraft in section 20.2.

20.1. Verification of Models Used

A number of models are used for the design of the IPMS; with varying degrees of in-house development. They are:

- **Systems ToolKit (STK)** developed initially by Analytical Graphics, later ANSYS [1]
- **TU Delft Astrodynamics Toolbox (TUDAT)** developed by researchers from the TU Delft
- **Orbit Selection Model** developed in-house
- **Perturbation Model** developed in-house
- **Propulsion Sizing Model** developed in-house

While the models utilised in STK are supplied with verification documentation, it remains important to verify (and validate) their application for the purposes of the Taking Control Mission. To do so, a number of runs were completed with simple parameters, for which hand calculations were made to cross-reference the output of the program with the expectation. Following this, STK was primarily utilised as a means for visualising orbits, verifying in-house code, and calculating up/down-link periods.

The TUDAT software, while also supplied by a 3rd party, is not supplied with an equal amount of V&V documentation to that of STK. As such, it also required the use of hand calculations (informed by *Space Mission Engineering: The New SMAD*, and checked by multiple team members) in order to verify the calculations, while more complex orbits could also be simultaneously modelled in both TUDAT and STK, to enable the verification of the throughput of each other.

With these tools verified, a number of models are used which the team developed in-house. The first of which is the model for the selection of the optimal orbit. The model is generated using equations derived from *Space Mission Engineering: The New SMAD*, for which each unit is tested individually. The model sizes the orbit for complete and optimal coverage of the area of interest, so verification is carried out by plotting the orbit in STK (verifying that the orbit has been correctly calculated), and then plotting in STK with adjusted parameters to confirm that the coverage is worsened with a change in the key parameters, thus verifying and validating the optimisation strategy of the in-house code.

With the orbit selected, a model for perturbations is required to calculate the ΔV required for orbit maintenance. This was also developed directly from the equations in *Space Mission Engineering: The New SMAD* and [2], with the fixed variables verified by multiple sources [33], [30]. The model was verified by unit testing of each of these functional blocks, before a pass-through test could be carried out, comparing with multiple known solutions for specific orbits provided in *Space Mission Engineering: The New SMAD*.

The final model which is utilised is the model for the sizing of the propulsion system, which is

[1] URL: www.ansys.com [accessed: 26/06/2023]
[2] URL: ocw.tudelft.nl [accessed: 19/06/2023]

primarily derived from the content of the TU Delft AE2230-ii reader [3]. Similarly, each equation block is validated with unit testing, before a full model test is carried out in which the known inputs (ΔV, dry mass, etc.) of a group of known satellites are given to the model, and the output (required propellant mass, tank size, etc.) are compared with the actual variables of the same satellites.

20.2. Spacecraft Verification

Product verification is a critical part of a system design. It is the process by which it is proven that the end product conforms to its requirements or specifications. In other words, it answers the question: "Was the end product realized right?" [4].

According to ESA's mission lifetime cycle, the verification process occurs during both the detailed definition of the product (Phase C) and the qualification and production (Phase D), although some review of the design verification may also occur once the mission is formally adopted (Phase 2B/C). In phase C the Structural and Thermal Model (STM), Engineering Model (EM) and Qualification Model (QM) are produced. These are used to test the launch conditions (vibrations and acoustic tests) and undergo environmental (vacuum, radiation and temperature) tests[5].

The focus of this section will therefore be on the aforementioned phases of the design providing a preliminary overview of the verification methodology (the verification of the subsystems' components is considered to be done at a later stage of the design). In Table 20.1, the verification matrix can be seen. It includes all the subsystem requirements, that have been categorized by type of requirement, the verification method (Test-T, Analysis-A, Simulation-S, Review of design-R and Similarities-SM), level (System-S, Subsystem-SB, Payload-P and Unit-U) and applicability (ESA's phase B/C/D). This leads to the description of the tests, presented in Section 20.2.1.

Table 20.1: Preliminary Verification Matrix

Require-ments Grouping	Requirements	Verification Method	Verification Level	Applicabil-ity
C&DH				
Functional	02, 05, 06, 10, 11, 17, 18, 19, 20, 21, 22	T, A, S, R	S, SB, P, U	Phase D
Performance	03, 04, 09, 12, 13	T, A	S, SB, P	Phase D
Interface	01, 07, 08, 14	T, A, S, SM, R	S, SB, P, U	Phase D
TT&C				
Functional	01, 02, 08, 10, 11	T, A, S, R	S, SB, U	Phase D
Performance	03, 04	T, A, S	S, SB, U	Phase D
Interface	05, 06 09	T, A, S	S, SB	Phase D
ADCS				
Functional	04, 07, 08, 09, 15	T, A, R	S, SB, U	Phase C-D
Performance	01, 02, 03, 05, 06	T, A, R	S, SB, U	Phase D
Interface	10, 11	T	S, SB	Phase D
Thermal				
Functional	04, 04.1, 04.2	T, A	S, SB, U	Phase C
Performance	01, 02, 02.1, 02.2, 02.3, 02.4, 02.5, 02.6, 02.7, 03, 03.1, 03.2, 03.3, 03.4, 03.5, 03.6, 03.7	T, A	S, SB, U	Phase C
EPS				
Functional	11, 12, 13, 14, 15, 16, 19, 20	T, A, S, R	S, SB, P	Phase D
Performance	03, 04, 05, 08, 09, 17, 18	T, A	S, SB, U	Phase D
Interface	07, 10	T, S, SM, R	S, SB	Phase C-D
Propulsion				
Functional	06	A, R	S, SB	Phase C-D

[3]URL: brightspace.tudelft.nl [accessed: 19/06/2023]
[4]URL: www.nasa.gov [accessed: 20/06/23]
[5]URL: www.esa.int [accessed: 20/06/23]

Performance	01, 02, 05	T, A	S, SB, U	Phase C-D
Structure				
Functional	07, 12, 13, 15, 16, 19, 20	T, A, S, SM, R	S, SB	Phase C-D
Performance	01, 02, 04, 05, 09, 10, 11, 17	T, A	S, SB, U	Phase C
Interface	03, 08	T, S, SM, R	S, U	Phase C-D
Navigation				
Functional	06	T, SM, R	S, SB, U	Phase D
Performance	01, 02, 03, 04, 05	T, A, R	S, SB, U	Phase D
General				
Mass	EPS-1, EPS-06, ADC-12, CDH-15, PRP-03, STR-06, TCS-05, TTC-07	T, S, R	S, SB, P, U	Phase C-D
Material	EPS-21, PRP-04, STR-14, STR-21, STR-22, STR-23	T, SM, R	U	Phase B-C-D
Power Consumption	ADC-13/14, CDH-16	T	S, SB, U	Phase C-D
Cost	EPS-02	A, R	S, SB, U	Phase C-D

20.2.1. Verification Procedures

In regards to the C&DH subsystem, because of its interconnected nature, it is a subsystem that will mainly be tested on the FM. The functional requirements can be tested once the subsystem is connected to the relevant subsystems. Tests, mainly software-based, as well as simulations can then be performed on them to test the communication, data transferring and processing requirements. Performance requirements - data storage and data transfer rates - can be verified through testing, both on the components themselves - once they are received - and when they are connected to the relevant subsystems. Lastly, for interface requirements, similarly to the functional requirements, they are to be verified once the C&DH is connected to the other subsystems and telemetry points around the spacecraft. It can then be concluded that all the C&DH verification tests are to be performed during Phase D, but 21 and 22, can already be verified during Phase 2B or C. During the latter-mentioned phases, analysis, review of the design and similarities are also to be reviewed in order to further verify the subsystem.

In relation to the TT&C subsystem, all of its requirements can be verified through a review of design and similarities with other spacecraft of the off-the-shelf equipment selected; testing, analysis through mathematical models, and communication simulations to prove the subsystem meets the required performance and functional specifications. Such simulations can be performed in facilities such as NASA's Communication System Simulation Laboratory, which they currently use to test the TT&C subsystem of their spacecraft. The verification of this subsystem is to be performed during Phase D.

The ADCS subsystem functional and performance requirements are to be verified during Phase D of the design. A review of design and analysis methods is to be used to verify off-the-shelf components of the subsystem. Further tests under specific radiation, force and electromagnetic conditions are to be used to verify functional requirements. Interface requirements are to be verified through testing once the subsystem is connected to the C&DH unit. All pointing tests are to be performed during Phase D [6]. Although environmental testing of the subsystem can already be performed in Phase C.

The thermal subsystem requirements are all to be verified through a combination of testing and analysis in the STM during Phase C in the environmental tests, as to see if the subsystem is able to maintain the intended temperature ranges for the spacecraft components under specific atmospheric conditions. The subsystem should also be tested in the FM when all the subsystems are attached and in their final disposition in Phase D.

The EPS subsystem requirements are to be verified through a review of design, simulation of the electrical system, similarities with other spacecraft, interface requirements, and a combination of

[6]URL: www.esa.int [accessed: 20/06/23]

analysis and tests. These are to be performed on the FM during Phase D, where the electrical system is to be tested. Some of the requirements, especially those referring to EOL performance can only be verified via analysis and similarities. Power output can be verified through tests once the subsystem components are obtained. And interface requirements can only be fully tested once the FM is constructed.

In regards to the propulsion subsystem, the functional requirement can only be verified through analysis, mathematical models, and review of design for the selected off-the-shelf components, as it could only be tested once the spacecraft is in orbit. Performance requirements would require the spacecraft to be in orbit for verification through testing only. However, a combination of mathematical models and testing during Phase C and D of the design are sufficient to verify these parameters.

Regarding the structural requirements of the spacecraft, those related to structural capabilities such as temperature ranges, load strengths and eigenfrequencies will be verified with the STM in the vibrations and acoustic test during Phase C. The interface requirement is to be verified during this same phase when the compatibility with the launch vehicle is to be tested [7]. Accessibility requirements are to be verified along Phases B-C-D. In all preliminary models and the FM.

The functional GN&C subsystem requirement is to be verified via review of the design when selecting the GNSS receiver. The performance requirements can be verified through a combination of testing, simulation and review of design with the FM during Phase C.

Regarding the general requirements, those related to the specific mass of the subsystems can be verified via testing (weighting them once they have been received or produced), review of design for off-the-shelf components and similarities with other spacecraft, especially for connectors and other components which can only be verified on the FM has been finished.

Because all the system requirements lead to at least one subsystem requirement, it can be concluded that the verification of the subsystem requirements constitutes a verification of the system requirements. Moreover, in Section 21.2, the verification results at the system level are shown. This would allow to continue into the next phase of the IPMS design.

In conclusion, a combination of tests - including environmental, structural or unit tests, analysis models, simulations, similarity analysis and review of designs are used to verify all of the system and subsystem requirements. All the models and simulations should be verified and validated independently to ensure a correct verification procedure of the system. Assuring that "the product has been realized right".

20.2.2. Verification Tests

From the previously presented analysis of the overall requirements verification procedure, three tests were identified as crucial as per the major risks. These are the environmental conditions test, the loads and vibrations test, and the communications test. A more detailed overview is presented hereafter. Other tests and test configurations are also to be developed for the full validation and verification process, nonetheless, these were considered as most critical, minimizing the chance of design failure.

The main purpose of the environmental test is to prove the required functioning of the structures, power generation, ADCS stability, accuracy and torque counteraction requirements, and most importantly, verify the thermal subsystem requirements. The test configuration is made up of the STM, a TCS model, ADCS model and an EPS model, as presented in Figure 20.1a. The latter four models would be incorporated into the STM and then subjected to extreme space conditions in terms of temperature, pressure and radiation. In this way, the aforementioned requirements can be verified and these subsystems can be expected to meet the requirements once the FM is up in space.

[7] URL: www.esa.int [accessed: 20/06/23]

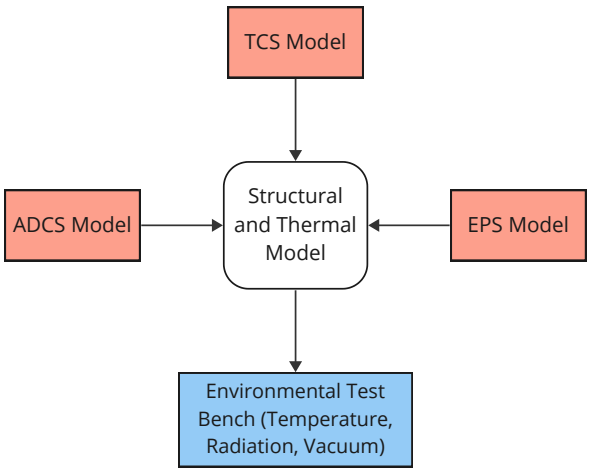

(a) Environmental Conditions Test Configuration

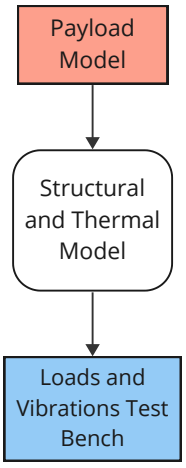

(b) Load and Vibrations Test Configuration

Figure 20.1: Figures showing test configurations for different tests

The second test configuration developed is that of the load and vibrations. In this case, the main verification parameters are those of the structure's load and vibration requirements. The STM is to be used together with a payload model, in order to investigate whether the instrument itself can withstand the launch conditions, this should normally be already verified through a review of the design. The aforementioned model is to be installed in the loads and vibrations test bench in order to proceed with the testing as can be seen in Figure 20.1b.

Finally, the third considered most critical verification test is the communications test. In this configuration, as can be seen in Figure 20.2, many subsystems are considered. The main purpose of the test is to verify the interface requirements of the system. Two major networks are considered in this test: data communication and power supply networks. The efficiency and compatibility of the power connections are to be verified. As well as the full functioning of the C&DH and TT&C subsystems. From the obtention of commands from a (simulated) ground station to their distribution to the relevant subsystems. And on the way back, from the collection of payload and telemetry data from the subsystems to the ground transmission; verifying all the relevant requirements.

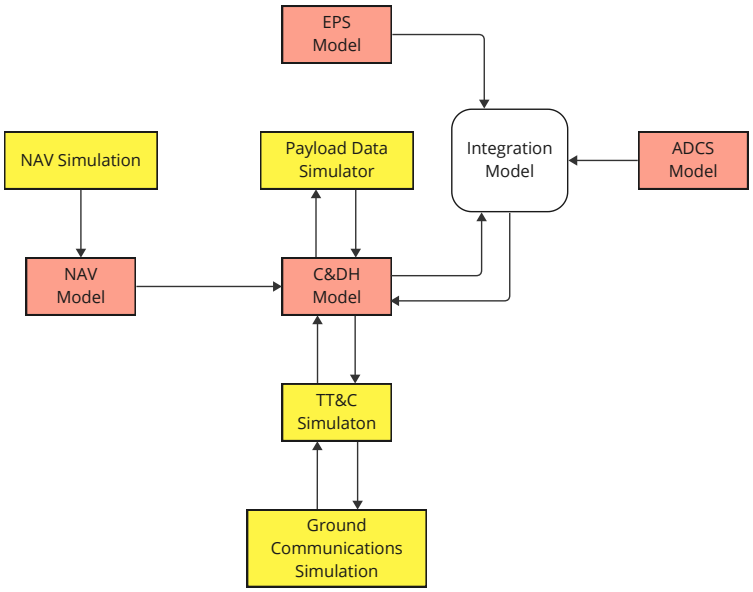

Figure 20.2: Communications Test Configuration

20.2.3. Verification & Validation and Sensitivity Anlysis

Although the design of each subsystem has been made with the utmost care and conservativeness to account for worst case conditions, therefore providing a flexible design, a requirement or mission change can greatly affect the design solutions found, and therefore the verification and compliance of these requirements. The effect of changes to the requirements on the design is presented in the respective sections for each of the subsystems. The verification and compliance of the new or modified requirements is something that will have to be dealt with in case of these changes. The verification tests have been designed with this in mind, and can therefore withstand moderate changes to the requirements. In case of critical changes, modifications to the current tests should be performed, and the compliance to the new or modified requirements reassessed.

20.3. Spacecraft Validation

The validation of a system entails that the system is compliant with the functions it was designed for. In other words "Does the system do what we intended it to do?". In this case, the project objective statement to be evaluated is: "Design a space-based platform that is capable of monitoring the radiative forcing effects and dynamic evolution of exhaust trails from air-breathing vehicles in NearSpace, in 12 working days by ten students". Since team Taking Control is the designer of the NOMS, and has identified this project objective from a self-designated need, the validation of the IPMS must be made entirely by checking the design made by Taking Control with the mission need and project objective established at the earliest stage. For this reason, the documentation of the process of requirements flow down provided in this report forms a first step in validation, which is to be carried on throughout the further design of the system. In conjunction with the verification measures already detailed, a number of full system simulations, tests, and demonstrations are required in order to ensure that the project objective has been fulfilled, this is in order to ensure that the design process has wholly fulfiled the mission need. At the first stage, this requires the check for validity of the mission, system, and subsystem requirements, which have been checked at this stage already. Any further requirements on lower level subsystems which are added at a later date should also be checked for validity.

In conclusion, the validation of the system is a conglomerate of different tests (let it be system, subsystem or unit tests, model or real instruments tests), together with analysis, simulations, review of design (especially for off-the-shelf components), and review and documentation of design flowdown that will lead to the safe conclusion that the system will be able to monitor radiative forcing effects and dynamic evolution of exhaust trails from air-breathing vehicles in the NearSpace, for the improvement of the NOMS.

21 Compliance with Requirements

To verify that the design complies with the requirements, a requirement compliance matrix is constructed. In order to make this matrix, the performance of the design is analysed in Section 21.1. Then, in Section 21.2, the compliance matrix is provided. In this matrix, each of the system, mission, and sustainability requirements are checked with the design.

21.1. Performance Analysis

This section provides an overview of the performance characteristics of the IPMS and the satellites. This performance analysis is used as a basis to verify that the requirements are met with the designed system. Each of the values in Table 21.1 are reported with an explanation in the respective subsection chapters, Chapters 7 to 15. It should be noted that: even though the payload is able to observe the entire globe in the chosen orbit, it was chosen to observe only the northern hemisphere from 13° upwards.

Table 21.1: Performance Analysis of the IPMS and the Spacecraft Subsystems

Parameter	Value
Mission Characteristics	
Mission lifetime	30 yr
Spacecraft lifetime	7.5 yr
Reliability	68.23%
Availability	97.7%
Dry mass	771
Wet mass	911
Astrodynamics	
Eccentricity	0.042 09
Semi-major axis	7 258 689 m
Inclination	90°
Right ascension of the ascending node	0° - 8.57° - 17.12°
Argument of periapsis	90°
True anomaly	0° - 0° - 0°
peri-centre altitude	575 km
Earth repeat, k	1 day
Temporal resolution	2 per day
Payload	
Horizontal resolution (at 13° latitude)	24 km
Vertical resolution	1 km to 2 km
Field of View	80°

Parameter	Value
C&DH	
Data storage	196 GByte
Computing power	1GiB Processing Memory; 32-bit processor @ 800 MHz; 3600 DMIPS
TT&C	
Groundstation 1	SvalSat Ground Station
Groundstation 2	TrollSat Ground Station
Modulation	SQPSK downlink BPSK uplink
Downlink speeds	100 Mbit s^{-1}
Uplink speed	192 kbit s^{-1}
ADCS	
Angular momentum stored reaction wheel	37.5 N m s
Slew rate	8.5×10^{-1} ° s^{-1}
Pointing stability	3×10^{-2}° over 60 s
Attitude knowledge accuracy	2×10^{-3}°
Navigation	
Position determination accuracy	1 m 3D
Propulsion	
# Thruster	2 (+ 2 redundant)
Specific impulse	285 s
Nominal thrust	19.3 N
ΔV contingency	100 m s^{-1}

Spectral range	645 cm^{-1} to 2760 cm^{-1}
Spectral resolution	0.25 cm^{-1}
EPS	
Power generation	2065 W[1]
Battery capacity	2246 W h
Degradation of solar cells	6%/lifetime
C&DH	
Latency	SpaceWire: 10 µs RS485: 1.1 ms

ΔV de-orbit	161.21 m s^{-1}
ΔV orbit maintenance	42.79 m s^{-1}
Thermal	
Minimum operation temperature	13.7 °C
Maximum operating temperature	20.0 °C
Structures	
Lateral eigenfrequency	415.2 Hz
Longitudinal eigenfrequency	614.2 Hz
Maximum stress	2.63 MPa

21.2. Compliance Matrix

To verify that all requirements are met, a compliance matrix is set up. In this matrix, all sustainability-, mission-, and system requirements are checked to verify that the designed system complies with them. Table 21.2 shows the overview of this process. In the first column, the requirement ID is shown. The second column shows if the system complies, where a green checkmark indicates compliance, a red cross is no compliance, and an orange tilde means that the requirement is not checkable, yet. The third column shows the achieved value of a parameter directly specified by the requirement, if applicable. Finally, the last column references a chapter or section in this report, where it is ensured that the requirement is complied with. For brevity, subsystem requirements are not included. As they all flowed down from the system requirements, the satisfaction of the system-level requirement is indicative that the associated subsystem requirements were also satisfied.

Table 21.2: System Requirements

Req. ID	✓ ~ ✗	Value	Source
Sustainability Requirements			
SUS-SPA-01	~		
SUS-SPA-02	✓		Section 21.1
SUS-SPA-03	✓		Section 23.3
SUS-SPA-04	✓		Section 17.4
SUS-SPA-05	~		
SUS-SPA-06	✓		Section 10.3.2
SUS-SPA-07	✓		Section 10.3.2
SUS-SPA-08	✓		Chapter 17
SUS-SPA-09	✓		Section 16.3.1
SUS-SPA-10	✓		Section 23.3
SUS-SPA-11	✓		Chapter 17
SUS-SPA-12	✓		Section 23.3
SUS-SPA-13	✓		Table 13.4a
SUS-SPA-14	✓		Section 9.4
Mission Requirements			
MIS-FUN-01	✓		Section 5.3
MIS-OPS-01	✓		Chapter 17
MIS-OPS-02	✓		Section 18.3

Req. ID	✓ ~ ✗	Value	Source
System Requirements			
SYS-OPS-02	✓		Section 15.3.1
SYS-OPS-03	✓		Table 14.7
SYS-OPS-04	✓		Section 11.3.2
SYS-OPS-05	✓		Section 10.3.1
SYS-OPS-06	✓	28 d^{-1}	Section 11.3.1
SYS-OPS-07	✓		Section 10.2
SYS-OPS-08	✓		Section 10.2
SYS-OPS-09	✓		Chapter 12
SYS-OPS-10	✓		Section 7.2.5, Section 12.3.4
SYS-OPS-11	✓		Section 12.3
SYS-OPS-12	✓		Section 9.3.2
SYS-OPS-13	✓		Section 10.2, Section 11.3
SYS-OPS-14	✓		Section 11.3.4
SYS-OPS-15	✓		Section 11.3.2
SYS-OPS-16	✓		Section 9.5
SYS-OPS-17	✓		Section 13.2.3
SYS-OPS-18	✓		Section 6.3
SYS-OPS-19	✓		Section 15.1.1

[1]At EOL, temperature 60 °C, without transfer losses.

MIS-CON-01	✓		Section 23.2
MIS-CON-02	✓		Section 23.2
System Requirements			
SYS-FUN-01	✓		Section 5.3
SYS-FUN-02	✓		Section 5.3
SYS-FUN-03	✓	0 km to 575 km	Section 5.3
SYS-FUN-04	✓	$2\,d^{-1}$	Section 7.1.2
SYS-FUN-05	✓	> 13° lat.	Section 7.1.2
SYS-FUN-06	✓	575 km	Table 7.1
SYS-FUN-07	✓	800 km	Table 7.1
SYS-OPS-01	✗	0.68 [-]	Section 18.2
SYS-OPS-20	✓		Section 12.2, Section 12.2
SYS-CON-01	✗	2207 M$	Section 22.1
SYS-CON-02	✓		Chapter 17
SYS-CON-03	✓		Chapter 17
SYS-CON-04	✓		Chapter 17
SYS-CON-05	✓		Table 7.1
SYS-CON-07	✓		Table 16.1
SYS-CON-08	✓		Section 15.3.2
SYS-CON-09	✓		Chapters 9 to 15
SYS-CON-10	✓	415.2 Hz	Section 15.3.3
SYS-CON-11	✓	614.2 Hz	Section 15.3.3
SYS-CON-12	✓	1.5 m	Section 15.2

SUS-SPA-01 requires that all countries where IPMS observes approve its operation. This requirement is not taken care of at this stage of the design process. However, when the design process is developed in more detail, it will be ensured that this requirement is met before the operation of the system. SUS-SPA-05 requires a certain amount of $CO_{2(eq)}$ emissions during the re-entry procedure. At this stage, it is yet uncertain how much emissions are emitted during the process. This needs to be determined at a later stage. SYS-OPS-01 states that the minimum reliability of one satellite shall be 87.5% after the lifetime of the spacecraft. Currently, this requirement is not met, partially due to the payload reliability. To mitigate this, the design can be made more redundant in future design phases. It could also be considered to have backup satellites in orbit, in case one fails. SYS-CON-01 states that the maximum cost of the system shall not cost more than 500 M$. This is currently not met. However, as explained in Section 22.3, if a sufficient amount of data is sold over the lifetime of the system, the IPMS can be profitable. Exceeding the cost budget is not critical, if this happens.

22 Economic Analysis

With the IPMS designed and its mission operation defined, an economic analysis can be done. A breakdown of the anticipated costs can be made for the whole system. This breakdown is given in Section 22.1. Then the meteorological market of the payload data is discussed in Section 22.2. With the total costs and prices defined, the operational profit and thus return on investment of the system can be determined. This is done in Section 22.3.

22.1. Cost Breakdown

To accurately estimate the total costs of the IPMS, the different cost categories of the system need to be determined. To find these, a cost breakdown structure of the whole system was created. This can be seen in Figure 22.1.

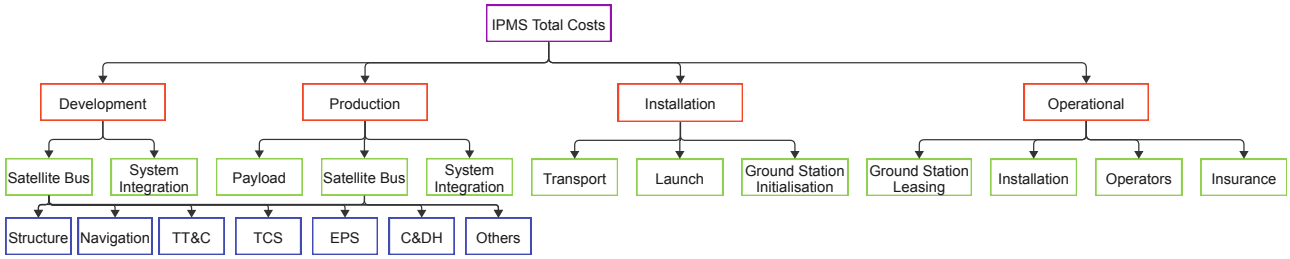

Figure 22.1: Cost Breakdown Structure of the IPMS

From Figure 22.1, it can be seen that the satellite bus and system integration must be developed and produced for all the different subsystems. Moreover, due to using an already existing payload, this does not have any development costs attached. Due to many components' prices being unavailable, an estimation has been made based on each subsystem's price per unit mass. This distribution was taken from Table 16.1 and scaled according to a NASA model-based cost engineering space missions estimation[1]. The cost breakdown of one satellite can be seen in Table 22.1. It should be noted that this is a breakdown estimate with currently available information. The values are not intended to be used as a budget and hence contingencies are not allocated.

Table 22.1: Cost Breakdown of One Satellite

Category	Development Cost [1,000 USD FY2023]	Production Cost [1,000 USD FY2023]
Structure	$ 39,700	$ 14,900
TCS	$ 949	$ 292
Navigation	$ 8,430	$ 9,240
TT&C	$ 1,960	$ 1,770
C&DH	$ 11,100	$ 4,640
EPS	$ 16,400	$ 11,300
Others	$ 16,000	$ 5,850
Payload	$ 0	$ 96,100
System Integration	$ 9,890	$ 245
Total	$ 104,000	$ 144,000

From Table 22.1, it should be noted that the development costs are only present once for all the satellites due to their similarity. A satellite cost of around 153 million USD FY2023 is determined, which is

[1]URL: www.nasa.gov [accessed: 20/06/2023]

well below the estimated 390 million in Section 8.3. Moreover, V&V is typically 30 to 35% of the total development costs, resulting in 33.9 million USD FY2023[75]. The satellite cost breakdown defined forms the input to the IPMS cost breakdown, which can be seen in Table 22.2.

Table 22.2: Cost Breakdown of IPMS

Category	Subcategory	Price [1,000 USD FY2023]
Development	Mission	$ 104,000
Production	Total of 12 Satellites	$ 1,732,000
Installation	**Total**	$ 11,900
	Satellite Transport	$ 90
	Launch	$ 11,700
	Initialisation Groundstation	$ 60
Operation	**Total**	$ 405,000
	Leasing Groundstation	$ 6,000
	Operators	$ 7,800
	Satellite Deployment	$ 35,500
	Satellite Insurance	$ 356,000
Total		$ 2,254,000

In Table 22.2, the total cost of the IPMS is 2254 million USD FY2023. However, it should be noted that due to the operations of the mission, this total can be reduced. This depends on whether all twelve satellites need to be produced or whether a reduction in satellites is sufficient for required model verification. The transport of the satellites to the launch sites will cost 30 000 USD FY2023 per shipment[2]. The launch cost was calculated from the specific price defined in Chapter 6 for the total mass determined in Section 16.4.1. With that, the ground station setup was assumed to be 1% of the leasing costs over the operational lifetime, which is derived similarly to the Midterm estimation of the leasing being 100 000USD FY2023 per ground station per year[1]. Finally, insurance accounted for 20% of the total launch and satellite costs[3].

22.2. Meteorological Measurements Market

Despite its unprecedented measurement regime, the Infrared Pollution Monitoring System is to exist within an existing and populated economic environment. This market must therefore be characterised to identify IPMS's competitive advantages, limitations, constraints, and positioning. Firstly, the capital costs of the supply-side competitors will be analysed. The demand side is then evaluated for the prices willing to be paid, and lastly the quantitative size of this demand.

22.2.1. Capital Costs

An investment cost comparison can be conducted against direct competitors that also possess at least similar capabilities if not more. This provides a starting point to provide further insight into the economic viability of the system. Whilst not indicative of its economic performance by itself, it is a key piece of context to be considered during revenue and profit analysis. A set of cloud profiling and species-identifying meteorological satellites was identified. The considered spacecraft, being in no way fully exhaustive of the market, include MetOp, Aura, Calipso, CloudSat, OCO-2, Glory, and EarthCare.

It should be noted however that the majority of these spacecraft carry with them significantly more instruments than IPMS. The capabilities of these spacecraft from an instrument standpoint, however, do not reflect the observation potential. IPMS's mission parameters allow it to observe above and beyond the tropospheric measurement being focused on by its competitors. IPMS's 7.5-year design operational duration also exceeds its competition 3.75-year average planned durations. Whilst most

[2]URL: heavyhaulandoversized.com [accessed: 20/06/2023]
[3]URL: brightspace.tudelft.nl [accessed: 20/06/2023]

examples far outlive these planned lifetimes, IPMS is also designed to allow for and accommodate such extensions.

With these discrepancies in mind, the competition set possesses an average of 665 million USD (FY2023), a minimum of 327 million USD (Calipso) and a maximum of 1250 million USD (MetOp 1st Generation). All costs are self-reported by each respective space agency but will be interpreted as accurate representations of the magnitude of the actual values. As a direct comparison of the single satellite undistributed development and production cost, IPMS at 248 million USD is highly competitive.

22.2.2. Present Prices

Prices currently accepted by the market can also be used to form the baseline of the system's rates and hence also revenue. Firstly, the prices at which competing or similar services operate can be investigated. The quantity of data produced by the system can then be applied to determine the per-unit sale turnover of the system.

- The European Centre for Medium-Range Weather Forecasts (ECMWF) sells their processed meteorological forecasted data at a rate of 9,000 Euros per Gigabyte of data with a base fee of 81,380. [4]
- Geocento sells satellite imagery at rates varying from 0.003 to 0.006 US cents per pixel to scale for total area and resolution. [5]
- EUMETSAT purchases meteorological data from Spire Global's nanosat constellation for a distributed three million Euros per year within a three-year agreement. [6]

Whilst ECMWF's data is highly processed, a direct application to IPMS's highly compressed but more minimally analysed data can be made. Considering IPMS recording its superior-to-MetOp regime above 13° latitude. A single coverage per day will be considered. Whilst IPMS measures more than this, these values are used as a baseline of a "single purchase" and may be multiplied as multiple purchases later on. Measurements every day are applied to determine the total amount of data produced in a year. This is representative of a single unit of sale of annual data, not that a single buyer purchases all of the data.

The spatial resolution was rounded to 25 km for simplicity and can therefore be used to determine the number of pixels that the system can produce. In comparison to the photographs sold by Geocento, IPMS data is of significantly greater scarcity as well as meteorological value. The unfilled niche is expected to confirm demand in contrast to trying to compete in the more highly saturated satellite photography market. Therefore, the asking price for IPMS data may be greater than this.

EUMETSAT's rates can be seen as a reasonable baseline due to the significant similarity in type, quantity, and context of the transaction. IPMS is expected to provide superior data. An average of the rates can be used as a first estimate for the potential unit revenue. A further specification of the data to that within a potential "interest zone" between the longitudes of New York and Frankfurt can be taken as a more realistic representation of the data that is desirable to purchase. The rate values are summarized in Table 22.3. Furthermore, in order to sell the data to customers, it should be considered that on ground ICT services, and perhaps infrastructure is to be provided for the acquisition and transmission of data to the customers.

[4] URL: www.ecmwf.int [accessed: 19/06/2023]
[5] URL: geocento.com [accessed: 19/06/2023]
[6] URL: www.eumetsat.int [accessed: 19/06/2023]

Table 22.3: Current Market Data Rates and IPMS Unit Revenue Estimate (USD FY2023)

	Rate	Annual Revenue All longitudes	Annual Revenue North Atlantic
ECMWF [4]	$ 88,704.20 + $ 9,810/GB	$ 99,344,322	$ 22,886,644
Geocento high [5]	$ 0.006/pixel	$ 692,609	$ 159,085
Geocento low [5]	$ 0.003/pixel	$ 346,305	$ 79,542
EUMETSAT [6]	$ 3,270,000/yr	$ 3,270,000	$ 3,270,000
Average		$ 25,913,309	$ 6,598,818

22.2.3. Data Demand

The meteorological data generated during the operation can be sold to a variety of different customers. As most governments in the northern hemisphere provide a national meteorological & hydrological service to their country, there are institutions active which can use this data. Examples of these institutions are the Royal Dutch Meteorological Institute[7] and the National Oceanic and Atmospheric Administration[8]. Moreover, there are also some multinational institutions which collaborate in this field, such as the European Meteorological Network[9] and the World Meteorological Organization[10].

Next to governmental organisations, there are also private weather consultancies which could benefit from the data. These are mostly located in North America, such as AccuWeather[11] who can improve their forecasting or the aviation weather plans from Spire Global[12]. Finally, there could also be interest from the academic community. Research centres such as for example the Toronto Magnetic and Meteorological Observatory and the Department of Atmospheric and Oceanic Sciences of McGill University could also have an interest in this data, however, those will not be expected to partake as their national meteorological institutes might already provide them with data.

22.3. Return on Investment and Operational Profit

When purely considering the commercial benefit of selling meteorological data on the market by the IPMS, the net present benefit over the system's lifetime for different amounts of customers can be calculated using the system costs. This case is considered, as the refined fining structure is part of the NOMS business case and thus does not bring in any direct profit to the IPMS, due to fees being applied no matter the presence of an emissions sensing system. Rather, it could be stated that the IPMS increases the cost of the NOMS if ultimately all SHT vehicles are less polluting and thus paying lower fees.

The system's cost components can be subdivided into initial capital investments, medium-term equipment renewal, and tactical year-to-year operational costs. The initial costs include development costs, verification & validation costs, and ground station setup costs. Equipment renewal consists of the production, transportation, and launch costs of any satellites that will need to be replaced, nominally all three of the constellation. The current cost estimates most likely overestimate real costs; as they assume the planned mission duration of the spacecraft, without further extension. Operational costs consist of ground station leasing, staff wages, and launch insurance paid per annum.

System revenue is as mentioned assumed to only consider the sale of collected measurement data. This is hence the linear relationship between the number of buyers of units of data and the assumed average selling price of the data. Whilst exact distributions of sale volume are difficult to predict due to the novel and niche dataset that IPMS is able to provide, effectively creating a new market.

[7]URL: www.luchtvaartmeteo.nl [accessed: 20/06/2023]
[8]URL: www.noaa.gov [accessed: 20/06/2023]
[9]URL: www.eumetnet.eu [accessed: 20/06/2023]
[10]URL: worldweather.wmo.int [accessed: 20/06/2023]
[11]URL: www.accuweather.com [accessed: 20/06/2023]
[12]URL: spire.com [accessed: 20/06/2023]

The European Central Bank's current and relatively stable bank rate of 4.00% is taken. [13] This discount rate is applied upon each year's costs and revenues. Economic performance metrics can thence be defined for the project. The net benefit is the gross cash flow considering costs and revenues. The net present value is defined as the summation of the net discounted benefit. Return on investment as the fractional net present value out of the total discounted costs. The internal rate of return is, inversely to the bank rate, the effective yearly compounded valuation growth of the net present value returned by the project.

For the IPMS, different net present benefit curves have been plotted for different amounts of customers in Figure 22.2. The performance metrics are summarized in Table 22.4. The baseline of five buyers was taken as these are the most interested parties on the IPMS's data, as mentioned in Section 22.2.3. Fourteen and fifteen buyers are represented to illustrate the break-even point. Whilst twenty buyers is a somewhat realistic, if perhaps optimistic estimation of the prospective sales volume considering the growth NearSpace transportation market.

Table 22.4: Economic Performance Metrics for Varying Sale Volumes

Annual Sales Quantity	Net Present Value [million USD FY2023]	Return on Investment [%]	Internal Rate of Return [%]
5	$ −989.0	-62.5 %	N/A
13	$ −39.6	-2.51 %	3.26 %
14	$ 79.0	4.99 %	5.46 %
20	$ 791.0	50.0 %	18.3 %

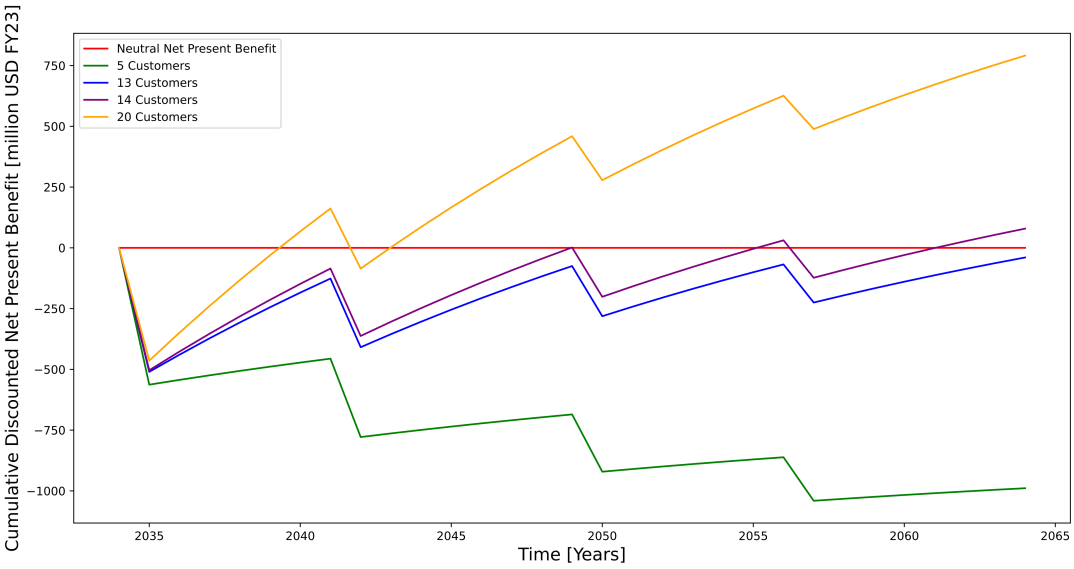

Figure 22.2: Net Present Benefit of IPMS over Time for Different Amount of Customers

From Figure 22.2, it can be concluded that in order to get a positive net present benefit during the system lifetime, a minimum of fifteen customers are required to buy a year-long unit of data at an average price of slightly under 6.6 million USD FY2023. Moreover, the number of customers will determine the possible discontinuation of the process, only losing the sunk costs. However, due to the many worldwide governmental and private institutions present in the meteorological field, this is not expected. Nonetheless, an elaborate customer analysis should be performed to confirm this.

[13] URL: www.ecb.europa.eu [accessed: 19/06/2023]

23 Future Development

With the system designed to sense emissions of airbreathing vehicles in NearSpace, the NOMS has been developed to allow for a payment structure to be implemented. Moreover, the meteorological data will be able to be supplied based on the payload data. This can allow for weather forecast creations, which can be outsourced and then used by the NOMS to allow for more efficient, effective and sustainable navigation of aerial vehicles. However, as the NOMS and its IPMS have now only been developed in a preliminary phase, a plan needs to be present in which the activities that need to be executed after the conclusion of the DSE are discussed. In Section 23.1, an order of those activities will be presented in a flow diagram for both the NOMS and the satellite system. Afterwards, these tasks are presented in a Gantt chart to estimate the schedule of the post-DSE activities in section 23.2. Additionally, the manufacturing, assembly and integration activities have been specified in more detail in Section 23.3 for one of the exhaust trail sensing satellites.

23.1. Project Design & Development Logic

After the DSE project phase, a detailed design must be made before both systems can be implemented. In this detailed design phase, the team composition will change and funds and clients need to be obtained. Additionally, the design needs to be detailed and reported before the NOMS can be simulated. With a manufacturing, assembly and integration plan created, the production and certification phase can get started where verification and validation of the different NOMS and IPMS components and systems takes place before both systems can get installed, and operated and retired. This includes the setup and integration of the NOMS, but also the launch of the first three IPMS satellites. During operation, the IPMS functions as a subsystem of the NOMS and allows for improved flight plans and ConOps. The whole project design and development, including the EOL of both systems, can be seen in Figure 23.1.

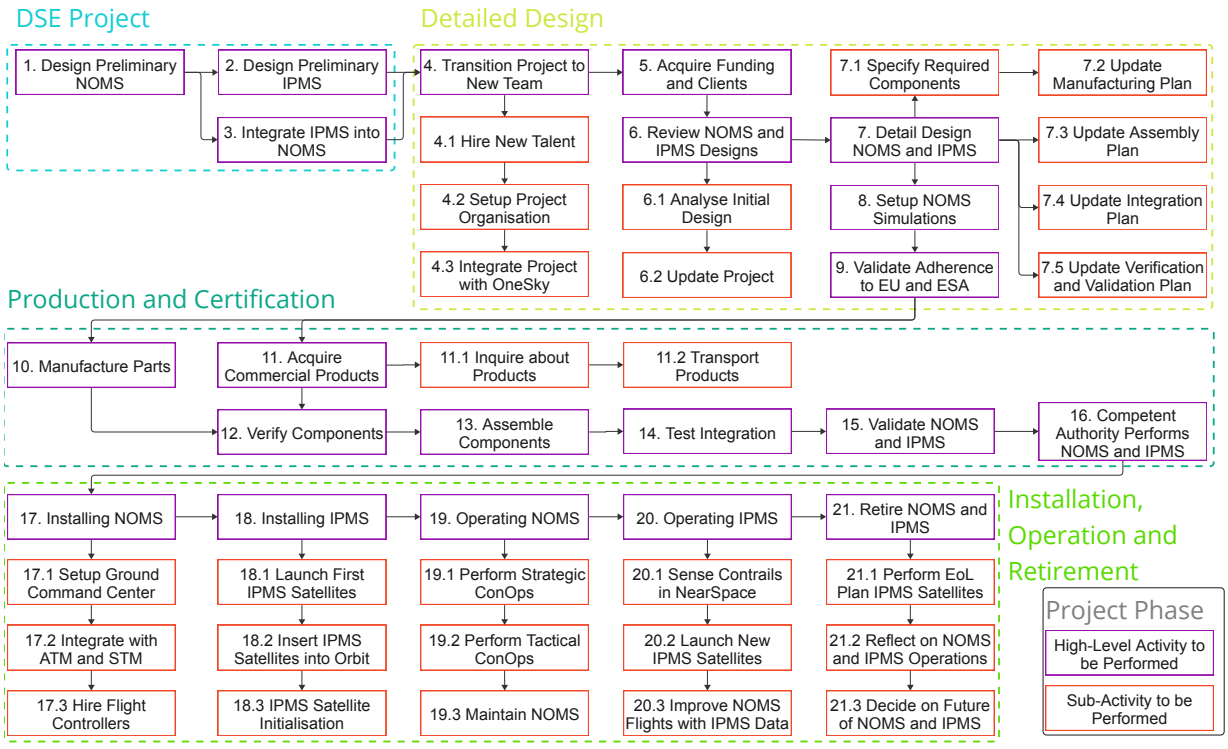

Figure 23.1: Project Design & Development Logic Diagram

23.2. Project Gantt Chart

With the four different phases presented in Section 23.1, they can be scheduled to ensure that both IPMS and NOMS are operational by 2035, as required by MIS-CON-01. The tasks have been assigned an approximate time interval to give an initial estimate of the project development and both systems' operation. Moreover, as they need to operate at least until 2065, due to MIS-CON-02, and the IPMS satellites have 25 years for their EOL, the timeline ends at 2090. This timeline is visualised in a Gantt chart (figure 23.2), where the approximate start and end dates of all the activities have been visualised. In the Gantt chart, the years until 2035 have been marked yellow and have a monthly schedule, whereas the years during operation have been highlighted blue and scheduled on a yearly basis, due to the little change in planned activities during that period.

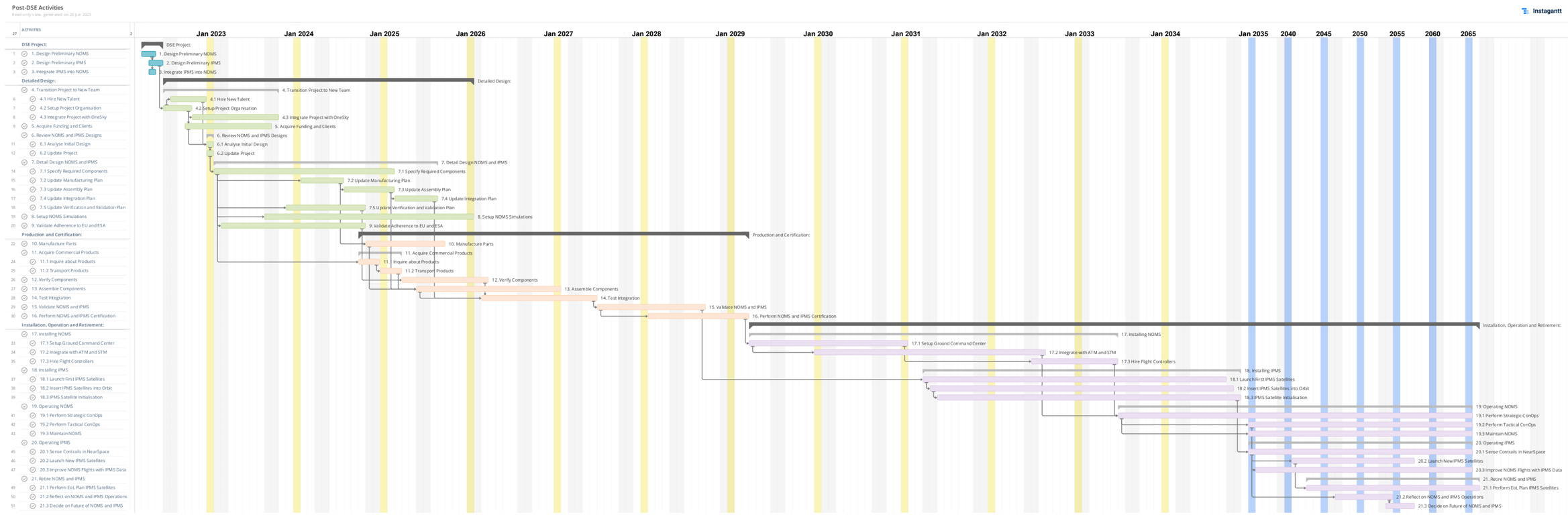

Figure 23.2: Gantt Chart of Post-DSE Activities to be Performed created using Instagantt

23.3. Manufacturing, Assembly, Integration Plan

Manufacturing and integration of the spacecraft system aim to produce a reliable system that complies with the requirements and stakeholders' needs. Production should be supported by engineering data, it should also include testing every time a new assembly is made. Manufacturing, integration and testing consist of the following steps. First, engineering data is gathered. It should include drawings, procedures and specifications like accuracy requirements, materials, spacing between parts, painting, coating, and lubrication. Once the parts are produced, they are assembled into components. Those are later tested and once successfully qualified, they are assembled into the spacecraft structure. Finally, the spacecraft is tested and qualified.

The production plan starts with a system breakdown to identify all the assemblies, components and piece parts, classifying their delivery method (i.e. off-the-shelf, in-house manufacturing). An overview is given in Figure 23.2. It is followed by a manufacturing, assembly and testing schedule that aims to make the processes parallel to limit production and certification time, Figure 23.3. Next, the in-house manufacturing and outsourcing of components are analysed, keeping in mind the sustainability requirements (SUS-SPA-03, SUS-SPA-12, SUS-SPA-10).

23.3.1. Components Breakdown Structure

The grouping into assemblies is done based on the structural or functional similarity of components as it is later used as a guide for integration. The division is provisional, it should be reassessed once all components and subsystems are fully designed and documented. Also, full documentation about manufacturing, integration, treatment and handling should be prepared and attached to each assembly, and should always travel with the components during integration and testing as recommended by *Space Mission Engineering: The New SMAD*.

Figure 23.2: Breakdown of subsystems into assemblies and components.

23.3.2. Production schedule

Figure 23.3 shows the order and groups in which components can be manufactured and tested. In Phase 1, all the in-house components are manufactured, put into small assemblies and tested. Integration and testing of small assemblies are beneficial as they can be highly parallelised resulting in a time gain. Also, if an assembly fails the tests, it is easier to investigate the reason if the assembly is small. The type of test depends on the assembly (subsystem), for instance, structural components will undergo vibrational analysis, and tanks will undergo pressure tests. The tests are part of the validation procedure which is described in Section 20.2. Phase 2 consists of the integration and testing of two subsystem assemblies to verify and validate the cooperation of key subsystems while still keeping the assembly conveniently small. Finally, Phase 3 is the integration and testing of multiple subsystems and, at the end, the entire spacecraft.

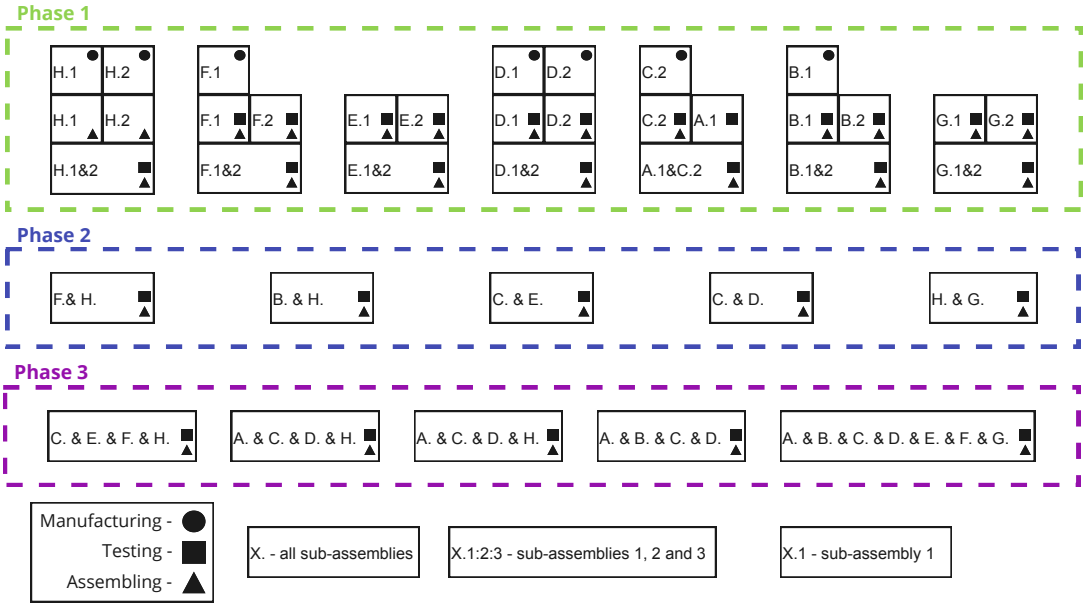

Figure 23.3: Manufacturing, integrity and testing execution order. Tasks at the same level can be executed in parallel.

23.3.3. Parts and materials sourcing

Integral to the satellite is the instrument for earth observation. The IASI-NG is proposed by CNES and developed and manufactured by Astrium, now integrated into Airbus Space and Defence. CNES has signed an agreement on the 2030 agenda of the United Nations, which include the Sustainable Development Goals. CNES shows extensive documentation on corporate social responsibility, pursuing a company-wide program to reduce the quantity of non-renewable resources consumed by development projects[1]. The contract and acquisition of Astrium as a provider of technology include adherence to these standards, as per CNES policy concerning stakeholders and partners[2].

In a similar fashion, components such as the solar array, solar cells, onboard computers and data storage components are sourced from companies that show attention and commitment to the need for sustainable sourcing of materials. Beyond Gravity, supplier of the OBC and GNSS receivers, as well SEAKR, a subsidiary of Raytheon Technologies, acknowledge the limits of resources of the planet and pledge to environmental, social and governmental sustainability[3] [4].

Another critical point of interest is the sourcing of raw materials needed for the manufacturing of the batteries. The required materials, tin, tungsten, tantalum and gold typically originate from conflict-affected and high-risk areas. The European Commission identifies these risks during the

[1]URL: cnes.fr [accessed: 20/06/2023]
[2]URL: presse.cnes.fr [accessed: 20/06/2023]
[3]URL: www.beyondgravity.com [accessed: 20/06/2023]
[4]URL: www.rtx.com [accessed: 20/06/2023]

mining stage and introduces requirements for ethical sourcing of these materials [76]. Contractors selected for the development of the battery pack should adhere to these standards.

Several key components of the spacecraft will be designed, developed and manufactured in-house to facilitate the need to tailor sizing and performance parameters to the need of the mission. This includes critical parts, such as the receiver and transmitter reflectors but also structural components and fuel tanks. The manufacturing of reflectors, temperature regulators and other structural components requires the sourcing and processing of aluminium, the development of composites and the generation of heat-conducting fluids. These processes are of high power consumption but also put a high strain on the environmental systems by expelling pollutants and requiring large amounts of water [77] [78].

To cope with these costs of In-house manufacturing, one should take measures such as selecting providers that adhere to voluntary standards set by cooperative organisations such as the Aluminium Stewardship Initiative [5] and simultaneously research opportunities in the production line to optimize value adding protocols and reducing waste. By conforming to standards set by ISO, such as the ISO Net Zero Guidelines [6] and the ISO 50001 Energy consumption standards [7], major advancements can be achieved.

[5]URL: aluminium-stewardship.org [accessed: 20/06/2023]
[6]URL: www.iso.org/netzero [accessed: 20/06/2023]
[7]URL: www.iso.org/energymanagement [accessed: 20/06/2023]

24 Conclusion

There is expected to be a rapid increase in activity in the NearSpace aerial region, between FL 660 and 100 km, in the near future. After the design of a NearSpace Operation Management System (NOMS) to manage and surveil objects and vehicles in this region, it was discovered that the most limiting factor in the initial stages of this system would be emissions from vehicles in the region. Water vapour, CO_2, NO_x, and CH_4 in NearSpace, emitted by air-breathing vehicles, was found to have increased negative effects on the environment therefore this study was focused on the design of a concept for an Infrared Pollution Monitoring System (IPMS) to observe these emissions was created.

The state-of-the-art Infrared Atmospheric Sounding Interferometer - Next Generation (IASI-NG) instrument provided was chosen as the primary payload after extensive analysis of existing options as it provides the capability to detect and separate emissions density by altitude. A polar Low Earth Orbit (LEO) was calculated to be the most optimal orbit track as it provided an area of interest with coverage from the payload twice every 24 h. Research indicated this prime area of interest to be the North Atlantic flight route between Europe and the East Coast of the United States. Therefore in order to provide coverage over the whole flight route a constellation of 3 satellites, launched and inserted by the Falcon 9, was chosen.

A suitable platform for the IASI-NG was developed through the analysis of individual subsystems of the spacecraft. A semi-monocoque structure and gimballed solar array provided the suitable conditions for power and structural integrity whilst external louvres and rear-mounted thrusters provided the required thermal management and propulsive capability. The management of these subsystems spurred the development of a high data rate On-Board Computer (OBC) with communication enabled by gimballed communication antennas. This design was complemented with 3-axis stability and nadir-pointing enabled by the Attitude Determination & Control System (ADCS).

While almost all requirements were met by this design a large limiting factor was the reliability of only 68.3% primarily due to the low reliability of the payload. Additionally, high unit costs arose due to the large form factor of the satellites. The combination of these poses further risks of uncontrollable cost overruns from inadequate service time and hence additional satellite number requirements. Future developments may provide the ability to create smaller and more reliable IASI-NG payloads therefore it is recommended to revise the design of this satellite as the technology of infrared interferometers develops.

Further revision efforts consist of performing multiple converging iterations until an insignificant difference in parameters is reached. The reduced total mass and power calculated in the resource breakdown compared to the initial budgeted mass and power can be used as a baseline for this process. Furthermore, it is needed to implement a true anomaly change in the three satellites to avoid close passes at the poles. For this, current contingency fuel might be sufficient but calculations have to be performed.

In conclusion, it was found that to create a safe and sustainable environment in NearSpace a NOMS is required to accurately surveil and manage vehicles and an IPMS is required to observe vehicle emissions. The design of both of these systems was performed in order to provide realistic and actionable solutions to the increasing activity in NearSpace in the coming future. By understanding the challenges and solutions in this report future engineers can work toward creating the best system for NearSpace.

References

[1] Taking Control. *Taking Control: Midterm Report, DID-8*. TU Delft, Faculty of Aerospace Engineering, June 2023.

[2] F. Bernelli-Zazzera et. al. "Re-entry predictions of space debris for collision avoidance with air traffic". In: *CEAS Space Journal* (2022). ISSN: 1868-2510. DOI: 10.1007/s12567-022-00463-y.

[3] H. J. Singer et. al. *Space Weather Forecasting: A Grand Challenge*. Mar. 2013, pp. 23–29. DOI: 10.1029/GM125p0023.

[4] J. Pletzer et. al. "The climate impact of hydrogen-powered hypersonic transport". In: *Atmospheric Chemistry and Physics* 22 (21 Nov. 2022), pp. 14323–14354. ISSN: 1680-7324.

[5] H. S. Johnston. "Pollution of the Stratosphere". In: *Environmental Conservation* 1 (3 Aug. 1974), pp. 163–176. ISSN: 0376-8929. DOI: 10.1017/S0376892900004513.

[6] European Environment Agency. *28. Stratospheric Ozone Depletion*. Apr. 2016.

[7] E. Dlugokencky et. al. "Observing Water Vapour". In: *World Meteorological Association Bulletin* 65-2 (2016).

[8] Council of European Union. *Council regulation (EU) 2018/1139*. 2018.

[9] Taking Control. *Taking Control: Baseline Report, DID-6*. TU Delft, Faculty of Aerospace Engineering, May 2023.

[10] E. Bucchignani. "Wind Predictions in the Lower Stratosphere: State of the Art and Application of the COSMO Limited Area Model". In: *Meteorology* 1 (3 Aug. 2022), pp. 311–326. ISSN: 2674-0494. DOI: 10.3390/meteorology1030020.

[11] IASI Sounding Science Working Group. "IASI-NG Science Plan". In: *CEAS Space Journal* (2018).

[12] W. J. Larson and J. R. Wertz. *Space Mission Engineering: The New SMAD*. eng. Space technology library ; v. 28. Hawthorne, CA: Microcosm Press, 2011. ISBN: 9781881883159.

[13] B. Mayer et. al. "Radiative Transfer: Methods and Applications". In: *Atmospheric Physics: Background – Methods – Trends*. Ed. by U. Schumann. Berlin, Heidelberg: Springer Berlin Heidelberg, 2012, pp. 401–415. ISBN: 978-3-642-30183-4. DOI: 10.1007/978-3-642-30183-4_24.

[14] B. Mayer et. al. "Validating the MYSTIC three-dimensional radiative transfer model with observations from the complex topography of Arizona's Meteor Crater". In: *Atmospheric Chemistry and Physics* 10.18 (2010), pp. 8685–8696. DOI: 10.5194/acp-10-8685-2010.

[15] B. Mayer and A. Kylling. "Technical note: The libRadtran software package for radiative transfer calculations - description and examples of use". In: *Atmospheric Chemistry and Physics* 5.7 (2005), pp. 1855–1877. DOI: 10.5194/acp-5-1855-2005.

[16] D. Kinnison et. al. "The Impact on the Ozone Layer of a Potential Fleet of Civil Hypersonic Aircraft". In: *Earth's Future* 8.10 (2020). e2020EF001626 2020EF001626, e2020EF001626. DOI: https://doi.org/10.1029/2020EF001626. eprint: https://agupubs.onlinelibrary.wiley.com/doi/pdf/10.1029/2020EF001626.

[17] K. Schäfer et. al. "Spectrometers". In: *Springer Handbook of Atmospheric Measurements*. Ed. by T. Foken. Cham: Springer International Publishing, 2021, pp. 799–819. ISBN: 978-3-030-52171-4. DOI: 10.1007/978-3-030-52171-4_28.

[18] D. W. T. Griffith et. al. "A Fourier transform infrared trace gas and isotope analyser for atmospheric applications". In: *Atmospheric Measurement Techniques* 5.10 (2012), pp. 2481–2498. DOI: 10.5194/amt-5-2481-2012.

[19] S. P. Davis et. al. *Fourier Transform Spectrometry*. Elsevier Science, 2001. ISBN: 9780080506913. URL: https://books.google.nl/books?id=gMXrvGg5hTQC.

[20] P. R. Griffiths. "Fourier Transform Infrared Spectrometry". In: *Science* 222.4621 (1983), pp. 297–302. DOI: 10.1126/science.6623077. eprint: https://www.science.org/doi/pdf/10.1126/science.6623077.

[21] I. Levin and M. Cuntz. "Measurement of Stable Isotopes in Carbon Dioxide, Methane, and Water Vapor". In: *Springer Handbook of Atmospheric Measurements*. Ed. by Thomas Foken. Cham: Springer International Publishing, 2021, pp. 509–532. ISBN: 978-3-030-52171-4. DOI: 10.1007/978-3-030-52171-4_17.

[22] H. J. Eichler et. al. "Spectrometers and Interferometers". In: *Lasers: Basics, Advances and Applications*. Cham: Springer International Publishing, 2018, pp. 397–406. ISBN: 978-3-319-99895-4. DOI: 10.1007/978-3-319-99895-4_22.

[23] N. Livesey. "Limb Sounding, Atmospheric". In: *Encyclopedia of Remote Sensing*. Ed. by E. G. Njoku. New York, NY: Springer New York, 2014, pp. 344–348. ISBN: 978-0-387-36699-9. DOI: 10.1007/978-0-387-36699-9_87.

[24] L.S. Rothman et. al. "The HITRAN 2004 molecular spectroscopic database". In: *Journal of Quantitative Spectroscopy and Radiative Transfer* 96.2 (2005), pp. 139–204. ISSN: 0022-4073. DOI: https://doi.org/10.1016/j.jqsrt.2004.10.008.

[25] D. W. T. Griffith. "Synthetic Calibration and Quantitative Analysis of Gas-Phase FT-IR Spectra". In: *Appl. Spectrosc.* 50.1 (Jan. 1996), pp. 59–70.

[26] M. Abd-Elghany et. al. "Environmentally safe (chlorine-free): new green propellant formulation based on 2,2,2-trinitroethyl-formate and HTPB". In: *RSC Advances* 8 (21 2018), pp. 11771–11777. ISSN: 2046-2069. DOI: 10.1039/C8RA01515E.

[27] ISO. "Space systems — Determining orbit lifetime". In: (Sept. 2007).

[28] R. Janovsky et. al. "End-Of-Life De-Orbiting Strategies for Satellites". In: Jan. 2002, pp. 1–10.

[29] S. Pessina et. al. *Metop long term free-dynamics attitude analysis, for improved re-entry prediction*.

[30] A. K. Singh and A. Bhargawa. "Prediction of declining solar activity trends during solar cycles 25 and 26 and indication of other solar minimum". In: *Astrophysics and Space Science* 364 (1 Jan. 2019). ISSN: 1572946X. DOI: 10.1007/s10509-019-3500-9.

[31] Y. Borthomieu. *Satellite Lithium-Ion Batteries*. Elsevier B.V., 2014, pp. 311–344. ISBN: 9780444595133. DOI: 10.1016/B978-0-444-59513-3.00014-5.

[32] Kh. I. Abdusamatov. "Optimal prediction of the peak of the next 11-year activity cycle and of the peaks of several succeeding cycles on the basis of long-term variations in the solar radius or solar constant". In: *Kinematics and Physics of Celestial Bodies* 23 (3 June 2007), pp. 97–100. ISSN: 0884-5913. DOI: 10.3103/s0884591307030026.

[33] Y. He et. al. "High-precision repeat-groundtrack orbit design and maintenance for Earth observation missions". In: *Celestial Mechanics and Dynamical Astronomy* 128 (2-3 June 2017), pp. 275–294. ISSN: 15729478. DOI: 10.1007/s10569-017-9753-0.

[34] C.D. Brown. *Elements of Spacecraft Design*. eng. AIAA Education Series, 2002. ISBN: 1-56347-524-3.

[35] C. M. Reid et. al. *Performance and Comparison of Lithium-Ion Batteries Under Low-Earth-Orbit Mission Profiles*. 2007.

[36] G. Kopp and J. Lean. "A new, lower value of total solar irradiance: Evidence and climate significance". In: *Geophysical Research Letters* 38.1 (2011). DOI: 10.1029/2010GL045777.

[37] M. Sumanth. "Computation of Eclipse Time for Low-Earth Orbiting Small Satellites". In: *International Journal of Aviation, Aeronautics, and Aerospace* (2019). ISSN: 23746793. DOI: 10.15394/ijaaa.2019.1412.

[38] *SPACECRAFT SOLAR CELL ARRAYS NASA SP-8074*. NASA, Jet Propulsion Laboratory, May 1971.

[39] S. Samwel et. al. “COMPARATIVE STUDY OF THE ENERGETIC PARTICLE FLUENCES FOR DIFFERENT ORBITAL TRAJECTORIES”. In: *International Journal of Astronomy and Astrophysics* (Jan. 2006), pp. 139–150.

[40] G. S. Arnold et. al. “Reaction of high-velocity atomic oxygen with carbon”. In: *AIAA Journal* 24.4 (1986), pp. 673–677. DOI: 10.2514/3.9324.

[41] J. Li et. al. “A Brief Review of High Efficiency III-V Solar Cells for Space Application”. In: *Frontiers in Physics* 8 (2021). ISSN: 2296-424X. DOI: 10.3389/fphy.2020.631925.

[42] TU Delft. *AE1222-II Aerospace Design & Systems Engineering Elements I Part: Spacecraft (bus) design and sizing*. English. TU Delft. 2013.

[43] A. T. Monham. “ENVISAT MISSION CONTROL: AN EFFECTIVE EVOLUTION FROM ERS”. In: *Space Mission Operations and Ground Data Systems - SpaceOps ’96, Proceedings of the Fourth International Symposium held 16-20 September 1996 in Munich, Germany.* (Sept. 1996), pp. 648–657.

[44] F. Bernard et. al. “Overview of IASI-NG the new generation of infrared atmospheric sounder”. In: *Society of Photo-Optical Instrumentation Engineers* (2017). Proceedings Volume 10563, International Conference on Space Optics — ICSO 2014; 105633H (2017). DOI: 10.1117/12.2304101.

[45] B. Ghodrati et. al. “Reliability considerations in automated mining systems”. In: *International Journal of Mining, Reclamation and Environment* (May 2015). DOI: 10.1080/17480930.2015.1091617.

[46] J. Menon. “Comparison of Sparing Alternatives for Disk Arrays”. In: *[1992] Proceedings the 19th Annual International Symposium on Computer Architecture* (1992). DOI: 10.1145/139669.140392.

[47] STAR-Dundee. *SpaceWire User’s Guide*. English. STAR-Dundee Limited. 2012.

[48] D. Donsez et. al. *Cubedate: Securing Software Updates in Orbit for Low-Power Payloads Hosted on CubeSats*.

[49] *FAQs for Protecting SMD Spaceborne Assets Command Uplink Encryption*. 2020.

[50] C. B. Smith and A. F. León. *AUTHENTICATION IN THE TELECOMMAND LINK TO IMPROVE SECURITY*.

[51] C. R. Bjornson and L. Johnson. *Licensing Reference Document | Athena LEOP*.

[52] S. H. Schaire and D. L. Carter. *Near Earth Network (NEN) Users’ Guide Signature/Approval Page Date NEN Wallops Manager, Near Earth Network Project, Code 453 NASA Wallops Flight Facility*.

[53] F. Concaro et. al. “The SNOWBEAR project: A Svalbard ground station for wide-band earth observation data reception”. In: American Institute of Aeronautics and Astronautics Inc, AIAA, 2018. ISBN: 9781624105623. DOI: 10.2514/6.2018-2478.

[54] H.T. Friis. “A Note on a Simple Transmission Formula”. In: *Proceedings of the IRE* 34.5 (1946), pp. 254–256. DOI: 10.1109/JRPROC.1946.234568.

[55] B. Koosha et. al. *Centralized Scheduler Interface for Communication Link Between SpaceLink’s Relay Satellites and LEO Assets*. 2022.

[56] M. Tolstoj. “Analysis of Disturbance Torques on Satellites in Low-Earth Orbit Based Upon Grace”. In: (July 2017).

[57] G. Wiedermann et. al. “THE SENTINEL-2 SATELLITE ATTITUDE CONTROL SYSTEM - CHALLENGES AND SOLUTIONS”. In: June 2014.

[58] J. J. Zipay et. al. *The Ultimate Factor of Safety for Aircraft and Spacecraft – Its History, Applications and Misconceptions*. 2015.

[59] R. C. Hibbeler. *Engineering Mechanics: Dynamics*. eng. Vol. 13. Prentice Hall, 2012. ISBN: 978-0132911276.

[60] G. Cros et. al. “European Astrix FOG In-Orbit heritage”. In: 144 (Jan. 2012), pp. 481–502.

[61] J. Levenhagen et. al. "EARTH ORIENTED SAFE MODE DESIGN BASED ON THE EADS ASTRIUM CESS". In: *IFAC Proceedings Volumes* 40.7 (2007). 17th IFAC Symposium on Automatic Control in Aerospace, pp. 301–304. ISSN: 1474-6670. DOI: 10.3182/20070625.

[62] J. Herman et. al. "Attitude control for grace the first low-flying satellite formation". In: 548 (Jan. 2004).

[63] J. D. Searcy. "Magnetometer-only attitude determination with application to the M-SAT mission". In: *Masters Theses* (2011). DOI: https://scholarsmine.mst.edu/masters_theses/6892.

[64] L. B. Winternitz et. al. "Global Positioning System Navigation Above 76,000 KM for NASA'S Magnetospheric Multiscale Mission". In: *NAVIGATION* 64.2 (2017), pp. 289–300. DOI: https://doi.org/10.1002/navi.198.

[65] F. Maggi et. al. *Trade-off analysis of a new liquid rocket engine*. 2019.

[66] S. A. Whitmore and S. N. Chandler. "Engineering Model for Self-Pressurizing Saturated-N2O-Propellant Feed Systems". In: *Journal of Propulsion and Power* 26 (2010), pp. 706–714. DOI: 10.2514/1.47131.

[67] SpaceX. *Falcon User's Guide*. English. Space Exploration Technologies Corp. Sept. 2021.

[68] M. M. Finckenor, and D. Dooling. *Multilayer Insulation Material Guidelines*. Technical Publication 19990047691. NASA, Apr. 1999.

[69] R. Carriere and A. Cherniaev. "Hypervelocity Impacts on Satellite Sandwich Structures—A Review of Experimental Findings and Predictive Models". In: *Applied Mechanics* 2 (1 Feb. 2021), pp. 25–45. ISSN: 2673-3161. DOI: 10.3390/applmech2010003.

[70] K.H.J. Buschow. *Encyclopedia of Materials: Science and Technology*. Encyclopedia of Materials: Science and Technology v. 10. Elsevier, 2001. ISBN: 9780080431529.

[71] M. DeVanzo and R. B. Hayes. "Ionizing radiation shielding properties of metal oxide impregnated conformal coatings". In: *Radiation Physics and Chemistry* 171 (June 2020), p. 108685. ISSN: 0969806X. DOI: 10.1016/j.radphyschem.2020.108685.

[72] H. Kjellberg. "Design of a CubeSat Guidance, Navigation, and Control Module". PhD thesis. Aug. 2011. DOI: 10.13140/2.1.1469.7767.

[73] Jean-Francois Castet and Joseph Homer Saleh. "Satellite and satellite subsystems reliability: Statistical data analysis and modeling". In: *Reliability Engineering & System Safety* 94 (11 Nov. 2009), pp. 1718–1728. ISSN: 09518320. DOI: 10.1016/j.ress.2009.05.004.

[74] B. Blanchard and W. Fabrycky. *Systems Engineering and Analysis*. Ed. by Rob DeGeorge and Denise Duggan. 2nd ed. Prentice-Hall, Inc., 1990, pp. 359–359.

[75] A. Pataricza et. al. *6 Cost Estimation for Independent Systems Verification and Validation*.

[76] L. Mancini et. al. *Responsible and sustainable sourcing of batteries raw materials : insights from hotspot analysis, corporate disclosures and field research.* ISBN: 9789276179504.

[77] B. O. Rosseland et. al. "Environmental effects of aluminium". In: *Environmental Geochemistry and Health* 12 (1-2 Mar. 1990), pp. 17–27. ISSN: 0269-4042. DOI: 10.1007/BF01734045.

[78] S. Ghavam et. al. "Sustainable Ammonia Production Processes". In: *Frontiers in Energy Research* 9 (Mar. 2021). ISSN: 2296-598X. DOI: 10.3389/fenrg.2021.580808.